PETROGRAPHY AND GEOCHEMISTRY OF A LIMESTONE–SHALE SEQUENCE WITH EARLY AND LATE LITHIFICATION: THE MIDDLE PURBECK OF DORSET, ENGLAND

by

Adam El-Shahat
M.Sc. (Cairo)

A thesis submitted for the degree of
Doctor of Philosophy

University of Southampton
1977

To my Mother and Father

بسم الله الرحمن الرحيم

CONTENTS

ACKNOWLEDGEMENTS

I am indebted to the Egyptian Ministry of Education for financial support. Special thanks are due to Professor M.L. Kabesh of the National Research Centre, Cairo, for his encouragement which made my study in this country possible.

My deepest gratitude goes to Dr. M.E. Cosgrove for his valuable guidance and supervision particularly the geochemical parts of this thesis. Ian West is fully acknowledged for supervision and continuous encouragement. His deep interest in the Purbeck environments and diagenesis has inspired the author.

I wish to thank Professor F. Hodson for his kind concern. I am most grateful to Mr. T.¢. Clayton for valuable help with the data-processing computer programs. I thank Mr. J. Merefield for his continuous help during the four months of spectrometer calibration. I am also grateful to Mr. R. Saunders, Mr. D. Utton and Mrs. A.M. Dunckley for their help. I extend my acknowledgements to other members of the academic and technical staff of the Geology Department, Southampton University for their advice and help.

I am grateful to Professor P. Allen, University of Reading, who provided valuable advice on heavy minerals. Dr. R. Clements, Leicester University, is acknowledged for providing access to unpublished data.

The appearance of the type-script results from the skill of Mrs. W. Rogers, to whom the author is most grateful.

Finally, I wish to express my gratitude to many friends who helped me directly or indirectly during the course of this study.

UNIVERSITY OF SOUTHAMPTON

ABSTRACT

FACULTY OF SCIENCE

GEOLOGY

Doctor of Philosophy

PETROGRAPHY AND GEOCHEMISTRY OF A LIMESTONE-SHALE SEQUENCE WITH EARLY AND LATE LITHIFICATION: THE MIDDLE PURBECK OF DORSET, ENGLAND.

By Adam El-Shahat

The Middle Purbeck Group (Upper Jurassic-Lower Cretaceous) consists predominantly of limestones and shales of shallow, brackish-water origins. The type-section, Durlston Bay, was investigated and correlations made with other exposures. Samples were studied petrographically, examined by X.R.D., and 200 of these were analysed for 28 elements mainly by X.R.S. Porosities and heavy minerals were studied.

The limestones, the "Purbeck Stone", are mostly bivalve biosparrudites. Bivalve biomicrudites, ostracod biomicrites and charophyte biomicrites also occur. The micrite was calcite mud, often argillaceous; most bivalves were aragonite and this is unchanged in thin shell beds within shales. Partial dissolution has led to precipitation of fibrous calcite or 'beef'. Porosities of biosparrudites increase with increase in aragonite, organic carbon and clay. Calcitized minor evaporites were discovered; calciostrontianite is reported.

Chemistry of the limestones is mostly controlled by clay content and by extent of diagenesis. Sparry calcite contains less Mg than micrite. Some migration of Ni, Fe, Zn, S and organic matter from shales into aragonitic beds has occurred. Manganese contents, however, have apparently undergone little change during aragonite-calcite inversion.

The shales consist of illite with montmorillonite. Kaolinite occurs above the Cinder Beds as do the heavy minerals kyanite and staurolite. The shales have chemical composition similar to the world average. Rubidium, Ba, Sr and Pb substitute for potassium. Zinc, Fe, Ni, Mn, P and organic carbon are relatively enriched in the calcareous shales. Sodium occurs in calcite. The clays have been derived from older marine sediments and there seems to have been a progressive increase in sedimentation rate upwards probably due to increase in rainfall.

Lithification of the biosparrudites, the most common limestones, took place in two major stages. Some were lithified early in vadose conditions. These are uncompacted, and occur as thick beds, occasionally with dinosaur footprints. Most biosparrudites, however, were compacted first and then lithified at a late stage. These, which retain more Sr, and organic matter, occur as thinner beds intercalated in shale sequences. Many characteristics, both chemical and petrographic, of these limestone types are detailed here and criteria given for their recognition.

1. INTRODUCTION

1. General

The middle Purbeck of Dorset is marginal freshwater, brackish and marine limestone-shale facies. Though the general stratigraphy and palaeontology have long been known (see below), relatively little work has been done on the geochemistry and petrography of these rocks. These topics are the subjects of this project.

The objectives of this research were the further understanding of the sedimentary environments and the diagenetic history of the middle Purbeck limestones and shales. These objectives were pursued by integrating systematic petrography, mineralogy and geochemistry in one study. Quantitative methods were used where possible and supplementary studies involve porosity and heavy minerals.

Two-hundred hand specimens were collected from the type-section of Durlston Bay. Vertical spacing of samples was primarily a function of lithology, and averaged a approximately 25 cm. These samples were subjected to all the above mentioned techniques. Additional samples were obtained from the quarries of the Isle of Purbeck (100 samples) and from the cliff sections of the Worbarrow and Lulworth areas (50 samples). These were subjected to petrographic and heavy mineral studies. The location of Dorset samples is given in the chapters 3 – 5. Few samples were obtained from the middle Purbeck outcrops in Wiltshire and Sussex. These samples were used in the heavy mineral study; and their location is given in chapter 10.

2. Summary of previous work

The Purbeck Group in south and south-east England represents a major regression phase at the end of the Upper Jurassic. After the shallow marine sedimentation of the Portland Group, the sea retreated leaving behind series of ephemeral lagoons, lakes and

swamps of varying salinities. At intervals throughout the Purbeck times, the nearby sea invaded this unstable area. As a result of such oscillatory changes, a wide range of sediment types were accumulated. These sediments are well-exposed and well-developed along the sea cliffs and in the quarries of the Isle of Purbeck, Dorset.

The name Purbeck Beds was first employed as a stratigraphic term by Webster in 1816 and the term Purbeck Stone was used by William Smith in 1812 (Woodward, 1895) During the last century, the Purbeck Group of Dorset were described in detail and most of the cliff sections were measured for the first time. These records were based essentially on field observations with little petrographic work. Nevertheless, the lithology and thickness of various strata were accurately determined.

Webster (1816) wrote the first description of the geology of the Isle of Purbeck and made the first geological map of the area. In a later paper (1826) he described the junction of the Portland and Purbeck Groups. Other detailed stratigraphic descriptions followed and include those of Fitton (1835 and 1836), Weston (1848), Forbes (1851), Austen (1852) and Fisher (1856). Forbes (1851, p. 79) divided the Purbeck into upper, middle and lower and found that these divisions are each "marked by a peculiar assemblage of organic remains". Bristow and Fisher (1857) and Bristow and Whitaker (1859) drew up the most detailed Purbeck descriptions of the coast exposures of Dorset.

In 1850, Damon published a "Geology of Weymouth, Portland and the Coast of Dorset" which in the second edition of 1884 contains Bristow's stratigraphic description of Durlston Bay. Woodward (1895) and Strahan (1898), in the first Geological Survey Memoirs dealing with the Isle of Purbeck and Weymouth, summarised the early work and gave more detailed descriptions. These two memoirs together with the memoir by Arkell (1947) remain the standard references on the Purbeck stratigraphy. Apart from

the Geological Survey memoirs, Arkell (1933) described the Purbeck in his classic work "The Jurassic System of Great Britain".

The subdivision of the Purbeck Group has often been a matter of some difficulty and controversy. The lower, middle and upper divisions were split into lithological units by Bristow and Fisher (1857). These units with their traditional names are used in this work. They probably have member status but have not been formally named as members. It seems undesirable to create a host of new names to replace them.

Owing to the absence of ammonites, ostracods have been used for correlation in Purbeck stratigraphy. The earliest attempts were made by Forbes (1851) and Lyell (1855) but it was Jones (1885) who first published detailed descriptions of genera and species. He assigned five species to the lower Purbeck and six to the middle and upper Purbeck. The next account on the Purbeck ostracods was by Strahan (1898) on which all subsequent subdivision was based. Anderson (1941, 1966 and 1971), Sylvester-Bradley (1949) and Clements (1969) pursued ostracod investigations in more detail.

Early petrographic descriptions of some Purbeck rocks dates back to the 1870's. In 1879, Sorby in his address to the Geological Society, mentioned briefly some petrographic features of some Purbeck limestones from the Weymouth area. Other early petrographic information was reported by Teal (Woodward, 1895, p. 233), Watts (Strahan, 1898, p. 98) and Chapman (1906). Chapman's work includes the earliest photomicrographs of some ostracodal limestone from Durlston Bay. More recently, interest in petrography and diagenesis, especially of the lower Purbeck of Dorset, commenced seriously in the 1960's. Diagenesis of the basal Purbeck evaporites have already been discussed by West (1960, 1964, 1965) and Shearman (1966). The petrographic features of some lower and middle Purbeck limestones from Dorset have been described by Brown (1963; 1964;

1966) and Pugh (1969).

Geochemical studies on the Purbeck rocks are extremely rare. Few reports only exist, dealing with palaeosalinities. Boron contents of some Purbeck illite were reported by Walker (1962; 1963), and carbon isotope ratios of a few Purbeck sediments and fossils, mainly from Dorset, were discussed by Allen and Keith (1965).

2. GENERAL STRATIGRAPHY

1. Age of the Purbeck Group

The Purbeck strata are difficult to date because they mostly lack remains of stenohaline organisms. In most early accounts such as those of Webster (1826) and Fitton (1836), the Purbecks were grouped with the conformably overlying Wealden. This was done because of their closely connected 'freshwater' fauna. Later, Forbes (1851), influenced by his discovery of the echinoid *Hemicidaris purbeckensis* in the Cinder Beds in Durlston Bay, classified the Purbeck with the Oolite (Jurassic) and the Wealden with Cretaceous.

The Purbeckian was defined by Arkell (1947) as the youngest of the Jurassic stages. More recently, the Colloquium on Jurassic System held in Lexemburg in 1962, recommended "by general accord, the Purbeckian was considered to be not a stage, but a facies, predominantly freshwater and continental, at the top of the Jurassic, of which a part might overlap into Cretaceous" (Lloyd, 1964). The name 'Purbeck' as a lithostratigraphic term will, nevertheless, remain in general usage.

Casey (1962 and 1963) suggested that the base of the Cinder Beds in the middle Purbeck of southern England, represents the Jurassic/Cretaceous boundary. He renamed the strata below the Cinder Beds the Lulworth Beds and the remainder of the Purbeck, he termed the Durlston Beds. Casey's thesis is, however, an attempt to correlate with the Boreal ammonite realms developed over northern Europe.

The British Mesozoic Committee adopted Casey's suggestions and the Lower Cretaceous was regarded as commencing at the base of the Cinder Beds (in Joffe, 1967). The problem of the Jurassic/Cretaceous boundary is, however, still debatable and the work Anderson (1962 and 1974), Donze and Le Hegarat (1972), Casey and Gallois (1973) and Clements (1973) should be consulted for further information.

Colloq. 1975 (MEM. BRGM. 86)	France du Sud-Est (Le Hegarat 1973)				Angleterre (R. Casey 1963, 1967, 1972)	
					Nord-Est	Sud
VALANGINIAN	VALANGINIEN (*pro parte*)	zone à *Roubaudi* (*pro parte*)		*Thurmanniceras pertransiens* f	*Tollia* cf. *tolmaschowi* *Tollia* cf. *payeri*	
						Hastings Beds
BERRIASIAN	BERRIASIEN	zone à *Boissieri*		*Berriasella (Berriasella) calisto* e	*Peregrinoceras albidum*	
				Berriasella (Picteticeras) picteti	*Surites stenomphalus*	Durlston Beds
				Malbosiceras paramimounum d	*Hectoceras kochi*	
		zone à *Occitanica*		*Dalmasiceras dalmasi* c	*Runctonia runctoni*	Cinder Bed
				Berriasella (Berriasella) privasensis b		
				Tirnovella subalpina		
		zone à *Grandis*		*Pseudosubplanites grandis* a		
TITHONIAN	TITHONIQUE	supérieur	zone à *Jacobi*	*Berriasella (Berriasella) jacobi*	*Subcraspedites* spp.	Lulworth Beds (*Fabanella ansata*)
			?			
			zone à *Transitorius*	« Calcaire blanc vocontien » *pro parte*		
				(Niveau du Chouet)		
		inférieur (*p. parte*)	zone à *Ciliata*	(niveau de Saint-Concors)	*Paracraspedites* spp. *Titanites giganteus*	Portland Stone
				(niveau du Pouzin)	*Glaucolithites gorei*	Portland Sand
					Zaraiskites albani	

RYAZANIAN

PURBECK BEDS

Table 1. Tentative correlation of the British Purbeck succession with the ammonite bearing marine sequences in south-east France (modified from Demboska and Marek, (1975)). Majority opinion at the Colloquium at Lyon in 1973 (Anon., 1975), was that the Tithonian-Berriasian boundary should be placed at the base of *Jacobi/Grandis* zones. This position is shown as an addition to the left of this table.

At the time of writing, an internationally-recognised marker point for the Jurassic/Cretaceous boundary has not been selected but at a recent colloquium (Anon., 1975) a location in south-east France was advocated. Majority opinion was that the base of the Berriasian should be the Jurassic/Cretaceous boundary and that the Berriasian should commence at the base of the *Jacobi/Grandis* zone (Table 1). Casey (p. 388 in Anon., 1975) suggested that only the *Boissieri* zone should be included in the Berriasian and on that basis it would be more likely that the Cinder Beds would represent the Jurassic/Cretaceous boundary in south England. If the base of the Berriasian is the base of *Jacobi/Grandis* zone, then most or all of the Purbeck Group will perhaps prove to be Cretaceous (see Table 1).

Throughout the present project, the traditional Purbeck terminology given by Bristow and Fisher (1857) and Bristow and Whitaker (1859) is retained. Since the terms upper, middle and lower are only for informal use (Harland *et al.*, 1972) and following some acceptance of Casey's divisions (Townson, 1975), the base of the Cinder Beds is considered as a boundary to the Durlston and Lulworth Formations, which constitute the Purbeck Group.

2. Outcrops in Southern England

The Purbeck Group outcrops in Dorset, Wiltshire, Buckinghamshire and Sussex and is known from subsurface data in Kent and Hampshire. The Purbeck Group reach their maximum thickness in central Kent and thin to the west of Dorset and also to the north around Oxford and Swindon (Fig. 1). The isopachyte maps of the Purbeck Group reveal the presence of two basins, one to the west in Dorset and the other to the east in Sussex and Kent, (Howitt, 1964). According to Howitt a north-west to south-east ridge extending from Portsdown to Winchester formed a shallow area between the two basins. Purbeck strata also outcrop in the English Channel (Anon., 1974, and several papers in Lyon Colloquium – Anon., 1975).

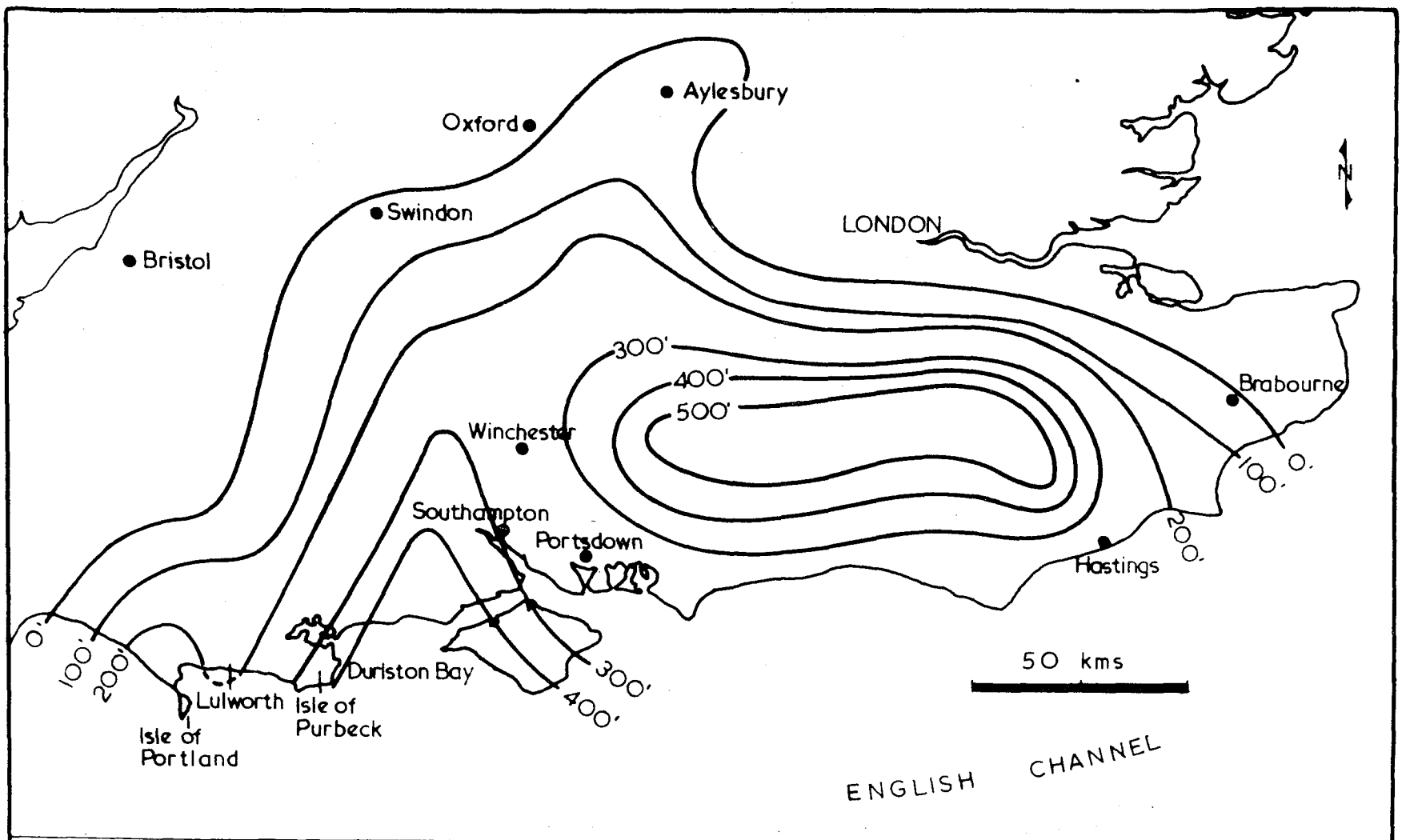

Fig 1 Isopachyte Map of the whole of the Purbeck Group. (after Howitt 1964) Contours at intervals of 100 feet.

The Dorset outcrops (Fig. 2) are the most extensive, occurring from Portesham in the west to Durlston Bay in the east, a distance along the strike of about 40 kms. They also outcrop on the Isle of Portland to the south. In Durlston Bay, the Purbeck Group attains a thickness of 121 m. They become thinner westwards (89 m. at Worbarrow), decreasing rapidly near Lulworth (55 m.), but become thicker again (58 m.) at Ridgeway.

The thicknesses of the Purbeck subdivisions, measured by Bristow and Fisher (1857), and converted into metres are as follows:-

Purbeck Beds	Durlston	Worbarrow	Mupe	Lulworth	Ridgeway
upper	18.5	15.0	15.4	8.4	15.0
middle	50.9	27.6	17.5	16.9	15.8
lower	51.7	46.3	43.3	29.4	26.9
Total	121.1	88.9	76.2	54.7	57.7

The tectonic thinning of the clays and shales especially at the west side of Lulworth Cove and Stair Hole recorded by Woodward (1895, p. 257) is one of the factors which influence the thickness values. Also the removal of unknown quantities of gypsum by solution and the differential degrees of subsequent calcitization represent another limitation. Lack of continuous exposures in sections due to tectonic disturbance makes accurate measurements more difficult to obtain.

3. Divisions of the Purbeck Group in Dorset

It is not easy to subdivide the Purbeck Group or to correlate the subdivisions in different parts of England. Lithologically there is little by which to be guided, for the many types of rocks alternate rapidly in short distance (Arkell, 1933). Forbe's divisions of upper, middle and lower in Dorset, except as a matter of local convenience are of little value, for with the exception of the Cinder Beds, there are no obvious lithologic

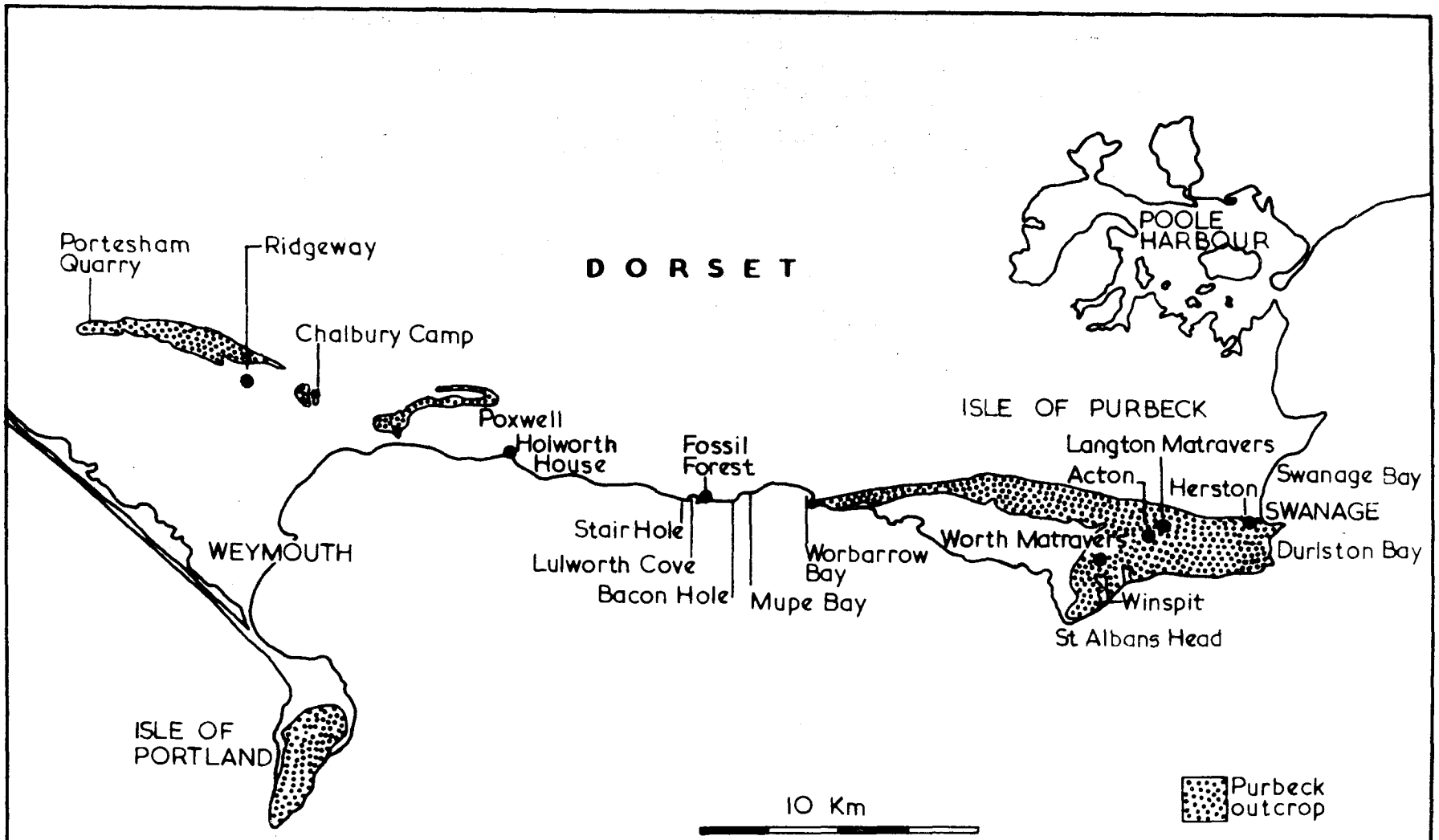

Fig 2. Purbeck outcrop in Dorset.

units nor significant palaeontolpgical breaks of any distinctive character (Casey, 1963). The Purbeck stratigraphy in Dorset is given in Table 2, with the ostracod zones of Anderson (1974).

Table 2

Purbeck stratigraphy and ostraced zone

Formations	Informal divisions	Strata in Durlston Bay	Cypridean. zones
Durlston Formation	upper	Upper *'Cypris'* Clays and Shales *Unio* Beds Upper Broken Shell Limestone	*C. setina*
	middle	Chief Beef Beds *Corbula* Beds Scallop Beds Intermarine Beds Cinder Beds Cherty Freshwater Beds	*C.g. fascicula*
Lulworth Formation		Marly Freshwater Beds Soft Cockle Beds Hard Cockle Beds	*C.g. granulosa*
	lower	*'Cypris'* Freestone Broken Beds Hard and Soft Caps	*C. dunkeri*

The base of the upper Purbeck is marked by the Upper Broken Shell Limestone consisting of about 3 metres (at Durlston Bay) of massive, creamy-grey porous bio-sparrudite, largely made up of *Neomiodon* shell fragments. The present work follows the traditional usage of the Mammal Bed as middle/lower boundary as originally used by Fisher (1856) and most of the early workers. Only at Durlston Bay, is it possible to locate the middle/lower boundary on the basis of Mammal Bed; elsewhere it is difficult to recognise. The boundary was taken at approximately a level 2–4 metres below the 'Flint Bed'; a bed which is easily recognised along the cliff sections.

4. Structure

The dominant structures affecting Portland and Purbeck Groups, exposed on the coast between the Weymouth area and Durlston Bay is the Weymouth-Purbeck anticline. Although this generally consists of two folds with axes 'en echelon', they can be regarded in simple terms as an eastward plunging assymetrical fold. The north limb of the anticline is much steeper and is seen in the coastal exposures between Durlston Bay and Durdle Door. The southern limb has been for the most part destroyed by the sea, but fragments still survive in the Isle of Portland. The southern limb is inclined at 1° and 3° while the northern limb dips at about 20°N. on the Isle of Purbeck and at about 40°N. north of Weymouth. In the central area between Mupe Bay and Durdle Door, the northward dip of the exposed Portland Group increases to 80°N. and the overlying Purbeck and Wealden strata are overturned to the north in many places (Phillips, 1964).

Smaller-scale structures associated with the main Weymouth-Purbeck anticline are the adjustment folds or 'crumples' which are well-exposed in the Lulworth area. Inland, the structures are further complicated by Intra-Cretaceous faulting and folding. For detailed accounts on the tectonic structures refer to Arkell (1938 and 1947), House (1961), and Ridd (1973).

3. FIELD RELATIONSHIPS – DURLSTON BAY

Most aspects of this research, petrology, mineralogy or chemistry, were concerned with the Durlston Bay section which receives most attention in this account. The middle Purbeck Group was extensively sampled and studied. As a foundation for this specialised investigation, the detailed and carefully measured section given by Clements (1969) was used, each bed from the Mammal Bed DB 83 to bed DB 219 was sampled (Fig. 3). Additional information was obtained from the bed-by-bed description of Durlston Bay given by Fisher (1856).

Durlston Bay provides the thickest exposed section of the Purbeck Group in this country. The lower boundary of the Purbeck Group with the Portland Group is isolated from the main section and confused by faulting. The junction of the Purbeck and Wealden strata is, however, concealed by the town and harbour of Swanage. Nevertheless, Durlston Bay has long been regarded as the type section of the Purbeck Group.

Durlston Bay has been formed largely by the erosion of the soft marls of the lower Purbeck Group. The hard Portland Stone at Durlston Head, and the limestone of the upper Purbeck Group at Peveril Point form headlands and 'reefs'. Small projections along the coast are produced where the stone bands descend to the sea-level and run out in ledges. At Durlston Bay the Purbeck Group are successively displayed in the cliffs and reach sea-level due to the inclination of the strata (see Figs. 4 & 5). This makes the section convenient for examination and sampling.

The continuity of the beds is disturbed by several faults. Those at Durlston Head are mentioned above. In the middle of the bay at the Zig Zag Path a considerable fault has thrown most of the middle against the lower Purbeck Group. At Peveril Point the beds are more disturbed by complicated folding and faulting of small amplitude (Cosgrove and

Hearn, 1966).

The middle Purbeck starts with the Mammal Bed (Fig. 6). It was the mammalian fauna (Owen, 1871 and Simpson, 1928) obtained from the Mammal Bed, which has made Durlston Bay world-famous. Moreover, Arkell (1933) regarded the Mammal Bed as the most important in the Jurassic System to the vertebrate palaeontologist. The boundary between the Marly Freshwater Beds and Cherty Freshwater Beds occurs at a level of 1.4 metres above the Mammal Bed.

The Cherty Freshwater Beds include the 'Feather Beds' (DB 108) which were formerly worked in the cliff, Woodward (1895, p. 251). Another important bed in this series which was reported by Woodward is the 'Flint Bed' (DB 97); a white-cream biomicrite with black chert nodules (Fig. 7). This 'Flint Bed' can be traced into the Weymouth area. Another bed in the Cherty Freshwater Beds is DB 101 or the 'New Vein' as it was known amongst the quarrymen.

The Cherty Freshwater Beds are overlain by the Cinder Beds, the most easily recognised beds in the Purbeck Group (Fig. 8). The Cinder Beds are very useful as a guide for fixing the position of the strata when they are disturbed. Above the Cinder Beds come the Intermarine Beds or Upper Building Stone (Figs. 9 & 10). These beds have been quarried in the cliffs as indicated by old excavations and tunnels; some still remain, especially in the upper part of the Intermarine Beds and, particularly in the 'White Roach' and 'Leaning Vein' (DB 144). No dinosaur footprints have been reported in the Intermarine Beds here although they frequently are recorded in the inland quarries, near Swanage (Delair and Lander, 1973 and Sarjeant, 1974).

Two important beds in the *Corbula* Beds, are worth a passing mention. The first, at the base of the *Corbula* Beds, is composed of calcareous sandstone (DB 157).

This is a good marker bed and can be traced to Lulworth area and Ridgeway. The second bed occurs near the top of the *Corbula* Beds, a massive grey and pinkish bivalve biomicrudite and biosparrudite with thin micrite seen in the middle (DB 183). This bed is also known as 'Toad's Eye Limestone' and two large tridactyl markings on its surface have been found (Jones, 1885, p. 323).

The Chief Beef Beds are the highest beds in the middle Purbeck Group. They are represented by dark shales and clays with layers of crushed, perished shells of *Neomidon,* formerly known as *Cyrena* (Arkell, 1947). Throughout this work these layers are termed 'perished bivalves'. The terms 'Beef' and 'Horse Flesh' were originally applied by the quarrymen to thin layers of fibrous calcite which represent a type of cone-in-cone structure. The "crystals of this mineral are usually shooting upwards from a band of perished bivalves" (Fisher, 1856, p. 559). The highest bed in the Chief Beef Beds (DB 219) shows faulted and folded layers of 'Beef' (Fig. 11).

The base of the upper Purbeck Group is represented by the Upper Broken Shell Limestone (DB 220) or 'Soft Burr' as it is known amongst quarrymen. These beds were also known as 'Comminuted Shell Limestone' or 'Marble Rag' (Fisher, 1856).

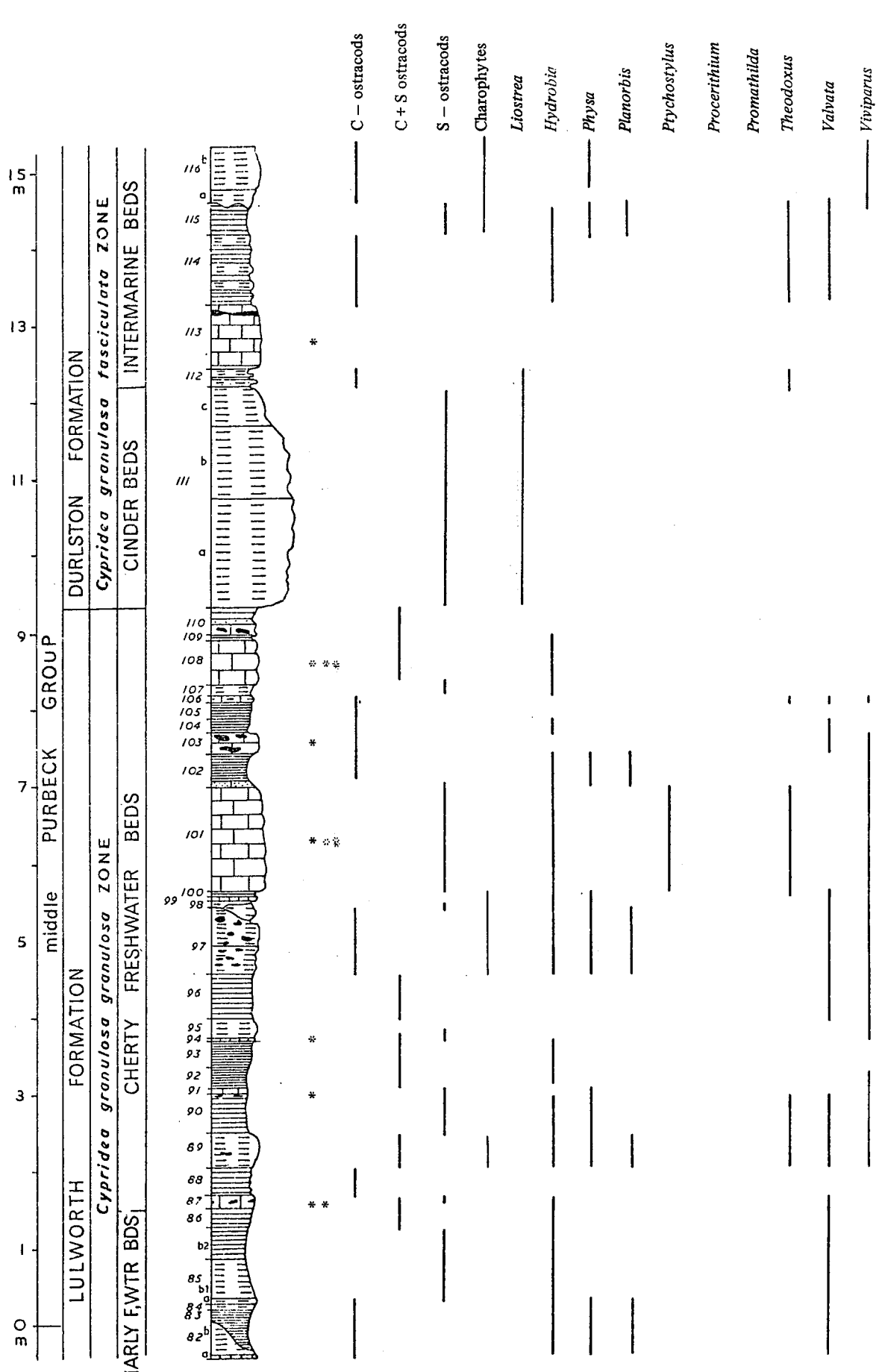

Fig. 3 Stratigraphic section of the middle Purbeck succession at Durlston Bay with summary of the fauna, based on Clements (1969) with modification to the stratigraphic log. Ostracod zones are those given by Anderson (1974). C-ostracods are dominated by the genus *Cypridea;* S-ostracods are mainly represented by other genera (*c.f.* Anderson *et al.*, 1967). For key see Fig. 15. Additional diagenetic data as follows: ★unlithified "perished bivalves"; * Type 1 biosparrudites, late lithified; ** Type 2 biosparrudites, intermediate; *** Type 3 biosparrudites, early lithified.

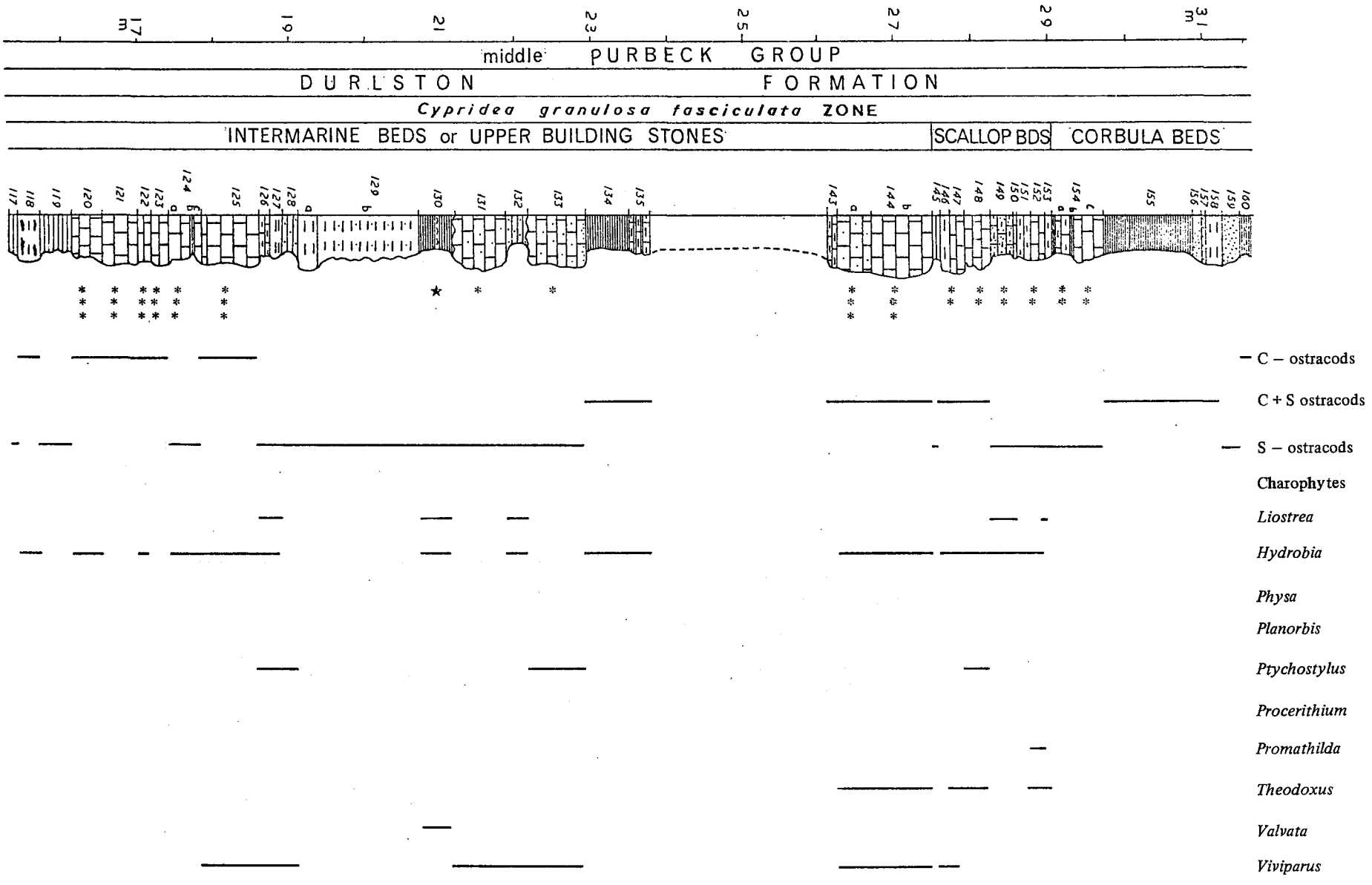

Fig. 3. Continued

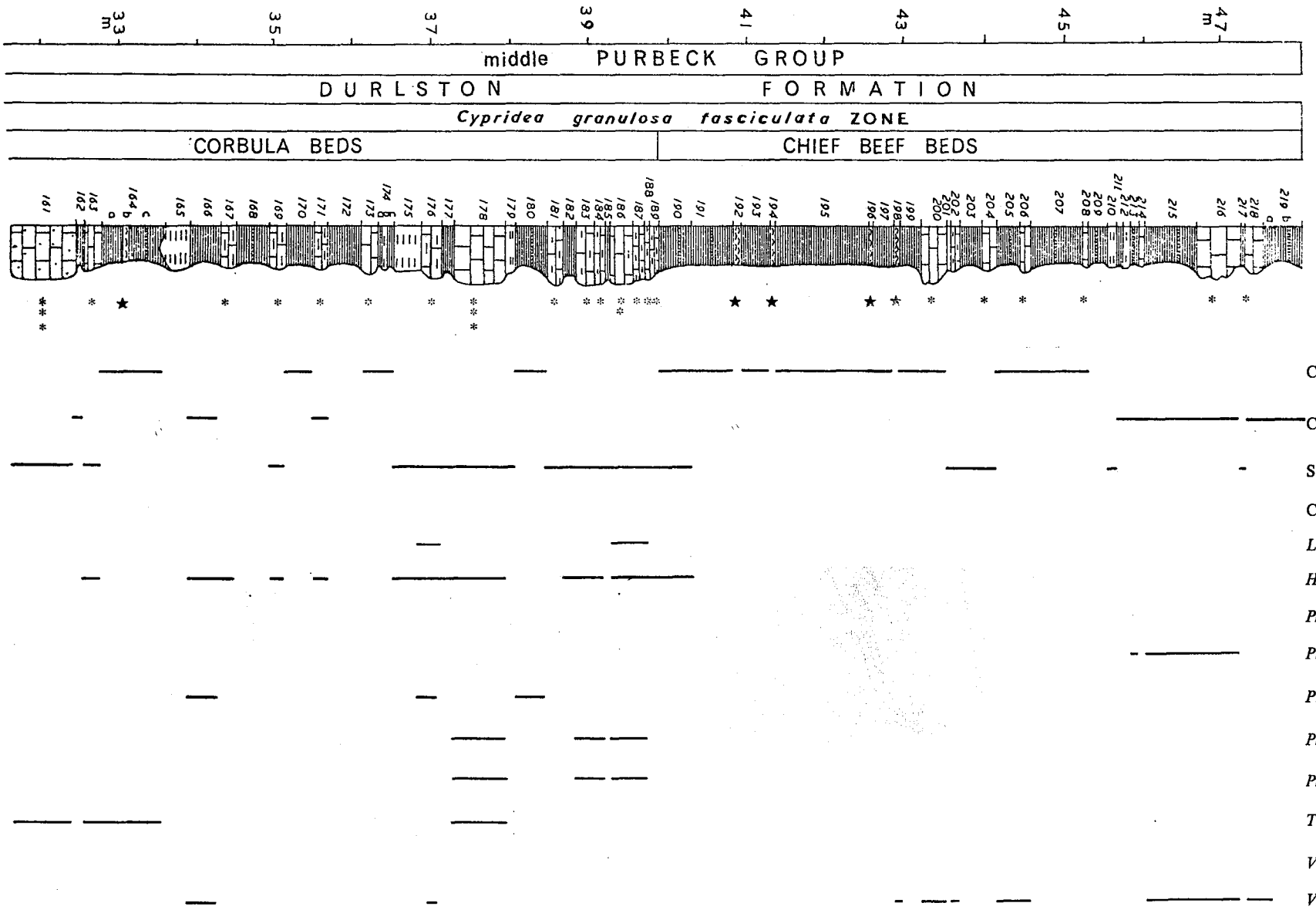

Fig. 3. Continued

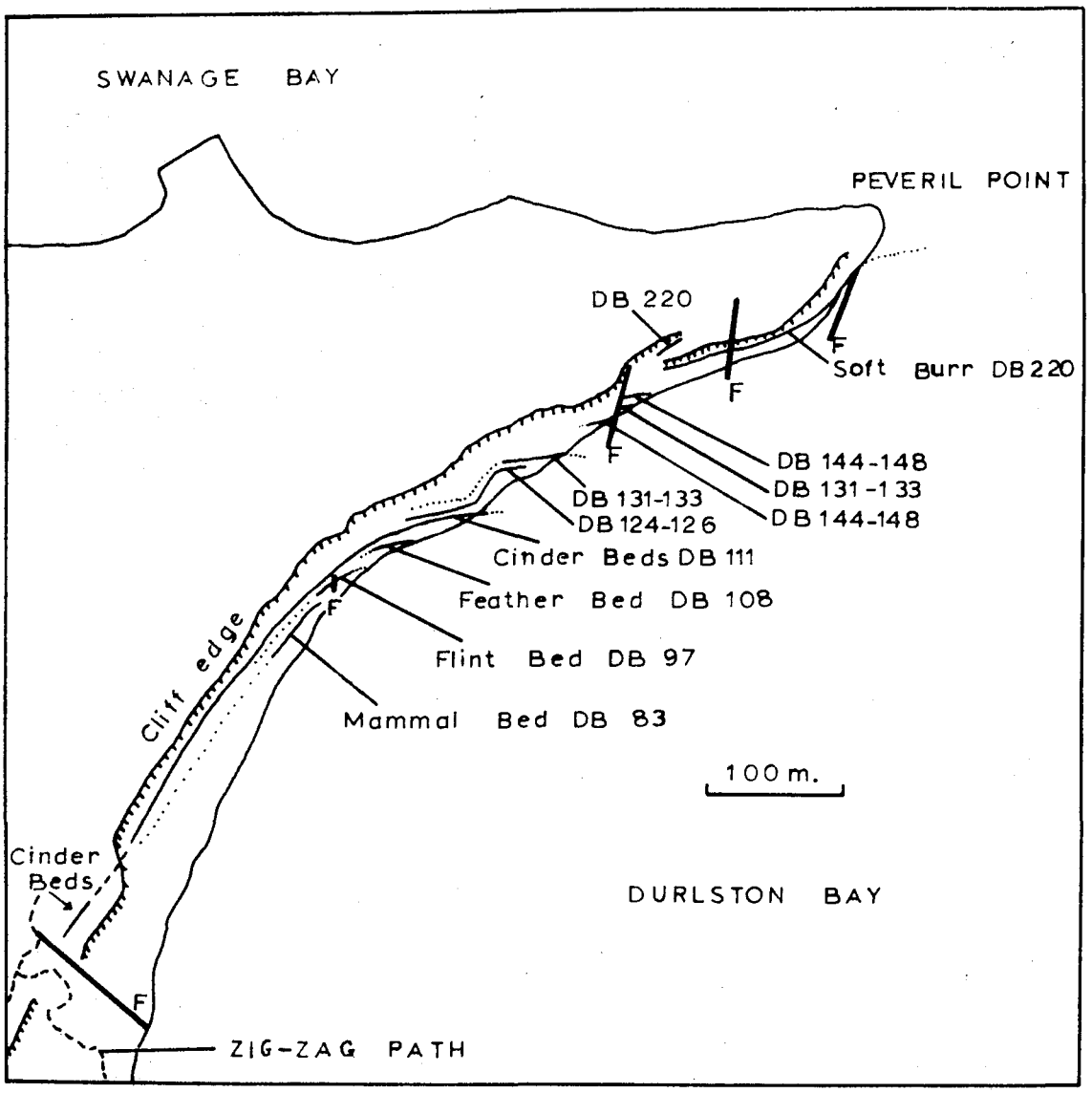

Fig. 4. Map of the northern half of Durlston Bay.

Fig. 5. General view of middle and upper Purbeck of Durlston Bay (looking N.E. towards Peveril Point).

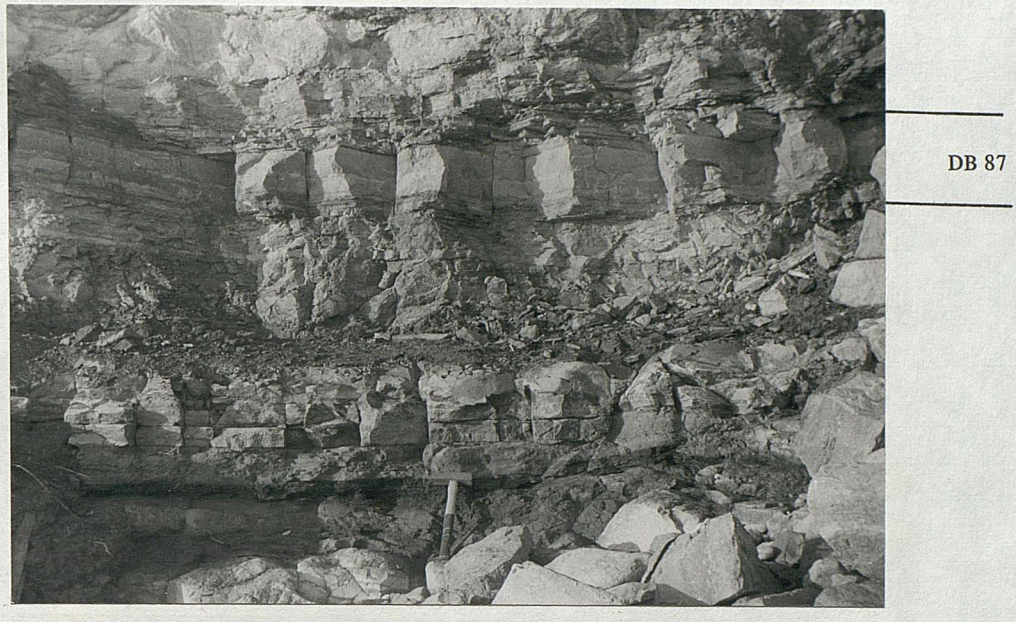

Fig. 6. Junction of lower and middle Purbeck, the hammer is on carbonaceous shale (bed DB 83; Mammal Bed) which represents this junction. The base of bed DB 87 is the boundary between Marly Freshwater Beds and Cherty Freshwater Beds. Durlston Bay.

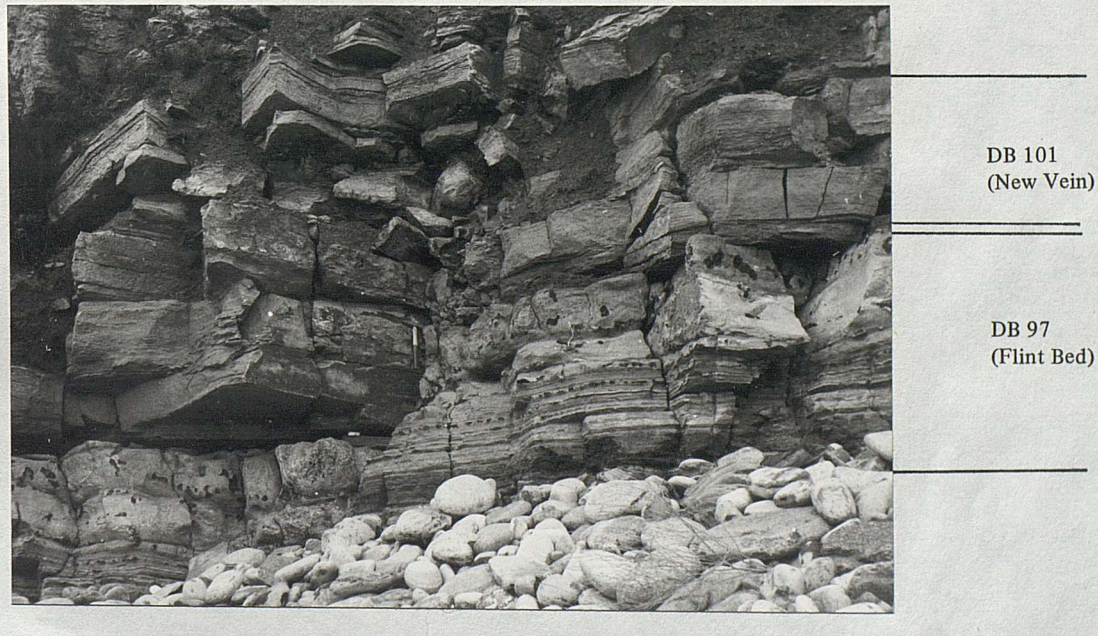

Fig. 7. Small fault in the Cherty Freshwater Beds

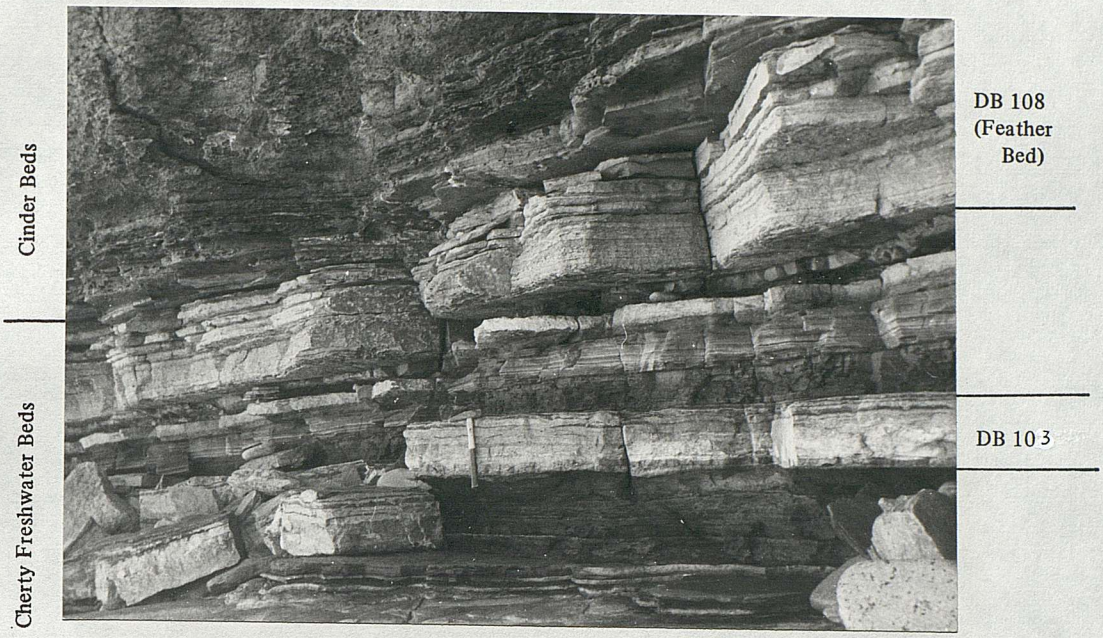

Fig. 8. Cherty Freshwater Beds and Cinder Beds at Durlston Bay.

Fig. 9. Intermarine Beds showing the uniform parallel bedding. Durlston Bay.

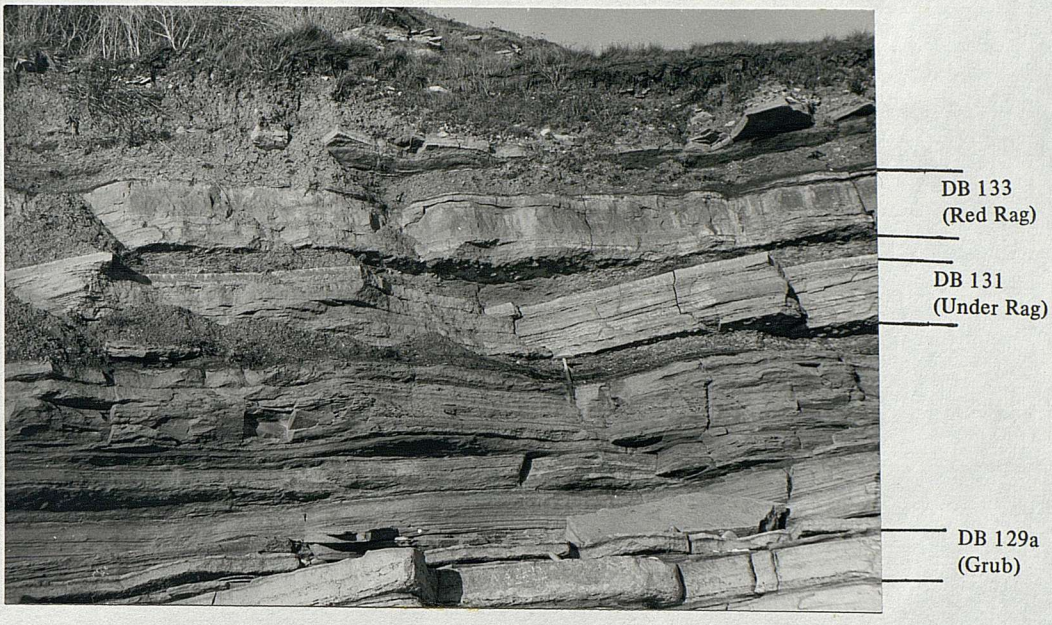

Fig. 10. Details of the Intermarine Beds showing the uniform parallel bedding. Hammer on bed DB 130 Durlston Bay.

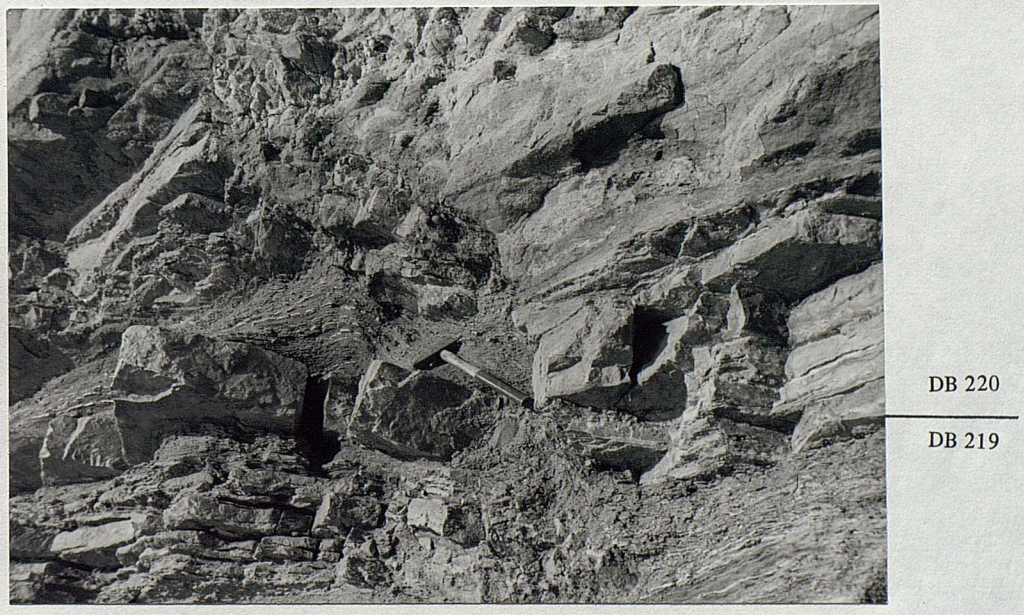

Fig. 11. Junction between upper and middle Purbeck. Hammer on the uppermost bed (DB 219) of the middle Purbeck. Note the folded and faulted 'beef' layers in bed DB 219. Durlston Bay.

4. FIELD RELATIONSHIPS – WORBARROW TO STAIR HOLE [1]

1. Worbarrow Bay

The Purbeck Group are well-exposed in the cliffs at the south-eastern sides of Worbarrow Bay, on both sides of the headland known as Worbarrow Tout. The middle/lower Purbeck boundary was approximately determined because the Mammal Bed which is considered to be the base of the middle Purbeck is difficult to recognise at Worbarrow Tout.

The upper/middle Purbeck boundary was taken as the base of the Upper Broken Shell Limestone. The measured succession of the middle Purbeck Group at Worbarrow Tout is correlated with Durlston Bay (Figs. 12, 13 and 14). The following section represents the measured strata:

Bed	At the top	metres
76b	Dark shale with 'beef' and thin limestone bands at the base	0.32
76a	Dark shale with thick and folded 'beef'	0.29
75	Grey, hard bivalve limestone	0.30
74	Alum shale with 'beef'	0.20
73	Grey biomicrite	0.10
72c	'Beef' with thin shale parting	0.15
72b	Band of perished bivalves	0.08
72a	Grey, papery shale with 'beef'	0.40
71d	Rubbly, sandy, bivalve limestone with ripple marks	0.80
71c	Grey micrites	0.06
71b	Pink, thin-laminated, bivalve limestone	0.07
71a	Grey, massive, biomicrite with thin 'beef' layer at the base	0.12

[1] Samples from localities described in this chapter were subjected to petrographic and heavy mineral studies (Chapters 8–10)

Bed		Metres
70	Grey nodular biomicrite	0.20
69	Pink, rubbly and sandy, bivalve limestone	0.07
68c	Grey micrites with conchoidal fractures	0.07
68b	Grey micrites with algal lamination, calcite pseudomorphs after gypsum.	0.12
68a	Bivalve limestone	0.22
67	Thin shale with 'beef'	0.05
66	Hard, pink, bivalve biosparite	0.28
65	Black shale with yellow weathering and thin layer of 'beef' at the base	0.20
64	Rubbly, sandy, argillaceous, thin-bedded limestone	0.40
63	Friable, rubbly, sandy, grey micrites with thin bands of biosparite, burrows and algal lamination	0.44
62	Hard, pink, biosparite rich in *Corbula*, rubbly and sandy at the base	0.22
61	Friable, grey, sandy and rubbly limestone with thin bands of 'beef' and perished bivalves	0.22
60	Grey micrites with conchoidal fractures	0.40
59	Black shales	0.06
58	Hard, grey, bivalve limestone, highly micritic near the base	0.11
57c	Black weathered shale with 'beef'	0.18
57b	Band of perished bivalves	0.05
57a	Alternating weathered shale and 'beef'	0.15
56b	Grey, rubbly, sandy limestone, burrows	0.16
56a	Grey, rubbly micrites	0.20
55	Weathered shale with 'beef'	0.35

Beds		Metres
54	Grey micrites with vertical fractures	0.14
53	Weathered shale	0.50
52	Calcareous sandstone, vertebrate remains and burrows, the upper surface shows ripple marks and limestone pebbles.	0.10
51	Highly bioturbated, grey, calcareous sandstone	0.20
50	Earthy, sandy, argillaceous limestone	0.15
49	Pink, sandy, rubbly, bivalve limestone	0.14
48	Grey, sandy, rubbly, argillaceous limestone and calcareous shale with *'Pecten'* and micrite lenses and bioturbation	0.50
47	Shale	0.08
46	Hard, massive, sandy, bivalve biosparite rich in *'Pecten'*, *Corbula* and gastropods	0.11
45	Grey, sandy, rubbly limestone with *'Pecten'* and micrite lenses	0.30
44	Black, calcareous shale	0.18
43	Pink, sandy, bivalve limestone, rubbly near the top, *'Pecten'*, burrows and micrite lenses	0.25
42	Grey, calcareous shale with micrite nodules	0.08
41c	Pink, massive, hard, bivalve biosparite, joints filled with pyrite	0.75
41b	Pink, sandy, rubbly limestone, cross-lamination and ripple marks	0.46
41a	Pink, hard limestone	0.11
40	Grey, rubbly, friable limestone and shale	0.21
39c	Grey, argillaceous micrites with vertical fractures	0.33
39b	Grey, rubbly, rough, argillaceous biomicrite	0.07
39a	Grey, argillaceous micrite	0.17
38	Thin-laminated, bivalve limestone	0.05

Bed		Metres
37d	Grey, earthy, friable calcareous shale with 'beef'	0.15
37c	Black, papery shale with bands of perished bivalves and 'beef'	0.28
37b	Bivalve limestone with small phosphate nodules	0.08
37a	Black, papery shale with 'beef' and bands of perished bivalves	0.60
36	Grey, massive, sandy, bivalve limestone in two units, *Liostrea* fragments, limestone pebbles on the upper surface	0.60
35	Friable, sandy, bivalve limestone, ostracods	0.20
34	Argillaceous micrites	0.08
33	Pink, thin-laminated, bivalve limestone in two units	0.35
32	Black, papery shale and ostracod limestone	0.20
31	Massive, grey biomicrite with some silicification	0.18
30	Argillaceous micrite	0.20
29	Grey, bivalve limestone with wavey surface, charophytes?	0.18
28	Argillaceous micrites and shales with vertebrate remains	0.14
27b	Hard, pink, bivalve biosparite	0.80
27a	Grey, rubbly, bivalve limestone with thin layer of 'beef' at the top	0.13
26	Cinder Beds, *Liostrea distorta*	2.10
25	Shale, poorly exposed	0.24
24	Earthy, grey biomicrites, ostracods, gastropods, some silicification and desiccation cracks	0.30
23	Shale	
22b	Biomicrite rich in charophytes and chert nodules. The top 10 cm. are made up of bivalve biosparite	1.12
22a	Calcareous shale and micrite with chert nodules	0.20

Beds		Metres
21	Grey, massive biomicrite, silicified near the top	0.41
20	Laminated, argillaceous charophyte biomicrite	0.20
19	Hard micrites	0.30
18	Thin-laminated, argillaceous micrites and shale	0.11
17	Argillaceous, ostracod biomicrite, bioturbation	0.38
16	Hard, grey, ostracod biomicrite	0.10
15	Alternating shale and ostracod limestone	0.15
14	Pink, ostracod, biosparite with small chert nodules	0.05
13	Alternating calcareous shale and thin-laminated argillaceous limestone	0.14
12	Alternating shale and limestone	0.16
11	Calcareous shale, poorly exposed	0.40
10	Argillaceous, ostracod biomicrite with shale parting	1.12
9	Calcareous shale	0.23
8	Argillaceous micrite	0.17
7	Alternating thin-laminated ostracod limestone and shale	0.13
6	Hard, pink, ostracod limestone, highly silicified, celestite	0.20
5	Calcareous shale, poorly exposed	0.53
4	Argillaceous, ostracod biomicrite	0.29
3	Argillaceous, micrite and shale	0.50
2	Argillaceous micrite	0.15
1	Calcareous shale grades into argillaceous micrite	0.80

2. **Bacon Hole** (Figs. 12, 13 and 14)

The complete Purbeck section from the Wealden to the Portland Stone occurs at Mupe Bay and Bacon Hole. The following account represents the middle Purbeck Group. The lower/middle Purbeck boundary occurs near the end of the following list.

Bed	At the top	Metres
48	Shale with layers of 'beef' and perished bivalves	1.41
47	Bivalve biosparite	1.02
46	Laminated, argillaceous micrites and mudstone	0.41
45	Pink, bivalve biosparite, rubbly at the base	0.19
44	Shale with layers of 'beef' and perished bivalves	0.31
43	Grey, sandy biomicrite	0.22
42	Calcareous mudstone, well-laminated at the base	0.30
41	Pink, bivalve biosparite	0.07
40	Argillaceous micrite grades into biosparite	0.38
39	Hard, pink, bivalve biosparite	0.28
38	Shale with 'beef'	0.21
37	Massive, argillaceous micrites	0.24
36	Alternating limestone and shale with 'beef'	0.15
35	Biomicrites with algal lamination	0.24
34	Alternating shale and 'beef'	0.35
33	Micrites with vertical cracks	0.10
32	Grey, calcareous sandstone, highly bioturbated	0.53
31	Calcareous, sandy shale	0.40
30	Argillaceous, rubbly, sandy limestone	0.14

Bed		Metres
29	Pink, massive, bivalve biosparite, rich in *Corbula* and gastropods	0.10
28	Grey, argillaceous, rubbly, sandy limestone with *'Pecten'* and *Liostrea*	0.10
27	Shale	0.12
26	Pink, rubbly, bivalve limestone, cross-lamination	0.79
25	Calcareous mudstone	0.36
24c	Shale with 'beef' and thin bands of perished bivalves	0.30
24b	Perished bivalves	0.05
24a	Calcareous shale with 'beef' and perished bivalves	0.41
23	Earthy, sandy, calcareous mudstone with *Liostrea*	0.28
22c	Sandy, argillaceous limestone	0.18
22b	Shale	0.12
22a	Sandy, earthy, argillaceous, rubbly, friable, bivalve limestone	0.16
21	Grey, calcareous, friable clays with thin sandy limestone at the base	0.31
20	Argillaceous, ostracod biomicrite	0.13
19	Earthy, rubbly, argillaceous biomicrite, desiccation cracks	0.16
18	Bivalve biosparite	0.13
17	Earthy, rubbly limestone with 'beef' and gypsum	0.12
16	Cinder Beds, *Liostrea distortata*	1.30
15	Brown shale and thin, ostracod limestone	0.42
14	Thin-laminated, bivalve biosparite with vertebrate remains mainly turtles	0.10
13	White, massive, charophyte biomicrite with chert nodules and chalcedony pseudomorphs after halite	0.82

Bed		Metres
12	Calcareous shale, poorly exposed	0.19
11	Massive, hard limestone, abundant ostracods and gastropods	0.35
10d	Earthy, calcareous clays with thin bands of perished bivalves	0.12
10c	Calcareous shale with perished bivalves	0.08
10b	Ostracod biomicrite	0.15
10a	Calcareous shale	0.12
9	Hard, grey micrites	0.29
8	Grey, laminated, argillaceous, ostracod biomicrite	0.16
7	Alternating shale and ostracod biomicrite with very small chert nodules at the base	0.35
6	Ostracod biomicrite	0.17
5	Black, calcareous shale	0.12
4	Green, argillaceous biomicrite in two units	1.30
3	Calcareous shale	0.30
2	Argillaceous micrite	0.20
1	Calcareous shale	0.31

3. Lulworth Area

The middle Purbeck succession was measured at Stair Hole. At Lulworth Cove, the east side, only the strata below the Cinder Beds were measured. Correlations with the other middle Purbeck outcrops at Durlston Bay and at Ridgeway are shown in Figs. 12, 13 and 14. The correlation indicates local thinning in most of the facies of the Lulworth area. The 'Mid-Dorset Swell' (of Drummond, 1970; Townson, 1975; West, 1975) which affected sedimentation from Portland to Upper Cretaceous times seems to have influenced facies distribution during de-

position of the middle Purbeck strata.

(a) **Lulworth Cove** (Fig. 12)

Bed	At the Top	Metres
21	Cinder Beds, *Liostrea distorta*	1.20
20	Alternating shale and thin-laminated limestone, turtle remains and small phosphate nodules	0.48
19	Pink, bivalve biosparite	0.05
18	Massive, charophyte biomicrite with chert nodules	0.73
17	Earthy, argillaceous micrite and shale with small chert nodules	0.12
16	Earthy, friable biomicrite with small white concretions	0.25
15	Calcareous clays with perished bivalves	0.20
14	Grey biomicrite	0.16
13	Calcareous mudstone	0.19
12	Hard, grey micrite	0.30
11	Alternating argillaceous micrite and calcareous mudstone	0.25
10	Calcareous shale and thin, laminated ostracod micrite	0.13
9	Grey, ostracod biomicrite	0.18
8	Shale and thin-laminated micrite	0.08
7	Laminated, calcareous mudstone	0.18
6	Soft micrite	0.46
5	Hard, grey micrite in two units; near the top there is a band of fish scales, burrows	0.73
4	Brown, calcareous mudstone	0.30
3	Grey, argillaceous micrite	0.35

Bed		Metres
2	Calcareous clays, poorly exposed	0.15
1	Grey, argillaceous micrite	0.35

(b) **Stair Hole** (Figs. 12, 13 and 14)

Bed	At the top	Metres
57	Weathered shale with 'beef'	0.60
56	Shale with 'beef' and thin micrite layers	0.20
55	Pink and hard, bivalve limestone	0.16
54	'Beef'	0.10
53	Friable, sandy limestone	0.30
52	Hard, grey, bivalve biosparrudite	0.95
51	Alum shale, poorly exposed	0.56
50b	Hard, grey biosparite	0.16
50a	Earthy, bivalve biomicrite	0.37
49	Alum shale with 'beef'	0.15
48	Grey micrite with algal lamination	0.27
47	Pink, sandy biosparite	0.15
46	Alum shale, poorly exposed	0.65
45	Thin-laminated biomicrite grades into biosparite, algal lamination	0.16
44	Shale	0.06
43	Grey micrite	0.45
42b	Sandy mudstone	0.13
42a	Black, sandy clay with thin, hard, grey biosparite band near the top	0.15

Beds		Metres
41b	'Beef'	0.10
41a	Alum shale with very thin bands of perished bivalves	0.42
40	Bivalve limestone	0.08
39	Hard, grey micrite	0.18
38	Alum shale with 'beef'	0.38
37	Brown, calcareous sandstone, burrows	0.63
36	Alum shale with 'beef', poorly exposed	0.90
35	Grey, calcareous mudstone, burrows are abundant at base	0.21
34	Pink, bivalve biosparite, *Corbula*	0.14
33	Brown, sandy limestone, *'Pecten'*	0.06
32	Blue, sandy clays with *'Pecten'* and *Liostrea*	0.10
31	Brown, sandy friable clays with *'Pecten'*	0.12
30c	Pink biosparite, *Corbula,* cross-lamination	0.18
30b	Hard, pink, bivalve biosparite, cross-lamination	0.30
30a	Pink, hard, sandy biosparite grades into biomicrite, algal lamination near the base	0.23
29	Earthy, calcareous clays	0.07
28	Hard, grey, mottled micrite, shale parting, bioturbation	0.59
27d	Alum shales with thin limestone bands	0.37
27c	Hard, bivalve limestone	0.07
27b	Alum shale stained with iron oxides	0.19
27a	Earthy, calcareous shale, and clays, thin bands of perished bivalves , 'beef'	0.48
26	Grey, mottled micrite, burrows and rootlets	0.65

Beds		Metres
25	Calcareous mudstone with a thin band of bivalve limestone	0.13
24	Earthy, sandy biomicrite	0.15
23	Hard, grey, bivalve biosparite	0.21
22	Earthy, argillaceous micrite with thin 'beef' layers	0.06
21	Grey, mottled micrite, desiccation cracks, burrows	0.53
20	Thin-laminated limestone and shale, thin 'beef' near the base, desiccation cracks	0.15
19	Cinder Beds, *Liostrea distorta*	1.00
18	Alum shale with thin limestone bands near the base	0.51
17	Pink, bivalve biosparite	0.05
16	Earthy charophyte biomicrite with chert nodules, desiccation cracks near the top	0.72
15	Shale with small chert nodules	0.50
14	Thin laminated, argillaceous micrite and clays	0.18
13	Very hard, grey micrite	0.20
12	Black, papery shale	0.06
11	Argillaceous micrite and shale	0.15
10	Thin-laminated, ostracod biomicrite and shale, desiccation cracks	0.22
9	Green and grey argillaceous micrite with shale parting	0.25
8	Thin ostracod limestone and shale, small chert nodules near the base	0.20
7	Argillaceous micrite with thin (5 cm) earthy limestone band at the top	0.35
6	Grey, friable argillaceous micrite with vertical cracks	0.60
5	Grey, hard micrite	0.55

Beds		metres
4	Black shale	0.30
3	Grey, argillaceous micrite	0.47
2	Black shale	0.17
1	Yellow and blue argillaceous micrite	0.33

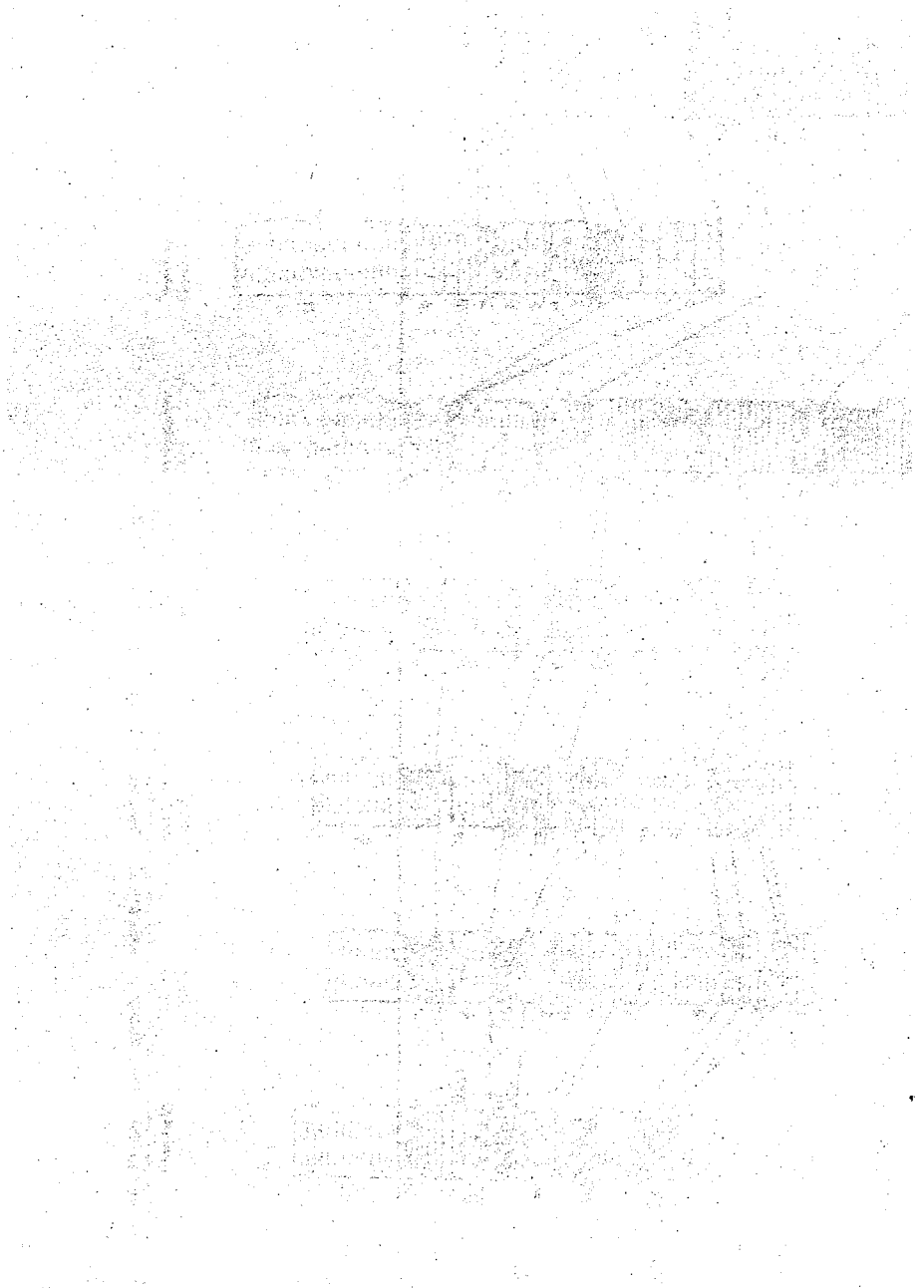

FIG. 12 CORRELATION OF MIDDLE PURBECK GROUP BELOW CINDER BEDS

Fig. 13. CORRELATION OF INTERMARINE BEDS

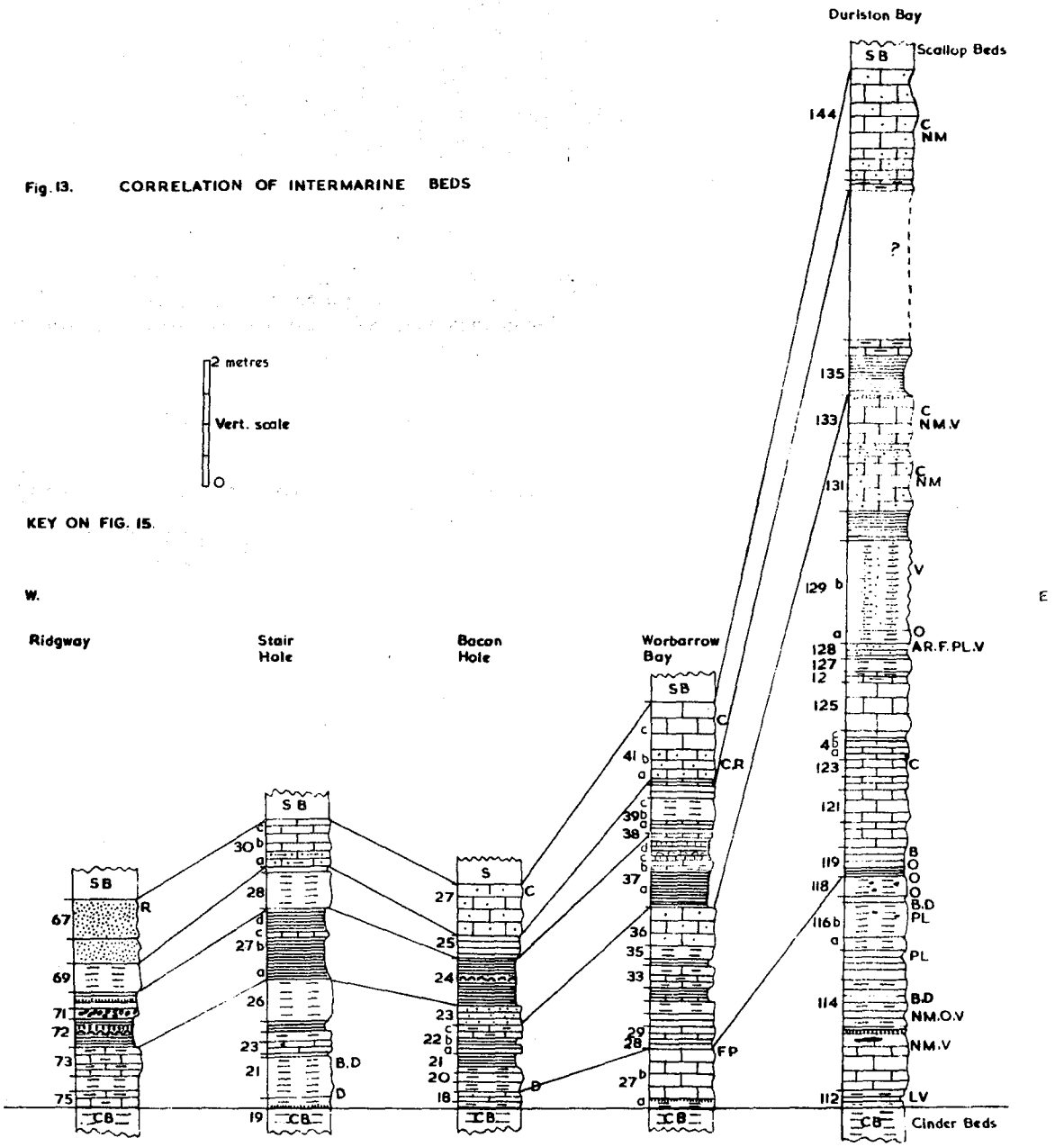

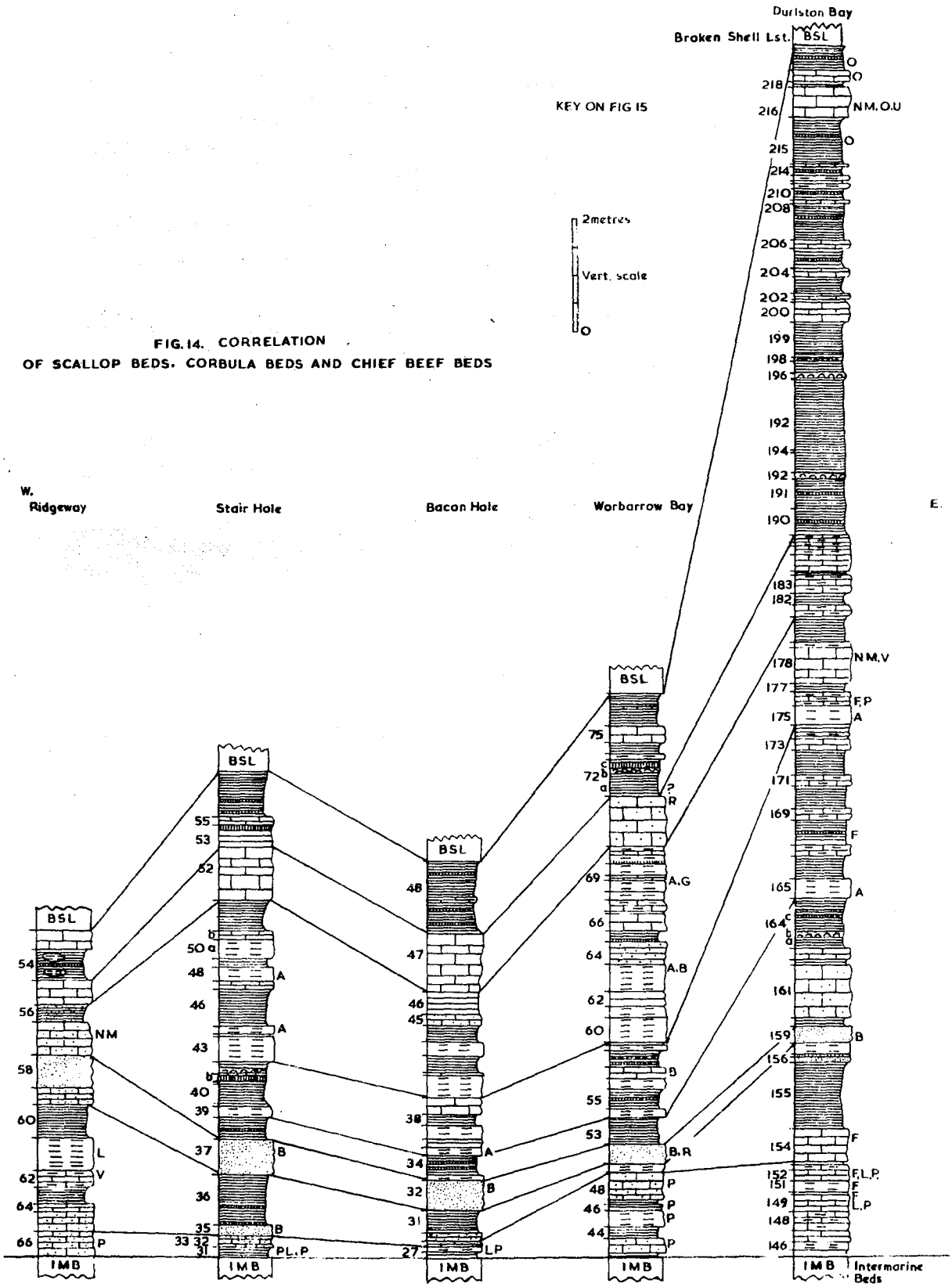

FIG. 14. CORRELATION
OF SCALLOP BEDS. CORBULA BEDS AND CHIEF BEEF BEDS

Fig. 15 Key to Measured Stratigraphic Sections

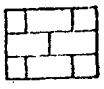
Biosparrudite, biosparite

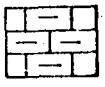
Biosparrudite grading into biomicrudite


Micrite, biomicrite, biomicrudite

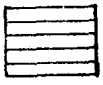
Argillaceous micrite, biomicrite


Shale, clay (usually calcareous)

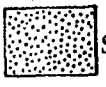
Sandstone

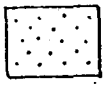
Sandy


Perished bivalves


'Beef'


Chert


Micrite nodules


Gravel

Fossils

AR	*Archaeoniscus*
F	Foraminiferas
GS	Gastropods
L	*Liostrea*
NM	*Neomiodon*
O	Ostracods
P	*'Pecten'*
PL	Plant remains (Charophytes)
V	Vertebrates
U	*Unio*

Sedimentary structure

A	Algal lamination
B	Burrows
C	Cross-lamination
D	Desiccation cracks
FP	Footprints (Dinosaurs)
G	Gypsum pseudomorphs
H	Halite pseudomorphs
R	Ripple marks

Note: Middle Purbeck sections of Ridgeway and Durlston Bay are modified after Fisher (1856) and Clements (1969) respectively.

5. FIELD RELATIONSHIPS – INLAND QUARRIES NEAR SWANAGE [1]

The area attracted attention for a long time mainly because the majority of dinosaur footprints in most British Museums came originally from the middle Purbeck quarries near and around Swanage. Nevertheless, no detailed published descriptions exist for the stratigraphy of these quarries. In general, there are very few marker beds in the Purbeck Group, a difficulty which contributes to the problems of correlating the inland quarries with the type-section. During the course of this work thirty working and disused quarries were measured in detail. In most of the quarries correlation with the type-section on bed-by-bed basis was found possible. It is relevant to mention that the middle Purbeck 'stratigraphy' especially of the Upper Building Stones, is well known among the quarrymen who have their own terminology. Such terms like 'Feather Bed', 'White Roach', 'Rag', 'Burr', etc. were found useful in the field. Most of the 19th-century stratigraphic descriptions of Durlston Bay used mainly the same terms. This was because Durlston Bay section itself was extensively quarried in the late nineteenth century. For additional information concerning the names of the Purbeck strata as chiefly used by quarrymen, refer to Arkell (1945) and Arkell and Tomkeieff (1953).

In the inland quarries, the Intermarine Beds are exposed at nearly every locality. The Scallop Beds, although they are difficult to recognise in the type section, have been identified overlying the Intermarine Beds in four quarries. The Cinder Beds and the underlying Cherty Freshwater Beds were also recorded in four quarries. With regard to the Chief Beef Beds, only the upper part, was recognised in one locality near Langton Matravers (SY/998793), below the 'Soft Burr' (Upper Broken Shell Limestone – upper Purbeck). Generally, in the whole inland area between Swanage and Worth Matravers, the Chief Beef Beds and most of the *Corbula* Beds have been destroyed by recent erosion.

[1] Samples from localities described in this chapter were subjected to petrographic and heavy mineral studies (Chapters 8-10).

To avoid repetition, only a few representative measured sections are given in this account.

1. Exposures of strata below the Cinder Beds: Cherty Freshwater Beds

(a) Worth Matravers (SY/997778)

This locality is about 100 metres south of Compact Farm, a locality which was described by Arkell (1941) as the source of the weathered chert scattered near the sea cliffs between Winspit and St. Alban's Head. Arkell reported in these chert the rare gastropod *Ptychostylus.* The section is poorly exposed and nearly half of the Cinder Beds have been eroded. No reduction in thickness was observed in this locality compared with the type-section in Durlston Bay, although this was suggested by Arkell. At this locality the Cherty Freshwater Beds show well-preserved desiccation cracks (Fig. 16).

(b) Harden's Quarry (SY/979790)

This is the most exposed inland section in the area showing the Cherty Freshwater Beds. There is a slight increase in thickness compared with the type-section (Fig. 12). The high silicified nature of bed 6, and the large irregular chert nodules, give the false impression that this bed can be correlated with the 'Flint Bed' (DB 97) at Durlston Bay.

Sedimentary structures include desiccation cracks similar to those reported in the foregoing locality. The following represents the measured section:

Bed	At the top	Metres
11	Cinder Beds (Fig. 17), masses of *Liostrea distorta* in micrite matrix.	2.20
10	Sandy shale and thin limestone shale	0.10
9	Hard, thin-laminated, bivalve biosparite and biomicrite	0.50
8	Massive, white, bivalve biosparite with highly micritized shell fragments	0.50

Fig. 16. Desiccation cracks in a slab from Cherty Freshwater Beds. Disused quarry at Worth Matravers (SY/99778)

Fig. 17. Cinder Beds at Harden's Quarry. The floor represents the junction between Lulworth and Durlston Formations.

Bed		Metres
7	Argillaceous, earthy biomicrite	0.10 – 0.30
6	Hard, grey, argillaceous, charophyte biomicrite with chert nodules	0.43
5	Earthy, poorly laminated, ostracod biomicrite	0.23
4	Argillaceous biomicrite grades vertically into calcareous mudstone, thin-laminated, desiccation cracks	0.29
3	Massive, earthy, charophyte biomicrite, chert nodules and well-preserved gastropods	0.30
2	Brown, calcareous shale and thin-laminated limestone	0.50
1	Massive, hard, white, bivalve biosparite	1.30

2. Exposures of strata above the Cinder Beds: Intermarine Beds

The term 'Swanage Stone' applied by many geologists in the last century, probably refers to some of these beds. These beds have been extensively quarried for many centuries especially the middle part of the sequence. In this part there are two relatively thick biosparrudite units separated by about 3 metres of sandy, argillaceous biomicrites and calcareous mudstone and shale (Fig. 18). The white bivalve biosparrudites are used mainly for building purposes, while the thin-bedded, brown, sandy, bivalve biosparrudites are favoured for decoration. The biomicrites are less quarried, although some of the thin-laminated charophyte and ostracod biomicrites are used for roofing or for 'Crazy Pavement'.

Sedimentary structures are clearly visible in the Intermarine Beds and are represented mainly by cross-lamination and uniform parallel bedding (Figs. 18 and 19). Dinosaur footprints occur mainly in one particular bed in almost every quarry; the

Fig. 18. Two bivalve biosparrudite units (A and C) separated by sandy argillaceous biomicrites and calcareous mudstones (B). Note the cross-lamination in unit C. Intermarine Beds at Harden's Quarry (SY/979790).

Fig. 19. Cross-lamination in a bivalve biosparrudite. Intermarine Beds at a disused quarry near Worth Matravers, (SY/979781).

'Roach' (Figs. 20 and 21). The 'Roach' can be recognised in the field by its stratigraphic position and by a thin red limestone crust. Desiccation cracks are common and are confined to certain horizons and are more frequent than those recorded in the Cherty Freshwater Beds. One particular bed approximately 0.5 metres thick yielded about 10 laminae; each with desiccation cracks (Fig. 22). An incipient development of desiccation cracks is a common sedimentary structure in the Intermarine Beds (Fig. 23). Donovan and Foster (1972) described similar structures (subaqueous shrinkage cracks) from the middle Devonian of north-east Scotland.

Small folds and faults in the Intermarine Beds run parallel to the main Weymouth-Purbeck anticlinal fold (Figs. 24 and 25). The small folds show some similarity to the adjustment folds, or 'crumples', exposed in the Lulworth area and at Peveril Point.

Only three representative stratigraphic sections are given in this account (Fig. 26a).

(a) **California Farm** (SY/017775)

Bed	At the top	Metres
27	Hard, brown, sandy, thin-laminated limestone	0.50
26	Hard, brown, bivalve limestone, cross-lamination	0.56
25	Grey, rubbly, sandy, bivalve limestone, cross-lamination	0.54
24	Calcareous mudstone	0.24
23	Sandy, friable, argillaceous limestone and shale with 'beef'	0.30
22	Grey and red, bivalve limestone rich in vertebrate remains	0.35
21	Grey, sandy limestone	0.10
20	Calcareous shales with thin bands of perished bivalves	0.17
19	Grey, earthy, argillaceous limestone	0.13
18	Alternating, friable, argillaceous limestone and sandy shale, vertebrate remains.	0.37

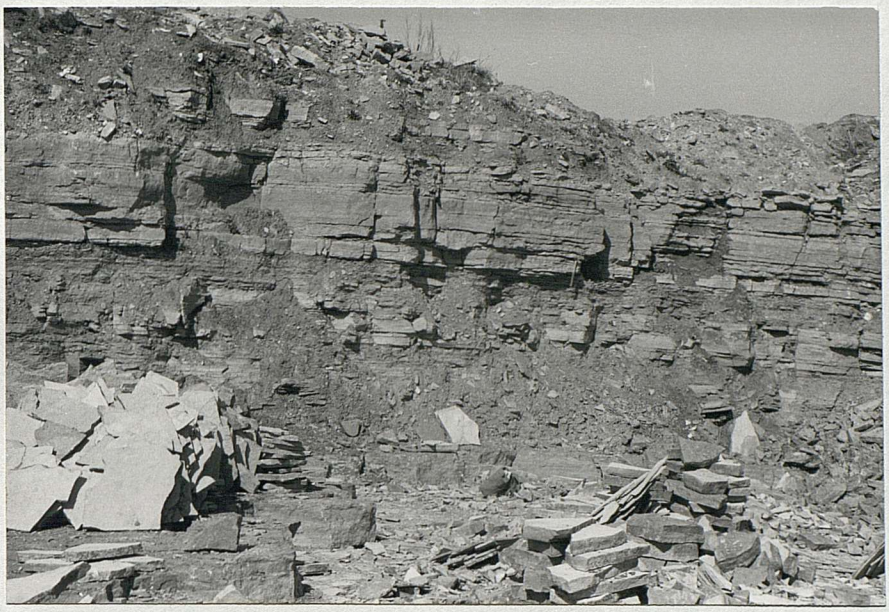

Fig. 20. Quarry at (SY/996776) showing the Intermarine Beds. The loose blocks at the quarry's floor are worked from the 'Roach' bed.

Fig. 21. Dinosaurs footprints in two slabs from the 'Roach' at the quarry shown above.

Fig. 22. Desiccation cracks in a thin-laminated sandy limestone. Intermarine Beds at a disused quarry near Acton (SY/987784).

Fig. 23. An incipient development of desiccation cracks, Intermarine Beds. Quarry near Acton (SY/989781).

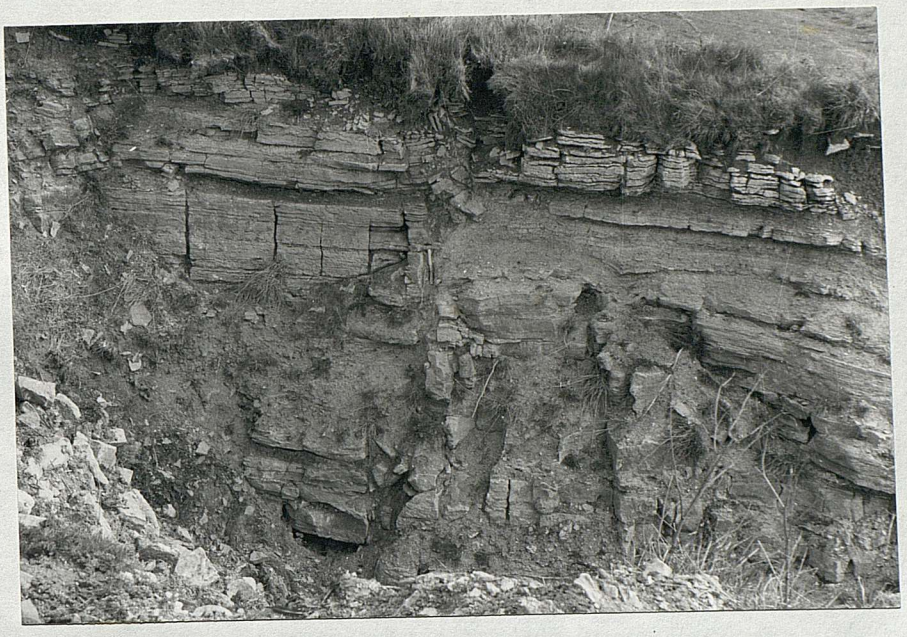

Fig. 24 Small vertical fault in a disused quarry at (SY/981790). The fault runs parallel to the main Weymouth-Purbeck anticline. Intermarine Beds.

Fig. 25. Small 'crumple' in the Intermarine Beds. The axis is nearly parallel to the main Weymouth-Purbeck anticline. Pencil is on a calcareous shale which correlates with bed DB 130 of Durlston Bay. Disused quarry at (SY/996776).

FIG. 26

b. CORRELATION OF THE SCALLOP BEDS IN THE PURBECK QUARRIES

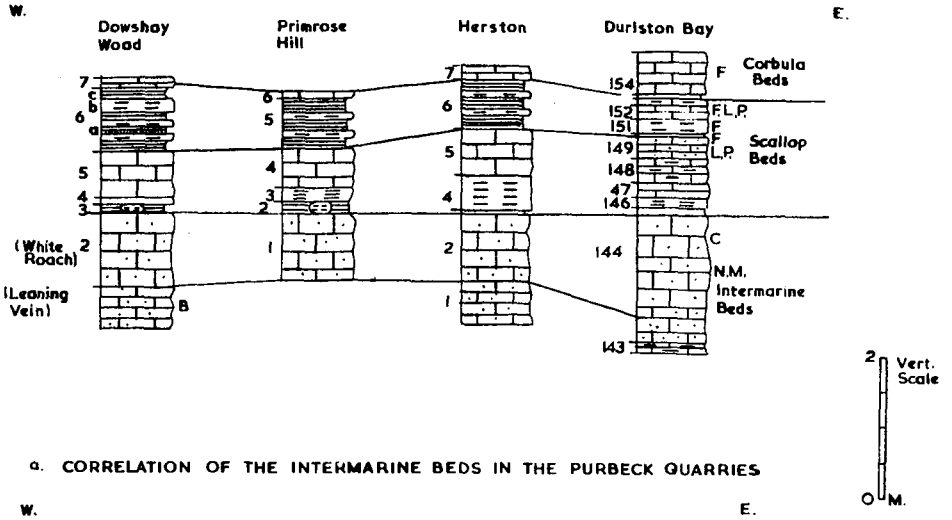

a. CORRELATION OF THE INTERMARINE BEDS IN THE PURBECK QUARRIES

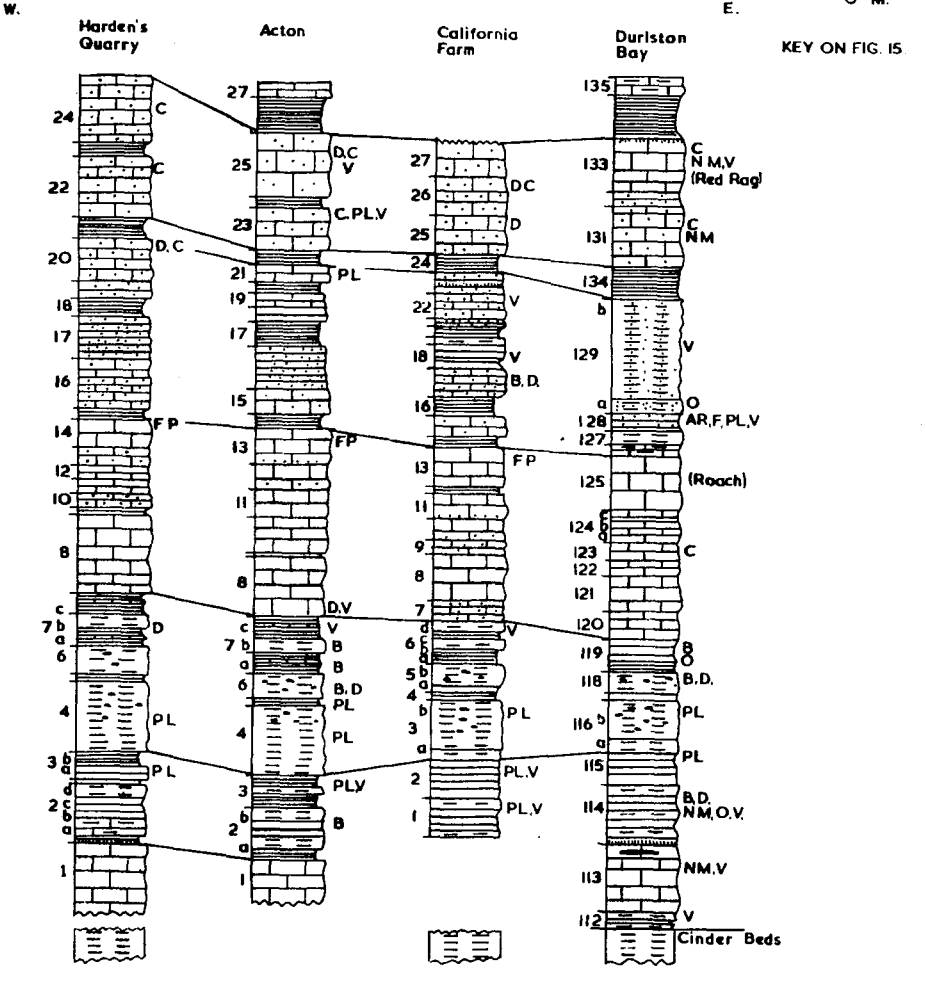

Bed	At the top	Metres
17	Hard, grey, sandy limestone, desiccation cracks and bioturbation	0.40
16	Laminated, calcareous mudstone with thin limestone bands, *Liostrea* fragments	0.23
15	Hard, grey, sandy limestone	0.30
14	Mudstone with thin limestone bands, sandy at the base	0.14
13	Thin-bedded, grey, bivalve limestone with 3 cm. red crust, *Liostrea* fragments and dinosaur footprints (Roach)	0.53
12	Sandy, calcareous clays	0.10
11	Hard, bivalve limestone, sandy at the base, *Liostrea* fragments	0.34
10	Hard, grey, bivalve limestone	0.32
9	Grey, sandy and rubbly limestone	0.22
8	White, hard, bivalve limestone	0.67
7	Hard, sandy, rubbly limestone	0.28
6d	Earthy, ostracod biomicrites rich in vertebrate remains	0.13
6c	Calcareous mudstone with thin limestone bands	0.10
6b	Hard, grey, earthy ostracod biomicrite	0.15
6a	Sandy, calcareous shale and thin limestone bands	0.26
5b	White, thin, laminated ostracod and charophyte biomicrites with small chert nodules	0.29
5a	Grey, ostracod biomicrite	0.08
4	Calcareous shale with thin limestone bands	0.16
3b	Thin-bedded charophyte and ostracod biomicrite, shale parting, plant and vertebrate ramains	0.68
3a	Hard, grey, charophyte biomicrite	0.16
2	Earthy, calcareous clays, very rich in plant and vertebrate remains	0.57

Bed	At the top	Metres
1	Grey, argillaceous micrite and mudstone, vertebrate and plant remains	0.56

(b) Acton (SY/991783)

Bed	At the top	Metres
27	Brown, blue-hearted bivalve limestone	0.20
26	Black to blue papery shale, 'beef' and perished bivalves	0.50
25	Thin-bedded, sandy, cross-laminated limestone with shale parting, plant remains, *Liostrea* fragments, turtle remains, desiccation cracks near the top	0.90
24	Sandy, calcareous shale	0.15
23	Thin-bedded, sandy, bivalve limestone, plant and vertebrate remains *Liostrea* fragments, cross-lamination	0.60
22	Brown, sandy, papery shale	0.20
21	Hard, sandy limestone, plant remains	0.25
20	Sandy, calcareous mudstone	0.16
19	Very hard, sandy limestone	0.21
18	Sandy limestone and shale	0.19
17	Brown, calcareous shale and mudstone	0.33
16	Brown, sandy, friable, argillaceous limestone	0.58
15	Very hard, sandy, bivalve limestone, *Liostrea* fragments	0.37
14	Mudstone with thin limestone bands	0.18
13	White, thin-laminated bivalve limestone, red crust, dinosaur footprints, (Roach)	0.50
12	Hard, massive, bivalve limestone, rubbly near the base, *Liostrea* fragments	0.35
11	White, hard, bivalve limestone, sandy and friable near the base, *Liostrea* fragments	0.40

Bed	At the top	Metres
10	White, hard, bivalve limestone, sandy and friable near the base, *Liostrea* fragments	0.50
9	Calcareous shale	0.05
8	White, bivalve limestone	0.40
	The rest of the section was measured in a nearby quarry about 100 m. to the east where bed 8 attains a thickness of 0.85 m.	
8	White, thick-bedded, bivalve limestone, vertebrate remains and desiccation cracks near the base	0.85
7c	Thin-bedded, calcareous shale with limestone bands, vertebrate remains	0.28
7b	Hard, grey micrites, burrows	0.22
7a	Calcareous shale and limestone bands, burrows	0.29
6	Grey, thin-laminated, ostracod and charophyte biomicrites, weathers white, small chert nodules, desiccation cracks	0.33
5	Brown, calcareous shale with plant remains	0.08
4	Ostracod and charophyte biomicrite, thin laminated, weathers white, rich in vertebrate remains; charophytes are abundant near the base	1.00
3	Sandy, calcareous mudstone very rich in vertebrate remains especially at the top	0.43
2b	Alternating grey biomicrite and calcareous shale, burrows	0.60
2a	Thin-laminated, calcareous shale with thin layer of 'beef' at the base	0.15
1	Hard, bivalve limestone	0.60

(c) **Harden's Quarry** (SY/979790)

Bed	At the top	Metres
24	Sandy, bivalve limestone with thin shale parting	0.95
23	Brown, calcareous shale	0.22

Bed	At the top	Metres
22	Thin-bedded, sandy limestone with *Liostrea* fragments cross-lamination	0.90
21	Sandy, calcareous shale with thin limestone bands, 'beef'	0.28
20	Thin-laminated, sandy limestone, plant remains, cross-lamination and desiccation cracks	0.60
19	Argillaceous, sandy biomicrite	0.23
18	Calcareous mudstone	0.20
17	Friable, brown, sandy, thin-bedded limestone	0.55
16	Hard, sandy, thin-bedded, bivalve limestone, *Liostrea* fragments	0.70
15	Calcareous mudstone with thin limestone bands	0.15
14	Massive white, bivalve limestone with thin red crust, dinosaur footprints (Roach)	0.32
13	Rubbly, sandy limestone	0.25
12	Hard, grey, massive, bivalve limestone	0.25
11	Hard, grey, massive, bivalve limestone	0.25
10	Rubbly, sandy limestone	0.21
9	Calcareous shale with thin limestone bands	0.10
8	Massive, bivalve limestone in two units	1.10
7c	Thin-laminated, friable limestone and calcareous shale	0.32
7b	Hard, grey, ostracod biomicrite, desiccation cracks	0.20
7a	Thin-laminated, calcareous shale and limestone	
6	Thin-laminated, grey, ostracod and charophyte biomicrite, weathers white, small chert nodules	0.35
5	Calcareous shale with thin carbonaceous bands	0.08
4	Thin-laminated, earthy biomicrite, ostracod and vertebrate remains, the lower part of the bed is very rich in charophytes (see Fig. 27)	1.00

Fig. 27. Lower part of the Intermarine Beds at Harden's Quarry (SY/979790). These limestones are dominated by ostracod and charophyte biomicrites.

Fig. 28. Scallop Beds and upper of Intermarine Beds at Downshay Wood (SY/981794). Hammer on the 'White Roach'. The overlying bed (arrowed) contains the rare mineral calciostrontianite.

Bed	At the top	Metres
3b	Calcareous clays rich in carbonaceous matter	0.17
3a	Calcareous mudstone and argillaceous micrites	0.22
2d	Thin-laminated, earthy micrites	0.26
2c	Argillaceous micrites and shales	0.28
2b	Very hard, massive bivalve limestone, glauconite	0.23
2a	Brown shale with 'beef'	0.10
1	Very hard, massive white bivalve limestone, *Liostrea* fragments	1.10

3. Exposures of strata above the Cinder Beds: Scallop Beds

The Scallop Beds and the lower part of the *Corbula* Beds are the highest middle Purbeck Group exposed in the inland quarries between Swanage and Worth Matravers. The Chief Beef Beds were recorded only in one quarry near Langton Matravers (SY/998793). The Scallop Beds are not easy to recognise in the field because they are relatively thin, i.e. about 1.5 metres. Nevertheless, the abundance of *Pecten*, the sandy nature of the beds and their stratigraphic position (usually they overlie the 'White Roach' and 'Leaning Vein'), are useful criteria to recognise the Scallop Beds in the field.

The Scallop Beds and the underlying Intermarine Beds ('White Roach' and 'Leaning Vein') have been recorded in four quarries. In one of these quarries (SY/981794), the rare mineral calciostrontianite was discovered. Details of this discovery are given in the petrographic section. Three measured sections are reported in this account and correlated with the type section (Fig. 26b).

(a) **Herston, Swanage** (SZ/009787)

Beds	At the top	Metres
7	Grey, hard, bivalve limestone, *Corbula*	0.22
6	Grey, friable biomicrite and sandy shale, *'Pecten'*	0.70
5	Rough, thin-bedded biosparite rich in gastropods	0.66
4	Grey, argillaceous nodular micrite	0.49
3	Thin-laminated, calcareous mudstone	0.05
2	Massive, bivalve biosparite (White Roach)	0.95
1	Thin-laminated, sandy biosparite (Leaning Vein)	0.60

(b) **Near Primrose Hill** (SY/989783)

Bed	At the top	Metres
6	Rubbly, friable sandy limestone with *'Pecten'*	0.10
5	Sandy limestone and shale, *'Pecten'*	0.65
4	Thin-laminated, rough bivalve biosparite, abundant gastropods	0.55
3	Nodular, argillaceous micrite	0.17
2	Argillaceous micrite and shale, micrite nodules up to 20cm. in diameter	0.23
1	Massive, white, bivalve limestone (White Roach)	0.90

(c) **Downshay Wood** (SY/981794)

Bed	At the top	Metres
7	Thin-bedded, hard, bivalve biosparite	0.15
6c	Sandy clays	0.15
6b	Hard, argillaceous, sandy biomicrite, *'Pecten'*	0.20
6a	Friable, sandy, brown limestone and shale with some 'beef'	0.53

Bed	At the top	Metres
5	Rough, pink, bivalve biosparrudite (Fig. 28), abundant gastropods and vertebrate remains. This bed contains the rare mineral calciostrontianite	0.63
4	Nodular, argillaceous micrites	0.12
3	Brown shale with small micrite nodules.	0.15
2	Massive, hard, white, bivalve biosparite (White Roach)	1.00
1	Sandy, thin-laminated, white, bivalve limestone, burrows, (Leaning Vein).	0.60

6. ANALYTICAL TECHNIQUES 1 : CHEMISTRY

A major part of this study is concerned with the chemical analyses of the middle Purbeck rocks. Major elements (Ti, Si, Al, Fe, Mg, Ca, Na and K) and minor elements (P, S, Cl, V, Mn, Ni, Cu, Zn, Ga, As, Rb, Sr, Zr, Ba, Ce, Pb and Th) were determined by X-ray spectroscopy. The rapid methods of Shapiro and Brannock (1962) were used for the determination of CO_2 and H_2O^+ Organic carbon was determined by a method similar to that of Bear (1964).

1. Sample Preparation

(a) Grinding

The samples were first sawn into halves, one half being kept for thin-sectioning purposes, the other being further reduced into pea-sized fragments. A 100 gm. sample of the fragments was washed thoroughly with tap water and was then soaked in deionized water overnight to reduce any sea-water contamination. The 100 gm. sample was loaded into Tema disc mill (lined with tungsten carbide) and pulverized for 10 minutes. Such a grinding ensures less than 200 mesh particle size (Sulaiman, 1972), which is reasonably adequate for chemical analysis. Between samples, the Tema disc mill was cleaned by grinding broken glass for a few minutes, followed by washing and drying. The Tema contributes a small quantity of tungsten preventing its determination; carbon contamination however, is low ($< 0.04\%$) compared with its contents in the samples.

(b) Pellet making

In X-ray spectrometry, samples can be prepared in different ways. Samples may be used as powders, fused discs and pellets. It is well known that an excellent procedure for sample handling is to make pellets (Adler, 1966). Pellets are easy to work with and can be made and reproduced simply.

An approximate weight of the powder (10 gm.) was placed in an agate morter. A few drops of the binder (2% aqueous solution of polyvinyl pyrrolidone) was added and thoroughly mixed with the powder. This damp paste was transferred into a loose-fitting cylinder placed in a special mould (Cosgrove, 1972a). The paste was tapped down to take the shape of the cylinder. The cylinder was then gently pulled out and finely powdered boric acid was added to fill the space between the paste and the outer part of the mould. More boric acid was added, covering the paste and filling the mould about three quarters full. A stainless steel plunger was inserted and the paste (surrounded and covered with boric acid) was pressed at about 500-600 kg/sq. cm. for three minutes in a hydraulic press. The pellet was then removed from the mould and labelled.

2. X-ray Spectrometry

In X-ray fluorescence analysis, the sample is irradiated with primary X-rays to produce secondary (fluorescent) radiation, which, after collimation, is dispersed by an analyzing crystal. The angle corresponding to a particular wave-length can be set on a goniometer and the intensity is determined by counting with a detector.

A Philips PW1212, 24 channel, fully automatic spectrometer with simultaneous, tape and printed output was used. The goniometer can be set for 24 angular positions; 15 angular positions only in one cycle and the remaining 9 positions if required, being used in a second analysis cycle. For each angular position different operating variables can be individually optimised i.e. voltage, current, collimator, time and sample-spinner. The established optimum conditions were entered onto a patchboard which controls the spectrometer. The analysis operation requires the insertion of the pellets and then pushing the start button after punching and printing specimen details for the computer.

Chromium target X-ray tube is used for exciting major elements and some of

the minor elements while molybdenum and tungsten tubes are used mainly for the trace elements. Extensive calibration has been already achieved by Cosgrove (1972a) and Sulaiman (1972). These two authors should be consulted for any details concerning the operational conditions and the calibration equations. Nevertheless, additional calibration has been carried out in the present work for seven elements (Mn, Ni, Rb, Sr, Zr, Ba and Ce). These seven elements were programmed using a molybdenum tube. A tungsten tube is more suitable since it gives maximum excitation for most of these seven elements, but it was not available during the calibration time. The calibration processes include standard preparation, establishment of optimum operational conditions, construction of the calibration equations and then evaluating precision and accuracy.

(a) Standard Preparation

Some middle Purbeck rocks which were already analysed for the major elements, were selected as rock standards for the purposes of calibration. This choice ensures that the particle-size range in both samples and standards is similar since both received the same treatment during grinding and pelleting. The calibration depends upon variation in mineralogy as well as mass-absorption, therefore the rock standards were selected to cover such variations. Ten rock powders covering the whole range from almost pure limestone to almost pure shale were taken as rock standards.

The rock standards were spiked by spectrographically pure chemicals in the form of solutions containing exact proportions (ppm) of elements to accurately weighed quantities of the powders (4 gm.). Each element was added in eight different amounts to the aliquot of the rock standards. With the blank this ensures nine points on the calibration curve. More than one element was added to the aliquot. To avoid spectral interference, Zr and Sr were spiked separately as were Ce and Ba. The liquid spiking

ensures homogeneity in the distribution of the trace elements added and the means of adding very small amounts of these elements (1-10 ppm) with great accuracy. One hundred and twenty rock powders representing 10 rock standards were spiked, left to dry at 60° C, homogenised by shaking with lucite balls, pelleted and labelled.

(b) **Operational conditions**

The different operational conditions for each element were established (Table 3). The goniometer angular positions for peaks and backgrounds were determined by scanning standards of spectrographically pure elements at $0.01^{\circ}2\Theta$ intervals. Using the molybdenum tube it was found that the background counting rate varies at different levels of background. This was the case at the vicinity of Zr Kα, Sr Kα and Rb Kα. This difficulty can be removed by taking two readings on both sides of the peak. This cannot always be applied due to the limitations of the 15 goniometer angular position. Also in the case of Zr Kα, the right hand side of the peak is mainly occupied by the MoKα compton scatter and to some extent by $SrK\beta_1$ and $K\beta_3$. Anderman and Kemp (1958) found that the mass-absorption is proportional to the background intensity at the vicinity of the element peak. This relationship was proved by plotting the background intensities against the corrosponding mass-absorption at three background levels for eighty rock pellets (Fig. 29). This means that once the mass-absorptions are known, one can calculate the background intensity at any level.

The relationship between the counting rates at the different background levels and mass-absorption was established by preparing artificial matrices free from trace elements. For Zr the following equation was obtained:

$$c/s = \frac{2660}{\mu m} + 60$$

where c / s is the counting rate for background under Zr Kα position and μ_m is the mass-

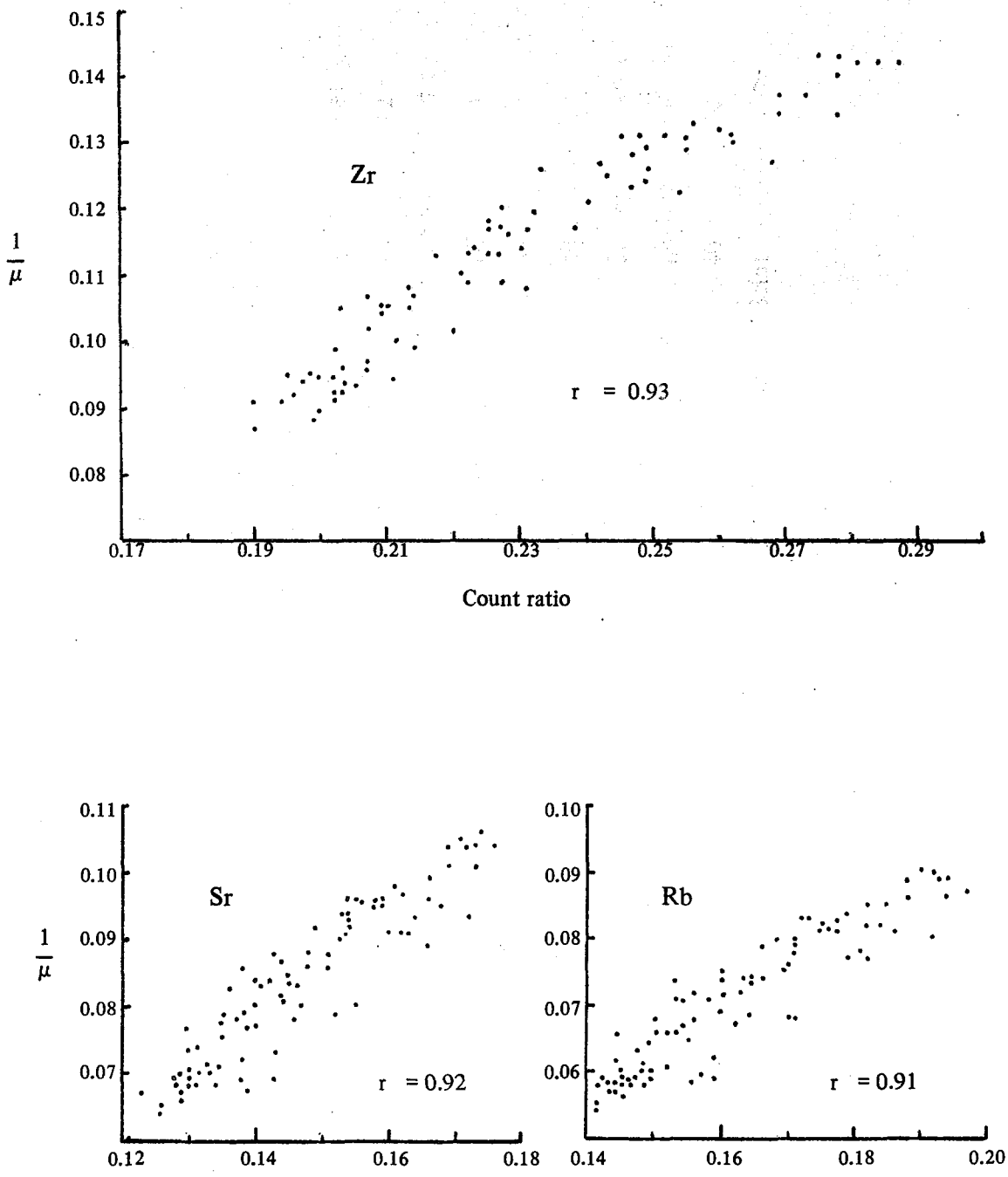

Fig. 29. Relation between mass-absorption and background intensities (ratioed to a master standard) at the vicinity of Zr Kα, Sr Kα and Rb Kα.

Table 3 **Operational conditions for the Molybdenum tube programme (Mo 9)**

	Zr	Sr	Rb	Ni	Ce	Mn	Ba
Peak	Kα	Kα	Kα	Kα	Lβ1	Kα	Lβ1
Peack channel	1	3	5	7	8	11	12
Background 2Θ	+ 0.47	+ 0.63	− 0.82	− 2.10	+ 3.08	− 2.24	+ 7.11
Background channel	2	4	4	6	9	10	13
Volts (kV)	100	100	100	100	60	60	60
Current (mA)	20	20	20	20	32	32	32
Collimator	Fine	Fine	Fine	Fine	Coarse	Coarse	Coarse
Crystal	LiF200	LiF200	LiF200	LiF200	LiF200	LiF200	LiF200
Time (Seconds)	40	20	20	40	40	40	40
Counter	← Scint →			← Flow + Scint →			

absorption at Zr Kα. Similar equations were established for Sr, Rb and Ce. They are given in the following order:

$$c/s = \frac{1427}{\mu_m} + 41 \qquad \text{for Sr}$$

$$c/s = \frac{1269}{\mu_m} + 37 \qquad \text{for Rb}$$

$$c/s = \frac{17840}{\mu_m} + 83 \qquad \text{for Ce}$$

These equations were tested by comparing calculated and determined background values and a fair agreement was found between them. The advantage of this approach is that all background angular positions can be saved if necessary, therefore, the 15 angular positions of the goniometer can accommodate more elements.

Similar approach to that described above was applied for correction of Ni in the molybdenum X-ray tube. It was found that the tube contamination Ni Kα is proportional to mass-absorption. Ni-free standards were used to calculate the net-peak counting rate of Ni in the molybdenum X-ray tube. The following equation was obtained:

$$\text{Ni contamination in c/s} = \frac{1421}{\mu_m} - 8$$

where μ_m is the mass-absorption at Ni Kα position.

(c) Calibration

The performance of the spectrometer is subject to long-term variation such as the deterioration of X-ray tube or electronic drift and much shorter irregularities such as differing vacuum, expansion and contraction of the analysing crystals (Leake *et al.*, 1969/70). Also when using gypsum as the analysing crystal, dehydration may be responsible for a sharp drop in the counting rate (Cosgrove, 1972a).Considering these limitations, absolute counting may lead to serious difficulties. High precision can be

achieved by taking the ratios of all measurements, both of the standards and of samples to one rock pellet, which is repeatedly measured every few minutes. The ratio method used consists of dividing the peak minus background obtained on samples by peak counts obtained on a master standard. The calibration curves are therefore based on plots of the element (ppm) against the ratio counts collected on the master standard. In order to minimise goniometer travelling time, the order of measurements is always determined by working with increasing 2 Θ angles.

All the primary calibrations for each matrix fulfil the equation: $Y = mX - c$, where Y is the added ppm; X is the count ratio; m is the slope and c is the original ppm present before spiking. The count ratio X is regressed on Y (the element concentration) assuming that the spiked amount is correct and the error lies in the determination of the count ratio. The total ppm becomes : Total ppm = m X. Plots of slopes against μ_m for each of the ten spiking matrices shows that generally slopes increase with the increase in μ_m. This is expressed in the equation : Slope = $a\mu_m + b$, where a and b are constants. Substituting for slopes in the calibration equations, the final equation becomes: Total ppm = $X(a\mu_m + b)$. The relationship between slopes and μ_m enables each sample analysed to be finally computed with the correct slope applicable to that sample. Thus, intermediate rocks or even those with μ_m somewhat outside the range of the spiking matrices, may be computed with the correct slopes.

(d) Precision

As far as instrumental precision is concerned, calibration was reasonably successful. The molybdenum tube programme was not adequate for Ba determination. The element was later determined using the existing tungsten tube programme (Cosgrove, 1972a). In general the elements involved in different corrections for spectral interference (Zr and

Ce) or a tube contamination (Ni) are less precise especially in the limestones which contain lower values of Zr, Ni and Ce in comparison with the shales.

The reproducibility of the results obtained from the spectrometer has been evaluated by repeating all standards used in the present calibration 10 times. Generally the coefficients of variation and standards of deviation are within acceptable limits for ordinary rock analyses. Instrumental precision for most of the elements involved in the calibration ranges from 1-6%.

(e) Accuracy

Chemical data dealing with sedimentary rock standards are relatively sparce. Ten reference carbonate rocks and mudstone standards were analysed. Only the carbonate standards are listed here since they have been analysed before by different authors. These were recommended for use as geochemical standards (Thompson *et al.*, 1970). The results of Zr, Sr, Rb, Ni and Mn analyses in three carbonate standards are reported in Table 4. For comparisons results reported by other workers are also included. It is difficult to make comments regarding the accuracy of the analyses with so few results and few standards. Again, with different grinding processes and different grain size range such comparison is more difficult. Nevertheless, the comparison shows a fair agreement between the results obtained by X-ray spectrometry and emission spectrography.

3. CO_2 and H_2O^+ determinations

The carbonates were determined by a method similar to that of Shapiro and Brannock (1962). The method was improved by reducing the boiling time to one minute. The sample was attacked by dilute HCl and was left to boil for one minute instead of three. The evolving CO_2 was absorbed by KOH. The weight percentage of

Table 4. Some trace element data (ppm) for some reference carbonate rocks*1

	Zr		Sr		Rb		Ni		Mn	
GFS 401 (Limestone)	7	* 2	153±(6)	* 2	3.0± (0.8)	* 2	6.2±(1.8)	* 2	131±(10)	* 2
	9.9±(2.5)	* 3	138±(7)	* 3	< 10	* 3	4.8±(2.8)	* 3	112±(9)	* 3
			152	* 4					85	
			140	* 5						
GFS 402 (Limestone)	10	* 2	120±(4)	* 2	6.7±(1.4)	* 2	9.4±(1.3)	* 2	184±(5)	* 2
	11±(2)	* 3	103±(12)	* 3	< 10	* 3	7.7±(1.1)	* 3	162±(16)	* 3
			101	* 4	1				147	* 4
			143	* 5						
GFS 400 (Dolostone)	?	* 2	750±(10)	* 2	< 2	* 2	< 4	* 2	50±(6)	* 2
	< 5	* 3	550±(27)	* 3	< 10	* 3	< 2	* 3	51±(4)	* 3
			1100	* 4					40	* 4

*1 Issued by G. Frederick Smith Chemical Co. P.O. Box 23344, Columbia, Ohio, 43223.
*2 Present work : X-ray spectrographic method
*3 Thompson *et al.*, (1970) : emission spectrographic method
*4 Ingamells and Suhr (1967) : neutron activition method
*5 Livingston and Thompson (1969) : neutron activition method
Note: Data between brackets represent ± one standard deviation

CO_2 was calculated by measuring the volume of the gas before and after the HCl attack. Analar $CaCO_3$ was used to calibrate the apparatus. The standard (0.1 gm. Analar $CaCO_3$) was run every five samples. The mean of 78 runs of the standard was 21.8 ml. with standard deviation of 0.67 and standard error of 0.08.

The combined water (H_2O^+) was determined in duplicates for all samples using the method of Shapiro and Brannack (1962). The reproducibility of the method is good.

4. Organic carbon determination

The organic carbon was determined according to the method described by Bear (1964). The sample was attacked by chromic acid, the unused chromic acid was back titrated against ferrous ammonium sulphate using diphenylamine as indicator. The organic carbon was calculated using the following equation:

$$\text{Organic carbon } \% = \frac{(b - u) \times d \times n \times a \times 100}{w \times b}$$

where

b = ml. of ferrous ammonium sulphate solution in ml. required for the blank.

u = ml. of ferrous ammonium sulphate required for the sample.

d = ml. chromic acid used (10 ml)

n = normality of chromic acid (0.4N)

a = m eq. weight of carbon (0.003 gm.)

w = weight of the sample used in grams.

By substituting for d, n and a, the equation becomes:

$$\text{Organic carbon } \% = \frac{(b - u) \times 1.2}{w \times b}$$

Since this method is not as efficient as the dry combustion method, results should be multiplied by a correction factor. Bear (1964) reported a correction factor of 1.2.

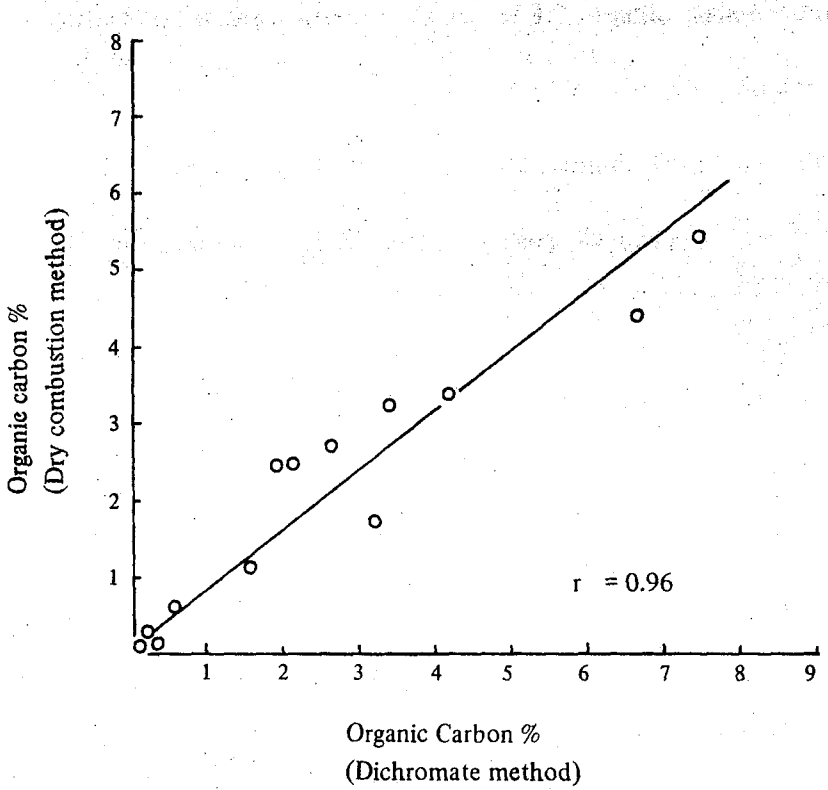

Fig. 30. A plot of organic carbon determined by dry combustion and dichromate methods.

A correction factor of 1.196 was obtained in the present work using tri-sodium citrate in which organic carbon was determined by dry-combustion and dichromate methods. On the other hand, organic carbon determined by dry-combustion method for 13 Purbeck samples is usually lower than that determined by the dichromate method (Fig. 30). The presence of elements in the reduced state could be responsible for higher organic carbon values when the dichromate method is used. It seems, therefore, unjustified to use the correction factor of 1.2 organic carbon values in the middle Purbeck rocks when the dichromate method is used. Thus no correction was applied.

The reproducibility of the method is good. Duplicate runs were carried out for all samples while the blank was run every 10 samples.

7. ANALYTICAL TECHNIQUES 2: MINERALOGY AND PETROGRAPHY

1. X-ray diffractometry

X-ray diffraction analyses have been used extensively for the determination of quartz, calcite and aragonite in all samples. Clay minerals determination was carried out only for the middle Purbeck shales.

For quartz, calcite and aragonite, the rock powder pellets which were initially prepared for chemical analyses by X-ray spectrometry were used for mineral determinations (Cosgrove and Sulaiman, 1973). Since a considerable directed pressure (500-600 kg/cm^2) was applied in making the pellets, some preferred orientation of minerals is to be expected. The effect of pelleting pressures was examined in seven pellets originally made from a clay-rich sample under different pressures. Quartz and calcite peaks (at 4.26Å and 3.04Å respectively) were recorded as counts per seconds and compared with the corresponding peak intensities in the random powder sample (Fig. 31.). Two main conclusions emerge:

1. Peak intensities are virtually unaffected in the pressure range of 200–4000 kg/cm^2. The small intensity variations are much less than the variation observed due to the fluctuation of the diffractometer. Below 200 kg/cm^2, peak intensities are greatly affected by pelleting pressure and the critical pressure is probably much lower than this. Powder samples pressed between two glass slides by hand have peak intensities similar to the intensities obtained on pellets prepared under 4000 kg/cm^2.

2. Between 200 and 4000 kg/cm^2 pelleting pressures, peak intensities increased in the pellets relative to the powder sample by a factor of 2.6 for quartz and 2.8 for calcite. Such intensity increase makes the determination of small amounts of minerals more reliable and much easier.

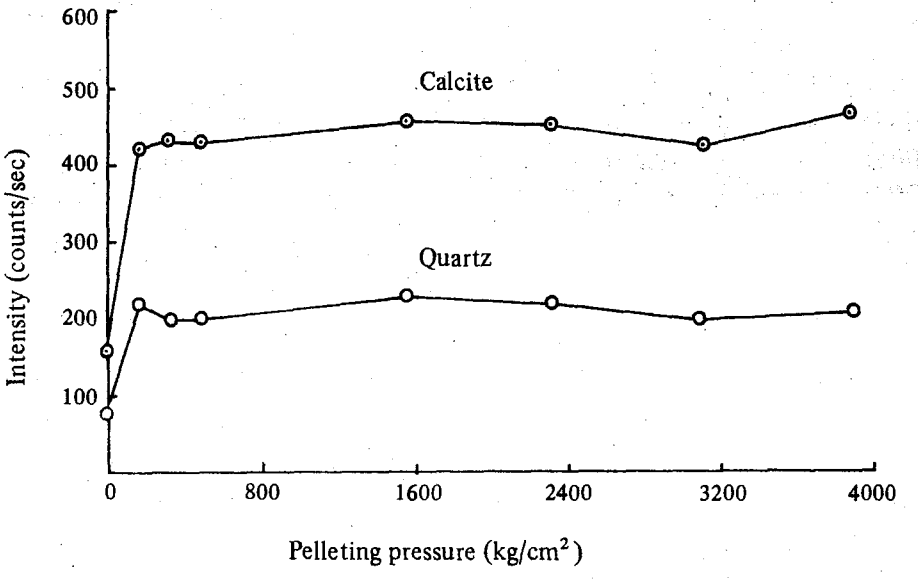

Fig. 31. Relation between pelleting pressure and peak intensities of calcite (3.04 Å) and quartz (4.26 Å)

To ensure that pelleting pressures above 200 kg/cm^2 have constant effects on mineral orientation, peak ratios for quartz, aragonite and calcite were compared in different pelleted samples. Although the samples have a wide range in composition (from limestones to shales), peak ratios for each mineral were more or less constant in all cases. This is supported by the statistics given in Table 5 below.

Table 5. Basic statistics[1] of peak ratios for quartz, aragonite and calcite

	Quartz 4.26Å peak/3.34Å peak	Aragonite 3.27Å peak/3.40Å peak	Calcite 3.86Å peak/3.04Å peak
Mean	0.204	0.484	0.086
Variance	0.0003	0.0004	0.0010
Standard deviation	0.017	0.020	0.001
Standard error	0.006	0.005	0.003
Coefficient of variation	9%	4%	11%
Number of pellets	10	14	12

[1] Computation methods and terminology used in the present work are from Griffiths (1967)

It seems reasonable to assume that the rock powder pellets represent oriented samples in which orientation is the same once the pelleting pressure exceeds 200 kg/cm^2. All the rock powder pellets were prepared under pressures between 500 and 600 kg/cm^2.

The samples were analysed on Philips diffractometer comprising a PW 1010 generator and a PW 1050 goniometer, with a proportional counter linked to a chart recorder. Copper Kα radiation (Ni filtered to give monochromatic beam) at 36 kV, 24 mA was used with 1.0°, 0.2mm., 1.0° slits, 1.0° 2Θ/min recording speed, a time constant of 4 sec. and 1200 cm/hr. chart speed.

The rock powder pellet fits into the diffractometer after slight modifications to the standard fixing clips thus presenting a flat powder surface to the X-ray beam.

(a) Quartz determination

Some middle Purbeck rocks were selected as rock standards for the purpose of calibration. This ensures that grain size in both samples and standards is similar since both received the same treatment during grinding and pelleting. Quartz in the rock standards was determined gravimetrically by the method of Trostell and Wynne (1940).

Peak intensities depend upon variation in mineralogy as well as upon mass-absorption. To reduce the effect of mineralogy, samples with more than 50% carbonate were grouped as a separate limestone series. The remainder of the samples are essentially shales and were treated as a second group. Mass-absorption correction was incorporated in the construction of the calibration curves.

The two main quartz peaks at 3.34Å and 4.26Å are preferred since the other quartz peaks have lower intensities. The main quartz peak at 3.34Å is overlapped by the (003) illite peak. Instead, the 4.26Å quartz peak was used although there is interference from the gypsum peak at 4.27Å. However, such interference can be corrected using the ratio between the intensities of the 4.27Å and 7.56Å gypsum peaks; a ratio which was reasonably constant.

The average height of the 4.26Å peak of quartz from three diffractometer scans was taken as quartz intensity. One sample was treated as a master standard and this was run during the analyses of each batch of samples so that minor electronic drift of the diffractometer affecting peak intensities could be corrected. The working equation is in the form:

$$\text{Quartz } \% = a \, \mu_m \, I + c$$

where a is the slope of the calibration curve; μ_m is the mass absorption of the sample at CuKα wave length (1.54Å) and calculated from the major element chemistry; I is the

peak intensity and c is a constant.

Table 6 shows some of the basic statistics of the calibration curve before and after mass-absorption correction. The mass-absorption correction did not improve the calibration curve of the limestones and so it was abandoned for these rocks.

In the shales, an improvement was observed after mass-absorption correction was incorporated in the calibration curve. This was indicated by the increase of correlation coefficient from 0.991 to 0.995 and the decrease in the standard error of the estimate from 2.60% to 2.04%. The working equations for quartz % in the limestones and shales were as follows:

$$\text{Quartz \% (in limestones)} = 0.0926\, I + 0.3$$

$$\text{Quartz \% (in shales)} = 0.0017\, \mu_m I - 0.7$$

Table 6. Basic statistics of the quartz calibration curve in the Purbeck limestones and shales

	Quartz % in limestones		Quartz % in shales	
	Against I	Against $\mu_m I$	Against I	Against $\mu_m I$
Correlation coefficient	0.996	0.991	0.991	0.995
Slope	0.0926	0.0016	0.0899	0.0017
S.E. of the slope	0.0023	0.0001	0.0040	0.0001
Intercept	0.3	−0.7	−1.1	−0.7
S.E. of the estimate	1.24%	1.88%	2.60%	2.04%

S.E. = standard error

The calibration curves ensure a reasonable reproducibility (Table 7). However the present method is not as precise as the widely-used gravimetric method of Trostel and Wynne (1940). The coefficient of variation quoted by Trostel and Wynne is about 1%. However their method takes about 8 hours per batch of analysis. The overall time per sample may be reduced by running several batches together, but this is not always possible as this may require a monopoly of laboratory space and equipment particularly

platinum ware. On the other hand, the X-ray diffraction method only requires 10 minutes to run the sample in triplicate.

Table 7 Reproducibility of quartz determination by X-ray diffraction method in four Purbeck samples.

	1	2	3	4
Mean	52.9%	25.1%	19.6%	10.8%
Standard deviation	6.0	2.1	2.0	1.3
Coefficient of variation	11.3%	8.6%	10.3%	11.8%
Number of runs	46	12	6	24

(b) Calcite and aragonite determination

Artificial calcite-aragonite standards were prepared using the bivalve *Ostrea edulis* (Recent) as calcite standard and the gastropod *Clavilithes macrospira* from the Barton Beds (Eocene) as an aragonite standard. Mineral purity was checked by X-ray diffraction. Neither shells have anomalous diffraction patterns, and thus they are acceptable as standards. The two shells were ground and a range of calcite-aragonite mixtures were prepared. After they were thoroughly mixed they were pelleted.

A scan was made from 25° – 31° 2Θ to include the 3.40Å and 3.27Å aragonite peaks and the 3.04Å calcite peak. The main calcite peak at 3.04Å is overlapped by the 3.06Å gypsum peak. Correction can be made using the ratio between 3.06Å and 7.56Å gypsum peaks.

Although peak areas of X-ray diffraction are more reliable (Milliman and Bornhold, 1973), peak heights were used as a measure of intensity since many lengthy corrections were involved. It was felt that the small additional improvement which might result from using peak areas is not justified in view of the time needed to measure the areas under the peaks. The average heights of the 3.40Å and 3.04Å peaks from three diffractometer scans were taken as the aragonite and calcite intensities.

Two calibration equations for calcite and aragonite were established as follows:

$$\text{Calcite } \% = 0.0583\ I - 1.9 \quad (1)$$

$$\text{Aragonite } \% = 0.179\ I - 2.6 \quad (2)$$

The correlation coefficients between peak intensities and mineral percentages are 0.998 and 0.996 for calcite and aragonite respectively. To reduce any electronic drift in the diffractometer, the ratio techniques was used to relate aragonite/calcite ratios to their peak ratios. This led to the following equation:

$$\frac{\text{Aragonite}}{\text{Calcite}} = 3.54 \times \frac{I\ (\text{Aragonite})}{I\ (\text{Calcite})} \quad (3)$$

Equation (3) was solved using the relation between the carbonate content and weight percentages of CO_2 available from the chemical analyses; the relation is in the following form:

$$\text{Calcite } \% + \text{Aragonite } \% = CO_2\ \% \times 2.27 \quad (4)$$

Calcite and aragonite are the essential carbonate minerals present in the samples studied. Dolomite traces below the detection limit of the diffractometer was recorded in one sample by staining.

As a check on reproducibility, calcite and aragonite in different pellets were repeatedly determined using the calibration equations. In calcite coefficient of variation ranges from 1.4 to 2.4% while in aragonite it varies from 5.2 to 12.2%. This figure indicate that the approach adopted for calcite and aragonite determinations is acceptable.

(c) Clay mineral determination

The weight percentage of the clay content in the middle Purbeck rocks was computed using the chemical data of the major elements. Assuming that the total percentages of

the major elements as oxides is equal to 100, and only clays, carbonates, quartz and organic carbon represent the essential rock components, the clay content is calculated as follows:

$$\text{Clay } \% = 100 - (\text{carbonate } \% + \text{quartz } \% + \text{organic carbon } \%)$$

However, the total percentage of the major elements as oxides differs slightly from 100%. Also, the other minerals such as pyrite and gypsum and rarely celestite, barite, geothite etc. are present in the order of 0.5 to 3%. To accommodate these limitations, the previous equation was slightly modified. The total of 100% was replaced by the actual sum of the major elements as oxides. The sulphur content was used to calculate pyrite and gypsum contents by multiplying the sulphur percentage by 1.87 and 5.38 respectively. When both minerals occur in the same sample as average factor of 3.63 was used.

The accuracy of the clay contents depends on accuracies of the major elements and quartz values. However, the correlation coefficient of 0.99 at the 0.1 level between the computed clay contents and determined Al_2O_3 indicates that the method is very reliable. Schultz (1964) concluded that this method of calculating the clay content is better than determining every clay mineral independently and summing them.

Identification of individual clay minerals was carried out only for the middle Purbeck shales. Initially the samples were treated with 5% acetic acid to remove the carbonates. Three sedimented clay samples ($> 2\mu$) were prepared on glass slides. This provides three films of clay with preferred basal orientation. After drying, one of the slides was heated to 575°C for one hour, the second was exposed to ethylene glycol vapour for two hours and the third was left untreated. The mounts were then run on the diffractometer between the angles of $2° - 16°$ 2Θ. Illite, kaolinite, montmorillonite and illite/montmorillonite mixed layers were the clay minerals most commonly identified

in the middle Purbeck shales.

The peak areas of the basal reflections in the glycolated mount were used to give semi-quantitative proportions of the clay mineral present in each sample (Shover, 1964). Knowing the total clay content, each clay mineral can be semi-quantitatively expressed as a percentage of the whole rock. Because it was difficult to separate the peak areas of montmorillonite and mixed-layer clay minerals, they were grouped together. It must be stressed that the contents of the individual clay minerals stated here are approximate values since during sample preparation differential settling can cause some inaccuracies (Gibbs, 1965; Stokke and Carson, 1973).

2. **Heavy mineral separation**

For this purpose about 400 gm. of each rock sample (mainly limestones) was treated with 1 : 1 hydrochloric acid. This was necessary to remove the carbonates and any ferrugenous material but solution of some of the 'heavies' such as apatite was anticipated. The grains in the size range 0.063 – 0.200 mm. were segregated by seiving. This size fraction contains the bulk of the heavy minerals in the sample (El-Shahat, 1968). The heavy minerals were separated from the light fraction using bromoform following the procedures outlined by Milner (1962). The heavy minerals were mounted on glass slides with Canada Balsam. Mineral identification was carried out with the aid of a petrographic microscope using the scheme given by Tickel (1965).

3. **Staining**

The staining technique described by Dickson (1965) was applied to more than 400 limestone thin-sections. The technique has been of great value in the study of the limestones of the Purbeck Group. Specifically, the distribution of ferrous ions can be revealed by the use of a potassium ferricyanide stain.

The staining of the thin-sections was performed in three steps:

1. The thin-section surface was etched with dilute HCl. Etching developed the intergranular boundaries and increased the clarity of the fabrics. Carbonate minerals have different rates of reaction with dilute HCl. Calcite and aragonite can be reduced greatly in thickness while dolomite is almost unaffected. Dolomite is rarely found in the middle Purbeck Group of Dorset; calcite and aragonite represent the carbonate minerals mainly identified in the present work.

2. Staining with acidified solution of alizarin red – S stains calcite red. Dolomite which is less affected by dilute HCl is unaffected. It was found that aragonite is less stained than calcite and gives a pale yellow colour. However, the colour developed by staining aragonite is insufficient for positive identification (Dickson, 1966). The degree of staining shown by calcite crystals is dependent upon optical orientation. Crystals parallel to the C-axis gave high colour-intensity whilst those normal to the C-axis stained very pale red and occasionally were unaffected. This difference provided an idea of the optic orientation of the calcite crystals. Organic remains such as charophyte fragments, ostracod carapaces and molluscan debris were stained a deeper red compared with the sparry calcite cements.

3. To differentiate between ferroan and non-ferroan varieties of calcite and dolomite, acidified solutions of potassium ferricyanide produce a precipitate of Turnbulls blue in the presence of ferrous ions. Ferroan calcite stains blue and ferroan dolomite stains turquoise. Non-ferroan varieties of calcite and dolomite are unaffected. Usually calcite with less than 0.5% FeO is not positively stained (Lindholm and Finkleman, 1972). Higher concentration of Fe^{2+} in the calcite lattice is indicated by deep blue stain (Evamy and Shearman, 1965; Oldershaw and Scoffin, 1967; Davies and Till, 1968; Colley and Davies, 1969; Evamy, 1969).

4. Porosity determinations

Two types of porosity are recognised, namely absolute and effective. Absolute porosity of a rock is defined as the ratio of total void space to bulk volume. Effective porosity is defined as the ratio of intercommunicating void space to bulk volume (Lalicker, 1949). Since rocks contain sealed pores, the absolute porosity is generally higher than the effective porosity.

Absolute porosity was determined for 150 samples from the middle Purbeck limestones following a method similar to that described by Lalicker (1949). The method is based on measuring absolute and bulk densities of the sample. Porosity in percent can be expressed in the following formula:

$$\text{Porosity } \% = \frac{(\text{absolute density} - \text{bulk density})}{\text{absolute density}} \times 100$$

Absolute density was measured using a density bottle. Determination of bulk density consists of the following steps:

1. The sample is weighed accurately in air
2. The bulk volume is measured after the sample was coated with water resistant liquid spray[1]. A correction can be made for the volume of spray coat knowing the weight and density of the spray used.

(1) Trycolag MK .IV made by Aerosol Marketing & Chemical Co., Limited, London.

8. PETROGRAPHY OF THE MIDDLE PURBECK GROUP 1: LULWORTH FORMATION

The middle Purbeck Group of Dorset affords an opportunity to study a wide variety of lacustrine and lagoonal carbonate rocks. The purpose of this part of the study is to present petrographic descriptions of diverse assemblage of carbonate lithologies of these lacustrine and lagoonal environments. This provides evidence for environmental interpretation and diagenetic synthesis.

It must be emphasised that this sequence is unusual in its thinly bedded and extremely varied character. It is not amenable to treatment in broad categories. It is the rocks which control the organisation of the petrographic chapters 8 and 9. This is stratigraphical rather than arranged in discrete sedimentological topics.

The rocks are considered in terms of 'facies' which have characteristic lithology and fauna. Thickness is not significant (*c.f.* Ainardi, 1975). Folk's limestone classification (1959) was used, with slight modifications, in describing the different limestone facies of the middle Purbeck Group. The term 'pellet' was replaced by the term 'pelletoid' which is used here as a descriptive term and does not connate origin (*c.f.* Milliman, 1974). Criteria for distinction between directly precipitated cement and neomorphic spar (pseudospar of Folk, 1959), have been taken from Bathurst (1975).

One of the facies, the bivalve biosparrudite, can frequently be subdivided into three petrographic types, based on degree of compaction and other criteria. In some stratigraphic units only one or two of these types are present. Differences exist within the same type at different stratigraphic units are described below.

The present chapter concerns the upper part of Lulworth Formation especially the strata located between the Mammal Bed and the base of the Cinder Beds. These strata comprise the Cherty Freshwater Beds and the upper part of the Marly Freshwater Beds.

1. Petrography of the Marly Freshwater Beds

At Durlston Bay, the Marly Freshwater Beds attain a thickness of 4.2 m. Only the upper part (1.9 m.) of the Marly Freshwater Beds belongs to the middle Purbeck Group. This part (beds DB83-DB86) was sampled and examined petrographically (see Fig. 12). The palaeontological importance of bed DB 83 (Mammal Bed) has been emphasized above (Chapter 3). Simpson (1928) and earlier authors have described the famous mammalian jaws of this bed. The most abundant fossils in the Marly Freshwater Beds, however, are the gastropods and ostracods. According to Clements (1969), the gastropods include many species which belong to the genera *Valvata, Hydrobia, Planorbis* and *Physa*. Ostracods include species of *Cypridea, Scabriculocypris* and less often *Fabanella, Mantelliana, Darwinula* and *Damonella* (Clements, 1969).

Petrographically, two limestone facies can be recognised in the Marly Freshwater Beds; ostracod-gastropod biomicrite and bivalve biosparrudite. These are described below.

(a) Ostracod-gastropod biomicrite facies.

In Durlston Bay, this facies is represented by beds DB84, DB85b and DB86 (Table 8). These limestones are poorly laminated, friable rocks which are medium light grey (N6) in colour[1]. The beds range from 10-100 cm. in thickness. The rocks are characterised by clay contents which range as high as 27%. The ostracod-gastropod biomicrite facies usually grades into friable calcareous shales and clays.

In thin-section, the bioclastic debris usually forms less than 20% of the rock volume. The matrix is essentially a mixture of micrite and clays. A few gastropods are well preserved. They are commonly infilled with ferroan calcite but occasionally with spherulitic chalcedony or quartz mosaics[2]. Some of the gastropods are still aragonitic

(1) Colour terms are from Goddard *et al.*, (1970).

(2) Quartz and chalcedony *sersu stricto* are the two varieties of silica encountered during the course of the present investigation.

especially in the samples which contain high clay contents. Bivalve fragements are extremely rare. When they occur, they are usually preserved as pseudo-pleochroic calcite mosaics, a good indication of the former presence of aragonite (Hudson, 1962; Hudson and Palframan, 1969; Kendal, 1975).

The composition and porosity of rocks of the ostracod-gastropod biomicrite facies are given in Table 8. Calcite contents range from 61-82%. Aragonite content is low and rarely exceeds 3%. Quartz content ranges from 3-8%. The porosity of the ostracod-gastropod biomicrite facies ranges from 3% up to the fairly high value of 17%. The porosity increases with increase of clay content.

(b) Bivalve biosparrudite facies[1]

This facies occupies the lower part of bed DB 85. In thin-section, the rock consists of a framework of large bivalve fragments up to 5 mm. in length and a matrix rich in smaller bivalve fragments, pelletoids, mud-clasts and less often ostracod fragments. The allochems represent about 80% of the rock volume; the rest is mainly ferroan calcite cements.

Spherical and ellipsoidal pelletoids are common. They are made of micrite which has a grain size less than 1μ diameter. Thin-sections made of fresh rock samples are usually rich in grey pelletoids while the brown pelletoids are more common in the weathered samples. The grey pelletoids are enriched in small (1–5μ) irregular black flakes, pyrite and organic matter, especially near the core of the pelletoids. The apparent length of the ellipsoidal pelletoids (in thin-section) ranges from 200-900 μ while the breadth varies

---

[1] The traditional boundary between 'rudite' and 'arenite' has been 2mm. (Pettijohn, 1957). Folk (1959) places the rudaceous/arenaceous boundary at 1 mm. In the middle Purbeck Group, the bivalve limestones usually have allochems with grain size either larger than 2mm. or smaller than 1 mm. Allochems ranging from 1–2 mm. are not common. It is, therefore, safe to use either the 2 mm. or 1 mm. as a rudaceous/arenaceous boundary. However, the 1 mm. boundary was adopted to ensure consistency with Folk's classification which is followed in the present work.

from 170-550 μ (Fig. 32). The dimensions of these pelletoids and the presence of organic matter and pyrite suggests that they are probably faecal in orgin (Bathurst, 1975).

Mud-clasts vary in size and are very irregular in shape. They usually show signs of fragmentation resulting from compaction. Syneresis cracks are abundant. Most of the mud-clasts are rich in small black inclusions. Some contain irregular filaments and probably are algal in origin. Small angular quartz grains occur in few clasts.

The bivalve fragments are preserved as ferroan calcite mosaics which show a gradual increase in grain-size away from the shell wall. Nevertheless, lines of inclusions revealing the original shell structure are common. Both pseudo-pleochroic and clear calcite occur in the same shell mosaics but their relative abundances vary considerably. Shell mosaics with up to 90% clear calcite and others entirely made of pseudo-pleochroic calcite occur side by side.

Most of the allochems are coated by a thin fringe of small calcite grains which represent the early cement precipitated. The fabrics of this early calcite cement are entirely dependent upon the nature of the substrate. When the substrate consists of heavily micritized bivalve grains, the early cements are extremely small in size and fibrous. In cases in which the bivalve grains are made of sparry calcite mosaics and lack micrite envelopes, the fringe cements are coarse and usually in optical continuity with the shell mosaics. In such cases the calcite fringe postdates the calcitization of the molluscan shell. The calcite cement which represents the main cementation phase is commonly rich in Fe^{2+} and much coarser than the early cements.

Silicification of the bivalves is mainly confined to those that are calcitized. Relics of the original shell structure are preserved in a few cases. The ostracod debris is partially silicified. Occasionally the early calcite cements are silicified in examples in which the main phase

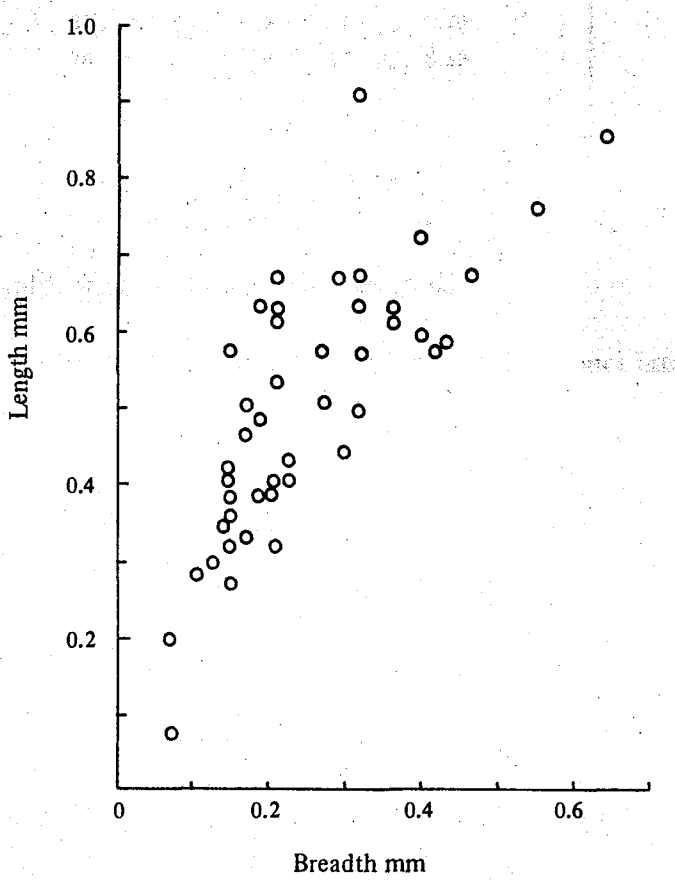

Fig. 32. Dimensions of some pelletoids in bivalve biosparrudite (bed DB85a).

calcite cements are unaffected. Silicification probably started shortly before calcitization and was completed before the main phase of calcite cementation.

Table 8. Mineralogy and porosity of the limestones of the Marly Freshwater Beds of Durlston Bay.

Bed Number	Sample Number	Calcite %	Aragonite %	Quartz %	Clay %	Organic Carbon %	Porosity (%)	Facies
DB 84	3	61	2	6	27	0.48	7	Ostracod-gastropod biomicrite
DB 85b	5	82	3	3	4	0.20	3	
DB 85b	6	76	–	3	15	0.59	7	
DB 86	7	63	3	8	22	1.21	17	
Average		71	2	5	17	0.62	8.5	
DB 85a	4	82	4	2	4	0.11	1	Bivalve biosparrudite

2. Petrography of the Cherty Freshwater Beds

These beds comprise several different types of limestones interbedded with calcareous shales. Most distinctive in this sequence is a bed of pinkish grey (5 YR 8/1) marl, in which most of the chert occurs. This bed is known as the 'Flint Bed' and is present in all localities in Dorset, forming a useful marker horizon (Fig. 12).

The Cherty Freshwater Beds are rich in their bioclastic content especially the ostracods and gastropods. Ostracods are represented by different species belonging to the genera *Cypridea, Theriosynoecum, Darwinula, Fabanella* and less often *Rhinocypris, Mantelliana* and *Orthonotacythere* (Clements, 1969). Among the gastropods found in the Cherty Freshwater Beds of Durlston Bay the most important are the following genera: *Valvata, Hydrobia, Viviparus, Planorbis* and *Physa* (Clements, 1969). The bivalves are locally very abundant especially in Durlston Bay. They include *"Cyclas"* (Fisher, 1856), *"Cyrena"* (Damon, 1884) and *Unio* (Clements, 1969). Among the Reptilia the most important are the goniopholid crocodiles (Joffe, 1967) found in the

'Feather Bed'. Sponge spicules of *Spongilla purbeckensis* Young are locally abundant in the 'Flint Bed' (Young, 1878; Hinde, 1912). From the same bed charophyte remains, mainly of the genera *Clavator* and *Perimneste,* have been described by Forbes (1851), Weathered (1890) and Harris(1939).

The Cherty Freshwater Beds in Durlston Bay comprise three limestone facies: charophyte biomicrite, ostracod biomicrite and bivalve biosparrudite facies (Table 9). Mineralogically, they mainly differ in the contents of calcite, clay and organic carbon. Porosity values are higher in the charophyte biomicrites and ostracod biomicrites in comparison with the bivalve biosparrudites.

(a) Charophyte biomicrite facies

In Durlston Bay, this facies appears in bed DB 89, DB 97 and DB 99 (Fig. 12). In outcrops, the rocks range from medium light grey (N4) to pinkish grey (5 YR 8/1) in colour and beds very from 10-85 cm. in thickness. Lamination is poor; it becomes more obvious with increasing content of clay. Burrows are locally abundant especially in bed DB 89. Desiccation cracks are common and small chalcedony pseudomorphs after halite occur in bed DB 97, the 'Flint Bed' (Meyer, 1872). Particularly interesting are large halite pseudomorphs up to 2 cm. in diameter which are common in the charophyte biomicrite facies at Bacon Hole. Chert nodules occur extensively in the facies and mainly confined to the 'Flint Bed' (Fig. 7). The nodules are brownish black (5 YR 2/1) in colour, varying in size up to 50 cm. in diameter. Only a few of the large nodules have some degree of elongation parallel to the bedding.

In thin-section, the bioclastic contents are up to 50% of the rock volume; usually present as floating allochems in a matrix of micrite rich in highly fragmental ostracod debris. Fossils are varied; they include charophyte, ostracods, gastropods, sponge

Table 9. Mineralogy and porosity of the limestone of the Cherty Freshwater Beds in Durlston Bay

Bed Number	Sample Number	Calcite %	Aragonite %	Quartz %	Clay %	Organic carbon %	Porosity (%)	Facies
DB 89	12	81	2	3	7	0.19	2	
DB 89	13	89	2	2	2	0.25	2	
DB 97	22	71	–	4	12	1.90	10	
DB 97	23	86	–	2	6	0.40	12	Charophyte biomicrite
DB 97	193	97	–	1	1	0.36	15	
DB 99	26	85	–	2	9	0.60	8	
Average		85	1	2	6	0.62	8	
DB 88	10	70	1	5	18	1.86	13	
DB 88	11	68	3	6	16	2.40	17	
DB 90	14	67	2	1	21	0.81	8	
DB 95	19	81	1	4	8	0.40	2	
DB 96	20	86	3	2	4	0.87	15	Ostracod biomicrite
DB 96	21	68	2	4	14	3.67	11	
DB 105	33	74	–	5	12	1.13	11	
DB 107	35	81	–	2	13	0.36	2	
DB 110	39	71	3	3	12	3.40	1	
Average		74	2	4	13	1.66	9	
DB 87	8	95	2	2	–	0.12	2	
DB 87	9	83	–	7	4	0.62	5	
DB 94	18	84	4	3	3	0.37	4	
DB 101	28	94	–	1	–	0.24	1	
DB 103	31	80	5	3	5	0.69	5	Bivalve biosparrudite
DB 106	34	88	2	2	2	0.21	4	
DB 108	36	96	–	1	–	0.16	5	
Average		89	2	3	2	0.34	4	

spicules, bivalve fragments and turtle and fish remains.

Charophytes are especially abundant in the chert nodules of the 'Flint Bed'. Charophyte remains were found in great quantities in this bed at Worbarrow Tout where they are locally rock builders. The local abundance of the plants suggests that the remains accumulated near the place where they grew. In thin-section, it is significant that charophyte stems up to 7 mm. diameter are common; nodes and inter-

nodes can be recognised (Figs. 33 and 34). It is unusual to find oogonia and charophyte stems together in these beds. This was observed by Carozzi (1948) in the Purbeck of the Jura. The cylindrical shape of the plant is usually undistorted in silicified samples but in some cases it has been distorted indicating that the plants were crushed before lithification (Fig. 33). In the 'Flint Bed', the stem walls of the plant are usually silicified while the cavities of the cortical tubes are infilled with sparry calcite (Fig. 34).

Ostracods are common in the charophyte biomicrite facies. Fragmented ostracods are very abundant and locally they are rock-forming. The fragments range from 5 μ upwards. Ostracods with preservation of paired valves are not common in this facies. Large and small ostracods occur in the same rock suggesting either different growth stages or different species. Ostracods are usually infilled with sparry calcite although some micritic sediment produces a geopetal structure.

Gastropods were occasionally seen in thin-section. They are commonly infilled with coarse sparry calcite (Fig. 35). Preservation is particularly good when they are preferentially silicified.

Although often difficult to find sponge spicules *(Spongilla purbeckensis)* are abundant at certain horizons and localities (Fig. 35). Locally, they are "exceedingly numerous, so as to constitute the main portion of the chert in which they occur" (Hinde, 1912; p.212). In the present investigation they were encountered in the charophyte biomicrite facies at Worth Matravers (SY/997778). These spicules have an average length of 330 μ. The longest measured was 530 μ, slightly higher than the 415 μ reported by Hinde (1912). The maximum diameter ranges from 20-40 μ. The original opaline silica of the sponges has often been replaced by calcite of crystal diameter between 3

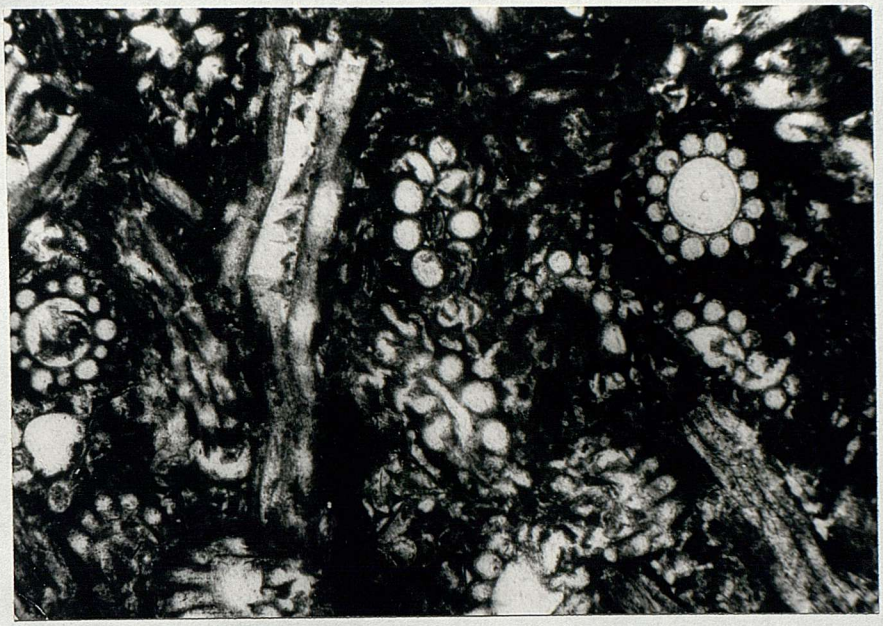

Fig. 33. Silicified charophyte biomicrite showing longitudinal sections in the node and traverse sections mainly in the internodes.

Plane polarised light Width of field 2.9 mm.

Charophyte biomicrite facies Cherty Freshwater Beds: bed DB 89, Durlston Bay

Fig. 34. Longitudinal section in charophyte stem showing the node and internode. The cavities within the cortical tubes are infilled with sparry calcite while the walls of the stems are silicified.

Plane polarised light Width of field 2.9 mm.

Charophyte biomicrite facies Cherty Freshwater Beds: bed 22b, Worbarrow Tout

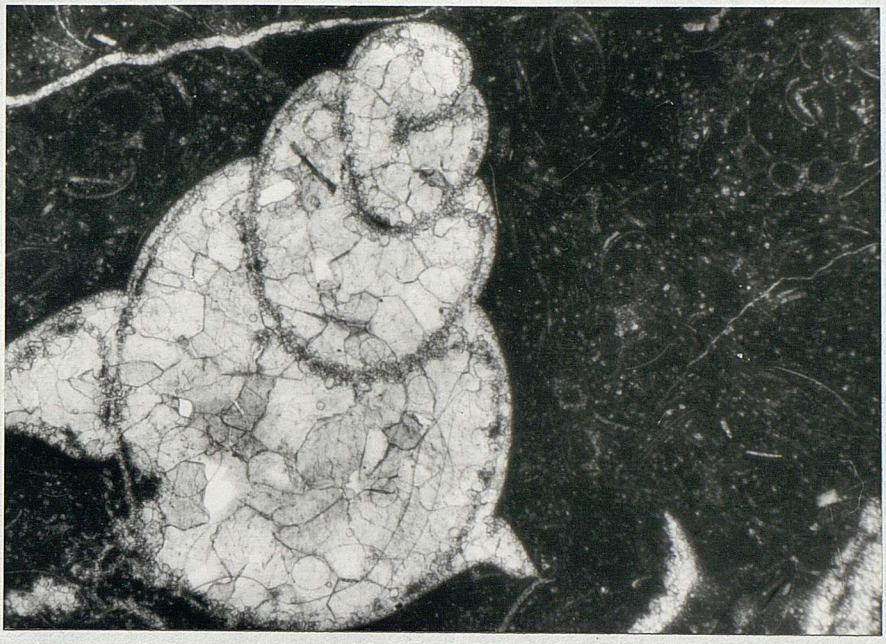

Fig. 35. Charophyte biomicrite with gastropods *(Viviparus?)* and *Spongilla purbeckensis.* The matrix is a micrite with ostracod and charophyte fragments. The small points are traverse sections of the sponge spicules.

Plane polarised light Width of field 2.9 mm.

Charophyte biomicrite facies Cherty Freshwater Beds: Worth Matravers

Fig. 36. Large fragmented vertebrate bones in a matrix of dense micrite.

Plane polarised light Width of field 2.9 mm.

Charophyte biomicrite facies Cherty Freshwater Beds: bed 13, Bacon Hole

and 10 μ. Acid-insoluble residues of the limestones around chert nodules are usually rich in silicified spicules.

Bivalves are rare in the charophyte biomicrite facies. They are present as small fragments mostly preserved as pseudo-pleochroic calcite, although few are still aragonitic. Partial silicification commonly preserves the details of the original shell structure.

Bone fragments are commonly encountered both in the hand-specimens and in thin-sections (Fig. 36). Fish scales are numerous in the 'Flint Bed' at Lulworth Cove and large fragments of turtle bones occur in the same bed at Bacon Hole.

Micrite (less than 2 μ) forms the main bulk of the charophyte biomicrite rocks. Some micritic sediment occasionally occurs within gastropod chambers and ostracods where it is developed geopetally and is overlain by coarse sparry calcite.

Veins are few; when they occur, they are usually infilled with ferroan calcite. Such veins cut all the fabric elements and postdate lithification.

The composition and porosity of limestone of the biomicrite facies are given in Table 9. Calcite content ranges from 74-97% while aragonite has only been detected in bed DB 89 where about 2% occur. Clay content ranges from 1% up to only 12%. Quartz content ranges from 1-4% and occurs mainly as quartz and grains which are usually subangular and up to 100 μ in diameter. Organic carbon ranges from 0.2% to 1.9%. The porosity of the charophyte biomicrite varies from 2% up to the fairly high figure of 15%.

(b) Ostracod biomicrite facies

This facies appears in several parts of the Cherty Freshwater Beds of Durlston Bay (Table 9). Individual beds range from 25-60 cm. in thickness. The rocks are soft

and range from light grey (N7) to medium grey (N5) as the clay content increases. Lamination is well-developed and visible both in hand-specimens and in thin-sections. In a few beds lamination is not well-developed probably as a consequence of bioturbation (e.g. bed DB 95).

Micrite forms the greatest proportion of the rocks. The grain size of the micrite components is usually less than 4 μ and crystal enlargement of the micrite has rarely occurred. Where it has, the micrite does not exceed 10 μ in diameter. Pelletoids are present within thin laminae rich in subangular quartz grains. They are darker than the surrounding micrite and usually contain small black inclusions (1-6 μ) particularly in the central parts. A few pelletoids have 'oolitic' coatings.

Content of bioclastic debris ranges from 20-50% of the rock volume, mainly represented by ostracods while shell fragments of gastropods and bivalves are less important. The ostracods are mostly fragmented (Fig. 37). Well-preserved ostracods are locally common and usually infilled with chalcedony or sparry calcite. When they are infilled with chalcedony, small euhedra of pyrite are common,especially near the ostracod walls (Fig. 38). Ostracods infilled with sparry calcite usually contain geopetal micrites (Fig. 39). In bed DB 95, extremely small ostracods occur and perhaps they are juveniles. Bivalves are highly fragmented and although commonly preserved as mosaics of pseudo-pleochroic calcite a few are still aragonitic.

Veins infilled with celestite were found in the ostracod biomicrite facies of Worbarrow Tout (Fig. 39). Ferroan calcite veins are present. From intersection relationships, the sequence of diagenetic events was: 1. non-ferroan calcite 2. chalcedony 3. ferroan calcite 4. celestite.

The composition and porosity of the ostracod biomicrite facies are given in Table 9.

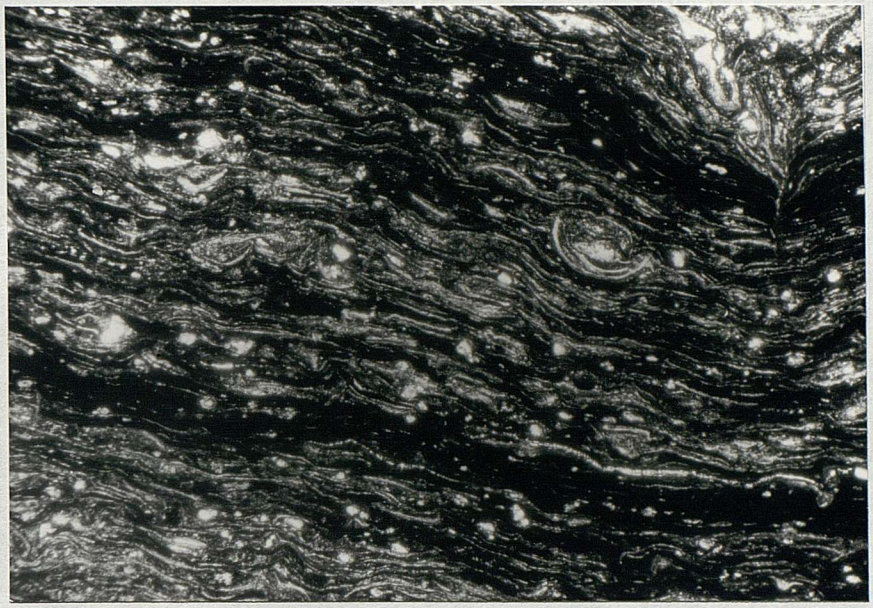

Fig. 37. Alternating laminae of ostracod biomicrite and calcareous shale rich in organic matter. Most of the ostracod valves are flattened by compaction.

Plane polarised light Width of field 2.9 mm.

Ostracod biomicrite facies Cherty Freshwater Beds: bed DB 110, Durlston Bay

Fig. 38. A well-preserved ostracod in a matrix of micrite and ostracod debris. The ostracod is infilled with spherulitic chalcedony. Euhedral pyrite are common adjacent to the ostracod wall.

Plane polarised light Width of field 1.3 mm.

Ostracod biomicrite facies Cherty Freshwater Beds: bed DB 88, Durlston Bay

Fig. 39. Ostracods infilled with sparry calcite and geopetal micrite. A post-lithification celestite vein forms the lower part of the field of view.

Plane polarised light Width of field 2.9 mm.

Ostracod biomicrite facies Cherty Freshwater Beds: bed 6, Worbarrow Tout

Fig. 40. Bivalve fragments preserved mainly as pseudo-pleochroic calcite and coated by thick micrite envelopes. The bivalve grain (in the middle) shows tubes resulted from algal boring. The opaque grains include pelletoids and mud-clasts.

Plane polarised light Width of field 2.9 mm.

Bivalve biosparrudite facies Cherty Freshwater Beds: bed DB 87, Durlston Bay

Calcite content ranges from 67-86% while aragonite is present in small amounts up to 3%. Clay and quartz contents vary from 4-21% and from 1-6% respectively. Organic carbon occurs in all samples and ranges between 0.4% and 3.67%. Porosity values vary considerably, from 1% to the high figure of 17%.

(c) Bivalve biosparrudite facies

In the Lulworth Formation of Durlston Bay, the bivalve biosparrudites are most abundant in the upper part of the Cherty Freshwater Beds. They are represented by beds up to 150 cm. of medium grey (N5) to pale yellowish brown (10 YR 6/2) in colour. At a short distance from Durlston Bay, at Harden's Quarry, the facies grades into biomicrites and biosparites (Fig. 12). At Worbarrow Tout, the bivalve biosparrudites are much reduced in thickness. Further west, from Bacon Hole to Ridgeway, this facies dies out completely (Fig. 12).

The bivalve biosparrudite facies is characterized by high carbonate contents which vary from 83-97%. Quartz occurs in small quantities up to 7%. Average organic carbon is low (0.34%) in comparison with most of the facies described before (Table 8 and 9). Porosity ranges from 1-5%.

In Durlston Bay, the bivalve biosparrudite facies of the Cherty Freshwater Beds comprises three petrographic types. They differ in the nature of bivalve preservation, content of sparry calcite between the allochems and degree of compaction. The three types are gradational.

Type 1. Typical examples of this type include beds DB 94, DB 103 and DB 106 of Durlston Bay. Type 1 is characterized by the abundance of pseudo-pleochroic calcite as a replacive fabric of the former aragonite. The amount of sparry calcite between the allochems is low and usually less than 10% of the rock volume. Compactional features

are very common. The bioclastic debris is dominated by bivalves; gastropods, ostracods and reworked charophyte fragments are present but volumetrically insignificant.

The rocks are essentially composed of disarticulated valves of bivalves, occasionally nested one within the other. Small localized areas appear to be entirely composed of valves which are in contact for most of their length with very little cement in between. Locally, many shells are fragmented into small pieces with various orientations which suggests some rotation. If these small fragments are reassembled they would form complete valves. There is no doubt that these compactional effects occurred before the main cementation phase. Lack of cement or a matrix supporting the originally loosely-packed structure, explains the highly fragmented nature of the bivalves. On the other hand, breakage of the shells occurred after the development of the early cement (thin fibrous calcite fringe) since it is absent on the fractures. Generally, breakage occurred as a result of direct load effects. Most of the broken shells have their long axis parallel to the bedding i.e. at right angles to the applied load. Here, compaction is mainly a direct function of the weight of the overlying sediments.

Calcitization of the former aragonite occurred before the main cementation phase but after the compaction. This is indicated by the following petrographic observations:

1. Shell mosaics are optically continuous across the shell boundaries towards the sparry calcite in the matrix.

2. When spar has filled the fractured shells it is controlled by shell mosaics i.e. in optical continuity of the shell fabrics.

3. Separate shell fabrics on either side of the fracture would be in optical continuity if reunited.

Post-lithification features are shown by ferroan calcite veins which intersect all the sedimentary fabrics.

Type 2. In Durlston Bay, this type occurs in bed DB 87 which represents the lowest horizon of the Cherty Freshwater Beds (Fig. 12). In type 2, the fabrics are more or less open since most of the allochems are in contact only for small proportions of their lengths. The allochems represent about 70% of the rock volume – the rest being occupied by sparry calcite. Apart from the bivalves, gastropods and ostracods are present. Pelletoids and mud-clasts are locally abundant (Fig. 40). Small chert nodules occur both in hand-specimens and in thin-sections. Most of the allochems have rounded edges suggesting abrasion prior to final deposition.

The bivalve fragments are preserved in a way similar to that described in the bivalve biosparrudite facies of the Marly Freshwater Beds. Clear calcite and pseudo-pleochroic calcite occur in the same shell fabric. Thick micrite envelopes, usually coat most of the bivalve fragments (Fig. 40). The early fibrous calcite cement was followed by granular calcite generation. Compactional features are not common. Type 2 represents an intermediate diagenetic stage between those attained by type 1 and type 3.

Type 3. This type is represented in Durlston Bay by beds DB 101 and DB 108, known locally as the 'New Vein' and the 'Feather Bed'. The content of sparry calcite between the allochems is low and represents about 15% of the rock volume. Micrite is present and commonly trapped in the concave side of bivalves. Complete bivalve valves are common. Gastropods and ostracods are rare. Reworked charophyte fragments are common particularly in bed DB 101 and probably derived from the main charophyte bed beneath (bed DB 97). Mud-clasts are locally abundant.

In type 3, the majority of the bivalves are preserved as moulds infilled

with non-ferroan calcite cement and surrounded by thick micrite envelopes. These fabrics suggest a stage of solution and the formation of cavities due to early leaching of some of the former aragonite[1]. Pseudo-pleochroic calcite is rarely present in the shell mosaics. Nevertheless, bivalve fragments consisting of calcite mosaics rich in inclusions relating to the original aragonitic shell structure do occur. Silicification is mainly confined to the ostracods and occasionally the early calcite fringe.

(d) Bivalve biosparite facies

This facies was only recognised in the Cherty Freshwater Beds in the inland quarries near Swanage particularly at Harden's Quarry. The facies is made up mainly of well-sorted bivalve fragments usually less than 1 mm. in diameter (Fig. 41). Whole bivalve shells are rare but when present they are commonly preserved as pseudo-pleochroic calcite mosaics (Fig. 42). Angular quartz grains are present in small quantities.

Most of the bivalve fragments are very rounded, ellipsoidal in shape and extremely micritized. A first impression is that these allochems are pelletoids (Fig. 41). Careful examination, however, reveals that they were products of intensive micritization of bivalve fragments. All degrees of micritization could be traced from grains slightly altered to others completely micritized. Skeletal grains in the early stages of micritization are readily identifiable. They occur as moulds infilled with sparry calcite and surrounded by thick micrite envelopes. The skeletal grains in a more advanced stages of micritization needed to be scanned carefully for traces of the original shell structure.

---

[1] The preservation of molluscan shells as moulds infilled with granular calcite indicates that they were aragonite. This was observed since 1858 by Rose (in Horwood, 1911). Bathurst (1964) described similar textures in which the micrite envelopes act as moulds when the skeletal aragonite is dissolved. Friedman (1964) reported similar fabrics developed in subaerially exposed carbonate of Pleistocene age. Brown (1964) described biosparites with these characteristics from the lower Purbecks.

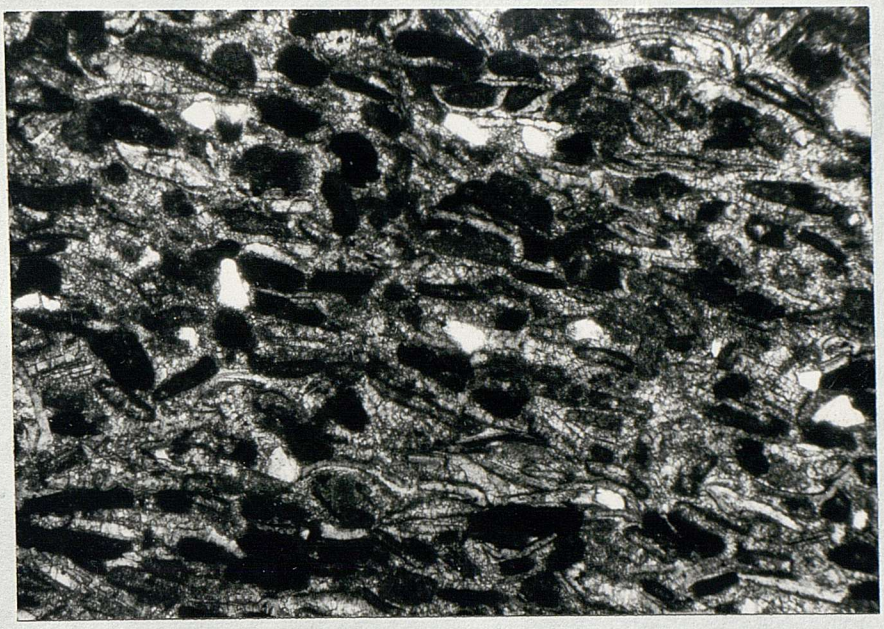

Fig. 41. Intensive micritization of bivalve fragments by boring algae. Most of the grains are rounded and resemble pelletoids.

Plane polarised light Width of field 2.9 mm.

Bivalve biosparite facies Cherty Freshwater Beds: bed 8, Harden's Quarry

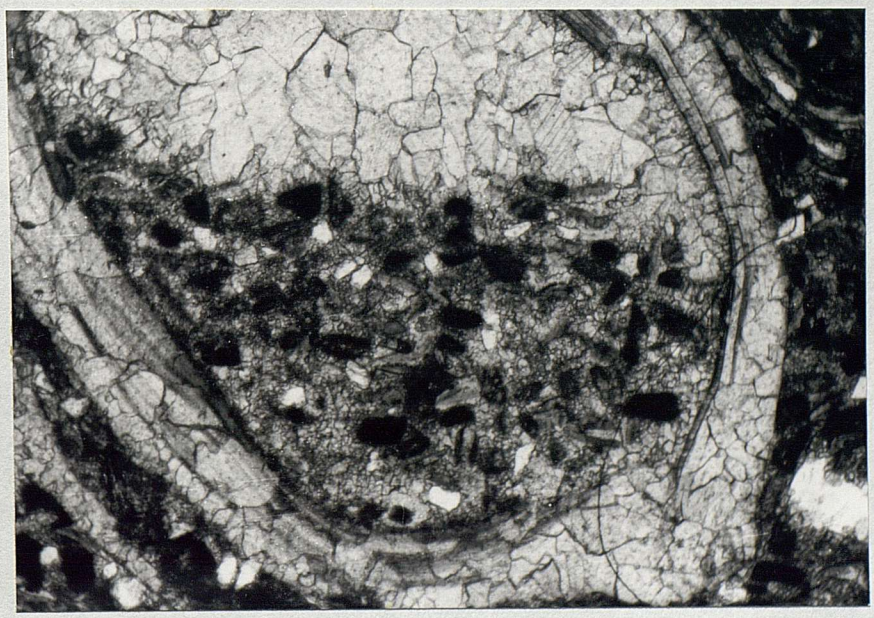

Fig. 42. Geopetal structure developed within a paired bivalve shell. The floor is rich in rounded micritized skeletal debris and angular quartz grains. Calcite cements include the early fibrous fringe and the main phase generation.

Plane polarised light Width of field 2.9 mm.

Bivalve biosparite facies Cherty Freshwater Beds: bed 8, Harden's Quarry

The fabric described above suggest that the skeletal grains were extensively micritized by boring algae. Micritized skeletal sands produced by boring algae form a considerable part of the recent carbonate sand in Bimini lagoon (Bathurst, 1966). He further pointed out that the "production of micrite peloids in this fashion may have played a big role in the sedimentation of ancient limestones. The Cherty Freshwater limestones described confirm this process.

(e) **Chert nodules**

These nodules occur extensively in the 'Flint Bed'. Examination of nodules shows that all fossil content and most of the primary sedimentary structures are similar to those of the surrounding host limestone. The nodules are not associated with fissures or joints. Thus silicification took place before uplift. A pre-compaction origin for the nodules is suggested since the original carbonate textures within the nodules show no signs of compaction at the time of silicification. In the host limestone many of the skeletal cavities are infilled with chalcedony or quartz mosaics. This indicates that silicification occurred before precipitation of calcite cements in the host sediments. The preservation of shell structures in some of the silicified aragonitic molluscs suggests that silicification began before calcitization.

Sponge spicules are abundant in the chert nodules. Most of the spicules which can be recognised in the host limestone are replaced by calcite while in the nodules the original opaline silica of the spicules has been replaced by chalcedony. If it is assumed that the spicules were originally equally distributed through the limestone, then most of the opaline silica of the spicules must have gone into solution and was localised as chert nodules.

9. PETROGRAPHY OF THE MIDDLE PURBECK GROUP: 2 DURLSTON FORMATION

The Durlston Formation commences at the base of the Cinder Beds and continues upwards to the Purbeck-Wealden boundary. Only the strata between the base of the Cinder Beds and the base of the Upper Broken Shell Limestone are included within the "middle Purbecks" (Arkell, 1947), and were investigated by the present writer.

1. Petrography of the Cinder Beds

These oyster beds are stratigraphically the most important beds within the whole Purbeck Group. They are traceable in borings and outcrops along a front of 240 km. from Dorset to Kent (Howitt, 1964). Within Dorset the Cinder Beds are readily recognisable from Durlston Bay in the east to Ridgeway in the west (Fig. 12).

The Cinder Beds can be divided into three parts which differ in the proportions of oyster valves present. The middle part is richer in oysters than the other two. Here there is a band about 30 cm. (the Urchin Band of Fisher, 1856), which contains the echinoid *Hemicidaris purbeckensis* and its spines with *Serpula coacervata* mingled with the oysters. The 'Urchin Band' can be traced to the inland quarries around Swanage and further west, probably to Worbarrow Tout.

The Cinder Beds mostly consist of valves of *Liostrea distorta* in a matrix of fine grained carbonate mud. The colour of the Cinder Beds depends on the quantity of oysters and on degrees of weathering. The rocks are generally medium dark grey (N4) in colour. They become very friable when they are weathered and then acquire a brownish grey (5 YR 4/1) colour. Bedding is very poor, though large fragments of oysters show rough orientation parallel to the general bedding.

Although the Cinder Beds have a dull argillaceous appearance, there is only 2-8% clay. Carbonate content ranges from 83-92%; it is essentially calcite. Aragonite was recorded in one sample from the Cinder Beds of Durlston Bay (Table 10). Quartz content (3%) appears to be constant through the Cinder Beds.

Table 10. Mineralogy and porosity of the Cinder Beds of Durlston Bay

Bed Number	Sample Number	Calcite %	Aragonite %	Quartz %	Clay %	Organic carbon %	Porosity (%)
DB 111a	42	86	3	3	5	0.17	3
DB 111a	197	83	–	3	8	0.28	3
DB 111b	41	92	–	3	2	0.11	3
DB 111b	196	91	–	3	2	0.36	3
DB 111c	40	87	–	3	5	0.30	4
Average		88	0.6	3	4.5	0.24	3

Petrographically, the bivalve biomicrudites of the Cinder Beds can be divided into two types according to the abundance of oysters. These are described below.

Type A. Generally the oyster content of this type are up to 40% of the rock volume. The oyster shells vary in size from less than 1 mm. to more than 2 cm. Most of the oyster fragments have few contacts and appear to be floating in a micrite-microspar matrix. Some of the oysters are silicified particularly some individual laminae forming the foliated shell structure.

Oyster valves are constructed mainly of calcite; only the adductor myostracum consists of aragonite (Stenzel, 1971). Two types of shell structures were recognised in *Liostrea distorta.* The first shell structure is a prismatic layer which consists of small parallel calcite prisms (6 μ in breadth) orientated obliquely to the main shell layers. A few oysters still retain this prismatic layer but in most cases it has been lost before final desposition. The early date of destruction was indicated by the common occurrence

Fig. 43. Large *Liostrea* fragments surrounded by dense micrite. Note the foliated shell structure of the oysters.

Plane polarised light Width of field 2.9 mm.

Bivalve biomicrudite facies (type A) Cinder Beds: bed DB 111, Durlston Bay

Fig. 44. Development of microspar at the expense of micrite. Non-oyster bivalves are readily recognisable by the pseudo-pleochroic shell mosaics.

Plane polarised light Width of field 2.9 mm.

Bivalve biomicrudite facies (type B) Cinder Beds: bed DB 111, Durlston Bay

of individual prisms in the groundmass.

The second structure found in *Liostrea* resembles the foliated structure described by Boggild (1930). It is built of successive calcite layers occasionally parallel to the surface of the shells (Figs. 43 and 44), but more often irregular with an appearance resembling cross-bedding (Fig. 51). The foliated structure aids identification of *Liostrea* even small fragments.

The bivalves other than oysters are present as calcite mosaics occasionally rich in pyrite. Micrite envelopes are not common and usually merge into the surrounding micrite-microspar matrix. Pseudo-pleochroic calcite is rare in the shell mosaics.

A few grains of detrital quartz are present in the matrix. They mainly range from 10-300 μ in diameter but larger grains occasionally occur when the oyster debris is abundant.

Type B. This type of limestone has a large proportion of non-oyster bivalves. Content of bioclastic debris ranges from 20-40% of the rock volume. Thin-sections show that the facies grades into bivalve biomicrites.

Most of the bivalves are heavily bored and fragmented. The non-oyster bivalves occur as shell mosaics of clear calcite, and less commonly as pseudo-pleochroic calcite (Fig. 44).

Micrite and microspar constitute more than 60% of the rock volume. Size distribution of the calcite matrix is given in Fig. 83. Typical micrite ($< 4\ \mu$), is usually less than 20% of the size population and more than 50% of the population occurs in the range 5-15 μ.

2. Petrography of the Intermarine Beds

The Intermarine Beds are readily recognisable in the field as the building stones

occurring between two nearly marine phases, the Cinder Beds below and Scallop Beds above.

The Intermarine Beds are rich in their fossil content. The fauna are dominated by bivalve especially *Neomiodon* and *"Cyclas"*. *Liostrea* fragments are common in small quantities in many beds. Ostracods are represented mainly by species of *Cypridea, Darwinula, Theriosynoecum* and *Macrodentina* (Clements, 1969). Gastropods include species of *Hydrobia, Viviparus, Ptychostylis, Planorbis* and, less often, *Theodoxus, Physa* and *Valvata* (Clements, 1969). Fish bones are common in the lower part of the Intermarine Beds especially in beds DB 112 and DB 115 of Durlston Bay. Turtle bones occur frequently in the middle part of the succession mainly in beds DB 129, DB 131 and DB 133. The arthropod, *Archaeoniscus* has been reported (Fisher, 1856). from a horizon corresponding to bed DB 128. During the present study foraminifera were discovered in this bed. Charophyte fragments are very abundant at a lower level in the succession (beds DB 115 and DB 116). The green alga *Ortonella* occurs as algal clasts particularly at the top of bed DB 133.

The Intermarine Beds are of varied lithology. At Durlston Bay the following limestone facies were recognised in the Intermarine Beds:

1. Charaphyte biomicrite
2. Ostracod biomicrite
3. Bivalve biomicrudite
4. Bivalve biosparrudite

Although most of these facies were previously recognised in the Lulworth Formation, in the Intermarine Beds they differ in many respects. The development of uniform parallel bedding, cross-lamination, ripple-marks and influx of coarse detritus,

Table 11. Mineralogy and porosity of the biomicrite and biomicrudite facies in the Intermarine Beds of Durlston Bay

Bed Number	Sample Number	Calcite %	Aragonite %	Quartz %	Clays %	Organic carbon %	Porosity (%)	Facies
DB 115	48	64	–	4	25	0.47	13	Charophyte biomicrite
DB 116a	49	98	–	1	–	0.22	3	
DB 116b	50	91	–	2	2	1.16	13	
Average		84	–	2	9	0.62	9	
DB 114	46	77	1	2	11	0.52	2	Ostracod biomicrite
DB 114	47	56	3	5	30	1.92	20	
DB 117	51	48	3	4	37	3.16	5	
DB 118	52	93	1	1	2	0.93	9	
DB 119	53	93	–	1	2	0.59	3	
DB 129a	68	86	3	3	3	1.90	8	
DB 129b	70	78	9	4	2	0.42	3	
DB 129b	71	68	6	4	13	3.35	8	
Average		75	3	3	13	1.72	7	
DB 112	43	89	3	2	2	0.06	4	Bivalve biomicrudite
DB 126	62	79	3	3	9	0.40	10	
DB 127	65	73	3	3	16	0.42	7	
DB 128	67	66	3	5	22	0.98	10	
Average		77	3	3	12	0.47	8	

especially at Ridgeway, mark a high energy environment.

(a) Charophyte biomicrite facies

The rocks belonging to the charophyte biomicrite facies are medium grey (N5) to pinkish grey (5 YR 8/1) in colour; they acquire a white chalky appearance (N9) when weathered (Fig. 27). They either thin-bedded or massive and are usually intercalated with calcareous shales. Individual beds range in thickness from 20-55 cms. Sedimentary structures include desiccation cracks and burrows. In Durlston Bay, beds DB 115 and DB 116 belong to the charophyte biomicrite facies.

In thin-section, proportion of bioclasts ranges from 20-70%. The matrix is mainly dark micrite and clay sometimes with scattered silt-sized grains of detrital quartz.

Fossils are represented by charophytes, ostracods, bivalves and gastropods. The charophytes are not as well preserved as in the Cherty Freshwater Beds. Vertebrate bones are abundant in beds belonging to this facies in the quarries near Swanage. Ostracods and gastropods are usually fragmented. Bivalves are present as calcite mosaics containing abundant lines of inclusions which are relics of the original shell structure. When the bivalves are locally concentrated, they are usually partially or completely silicified and in such cases a palimpest of the original shell structure is preserved (Fig. 45). Calcitization of the silicified bivalve fragments usually result in coarse calcite mosaics (Fig. 46).

The mineralogical compositions and porosities of the charophyte biomicrite facies are given in Table 11. Calcite content ranges from 64-98%, the quartz content is low (1-4%) and clay percentage varies considerably (from 0 -25%). The porosity ranges from 3% up to the fairly high figure of 13%. Although the charophyte biomicrite facies is rich in plant remains, organic carbon is low (0.22-1.16%). The similarities in mineralogic composition and porosity of the charophyte biomicrite facies described from the Intermarine Beds and Cherty Freshwater Beds are striking (Table 12).

Table 12. Composition of charophyte biomicrite facies in the Cherty Freshwater Beds and Intermarine Beds of Durlston Bay

	Cherty Freshwater Beds	Intermarine Beds
Calcite %	85	84
Aragonite %	1	–
Quartz %	2	2
Clay %	6	9
Organic carbon %	0.6	0.6
Porosity (%)	8	9

Fig. 45. Bivalve fragment in which details of the shell structure have been preserved by silicification.
Plane polarised light Width of field 1.1 mm.
Charophyte biomicrite facies Intermarine Beds, Harden's Quarry

Fig. 46. Large bivalve fragment showing a phase of silicification followed by a phase of calcitization (to the right). The ostracod (to the left) is infilled with quartz mosaics and coated with chalcedony (black) which shows banding.
Crossed polars Width of field 2.9 mm.
Charophyte biomicrite facies Intermarine Beds, Harden's Quarry

(b) Ostracod biomicrite facies

This facies appears in several parts of the Intermarine Beds of Durlston Bay (Table 11). Beds range in thickness from 10 cm. to 140 cm. but they are thinly bedded and evenly laminated, split readily into layers of 1-4 cm. thick. Calcareous shale parting are common while in bed DB 129 sandy laminae are frequent. Burrows are common especially in beds DB 114 and DB 118. Desiccation cracks are locally abundant.

Petrographically, the ostracod biomicrite facies cannot be differentiated from the similar facies in the Cherty Freshwater Beds. Ostracods are the main fossils encountered in the facies and gastropod and bivalve remains are common. When the bivalves occur they usually lie parallel to the bedding and are preserved as non-pleochroic calcite mosaics. Teeth and fish spines have been reported (Fisher, 1856) from bed DB 129.

The matrix is a mixture of micrite, clays and poorly-sorted ostracod debris. Angular quartz grains of 100-200 μ diameter are locally numerous especially in bed DB 129. A few grains of a green, glauconite-like mineral are also present in the matrix.

The ostracod biomicrite facies can be divided into several different petrographic types. In one type, complete ostracod valves occur in large numbers and in thin bands separated by layers rich in small fragments of ostracods. Usually in this type, the ostracod valves are oriented parallel to the bedding (Fig. 47). In another type, the ostracods show no preferred orientation. Also the paired ostracods are usually lined with pyrite and infilled with coarse sparry calcite which shows a gradual increase in size away from the substrate. Occasionally the residual micrite inside the ostracods shows a clotted appearance. The matrix is extremely rich in ostracod fragments from 20 μ upwards (Fig. 48).

The ostracod biomicrite facies includes many beds which were subaerially exposed

Fig. 47. Bands of ostracods infilled with calcite alternating with micrite layers containing fragmented ostracods.

Plane polarised light Width of field 2.9 mm.

Ostracod biomicrite facies Intermarine Beds: bed DB 118, Durlston Bay

Fig. 48. Paired ostracods with sparry calcite and lined with pyrite (black). Geopetal micrite occurs in some of the ostracods. The matrix is of ostracod fragments of various sizes.

Plane polarised light Width of field 2.9 mm.

Ostracod biomicrite facies Intermarine Beds: bed DB 119, Durlston Bay

during deposition. Rocks of this facies are petrographically different from those described above. There is less micrite in the matrix since such micritic sediments have neomorphosed into microspar. Coarse subangular and subrounded grains of quartz are more abundant (Fig. 49). The ostracods are commonly lined with brownish-red material, probably iron oxides, resulting from the oxidation of the original pyrite.

Bands with desiccation cracks are usually extremely rich in ostracods. The notable red crust which caps the 'Roach' and contains the famous dinosaur footprints is full of ostracods. Perhaps ostracods are abundant in other facies when there were desiccation periods and evidences of subaerial exposure. Grabau (1913) reported that the eggs of *'Cypris'* have the power to withstand desiccation for long time and hence the species can continue in water bodies which become periodically dried up. Similar observations were mentioned by Kesling (1961) who stated that the ostracod eggs can withstand long periods of subaerial exposures. With subsequent reflooding, a population of living ostracods would be rapidly re-established.

The mineralogical composition and porosity of the ostracod biomicrite facies of the Intermarine Beds are given in Table 11. The average composition and porosity are very close to that of the ostracod biomicrites described from the Cherty Freshwater Beds.

(c) Bivalve biomicrudite facies

In Durlston Bay, this facies is represented by beds DB 112, DB 126, DB 127, and DB 128 (Table 11). They are evenly laminated and medium grey (N5) in colour. Individual beds vary in thickness from 5-30 cm. In hand specimens, the rocks grade into sandy biomicrite, calcareous shale and mudstone. Occasionally they pass into bivalve biosparrudites.

In thin-section, the content of bioclastic debris is high, usually more than 50%

Fig. 49. Ostracods in a matrix of neomorphic spar. Note the abundance of rounded and sub-angular quartz grains.
Plane polarised light Width of field 2.9 mm.
Ostracod biomicrite facies Intermarine Beds Red crust at the top of the 'Roach' Quarry near Acton (SY/982783).

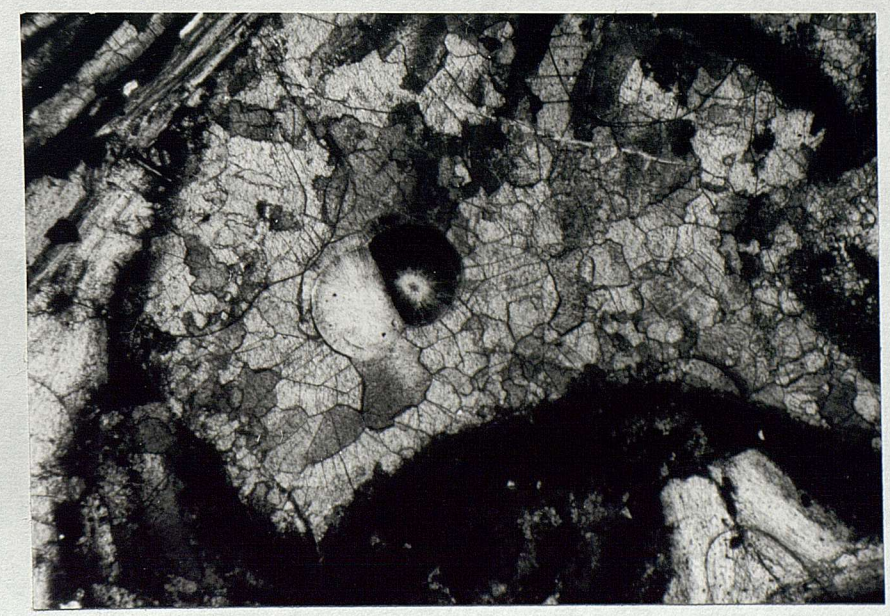

Fig. 50. Bivalve fragment preserved as pseudo-pleochroic calcite. Partial silicification is shown by spherulitic chalcedony which post-dates the calcitization of the original aragonite in the bivalve grain.
Plane polarised light Width of field 2.9 mm.
Bivalve biomicrite facies Intermarine Beds. Bed DB 127, Durlston Bay.

of the rock volume, and of course represented mainly by bivalves. Particular rocks are constituted of either small (< 1 mm.) or large (> 4 mm.) bivalve fragments. Occasionally, alternating laminae of coarse and fine bivalve fragments occur within the same thin section. Generally the shell fragments, particularly the larger sizes, are parallel to the bedding. Most of the bivalves are heavily bored, especially the finer fragments. Bores of up to 100 μ in diameter are commonly infilled with micrite derived from the matrix. Bivalve fragments are mainly preserved as mosaics of pseudo-pleochroic calcite. These mosaics are occasionally rich in Fe^{2+} especially in bed DB 127. Partial silicification is not common and when it occurs it is essentially confined to the bivalves. Silicification post-dates calcitization of the aragonitic bivalves since chalcedony replaces the pseudo-pleochroic shell mosaics (Fig. 50). *Liostrea* fragments are readily recognised, as in other facies, by their foliated shell structure (Fig. 51).

Gastropods occur as spar-filled shell casts with geopetal micrite and neomorphic microspar within the body chamber. Ostracods are commonly infilled with micrite or with non-ferroan calcite mosaics. In other instances, the ostracods are lined with fibrous non-ferroan calcite followed by ferroan calcite generation. Most of the ostracods show signs of partial silicification.

Micrite in the bivalve biomicrudite facies occurs as a matrix which constitutes up to 40% of the rock volume. The matrix also includes angular quartz grains, 60-250 μ in diameter, which may form up to 5% of the rock weight. Spherical and ovoid pelletoids (60-200 μ in length), are locally abundant specially in bed DB 127. They are much darker than the surrounding micrite and have well-defined boundaries. Dark inclusions probably of organic matter and pyrite tend to concentrate in the central parts of these pelletoids suggesting them to be faecal in origin. Large irregular mud-clasts are common

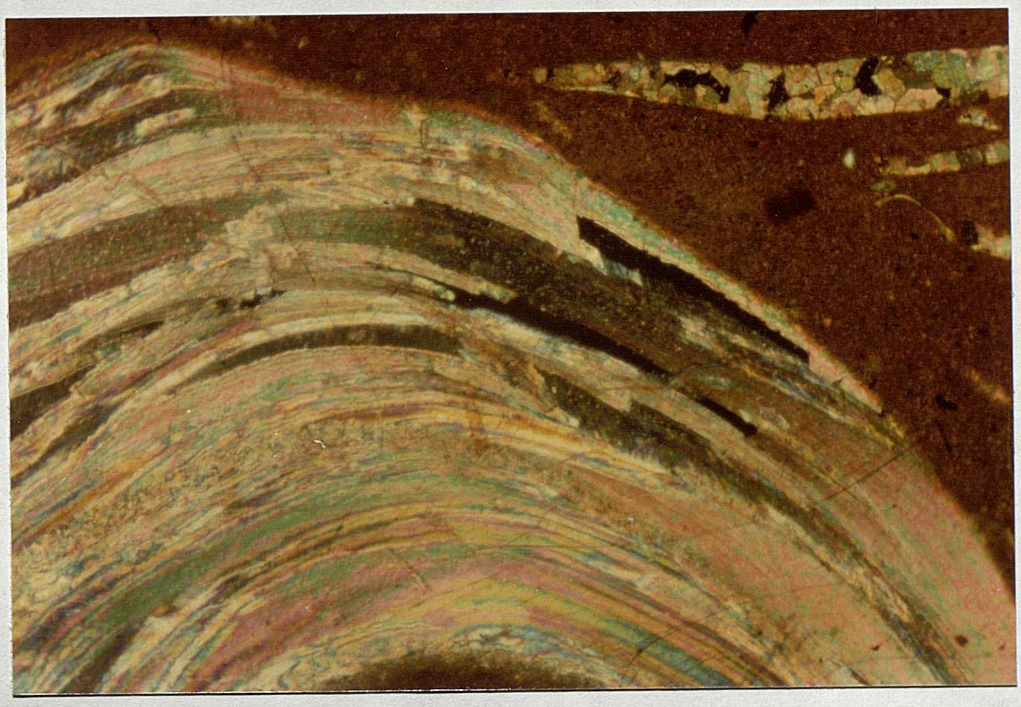

Fig. 51. Foliated shell structure in *Liostrea.* Stained thin-section with potassium ferricyanide and alizarin red-S.
Crossed polars Width of field 3.2 mm.
Bivalve biomicrudite facies Intermarine Beds Bed DB 127, Durlston Bay.

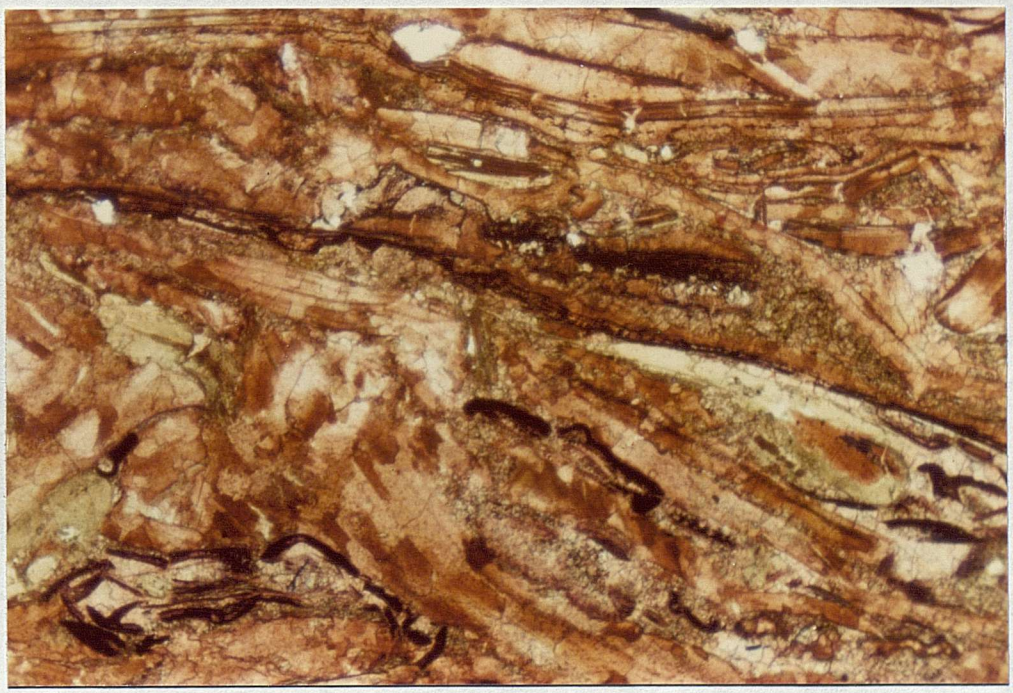

Fig. 52. Closely-packed bivalve fragments with little calcite cement. The bivalves are preserved as pseudo-pleochroic calcite. A few are still aragonitic (yellow).
Stained thin-section with potassium ferricyanide and alizarin red-S.
Plane polarised light Width of field 3.2 mm.
Bivalve biosparrudite facies (type 1) Intermarine Beds Bed DB 135, Durlston Bay.

in bed DB 128 and they contain syneresis cracks. Penetration of shell debris into these mud clasts is common which suggests that they are intraclasts (derived from within the basin) rather than extraclasts.

The carbonate of the bivalve biomicrudite facies is predominantly calcite. Aragonite is nearly constant, about 3%. Non-carbonates are represented mainly by clays which have a wide range in percentage from 2-22% but there is also quartz ranging from 2-5%. Porosity values vary from 4-10%. Average mineralogical composition and average porosity of the bivalve biomicrudite facies are very close to those of the ostracod biomicrite facies (Table 11). The organic carbon content of the bivalve biomicrudite facies, however, is only a third of that of the ostracod biomicrite facies.

(d) Bivalve biosparrudite facies

The facies includes several beds which are composed essentially of bivalve fragments usually larger than 2 mm. in diameter. At the outcrops, the limestones of this facies show uniform parallel bedding, ripple-marks, dinosaur footprints, and, less commonly, desiccation cracks. The facies is well developed in Durlston Bay and in the inland quarries around Swanage. The bivalve biosparrudite facies thins rapidly westward losing its petrographic identity. At Stair Hole (Lulworth area), the facies grades into biomicrites. Further west at Ridgeway, it is replaced by sandstones, and biomicrites (Fig. 13). Nevertheless, individual beds in Durlston Bay such as DB 113, DB 133 can be traced along the cliff sections to Bacon Hole (Fig. 13).

The bivalve biosparrudite facies has very high carbonate contents which range from 90-98% (Table 13). Average organic carbon content is low (0.3%) in comparsion with the other facies described before. Average porosity is 4% which is lower than that of most of the other facies of the Intermarine Beds (Table 11).

Table 13. Mineralogy and porosity of the bivalve biosparrudites of the Intermarine Beds of Durlston Bay

Bed Number	Sample Number	Calcite %	Aragonite %	Quartz %	Clay %	Organic carbon %	Porosity (%)	
DB 113	45	91	3	1	–	0.23	5	
DB 126	63	88	5	2	2	0.37	3	
DB 127	64	86	9	2	–	0.18	1	
DB 131	74	91	3	2	2	0.18	1	Type 1
DB 133	76	88	2	2	–	0.16	4	
DB 135	82	80	13	2	2	0.83	3	
Average		87	6	2	1	0.33	3	
DB 120	55	94	–	1	–	0.14	4	
DB 121	56	98	–	–	–	0.08	8	
DB 122	57	90	–	2	4	0.43	2	
DB 123	58	94	–	1	–	0.12	2	
DB 124a	59	93	–	1	3	0.18	3	Type 3
DB 125	61	92	–	4	–	0.06	5	
DB 143	83	91	–	3	2	0.08	2	
DB 144a	84	92	–	4	–	0.04	8	
Average		93	–	2	1	0.14	4	
Average of both types		90.5	2.5	2	1	0.22	4	

The bivalve biosparrudite facies comprises two petrographic types; type 1 and type 3 and there is no intermediate gradation. The different petrographic and diagenetic features of both types are summarised in Table 14. Field occurrence and detailed petrographic study of each type are given below.

Type 1. This type is represented in Durlston Bay by beds DB 113, DB 126, DB 127, DB 133, DB 134 and DB 135. Individual beds vary from 23-86 cm. in thickness. They are pale yellowish brown (10 YR 6/2) and medium dark grey (N4) in colour. Cross-lamination and desiccation cracks are developed in the inland quarries near Swanage (Figs. 18 and 22). Thin lenticular chert occurs near the top of bed DB 113. Mud-clasts up to 5 cm. in diameter are abundant on the top of bed DB 133 and can be traced at this

horizon to Worbarrow Bay (bed 36).

Bioclastic debris is abundant and usually exceeds 80% of the rock volume (Fig. 52). The calcite groundmass is spar and microspar. Occasionally a little micrite occurs and commonly trapped between the bioclasts.

Fossils are mainly bivalves particularly *Neomiodon* (Clements, 1969) and *'Cyclas'* (Fisher, 1856). *Liostrea* fragments are commonly encountered. Gastropods and ostracods are volumetrically of minor importance. Vertebrate remains especially of turtles are locally common in the inland quarries. Algal clasts are common on the top of bed DB 133. They are composed of the green alga *Ortonella* which is similar to that described from the lower Purbeck (Pugh, 1969; Brown, 1963). The branching filaments vary from 20-30 μ in diameter (Fig. 53).

Bivalves are very closely packed with compactional fabrics similar to those described earlier from the Cherty Freshwater Beds. The bivalves are preserved as pseudo-pleochroic calcite mosaics which have replaced aragonite (Figs. 52 and 54). Evidences of post-compactional calcitization of the former aragonite are numerous (see p. 99). Occasionally the pseudo-pleochroic shell mosaics are rich in Fe^{2+}. Pyrite inclusions are locally common in these mosaics.

Occasionally, the pseudo-pleochroic shell mosaics are replaced by a very coarse euhedral calcite up to 900 μ (bed DB 133). Rarely, euhedral ferroan dolomite up to 400 μ in diameter occurs in these coarse calcite fabrics. The diagenetic sequences are as follows: Aragonite was paramorphically replaced by the pseudo-pleochroic calcite of the shell mosaics which in turn was neomorphosed into coarse calcite. This was finally replaced by ferroan dolomite.

The mechanism responsible for the development of coarse calcite fabrics at the

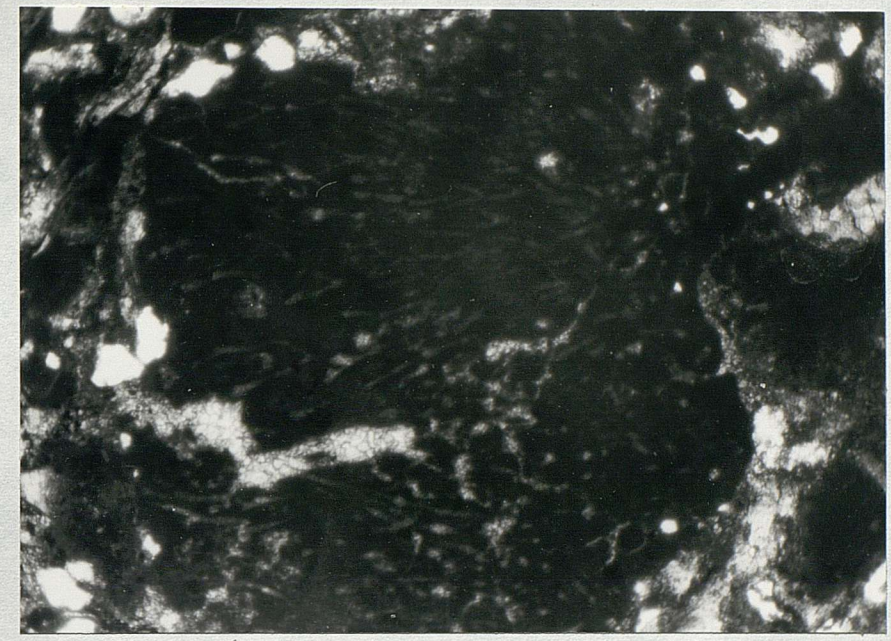

Fig. 53. Algal clast showing the green alga *Ortonella.*
Plane polarised light Width of field 2.9 mm.
Bivalve biosparrudite facies (type 1) Intermarine Beds Bed DB 133, Durlston Bay.

Fig. 54. Closely-packed bivalves showing high compactional features. The bivalves are mainly preserved as pseudo-pleochroic calcite. The fractured bivalve fragment (black) was completely micritized by boring algae.
Plane polarised light Width of field 2.9 mm.
Bivalve biosparrudite facies (type 1) Intermarine Beds Bed DB 135, Durlston Bay.

Table 14. **Comparison between type 1 and type 3 of the bivalve biosparrudite facies in the Intermarine Beds of Durlston Bay.**

	Type 1	Type 3
Content of bioclastic debris	> 80%	< 70%
Pseudo-pleochroic shell mosaics	very common	absent
Moulds infilled with sparry calcite	absent	very common
Micrite envelopes	rare	very common
Content of calcite cement relative to the rock volume	< 10%	> 40%
Composition of the calcite cement	mainly ferroan	mainly non-ferroan
Packing	closed	open
Compaction features	very common	rare
Calcite %	80–91	90–98
Aragonite %	2–13	–
Organic carbon %	0.16-0.83	0.04–0.43
Porosity (%)	1–5	2–8
Pyrite	Common	rare
Environment of diagenesis	mainly reducing	mainly oxidising
Time of cementation	after compaction and calcitization of aragonite	before compaction, during and after calcitization
Place of lithification	deep after burial	shallow probably subaerial

expense of the pseudo-pleochroic calcite has not been documented before in the literature. However, it seems that processes of size-enlargement were involved as indicated by (1) occurrence of traces of the original shell in the coarse calcite fabrics and (2) the considerable increase in grain size. Size-enlargement is not restricted to the shell mosaics but also affected the calcite groundmass. Occasionally angular quartz grains are partially or completely engulfed by very coarse calcite.

Aragonite bivalve fragments are locally common. They consist of very fine aragonite crystals less than 1 μ in length. Aragonite shell fragment extinguish uniformly between crossed-nicols as though all crystals are of parallel orientation. Remains of aragonite commonly occur as small islands in the pseudo-pleochroic shell mosaics (Fig. 52).

Type 3. In Durlston Bay, this type is represented by two separate and relatively thick units. The lower (2.55m.) occurs near the middle of the Intermarine Beds and comprises the beds DB 120-DB 125. Within these is the 'Roach' (bed DB 125); one of the most interesting beds in the Purbeck Group of Dorset with its well-known impressions and natural casts of dinosaurs footprints (see Chapter 5). The upper unit occurs near the top of the Intermarine Beds and includes the beds DB 143 and DB 144 known as the Leaning Vein and White Roach (Fisher, 1856). This unit can be traced from Durlston Bay to Ridgeway although in the latter locality it is represented by sandstones (Fig. 13).

In outcrops, beds of type 3 are massive or thin-bedded and pale yellowish brown (10 YR 6/2) or light grey (N7) in colour. Individual beds range from 23-125 cm. in thickness. Sedimentary structures include desiccation cracks and cross-lamination, which was recorded at Durlston Bay (beds DB 123 and DB 144) and in the inland quarries (Fig. 19).

In thin-section, type 3 of the bivalve biosparrudites contains up to 70% bioclastic debris. The matrix is essentially a mixture of spar and microspar. Apart from the dominant bivalves, ostracods occasionally occur. They are sometimes present in laminae with desiccation cracks or when there is other evidence of subaerial exposure (see p. 114). Gastropods were rarely encountered in thin-sections.

Type 3 can be recognised by the type of preservation of bivalves. They mainly occur as moulds infilled with granular non-ferroan calcite. Only in beds DB 143 and DB 144 the moulds are partially infilled with ferroan calcite. The outlines of the bivalve moulds are usually preserved by thick micrite envelopes (Fig. 55). No features are preserved to indicate that such moulds were molluscan debris; however, examination of the hand specimen frequently reveals such problem. Pseudo-pleochroic calcite is completely absent in the shell fabrics. This is another diagnostic criterion of type 3.

Collapsed micrite envelopes are locally common (fig. 56). Nevertheless, no compactional features are present to suggest that the breakage of the envelopes is product of compactional effects. Although Bathurst (1964; 1966), has stated that the micrite envelopes provide the strength and support which preserve the shell shape, it seems that the collapse of the micrite envelopes is not always due to external pressure. The micrite envelopes could be broken if the moulds formed after aragonite leaching were not infilled with calcite in the early stages of cementation. Movement of the pore fluids during the early stage of diagenesis while the sediment was still permeable and the moulds were still empty could be the reason for the breakage of the micrite envelopes. The chances of breakage would have been greater if the micrite envelopes were relatively thin and discontinuous.

A different type of collapse of micrite envelopes was observed in beds DB 143

Fig. 55. Bivalve fragments preserved as moulds infilled with sparry calcite. A few collapsed micrite envelopes are scattered in the calcite groundmass. Note the highly micritized bivalve fragment (black).
Crossed Polars Width of field 2.9 mm.
Bivalve biosparrudite facies (type 3) Intermarine Beds Bed DB 125, Durlston Bay.

Fig. 56. Collapsed micrite envelopes. Note the fibrous calcite fringe (early cement) around the collapsed micrite envelopes. The black grains are highly micritized bivalve fragments.
Plane polarised light Width of field 2.9 mm.
Bivalve biosparrudite facies (type 3) Intermarine Beds Bed DB 125, Durlston Bay.

and DB 144. In this case the collapse was due to external pressure probably produced by the weight of the overlying sediments. Compactional effects are visible such as shell penetration and welded grains.

Another important characteristic feature of type 3 is the common occurrences of intensively micritized grains. Different stages of micritization can be recognised in skeletal grains with very thin micrite envelope and grains entirely composed of micrite. Intermediate stages are represented by grains where some skeletal residue can be observed (Fig. 57). Skeletal grains with intense micritization are more rounded suggesting that the shell surface has been weakened by prolonged boring. When there has been more rounding the rock appears to be composed of micrite 'pelletoids'. These are, however, products of biological and mechanical breakdown of original molluscan debris. Rocks entirely made up of sorted micrite pelletoids have been described before from the Cherty Freshwater Beds from Harden's Quarry.

Two generations of calcite cements can be recognised in type 3. The early generation is represented by the fringe cements which are fibrous calcite and coat the allochems. The late cements are coarse granular calcite. Both generation cements are commonly non-ferroan calcite.

Silicification is not a common feature of type 3. A few moulds are infilled with chalcedony suggesting that silicification postdates calcitization of the molluscan shells. However, the absence of chalcedony from the calcite cements in the matrix suggests that silicification was completed before the main phase of calcite cementation.

Bivalve biosparites or biosparrudites with abundant skeletal moulds infilled with granular calcite, and micrite 'pelletoids' are products of prolonged colonization by algae, leaching of the skeletal aragonite and early cementation. The aragonite was

Fig. 57. Bivalve fragments showing different degrees of micritization.
Plane polarised light Width of field 2.9 mm.
Bivalve biosparrudite facies (type 3) Intermarine Beds Bed DB 123, Durlston Bay.

probably dissolved by low-Mg water (Friedman, 1964 and Bathurst, 1966). Early exposures to meteoric water is a likely possibility probably because of the development of extensive moldic porosity (Friedman, 1964; Land *et al.*, 1967; Matthews, 1967; Stephen and Humbert, 1969). Dinosaur footprints, desiccation cracks and crusts and low organic carbon content are evidences which strongly indicate that the rocks of type 3 were subaerially exposed during sedimentation. The diagenetic fabrics outlined above might be important and could be used to indicate subaerial exposure when other criteria are not available.

3. Petrography of the Scallop Beds

These are important since they represent one of the few nearly marine phases of the middle Purbeck Group. The Scallop Beds can be recognised in the field by the abundance of "*Pecten*"[1] (Fisher, 1856). They are recognisable from Durlston Bay to Ridgeway (Fig. 14) and for the first time are reported from the inland quarries near Swanage and correlated with the type-section in Durlston Bay (Fig. 26).

The Scallop Beds have a high bioclastic content, particularly of bivalves. Apart from *Pecten, Corbula, Liostrea* other unidentified bivalves are common. The gastropods are locally important and include *Hydrobia, Viviparus, Theodoxus* and *Procerithium* (Clements, 1969). Ostracods of species of genera *Dicrorygma, Macrodentina, Orthonotacythere, Theriosynoecum, Scabriculocypris* and *Cypridea* have been identified in the Scallop Beds in Durlston Bay (Clements, 1969). Foraminifera occur in beds DB150 and DB151. Small bone fragments are present at different horizons. Large plant remains are locally abundant especially in bed DB151.

The Scallop Beds comprise two main facies: bivalve biomicrudite and bivalve

[1] More recently this was tentatively identified as *Chlamys* (Clements, 1969).

biosparrudite. Mineralogically, they mainly differ in the amounts of calcite, clays and organic carbon (Table 15).

Table 15. Mineralogy and porosity of the Scallop Beds of Durlston Bay

Bed. No.	Sample Number	Calcite %	Aragonite %	Quartz %	Clay %	Organic Carbon %	Porosity (%)	Facies
DB145	85	57	1	7	34	0.30	8	Bivalve biomicrudite
DB146	86	90	1	2	6	0.23	4	
DB148	89	93	1	2	2	0.08	3	
DB149	90	60	–	16	16	0.49	4	
DB151	92	81	3	3	9	0.34	3	
DB153	94	81	3	3	9	0.61	3	
Average		77	1.5	5.5	13	0.34	4	
DB147	87	89	1	5	–	0.04	4	Bivalve biosparrudite
DB147	88	–	–	5	1	0.04	4	
DB149	91	74	4	11	6	0.18	2	
DB152	93	88	–	4	–	0.14	2	
Average		85	1,5	6	1,5	0.10	3	

(a) Bivalve biomicrudite facies

In Durlston Bay, the facies is represented by several beds (Table 15). In outcrops, these limestones are medium grey (N5) or greenish grey (5 GY 6/1) in colour, and ranging from 10–35 cm. in thickness.

In thin-section, the rocks are characterized by high micrite content which constitutes up to 80% of the rock volume. The facies is rich in clay content which ranges as high as 34%. Bioclastic content is of a minor importance in this facies and mainly dominated by *Pecten*. In general *Pecten* valves are built of a prismatic layer of calcite and a crossed-lamellar aragonitic layer (Bøggild, 1930). In *Pecten* of the Scallop Beds the calcitic layer is made up of nearly parallel prisms (30μ wide) while the aragonitic layer has been altered into pseudo-pleochroic calcite. Other unidentified bivalve fragments are mainly preserved as pseudo-pleochroic shell mosaics which are occasionally rich in

Fe^{2+}. Pyritized shell-mosaics are locally abundant especially in bed DB153. Pyrite contents vary considerably from bivalve fragments completely masked by pyritisation to others where pyrite is localised along the crystal boundaries in the shell mosaics. Pyrite is also common in the micrite matrix, occurring as small nodules and scattered euhedral crystals about 8 μ in diameter.

Neomorphic fabrics particularly those of size-enlargement are common in the bivalve biomicrudite facies of the Scallop Beds. The pseudo-pleochroic shell mosaics are occasionally altered into coarse ferroan calcite. Size-enlargement of the micrite in the matrix is indicated by the gradation from typical micrite size to a microspar up to 15μ in diameter. The original sediment was mud-supported as indicated by the very open fabrics in which the allochems are floating in a micrite groundmass. This suggests that neomorphism affected the original micrite.

(b) Bivalve biosparrudite facies

This facies appears in several parts of the Scallop Beds at Durlston Bay (beds DB147, DB149 and DB152). These limestones range from medium light grey (N6) to light brownish grey (5 YR 6/1) in colour and up to 33 cm. in thickness.

Petrographically, the rocks of this facies consist mainly of large bivalve fragments and a matrix of well-sorted and well-rounded smaller shell fragments, pelletoids and coated grains (Figs. 58; 59). Subangular quartz grains up to 300μ are abundant. Complete bivalve shells and whole valves are common especially in bed DB152. The bivalves are preserved as shell mosaics composed mainly of pseudo-pleochroic calcite. A few grains occur as moulds infilled with granular calcite indicating leaching of former aragonite. The co-occurrence of paramorphic replacement and of leaching of former aragonite in the same sample is interesting. It represents an intermediate diagenetic stage between that

Fig. 58 Rounded bivalve fragments with micritic and oolitic coatings. Some fragments contain thick micrite areas (dark) in the concave side of the shells. Fragmentation is clear in the bivalve fragment in the middle.

Plane polarised light. Width of field 2.9 mm.

Bivalve biosparrudite facies. Scallop Beds: bed DB152, Durlston Bay.

Fig. 59. Effect of pressure solution on micritic and oolitic coatings. The micrite coating was partially destroyed (in the middle) while the oolitic coating was unaffected.

Plane polarised light. Width of field 2.9 mm.

Bivalve biosparrudite facies. Scallop Beds: bed DB152, Durlston Bay.

attained by type 1 and type 3 of the bivalve biosparrudites of the Intermarine Beds. Pyritised bivalves with traces of the original shell structure are common. Pyrite inclusions tend to be concentrated along the crystalline boundaries of calcite crystals of the shell mosaics.

Some of the large bivalve fragments contain micrite areas in the concave side of the shell and appear to be intraclasts. The boundaries between the micrite and the surrounding sparry calcite are sharp. The smaller bivalve fragments usually have thick micrite coatings surrounded by oolitic coating especially in Durlston Bay (bed DB152). The micrite coatings have occasionally been affected by pressure solution. In this case, dissolution is always associated with pressure-welded grains (Fig. 59). The oolitic coatings are usually more resistant to the pressure solution than the micrite coatings (Fig. 59). Ruptured micrite envelopes which resulted from the displacive growth of neomorphic spar are locally common (Fig. 60). Compactional features include fragmentation of allochems and penetration of the shells (Figs. 58, 59, 61). These features indicate that deformation occurred when the sediment was only partially lithified. Such compactional features were developed when the overburden was thick enough to provide sufficient load for shell penetration and fragmentation.

Calcite cements are well-developed in the large shell-cavities. Three generations of cements were recognised; early, main-phase and late cements. The early cements predate compaction and occur as thin fibrous non-ferroan calcite fringes. The individual crystals in the early cements are usually oriented normal to shell walls. The main phase cements postdate compaction and calcitization of the aragonitic molluscs. They are slightly elongated and commonly normal to the substrate. They are usually non-ferroan

Fig. 60. Ruptured micrite envelopes resulted from the displacive growth of neomorphic spar.
Crossed polars. Width of field 2.9 mm.
Bivalve biosparrudite facies Scallop Beds: bed 5, Downshay Wood (SY/981794).

Fig. 61. Clotted micrite filling a gastropod cavity. Penetration by a bivalve fragment has resulted from compaction.
Plane polarised light Width of field 2.9 mm.
Bivalve biosparrudite facies Scallop Beds: bed 5, Downshay Wood (SY/981794).

and have planar crystalline boundaries (Fig. 62). The late calcite cements are commonly rich in Fe^{2+} and have much larger grain sizes. They are occasionally represented by a single calcite crystal with marked twinning. In many cases, the ferroan calcite crystals of the late cements are in optical continuity with the underlying non-ferroan calcite (Fig. 63). This indicates that the boundary between both cements is a chemical rather than a physical boundary. Transitions from iron-free calcite to iron-bearing calcite may be abrupt (Fig. 62) or gradual (Fig. 63). The abrupt transition probably indicates that iron was always available for incorporation in the cement, but that only when the environment became reducing was such inclusion possible (Evamy, 1969). The gradual transition indicates a progressive concentration of Fe^{2+}. The iron-bearing calcite cements indicate precipitation below the water table (Evamy, 1969; Bathurst, 1975). Generally, the iron-free calcite cements indicate precipitation in the vadose zone. It should be emphasised that sometimes there is a complete absence of Fe^{2+} so that it is not possible to distinguish by staining between cements precipitated below and above the water table.

Veins infilled with ferroan calcite are common. They usually postdate all the cement fabrics described above. These veins provided channels for very late carbonate solutions rich in ferrous ions. These solutions locally altered the early fibrous cements, precipitating a thin film of ferroan calcite along their crystalline boundaries. This may give an impression that the early cements were rich in ferrous iron. However, a careful examination reveals that such effects were closely connected with minute fractures and veins (Fig. 63). In other areas, unaffected by veins and fractures, the early fibrous calcite cements are non-ferroan.

Micrites in the bivalve biosparrudite facies of the Scallop Beds are polygenetic. Micrites occur as pelletoids, micrite coatings, in geopetal structures, and in the matrix.

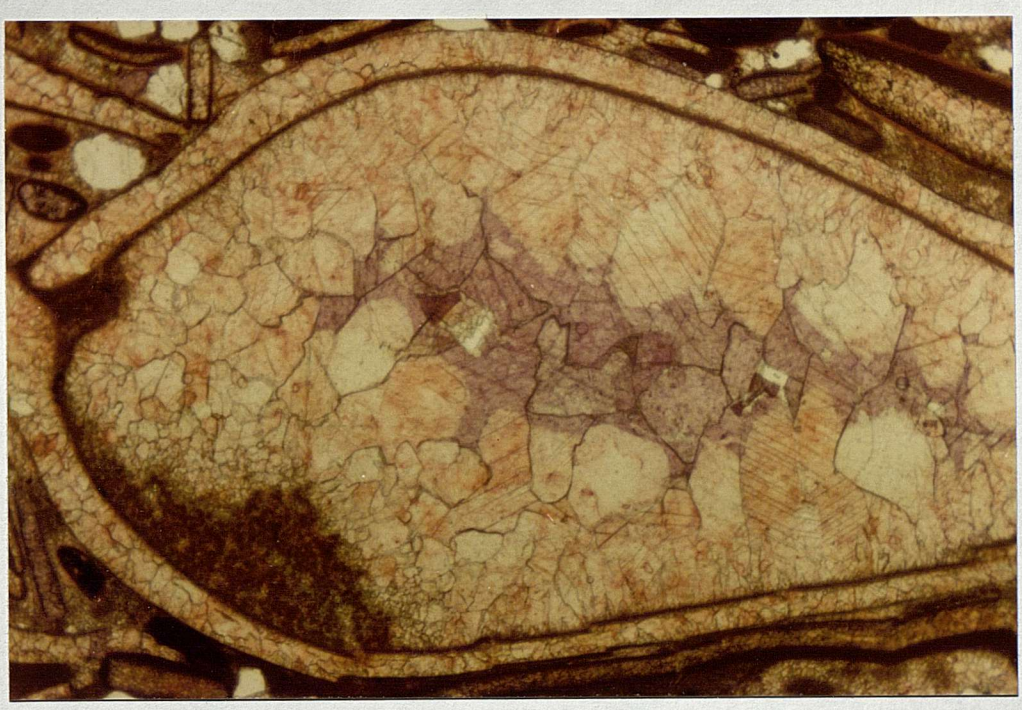

Fig. 62. Calcite cements within bivalve cavity. The early generation is a fibrous calcite fringe. The main-phase and late generations include the coarse non-ferroan and ferroan calcite.
Thin-section stained with alizarin sed-S and potassium ferricyanide.
Plane polarised light Width of field 3.2 mm.
Bivalve biosparrudite facies Scallop Beds: bed DB152, Durlston Bay.

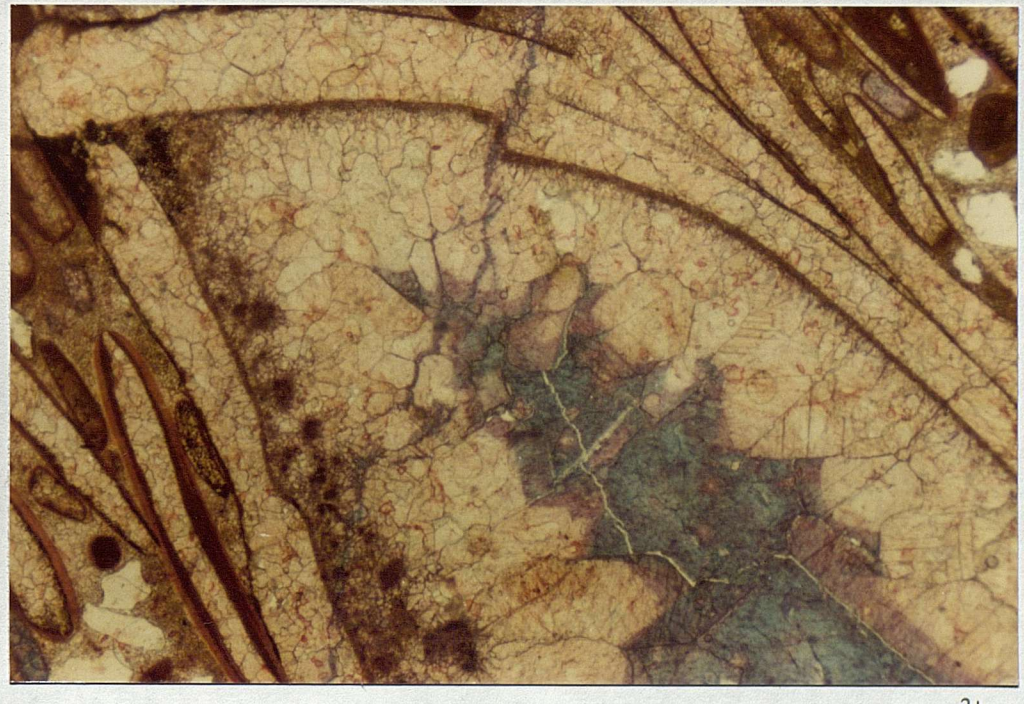

Fig. 63. Similar calcite cements to those of Fig. 62 except that the early cement is affected by Fe^{2+} rich solution, brought by post-complete cementation fissures. As a result, a film of ferroan calcite was developed along the crystal boundaries of the early fibrous calcite generation.
Thin-section stained with alizarin red-S and potassium ferricyanide.
Plane polarised light Width of field 3.2 mm.
Bivalve biosparrudite facies Scallop Beds: bed DB152, Durlston Bay.

Fig. 64 Clotted micrite overlain by calcite cements in a gastropod cavity. The difference between the early fibrous cement and the coarse equant main phase generation is marked. There is a vectorial change in grain size away from the shell wall.

Plane polarised light Width of field 2.9 mm.

Bivalve biosparrudite facies Scallop Beds: bed 5, Downshay Wood (SY/981794).

Pelletoids are either black or brown in colour and up to 500 μ in diameter. The micrites occurring in cavities and forming geopetal structures usually have a clotted appearance (figs. 61-64). These clotted micrites are very similar to the *'structure grumeleuse'* described by Cayeux (1935, figs. 67-69). The apparent blurring of the outlines of these clots is difficult to explain. It is unlikely that the clotted structure is a product of patchy neomorphism. Possibly these clots represent pelletoids since well defined pelletoids similar in size to that of the clots which occur in the shell cavities. Also the absence of clots in other micrite areas such as those of the intraclasts is a further evidence against the diagenetic origin of the clotted structure. Schwarzacher (1961) described similar structures and suggested that the clotting processes took place very early and it is possibly a pre-depositional feature.

Calciostrontianite: Mineralogically the bivalve biosparrudites of the Scallop Beds are far more interesting than any other facies described before. Patches of a white mineral were observed in hand-specimens that were obtained from bed 5 at Downshay Wood (fig. 28). The mineral is soluble in dilute hydrochloric acid and does not react to alizarin red-S, is identified by X-ray diffractometry as the rare mineral calciostrontianite. This is probably the second occurrence of the mineral in Britain since it was first reported from the basal Purbeck Group of Durlston Head, Dorset (Salter and West, 1965).

The calciostrontianite is composed of acicular cyrstals (fig. 65) arranged as spherulites. In thin section, the calciostrontianite can be seen to have replaced large celestite crystals (figs. 66; 67). The former celestite crystals seem to have occurred in cavities especially those associated with geopetal fabrics. Crystals of unaltered celestite are rare but occasionally found. Neither celestite or calciostrontianite was encountered in veins or cracks. This indicates that these minerals are not related to local tectonics

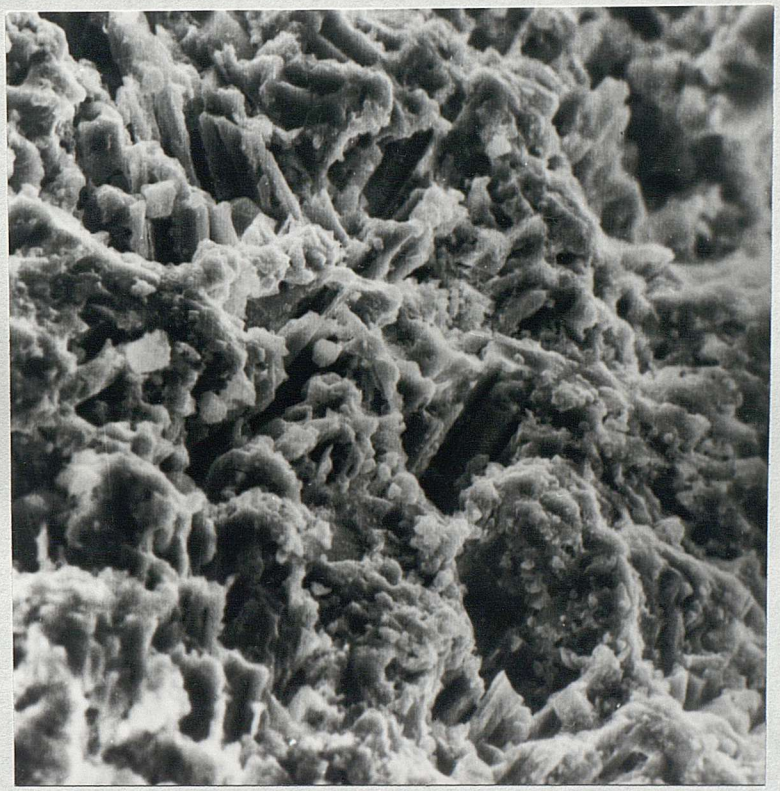

Fig. 65 SEM photograph of calciostrontianite showing prismatic crystals. Fractured surface coated with gold and carbon.

Width of field 0.135 mm.

Bivalve biosparrudite facies Scallop Beds: bed 5, Downshay Wood (SY/981794)

Table 16. X-ray powder data for calciostrontianite from the Scallop Beds compared with other data and pure strontianite

Calciostrontianite								Strontianite (A.S.T.M. card 5-0418)		
(1)		(2)		(3)		(4)				
d	I(obs)	d	I	d	I	d	I	d	I	hkl
4.358	3	4.32 Å	10	4.33 Å	vw	4.34 Å	w	4.367 Å	14	110
4.189	2	4.16	4	4.16	vvw	4.17	vvw	4.207	6	020
3.527	100	3.506	100	3,51	vvs	3.51	vvs	3.535	100	111
3.436	46	3.411	45	3.40	vs	3.41	vs	3.450	70	021
3.005	6	2.98	7	2.98	mw	2.98	w	3.014	22	002
–	–	–	–	–	–	–	–	2.859	5	121
2.828	10	2.80	14	2.81	m	2.815	w	2.838	20	012
2.585	8	2.57	7	2.58	w	2.58	vw	2.596	12	102
2.548	17	2.536	30	2.53	mw	2.54	s	2.554	23	200
–	–	2.50	4	–	–	–	–	–	–	–
–	–	–	–	–	–	–	–	2.481	34	112
2.473	20	2.45	20	2.46	m	2.46	m	2.458	40	130
2.447	29	2.428	48	2.43	s	2.43	vs	2.4511	33	022
2.260	2	2.24	3	2.25	vw	2.25	vw	2.2646	5	211
2.176	6	2.16	22	2.16	mw	2.165	m	2.1831	16	220
2.093	2	2.07	4	2.07	vw	2.075	vw	2.1035	7	040
2.046	23	2.034	36	2.04	s	2.04	s	2.0526	50	221
1.978	11	1.96	15	1.96	mw	1.96	m	1.9860	26	041
1.943	9	1.93	9	1.93	mw	1.935	mw	1.9489	21	292
1.900	21	1.88	13	1.88	m	1.885	m	1.9053	35	132
–	–	–	–	–	–	–	–	1.8514	3	141
1.821	16	1.80	7	1,81	mw	1.81	m	1.8253	31	113
1.808	7			–	–			1.8134	16	023
–	–	1.79	4	1.79	w	1.80	mw	1.8023	4	231
1.762	2	1.75	2	1.75	vw	1.75	vvw	1.7685	7	222
1.719	2	1.70	1	1.70	vvw	1.705	vvw	1.7253	5	042
1.666	1	1.65	3	1.65	vw	1.66	vw	1.6684	3	310
1.617	1	–	–	–	–	–	–	1.6236	4	240
1.613	2	1.59	6	1.60	mw	1.60	mw	1.6080	13	311
1.604	3			–	–			1.5981	3	150
1.562	3	1.54	3	1.55	mw	1.55	mw	1.5676	13	241
1.537	3	1.52	4	1.53	w	1.53	vw	1.5447	11	151
1.502	2	–	–	1.49	vvw	1.49	vvw	1.5072	3	004
1.000	2	–	–	1.47	vvw	1.47	vvw	1.4782	6	223
–	–	–	–	–	–	–	–	1.4596	4	312
1.454	3	1.44	4	1.44	vw	1.44	vw	1.4551	9	330
–	–	–	–	1.41	vw	–	–	1.4293	6	242
1.418	5	1.41	2	–	–	1.41	vvw	1.4246	7	114
–	–	–	–	–	–	–	–	1.4120	5	152
1.400	2	1.38	2	1.38	vvw	–	–	1.4024	4	060
1.395	7	1.29	3	1.30	mw	1.30	vw	1.3103	10	332
–	–	1.28	1	–	–	–	–	–		313 *
–	–	1.26	4	1.27	mw	1.27	mw	–		134 *

(1) Present work

(2) Salter and West (1965)

(3) Mitchell and Pharr (1961)

(4) Dietrich (1960)

* Indices according to Mitchell and Pharr (1961)

Fig. 66 Calciostrontianite after celestite crystals. The former celestite replaced the calcite cements developed in the shell cavity.

Plane polarised light Width of field 2.9 mm.

Biosparrudite facies Scallop Beds, bed 5, Downshay Wood (SY/981794)

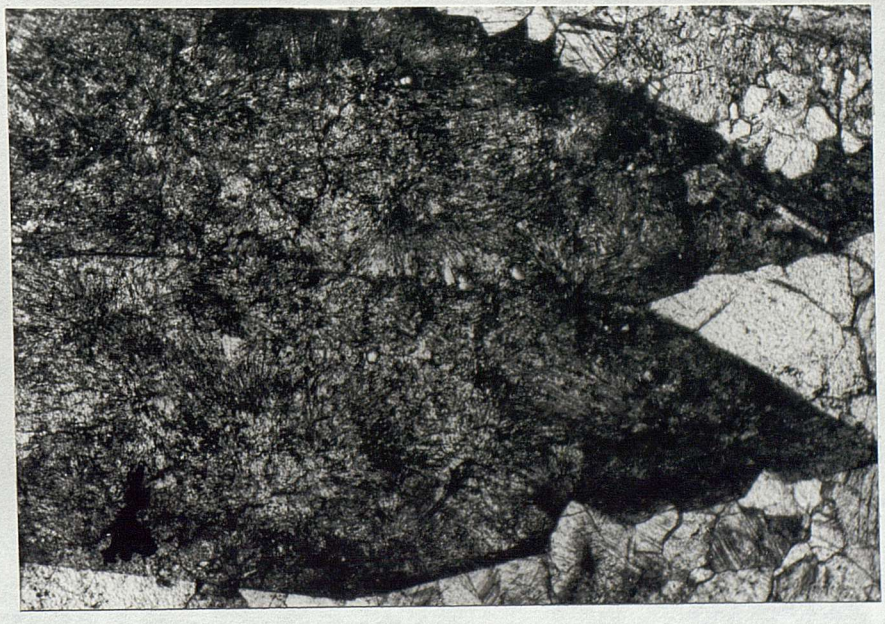

Fig. 67 Spherulitic calciostrontianite replacing a large celestite crystal.

Plane polarised light Width of field 2.9 mm.

Bivalve biosparrudite facies Scallop Beds: bed 5, Downshay Wood (SY/981794)

or jointing. However, the replacement of celestite by calciostrontianite occurred at a late stage of diagenesis. The former celestite crystals postdate all compaction and cementation phases.

The powder samples were prepared for X-ray diffractometry using Cu-Kα radiation (Ni filtered), and a complete scan up to $2\theta = 75°$ was run at ½° 2θ/min. recording speed, a time constant of 4 sec. and 1200 cm/hr. chart speed. Peak positions was corrected for diffractometer shift using pure quartz as an internal standard. Peak heights were used as measures of intensities. The results are given in Table 16, where they are compared with d-spacings obtained for a calciostrontianite containing about 8.1% CaO by Dietrich (1960), with averaged data by Mitchell and Pharr (1961), who reported calcium contents of their calciostrontianite ranging from 9.1 to 10.6% CaO, with d-spacings for calciostrontianite given by Salter and West (1965), and also with the A.S.T.M. data for calcium-free strontianite (less than 0.01% CaO). The X-ray data for calciostrontianite from the Scallop Beds indicates that the mineral has greater d-spacings than most other calciostrontianites. The d-spacing of calciostrontianite decreases with the increase of calcium content due to the substitution of the smaller calcium ion for strontium (Dietrich, 1960). Consequently, the calciostrontianite from the Scallop Beds probably contains a higher percentage of calcium than the specimens examined by Dietrich (1960) and Mitchell and Pharr (1961).

4. Petrography of the *Corbula* Beds

These beds comprise several different types of limestone and intercalations of shale. Near the base of the succession a calcareous sandstone bed is readily recognised and can be correlated throughout the coastal exposures and at Ridgeway (Fig. 14). The *Corbula* Beds have a relatively rich fauna particularly bivalves. They include species

of *Corbula, Neomiodon, Liostrea, Pecten* and *Cardium.* The main gastropod genera are *Hydrobia, Procerithium* and less commonly *Theodoxus* and *Promathilda* (Clements, 1969). The ostracods are represented by different species of the genera *Macrodentina, Orthonotacythere, Cypridea, Dicrorygma, Rhinocypris* and *Darwinula* (Clements, 1969).

The following facies were recognised in the *Corbula* Beds of Durlston Bay:

a. Micrite and pelmicrite

b. Algal pelmicrite with pseudomorphs after gypsum

c. Bivalve biomicrudite

d. Bivalve biosparrudite

e. Calcareous sandstone

f. Shale

Composition and porosity of the different limestone facies in the *Corbula* Beds are given in Table 17. Higher contents of clay and organic carbon characterise the micrites, pelmicrites and the bivalve biomicrudite facies. The bivalve biosparrudite facies have higher percentages of calcite and aragonite while clay and organic carbon contents are low.

(a) Micrite and pelmicrite facies

In Durlston Bay, the facies is represented by three beds: DB 165, DB 175 and DB 179. In outcrops, these beds are medium grey (N4) to greyish yellow green (5 GY 7/2) in colour and up to 35 cm. in thickness. They usually show a false nodular appearance and occasionally vertical jointing, especially in bed DB 179. The facies can be traced laterally to Bacon Hole near Lulworth.

In thin-section, the rocks range from a dense homogenous micrite (rarely exceeds 6 μ in diameter), to *grumeleuse* micrite rich in black pelletoids up to 150 μ in length. Pelletoids are more common in rocks which have high contents of organic carbon.

Table 17. Mineralogy and Porosity of the Limestones of the *Corbula* Beds of Durlston Bay

Bed Number	Sample Number	Calcite %	Aragonite %	Quartz %	Clay %	Organic carbon %	Porosity (%)	Facies
DB 165	118	73	–	3	15	0.93	4	Micrite and pelmicrite
DB 175	133	72	–	4	15	0.76	4	
DB 179	137	71	–	5	17	0.48	4	
Average		72	–	4	16	0.72	4	
DB161	107	74	2	4	11	0.36	4	Bivalve biomicrudite
DB 167	121	70	–	4	18	0.72	4	
DB 169	124	77	3	2	13	0.52	3	
DB 171	127	74	2	3	13	0.68	1	
DB 173	129	96	–	1	2	0.30	2	
DB 174	131	78	2	2	11	1.13	10	
DB 176	134	76	–	4	14	0.84	2	
DB 181	141	79	3	3	10	0.57	4	
DB 181	142	71	2	4	17	0.57	8	
DB 183	144	82	9	–	2	0.34	2	
DB 183	145	77	2	5	10	0.66	2	
DB 184	146	66	4	5	18	1.26	3	
DB 186	151	81	–	3	10	0.71	2	
DB 187	153	63	2	6	23	0.77	4	
Average		76	2	3	12	0.67	3	
DB 163	111	87	4	2	–	0.44	4	Bivalve biosparrudite Type 1
DB 167	122	89	8	1	1	0.32	1	
DB 171	126	90	3	1	3	0.28	1	
DB 187	152	81	3	4	7	0.68	3	
DB 188	154	87	9	2	1	0.31	1	
DB 189	155	72	8	3	12	0.55	3	
Average		84	6	2	4	0.47	2	
DB 186	150	94	–	1	—	0.84	1	Type 2
DB 161	108	90	–	7	2	0.35	1	Type 3
DB 178	136	96	–	1	–	0.32	1	
Average		93	–	4	1	0.33	1	
Average of 1, 2 & 3		86	4	2.5	3	0.45	2	

Occasionally, the pelletoids have been flattened by mild compaction. Locally they are more distorted and merge into the surrounding micrite loosing their outlines. Lamination is well-developed in bed DB175 although it is locally disturbed by vertical burrows. Veins are not common but when they occur they are infilled with ferroan calcite. Bioclastic debris rarely exceeds 10% of the rock volume.

Calcite is the only carbonate mineral present in the facies (Table 17). Quartz content varies from 3–5% while clay content is much higher, ranging from 15 – 17%. Organic carbon content varies from 0.48 – 0.96%. Porosity value is 4% in all cases.

(b) Algal pelmicrite with pseudomorphs after gypsum

This facies was discovered during the field work at Worbarrow Tout. It is confined to 12 cm. bands of micrite with algal lamination (bed 68b). This band is overlain by medium dark grey (N4) micrite and passes down into bivalve biosparrudites. A similar facies was recognised in Durlston Bay; it is represented by a very thin laminae (less than 1 cm. thick) which occurs in the middle part of bed DB183.

In thin-section, the rocks consist of layers rich in calcite pseudomorphs after gypsum (referred to briefly as gypsum pseudomorphs) occurring in layers of algal pelmicrite (Fig. 68). The gypsum layers are discontinuous and up to 0.6 mm. thick. The layers are marked by a thin film of black material probably of organic matter. The gypsum pseudomorphs have a roughly lenticular shape[1] (Fig. 69). Many of the gypsum pseudomorphs show preferred orientation with their short axes more or less parallel to the bedding. Most of the 'gypsum' crystals have a constant elongation at 5:1, with breadth of 20 – 150 μ and 100 – 700 μ in length. The gypsum pseudomorphs are partially infilled

---

[1] Gypsum crystals of this habit are flattened in a plane approximately normal to the crystallographic c-axis (Masson, 1955; West, 1964; Shearman, 1966). Experimentally produced gypsum crystals of this habit have been reported by Cody (1976).

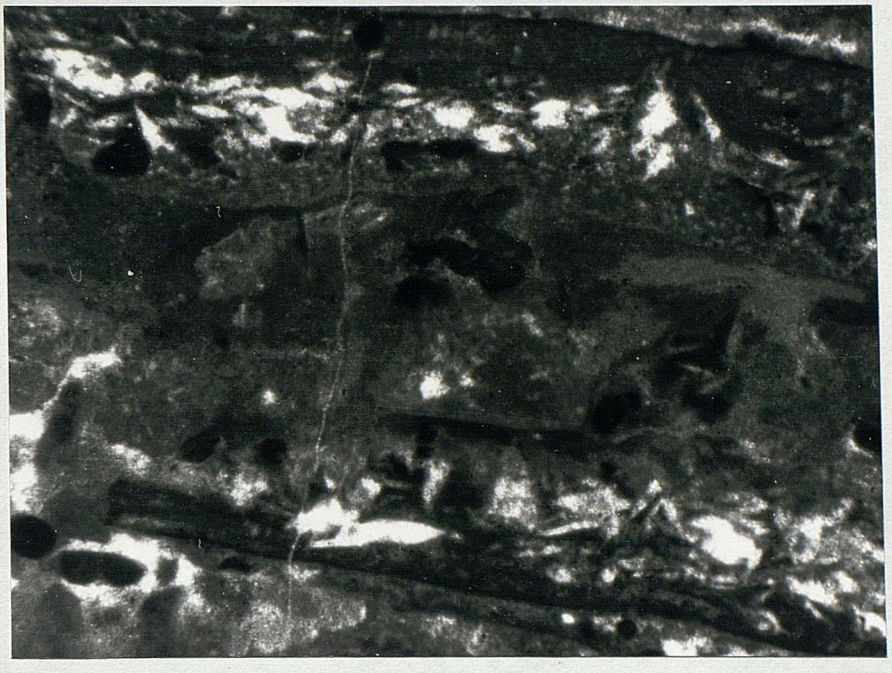

Fig. 68 Interbedded laminae of gypsum pseudomorphs and algal layers separated by a thin film of organic matter.

Plane polarised light Width of field 2.9 mm.

Corbula beds: bed 68b, Worbarrow Tout.

Fig. 69 Gypsum pseudomorphs partially infilled with internal sediment. Note the lenticular shape of the gypsum pseudomorphs.

Plane polarised light Width of field 2.9 mm.

Corbula Beds: bed 68b, Worbarrow Tout.

with spar and partially infilled with micrite derived from the surrounding sediment (Fig. 69). This implies that the gypsum outlines were stabilised by early cementation while the sediment was still mobile. Hudson (1970), while studying some algal limestones from the Middle Jurassic of Scotland, attributed the early stabilisation of the gypsum outlines to the effect of algal mucilage. Careful examination reveals the presence of a thin film of organic matter coating the well-preserved gypsum pseudomorphs (Fig. 69). Possibly the role of algal secretions in stabilising the gypsum outlines is similar to their role in preserving the outlines of the aragonitic skeletal debris during the early stages of diagenesis (Shearman and Skipwith, 1965).

The smaller gypsum pseudomorphs usually have well-developed crystal facies. They are not confined to the gypsum layers but are usually scattered in the algal layers and lack any preferred orientation. Masson (1955), described similar textures from the mud flats of the Laguna Madre, Texas, where the euhedral selenite crystals are scattered through the mass of dead algal fibres just below the surface of green, living algae.

The algal lamina are up to 2 cm. wide and are composed of structureless algal clasts with marked clotted appearance and fine black disseminated material (figs. 70, 71). Small spherical black pelletoids up to 150 μ in diameter occur in thin layers and a few are flattened by slight compaction (Fig. 71). Most of these pelletoids are probably faecal in origin. Hudson (1970), reported faecal pellets in a similar facies (algal limestones with gypsum pseudomorphs) in the Great Estuarine Series of the Hebrides (Middle Jurassic).

The fossil content (apart from algae), is very low and includes small bivalve fragments, ostracod debris and vertebrate bones.

By comparison with modern environments, the algal pelmicrite with gypsum pseudomorphs (orientated with the original c-axis parallel with the bedding) strongly suggests

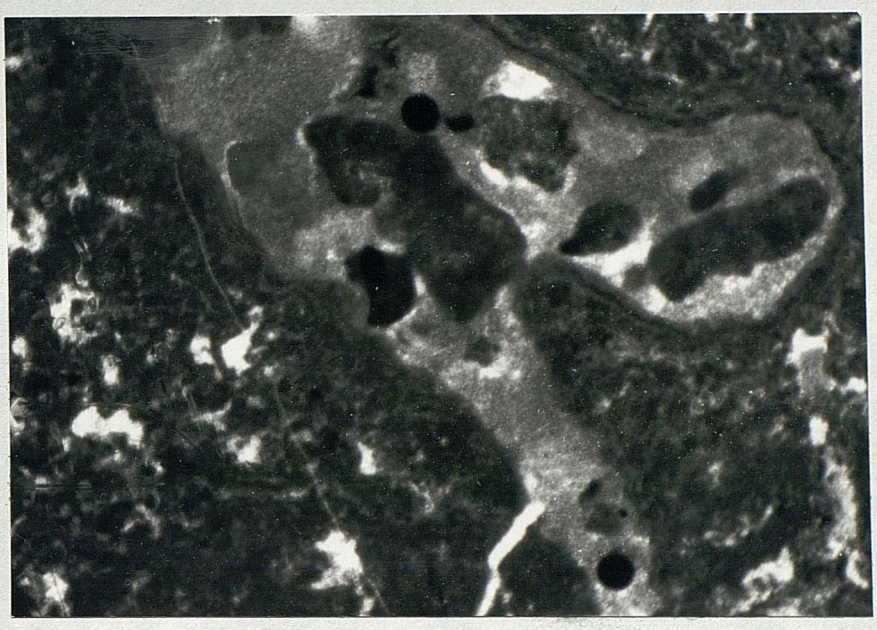

Fig. 70 Structureless algal biomicrite inclosing irregular micrite areas and faecal pellets.
Plane polarised light Width of field 2.9 mm.
Corbula Beds: bed 68b, Worbarrow Tout.

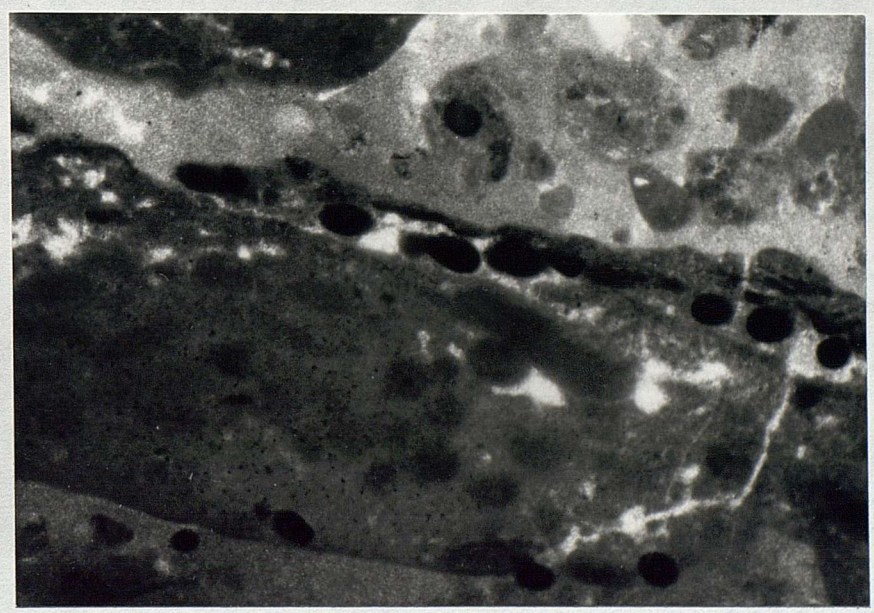

Fig. 71 Layers of faecal pellets interbedded with algal areas rich in black fine scattered material. A few pellets are slightly flattened by slight compaction.
Plane polarised light Width of field 2.9 mm.
Corbula Beds: bed 68b, Worbarrow Tout.

a tidal flat origin (e.g. Masson, 1955; Shearman, 1966).

(c) Bivalve biomicrudite facies

This facies is represented in Durlston Bay by at least 14 beds which are listed in Table 17. These beds are thin-bedded and range from medium grey (N4) to greenish grey (5 G 6/1) in colour. Individual beds range from 6 – 45 cm. in thickness. Algal lamination was observed in the middle part of bed DB183 known as the 'Toad's Eye Limestone' (Fisher, 1856).

In thin-section, the bivalve biomicrudites include several types differing in the fossil content, size of shell fragments and degree of neomorphism of the micrite groundmass. Generally the facies passes laterally and vertically into bivalve biosparrudites.

Bioclastic contents range from 20% upwards. The facies has a greater content of *Pecten, Liostrea* and foraminifera compared with the other facies of the *Corbula* Beds. The bivalves occur as large fragments (Fig. 72) up to 1 cm. long; roughly oriented parallel to the bedding. Whole valves of bivalves and complete articulated shells are not common. Small bivalve fragments from 20 – 500 μ in length occur either in thin bands (Fig. 73) or scattered in the matrix (Fig. 74). Locally, the large bivalve fragments have circular borings up to 60 μ in diameter. These are usually infilled with micrite similar to that in the matrix (Fig. 74). The abundance of these borings suggests effective biological breakdowns of the bivalves. Most of the bivalve fragments are preserved as pseudo-pleochroic calcite mosaics, locally with some pyrite, and occasionally rich in Fe^{2+}. Small pyrite nodules are common in the matrix.

The micrite in the matrix is usually altered into neomorphic spar with crystal sizes up to 55 μ. The majority of the size populations occur in the range 5 – 20 μ (Fig. 83). Usually, the micrites adjacent to the bivalve fragments were more altered by

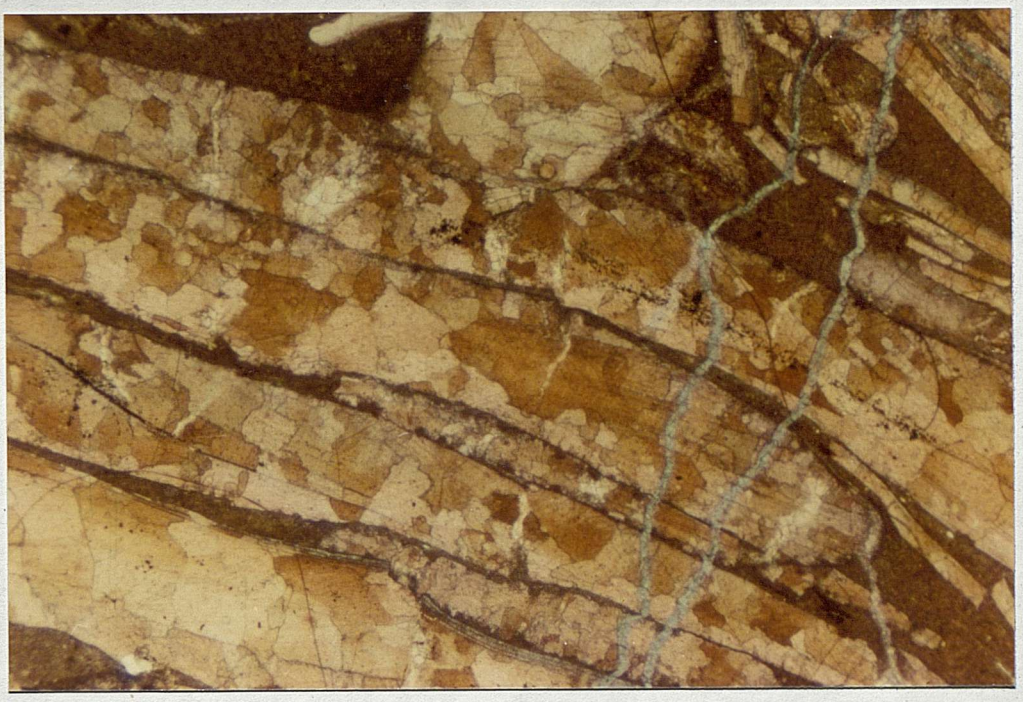

Fig. 72 Large bivalve fragments preserved as pseudo-pleochroic calcite and orientated parallel to bedding. Note the compactional feature of penetration (at the top). Veins are infilled with ferroan calcite. Thin-section stained with alizarin red-S and potassium ferricyanide.

Plane polarised light Width of field 3.2 mm.

Bivalve biomicrudite facies. *Corbula* Beds: bed DB183, Durlston Bay.

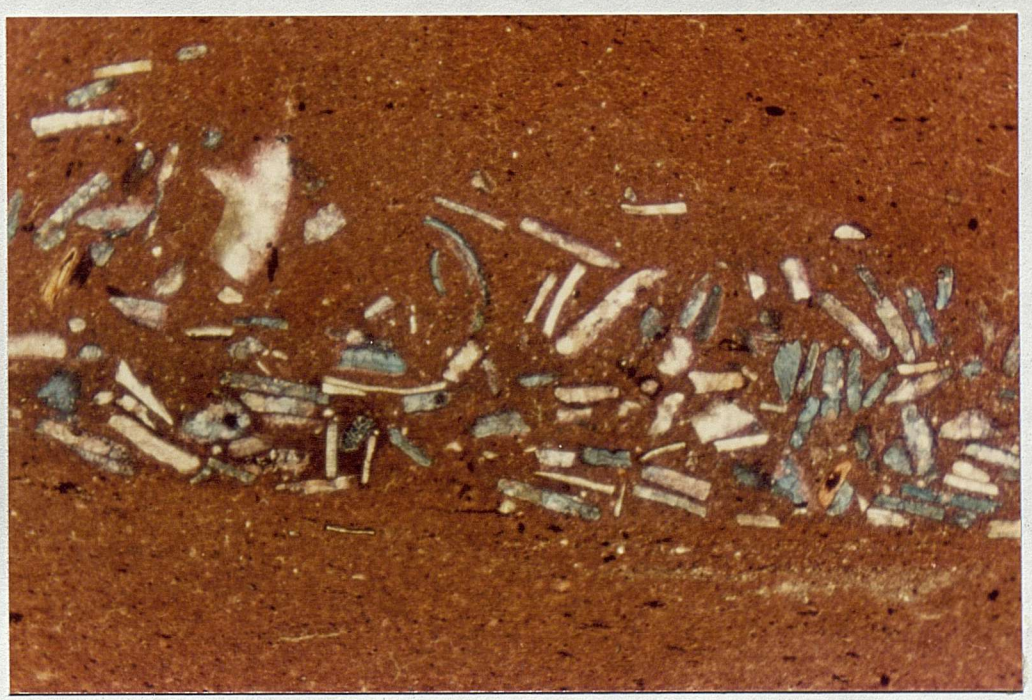

Fig. 73 Thin band of small bivalve fragments. The bivalves are preserved as pseudo-pleochroic calcite. Note the difference in Fe^{2+} content of the shell mosaics. Thin-section stained with alizarin red-S and potassium ferricyanide.

Plane polarised light Width of field 3.2 mm.

Bivalve biomicrudite facies. *Corbula* Beds: bed DB167, Durlston Bay.

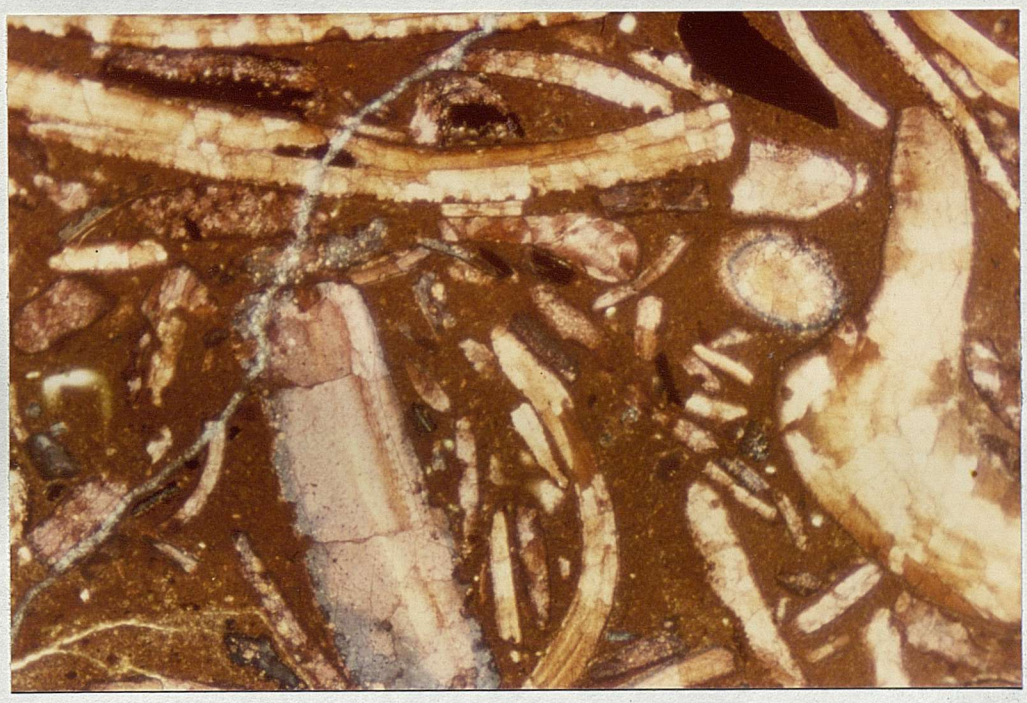

Fig. 74 Poorly-sorted bivalve biomicrudite. Note the large circular borings in the large shell fragments. This suggests effective biological breakdown of the bivalves. Thin-section stained with alizarin red-S and potassium ferricyanide.

Plane polarised light Width of field 3.2 mm.

Bivalve biomicrudite facies *Corbula* Beds, bed DB183, Durlston Bay

neomorphism. Incipient development of 'beef' (fibrous calcite) is common as elongated calcite crystals which have developed between shell fragments and forced them apart. This is a clear evidence of displacive crystal growth. Typical examples of these fabrics are found in beds DB169 and DB181.

The minerology and porosity of the bivalve biomicrudites are given in Table 17. These rocks are characterised by clay content which ranges as high as 23%. Quartz is present in small quantities up to 6%. The bivalve biomicrudites contain 76% calcite and 2% aragonite on average. Organic carbon varies from 0.30 – 1.26%. Barite is present as traces in bed DB187. Glauconite occurs especially in bed DB184 and is usually associated with calcitized shell fragments.

This bivalve biomicrudite facies of the *Corbula* Beds is the last of its type to be described in the middle Purbeck Group of Durlston Bay. Therefore, it is useful to compare all the bivalve biomicrudite facies here. The average composition and porosity of every bivalve biomicrudite facies is given in Table 18. The similarities among the bivalve biomicrudites of the Intermarine Beds, Scallop Beds and *Corbula* Beds are clear, especially in the contents of calcite, aragonite and clay. They differ slightly in the contents of quartz and organic carbon, and to some extent in their porosities. On the other hand, the bivalve biomicrudites of the Cinder Beds have the lowest contents of clay, aragonite and organic carbon and consequently the highest content of calcite.

Table 18 Average composition and porosity of the bivalve biomicrudite facies of Durlston Formation of Durlston Bay.

	Cinder Beds	Intermarine Beds	Scallop Beds	*Corbula* Beds
Calcite %	88	77	77	76
Aragonite %	0.6	3	1.5	2
Quartz %	3	3	5.5	3
Clay %	4.5	12	13	12
Organic carbon %	0.24	0.47	0.34	0.67
Porosity (%)	3	8	4	3

(d) **Bivalve biosparrudite facies**

This facies appears in several parts of the *Corbula* Beds of Durlston Bay (Table 17). Individual beds range from 15 – 85 cm. in thickness. They are either thin-bedded or massive and range from medium dark grey (N4) to pale yellowish brown (10 YR 6/2) in colour.

In thin-section, the rock grades into bivalve biomicrudite even within the same hand-specimen. The bivalve biosparrudite facies is subdivided into three petrographic types according to the nature of the bivalve preservation, packing, and degree of skeletal breakdown. The main petrographic features of each type are outlined in Table 19. They are discussed in some detail in the following pages.

Type 1: Fossil content of this type is high, up to 80% of the rock volume. The rocks consist of a framework of bivalve fragments, usually larger than 2 mm. The matrix contains smaller bivalve debris, angular and rounded quartz grains, bone fragments and small areas of sparry calcite. Compactional features increase with increase of the fossil content.

Biological and mechanical breakdown of the bivalves is common. Evidence of biological breakdown is best seen in the smaller bivalve fragments where large circular borings, up to 150 μ in diameter, are very common. Usually these borings are filled with ferroan calcite which is in optical continuity with the pseudo-pleochroic shell mosaics. This suggests that the borings remained empty until the original aragonite was calcitised. Evidences of mechanical breakdown of the bivalves are thin bands made up of well-sorted small shell fragments. The parallel orientation of these bivalve fragments probably resulted from current activity.

The bivalves are essentially preserved as pseudo-pleochroic shell mosaics which stain deep blue with potassium ferricyanide. Due to the high proportion of bivalve

percent, the thin-sections appear completely blue. Sparry calcite in the matrix stains pale blue suggesting lower content of Fe^{2+} compared with the pseudo-plerchroic shell mosaics. A few thin-sections have Fe^{2+}-free sparry calcite in the matrix although the pseudo-pleochroic mosaics are extremely rich in Fe^{2+}. This seems to suggests that the original sediment was "bathed" with Fe^{2+}-rich solutions for a long period until all the original skeletal aragonite was replaced by the pseudo-pleochroic mosaics.

Calcite cements are well-developed in the shell cavities. The crystals rarely exceed 100 μ in diameter but there are none of the small fibrous crystals of the calcite fringe which usually represent the early cement. The main-phase calcite cement (essentially non-ferroan) lies "unconformably" on a substrate of calcitised bivalves and followed by the late ferroan calcite cement. Occasionally the late calcite cement is followed by chalcedony (especially in bed DB171).

Pyrite is common in type1 of the bivalve biosparrudite facies and occurs as thin irregular layers more or less parallel to the bedding. Pyrite is also common in the calcitized bivalves as fine scattered crystals. Bivalves which still retain their original aragonite contain very little pyrite. This indicates that the processes of calcitization and pyritization were closely connected.

Type 2: The similarities between this type and the bivalve biosparrudite facies described in the Scallop Beds are striking. Rounded grains with micrite and oolitic coatings are abundant. Micrite envelopes are well-developed while the pseudo-pleochroic calcite in the shell mosaics is not common. Nevertheless, lines of inclusions forming palimpests of the original shell structure are abundant in some grains. Black ovoid pelletoids are common and range from 230–420 μ in length and from 100 – 150μ in breadth.

Although most of the allochems are very rounded, indicating high degree of

Fig. 75. Pyrite layers within a large bivalve fragment. The layers are folded by the pressure produced by shell penetration. The matrix contains rounded bivalve fragments, pelletoids and angular quartz grains.
Plane polarised light Width of field 2.9 mm.
Bivalve biosparrudite facies (type 2) *Corbula* Beds: bed DB186, Durlston Bay

Fig. 76 Pyritised bivalve fragments surrounded by pyrite-free sparry calcite. The pyrite rims and micrite envelopes (black) are fractured by compaction.
Plane polarised light Width of field 2.9 mm.
Bivalve biosparrudite facies (type 2) *Corbula* Beds: bed DB186, Durlston Bay

maturity, complete shells and whole valves are also common. The frequent occurrences of paired bivalves suggest that many of the shells have not been transported far after death. On the other hand, the high maturity of the allochems especially in the matrix indicates effective current activity. However, the rock as a whole was a product of mixing of allochems developed in different energy regimes.

Pyrite is usually associated with the calcitised bivalves. Occasionally, pyrite occurs as layers in paramorphically replaced bivalve fragments. These layers are locally folded by the pressure produced by shell penetration (Fig. 75). Pyrite rims surrounding the calcitized bivalves are occasionally broken by compaction (Fig. 76). These fabrics suggest that pyrite is pre-compaction and possibly post-calcitization. Pyrite rarely occurs in the calcite cements (Fig. 76), which indicates that pyritisation predates the cementation phases.

Three generations of calcite cements; early, main phase and late, were recognised (Fig.77). These calcite cements have textural fabrics similar to those described earlier in the Scallop Beds. Veins infilled with ferroan calcite post-date all the textural fabrics (Fig. 78).

Type 3: This type usually grades into bivalve biosparites. Bivalves are abundant and preserved as moulds formed by leaching of the original aragonite and then infilled with sparry calcite (Fig. 79). Bivalve fragments with oolitic coatings, particularly in bed DB178, show some similarities with the biosparrudite facies described in the Scallop Beds. Broken micrite envelopes and some small-scale shell penetration can be related to mild compactional effects.

Mud-clasts are locally common and range from 0.2 – 2 mm. in diameter. They are rounded and have sharp contacts with the surrounding calcite cements. They were probably derived from areas surrounding the basin of sedimentation. Reworked charo-

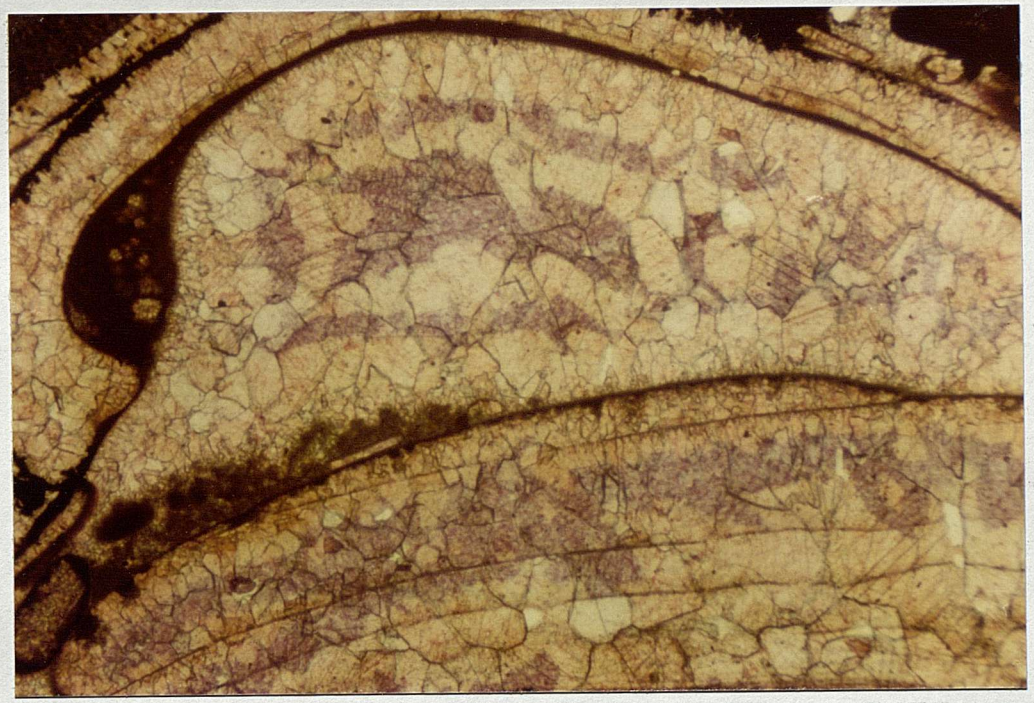

Fig. 77 Calcite cements well-developed in a large cavity between two bivalve valves. Note the oscillation in the Fe^{2+} content of the calcite cements which indicate that the ferroan and non-ferroan calcite are separated by chemical boundaries. Thin-section stained with alizarin red-S and potassium ferricyanide.
Plane polarised light Width of field 3.2 mm.
Bivalve biosparrudite facies (type 2) *Corbula* Beds: bed DB186, Durlston Bay.

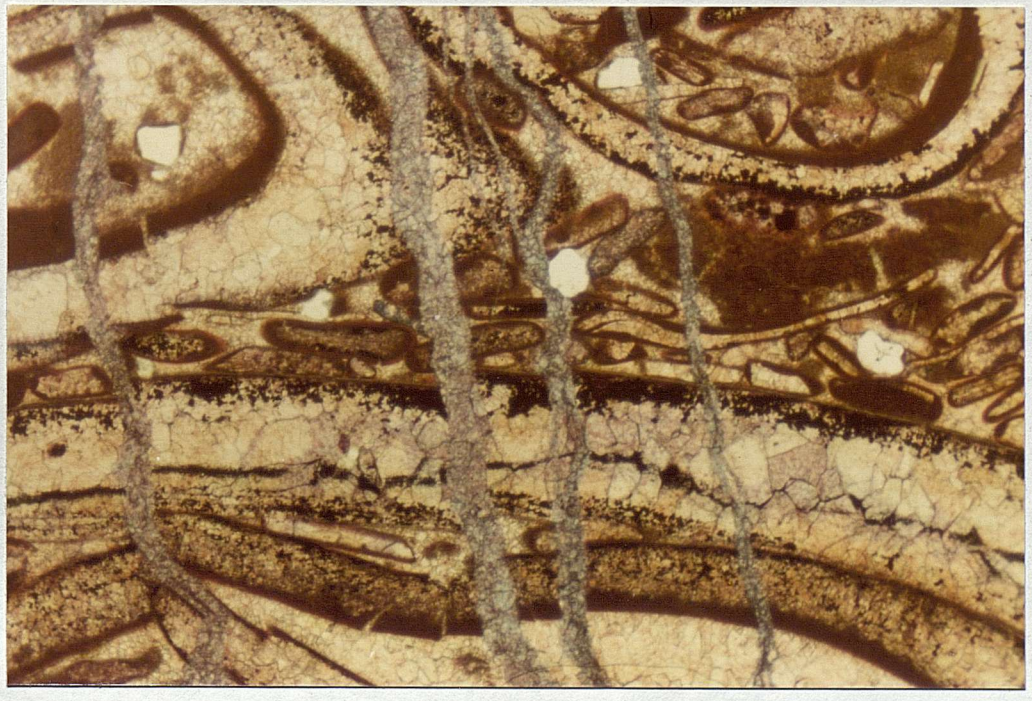

Fig. 78 Large bivalve fragments in a matrix of smaller rounded skeletal debris and subangular quartz grains. Pyrite (black) is common at the shell margins. Ferroan calcite veins postdate calcitization, pyritization, cementation and compaction phases.
Plane polarised light Width of field 3.2 mm.
Bivalve biosparrudite facies (type 2) *Corbula* Beds: bed DB186, Durlston Bay

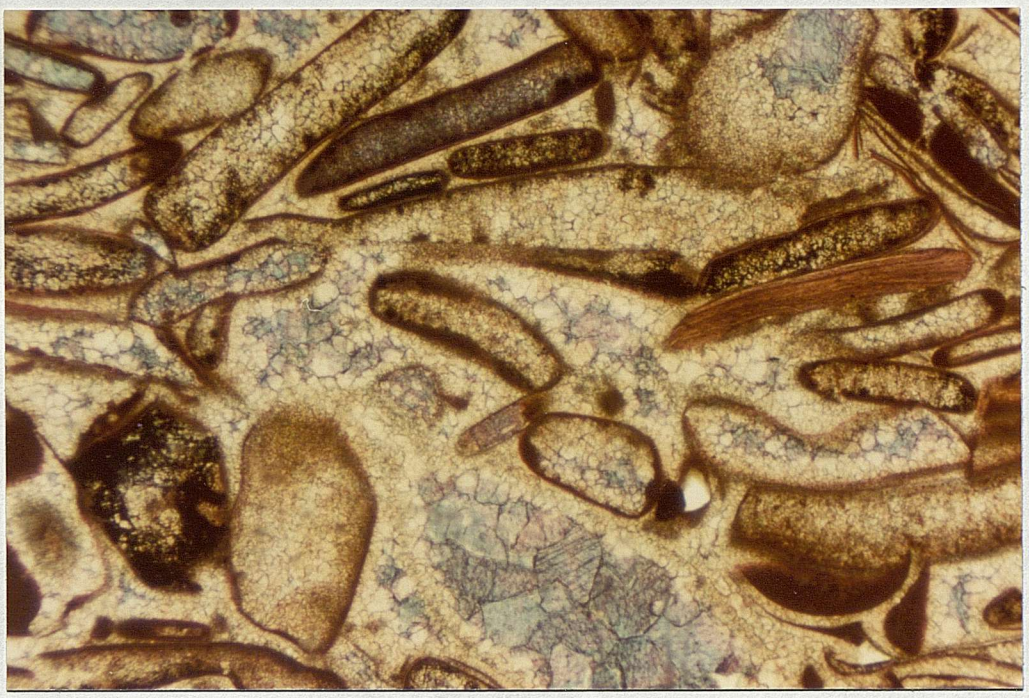

Fig. 79 Rounded bivalve fragments preserved as moulds filled with ferroan and non-ferroan sparry calcite after leaching of the former aragonite. Most of the allochems are coated with thick micrite envelopes. A *Liostrea* fragment (to the right) can be recognised by its foliated shell structure. Thin-section stained with alizarin red-S and potassium ferricyanide.

Plane polarised light Width of field 3.2 mm.

Bivalve biosparrudite facies (type 3) *Corbula* Beds, bed DB178, Durlston Bay

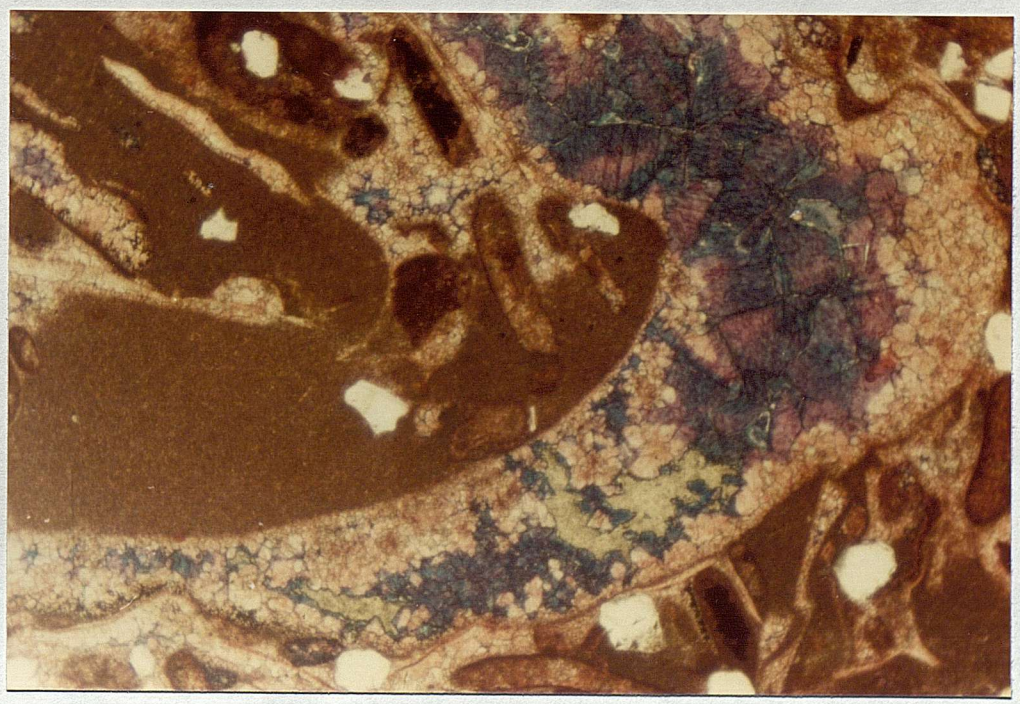

Fig. 80 Large bivalve fragment filled with ferroan and non-ferroan calcite after leaching of the former aragonite. Chalcedony (yellow) replaces the ferroan calcite. Thin-section stained with alizarin red-S and potassium ferrcyanide.

Plane polarised light Width of field 3.2 mm.

Bivalve biosparrudite facies (type 3) *Corbula Beds*: bed DB161, Durlston Bay

phyte fragments occur in bed DB178 of Durlston Bay.

Three generations of calcite cements occur in type 3. The early fibrous calcite fringe and the main-phase calcite cement are non-ferroan. The late calcite cements are essentially ferroan. Some of the bivalve moulds were completely or partially filled with ferroan calcite. The latest phase of cementation is represented by chalcedony which follows the ferroan calcite mosaics (Fig. 80). Most of the textures observed in type 3, suggest that diagenesis commenced under subaerial exposures and was completed under shallow overburden.

Table 19 Comparison between type 1, type 2 and type 3 of the bivalve biosparrudite facies in the *Corbula* Beds of Durlston Bay

	Type 1	Type 2	Type 3
Pseudo-pleochroic shell mosaics	very common	not common	absent
Moulds infilled with sparry calcite	absent	rare	very common
Micrite envelopes	rare	not common	very common
Content of calcite cement relative to the rock volume	< 10%	20 – 40 %	30 – 50%
Packing	closed	open	open
Compactional features	very common	common	rare
Skeletal breakdown	mainly biological	mainly mechanical	biological by algae and then mechanical
Pelletoids	absent	very common	not common
Aragonite	6	–	–
Organic carbon	0.47	0.84	0.33
Porosity (%)	2	1	1
Pyrite	common	common	rare

(e) Calcareous sandstone facies

This facies occurs near the base of the *Corbula* Beds and can be traced along the cliff sections from Durlston Bay westward to the Lulworth area and beyond Ridgeway (Fig. 14). In outcrops, the rocks of this facies are medium grey (N5) in colour and highly bioturbated. Ripple marks were observed in the calcareous sandstone facies in

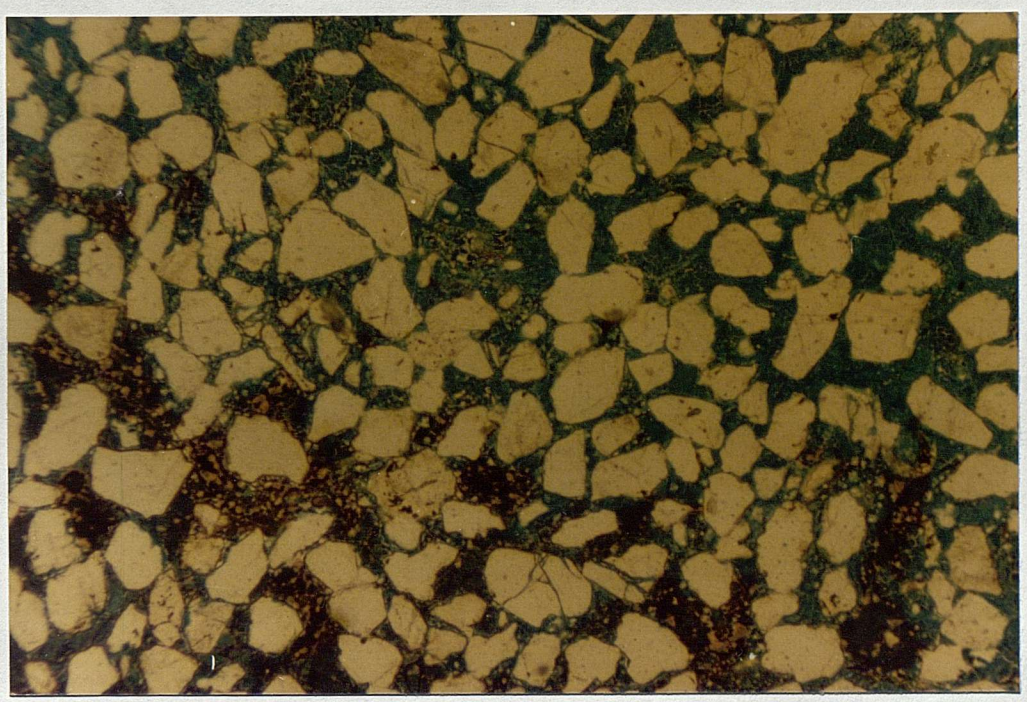

Fig. 81 Moderately-sorted subangular quartz grains cemented by ferroan calcite. Thin-section stained with alizarin red-S and potassium ferricyanide.

Plane polarised light Width of field 3.2 mm.

Calcareous sandstone facies *Corbula* Beds: bed DB157, Durlston Bay

Worbarrow Tout.

Petrographically, there is a complete gradation from calcareous sandstone to sandy limestone (Table 20). In Durlston Bay, the calcareous sandstone facies contains about 52% detrital quartz sand. Quartz grains are usually subangular, moderately-sorted, and up to 800 μ in diameter (Fig. 81). The bioclastic content rarely exceeds 20% of the rock volume. It usually includes small fragments of bivalves, ostracod debris and vertebrate bones. The sparry calcite of the groundmass is very rich in Fe^{2+} and has grain size up to 200 μ. Occasionally, the detrital quartz grains appear to be floating in a large area of sparry calcite which acts as a single calcite crystal. Such fabrics indicate a considerable size-enlargement. Compactional effects are indicated by the common penetration of the detrital quartz grains into bivalve fragments.

Pyrite is present as small spherical nodules up to 1.5 mm. in diameter. These nodules are locally fractured by compaction. Pyrite is also common in the calcitised bivalves.

The calcareous sandstone facies at Worbarrow Tout differs from that of Durlston Bay in two respects. It is less well-sorted and the sparry calcite in the matrix is non-ferroan.

Table 20 Mineralogy and porosity of the calcareous sandstone and sandy limestone facies in the *Corbula* Beds of Durlston Bay

Bed No.	Sample No.	Calcite %	Aragonite %	Quartz %	Clay %	Organic Carbon %	Porosity (%)
DB157	101	48	–	52	–	0.30	2
DB157	102	32	10	36	15	2.17	8
DB159	104	56	9	17	6	0.56	5
DB159	105	49	4	17	18	1.39	–
DB162	109	36	–	25	11	0.27	5

The mineralology and porosity of the calcareous sandstone and sandy limestone facies are given in Table 20. The contents of aragonite, clay and organic carbon are higher in the sandy limestones. Small amounts of barite was found in bed DB157.

5. Petrography of the Chief Beef Beds

These form the highest subdivision in the middle Purbeck Group according to the traditional Purbeck stratigraphy. They can be traced in Dorset from Durlston Bay to Ridgeway (Fig. 14). The Chief Beef Beds are dominated by shale which occupies 73% of the sequence at Durlston Bay. The shale usually contains thin bands of fibrous calcite, the 'beef', and thin layers of crushed bivalves referred in the present work as perished bivalves.

The bioclastic content of the Chief Beef Beds at Durlston Bay is dominated by ostracods and bivalves while the gastropods are less important. The main ostracod genera are *Cypridea, Darwinula* and *Theriosynoecum* and less commonly *Macrodentina* and *Rhinocypris* (Clements, 1969). The bivalves include *Neomidon* and *Unio* while the gastropods are represented by different species of the genera *Viviparus, Planorbis* and *Hydrobia* (Clements, 1969). Bone fragments and plant remains are locally abundant.

At Durlston Bay, three limestone facies were recognised in the Chief Beef Beds. These are:

a. Ostracod biomicrite

b. Ostracod biosparite

c. Bivalve biosparrudite

The mineralogy and porosity of the three facies are given in Table 21.

Table 21 Mineralogy and porosity of the limestones of the Chief Beef Beds of Durlston Bay

Bed No.	Sample No.	Calcite %	Aragonite %	Quartz %	Clay %	Organic Carbon %	Porosity (%)	Facies
DB201	167	66	–	8	22	2.63	11	Ostracod biomicrite
DB210	178	70	2	3	19	2.53	7	
DB211	181	72	4	2	15	1.13	5	
DB212	182	71	2	4	14	2.50	5	
Average		70	2	4	18	2.20	7	
DB202	168	81	–	4	9	1.34	6	Ostracod biosparite
DB214	184	62	4	4	3	4.81	4	
DB216	187	88	–	2	2	0.55	3	
DB218	189	98	–	1	–	0.39	2	
Average		82	1	3	3	1.77	4	
DB200	166	92	2	2	2	0.45	3	Bivalve biosparrudite
DB204	170	95	2	–	–	0.16	1	
DB206	172	96	2	–	–	0.44	1	
Average		94	2	0.7	0.7	0.35	2	

(a) Ostracod biomicrite facies

In Durlston Bay, the facies is represented by beds DB201, DB210, DB211 and DB212. These are thin-bedded and medium dark grey (N4) in colour. Individual beds range from 5 – 10 cm. in thickness.

The bioclastic debris of the facies is, of course, predominantly ostracod valves and these constitute from 15 – 60% of the rock volume. Bivalve fragments and vertebrate remains are locally present in small quantities. Unlike similar facies recognised earlier, the ostracod biomicrite facies of the Chief Beef Beds lacks gastropods.

In thin-section, the ostracods are commonly well-preserved and tend to be concentrated in thin bands separated by micrite layers rich in fragmental ostracod valves. The paired ostracods vary considerably in size i.e. from 100–1000 μ in length. Such a wide variation in size probably represents normal growth stages which in turn suggest

limited transport (Jones, 1958). Most of the paired ostracods are infilled with ferroan calcite (Fig. 82). Ostracods infilled with micrite and pyrite are also common. Although most of the paired ostracods appear to be floating in the micrite matrix, they are commonly flattened by compaction. Usually the long axes of the flattened ostracods lie parallel to the bedding which indicates that compaction was a direct effect of the overburden.

Micrite is the main component of the matrix. Clay and fine detrital quartz grains are also common. The micrite shows signs of size-enlargement especially in beds DB201 and DB211. Incipient development of 'beef' is common in bed DB201. Size distribution of 100 micrite grains in bed DB201, measured with the optical microscope, is given in Fig. 83. About 70% of the micrite grains occur between 5 – 15 μ. Of particular interest is the patchiness of the microspar. Micrite areas with much clay are usually less affected by the processes of size-enlargement. Folk (1965) has put forward a different explanation. He suggested the possibility that the clay content in a limestone might cause micrite to recrystallise to microspar. It is difficult to decide whether the organic matter aided the process of size-enlargement of the original carbonate mud leading to the development of microspar (Alberstadt, 1973). Examples of considerable size-enlargement in the micrites of limestone facies with low organic carbon content, such as the Cinder Beds, have been described earlier. However, it can be argued that the low contents of organic carbon may be due to oxidation which occurred after the process of size-enlargement. If this is true, it is difficult to explain why other fine-grained limestone (in the Purbecks) were slightly affected by size-enlargement although they contain higher contents of organic matter.

Table 22 summarises the mineralogy and porosity of the ostracod biomicrite

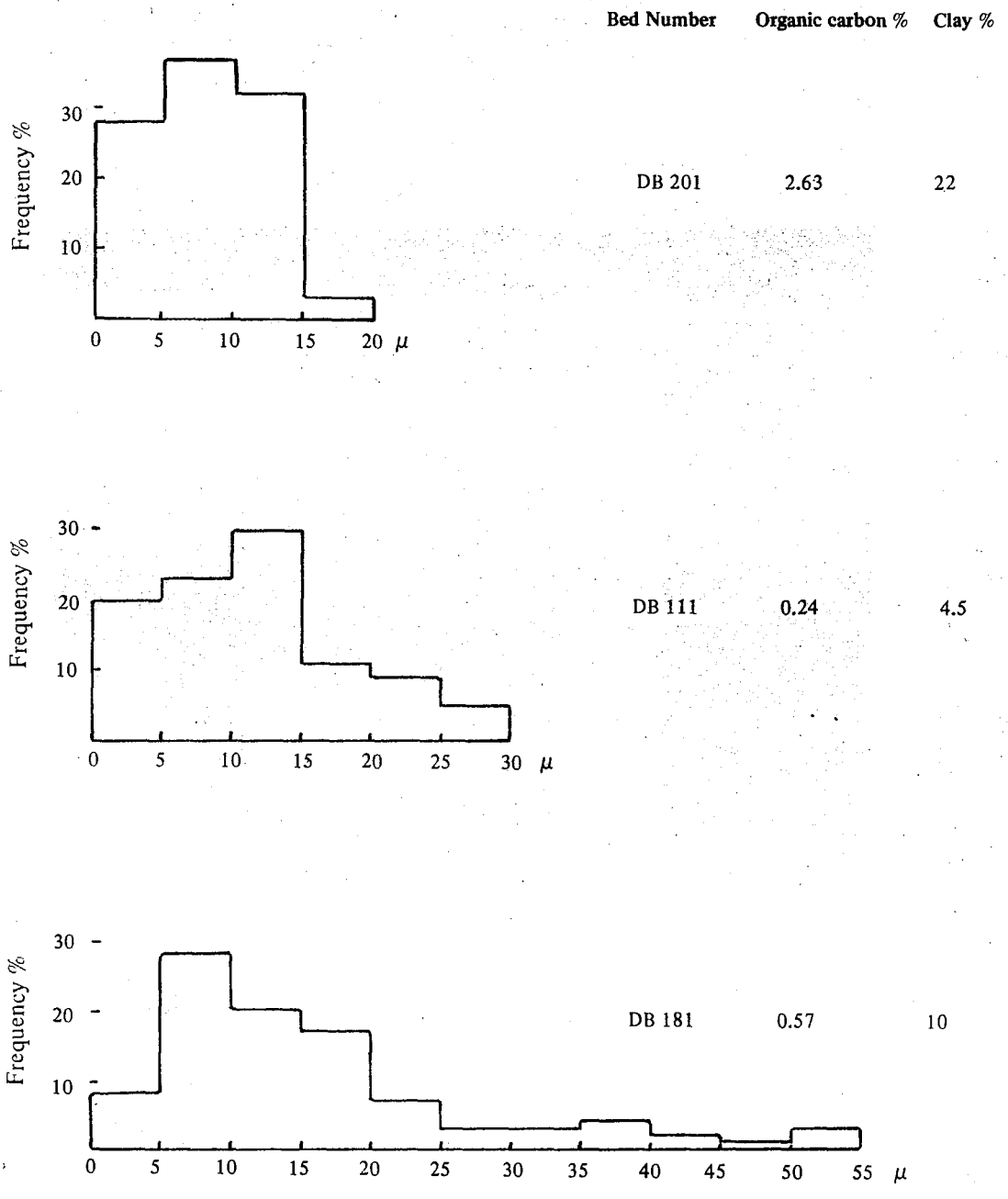

Fig. 83. Crystal-size distribution of the calcite groundmass in the bivalve biomicrudites (DB 111 and DB 181) and the ostracod biomicrite (DB 201).

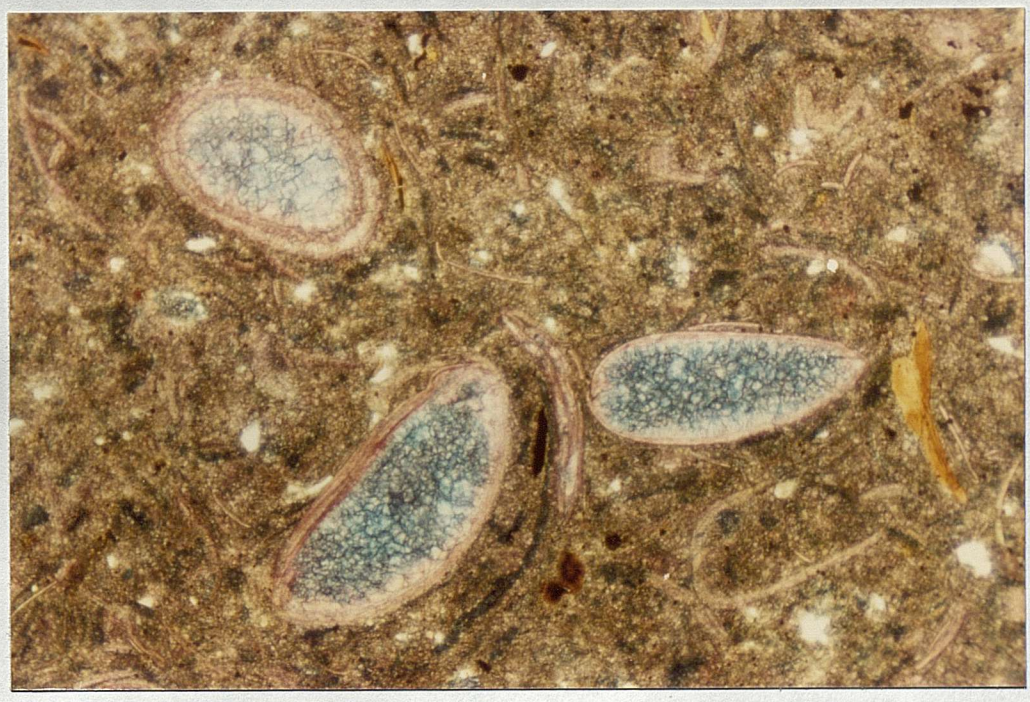

Fig. 82 Ostracods infilled with ferroan calcite. The matrix is a neomorphosed micrite with ostracod fragments, fine quartz grains and bone fragments (yellow). Thin-section stained with alizarin red-S and potassium ferricyanide.

Plane polarised light Width of field 3.2 mm.

Ostracod biomicrite facies Chief Beef Beds: bed DB211, Durlston Bay.

Table 22 Average composition and porosity of the ostracod biomicrite facies in the middle Purbeck Group of Durlston Bay

	Lulworth Formation	Durlston Formation	
	Cherty Freshwater Beds	Intermarine Beds	Chief Beef Beds
Calcite %	74	75	70
Aragonite %	2	3	2
Quartz %	4	3	4
Clays %	13	13	18
Organic Carbon %	1.7	1.7	2.2
Porosity (%)	9	7	7

facies of the middle Purbeck Group. The facies are more common in the Cherty Freshwater Beds and the lower parts of the Intermarine Beds. They are not represented in the Scallop Beds and the *Corbula* Beds. In the Chief Beef Beds, the ostracod biomicrites are of local importance. The general similarities in mineralogy and porosity of the ostracod biomicrite facies are striking.

(f) Ostracod biosparite facies

This facies was not encountered in the Lulworth Formation. In Durlston Bay, it is represented by beds DB202, DB214, DB216 and DB218. These beds are light bluish grey (5 B 7/1) when unoxidised but light brownish grey (5 YR 6/1) when weathered. They show massive bedding and range from 5-55cm. in thickness.

Bioclastic content is up to 70% of the rock volume, mainly represented, of course, by ostracods. Well-preserved ostracods are locally common and usually infilled with ferroan calcite. Bivalve fragments occur locally, especially in beds DB216 and DB218, and in thin-section, fragments up to 2 mm. in length are most common. They are preserved as pseudo-pleochroic calcite rich in Fe^{2+}. Fish and plant remains are locally abundant, particularly in bed DB214.

The sparry calcite in the matrix is extremely rich in Fe^{2+} as indicated from the

deep blue colour developed using a potassium ferricyanide stain. Pyrite is very common in all samples and extremely abundant in bed DB214 where it reaches up to 20% by weight of the rock. Incipient development of 'beef' in common in bed DB202. Compactional features occur locally and are similar to those described in the previous facies.

The composition and porosity of the ostracod biosparite facies are given in Table 21. Very high percentages of pyrite and organic carbon was found in bed DB214.

(c) Bivalve biosparrudite facies

In Durlston Bay, the facies is represented by beds DB200, DB204 and DB206. These are either thin-bedded or massive and bed thicknesses range from 17-33 cm. In outcrops the rocks vary in colour from medium bluish grey (5 B 5/1) to light grey (N7). Burrows were recorded from beds DB204 and DB206.

The facies is very rich in the bioclastic debris, particularly the bivalves which form up to 90% of the rock volume. The bivalve fragments are generally oriented parallel to the bedding. They are closely packed and show compactional features similar to those described in the bivalve biosparrudite facies of the Cherty Freshwater Beds. The bivalve fragments are preserved as pseudo-pleochroic calcite, a good indicator of the former presence of aragonite. Both the pseudo-pleochroic shell mosaics and the sparry calcite cements in the matrix are extremely rich in Fe^{2+}. This suggests that calcitisation and cementation phases were completed in a reducing environment. Most of the sparry calcites adjacent to the bivalve fragments are in optical continuity with the pseudo-pleochroic shell mosaics. This indicates that cementation postdates calcitization of the former aragonite.

Pyrite occurs as small spherules which range from few microns to 40 μ in diameter. These spherules are probably framboids, the very early diagenetic type of pyrite which

forms in unconsolidated recent mud (Love, 1964; 1967). Pyrite is also common in the calcitized bivalves and is usually more abundant along the crystalline boundaries of the pseudo-pleochroic shell mosaics.

The composition and porosity of the bivalve biosparrudite facies in the Chief Beef Beds are given in Table 21. Comparison with the other bivalve biosparrudites recognised earlier suggests a general similarity in composition and porosity (Table 23).

Table 23. Average composition and porosity of the bivalve biosparrudites in the Middle Purbeck Group of Durlston Bay

	Lulworth Formation		Durlston Formation		
	Cherty Fresh-water Beds	Intermarine Beds	Scallop Beds	*Corbula* Beds	Chief Beef Beds
Calcite %	89	91	85	86	94
Aragonite %	2	3	2	4	2
Quartz %	3	2	6	3	1
Clay %	2	1	2	3	1
Organic Carbon %	0.34	0.22	0.10	0.45	0.35
Porosity (%)	4	4	3	2	2

(d) Layers of perished bivalves

These are white (N9) and friable aragonite-rich bivalve layers up to 10 cm. in thickness. They are so friable that they can easily be broken down, by hand, into white powdery material. These layers of perished bivalves are common in the Purbeck shales and, particularly, those of the Chief Beef Beds.

Thin-sections of the perished bivalves (which usually are very difficult to make) reveal that they suffered considerable compaction without noticeable cementation. The majority of the bivalves are still aragonitic and a high aragonite content (40-75%) is one of the striking features of bands rich in perished bivalves (Table 24). The bivalve fragments consist of very fine aragonite grains which are less than 1μ in

Table 24. Composition and porosity of the perished bivalves, friable bivalve limestone and 'beef' in the middle Purbeck Group of Durlston Bay

Bed Number	Sample Number	Calcite %	Aragonite %	Quartz %	Clay %	Organic Carbon %	Porosity (%)	
DB 130	72	16	40	12	18	2.07	n.d	Perished bivalves
DB 180	139	8	63	4	12	6.99	29	
DB 192	159	12	68	2	2	1.62	37	
DB 194	161	6	75	2	2	1.44	40	
DB 198	164	2	62	4	25	0.96	30	
Average		9	62	5	12	2.62	34	
DB 91	15	68	14	3	7	0.41	8	Friable bivalve limestone
DB 129b	69	44	26	5	12	6.65	7	
DB 134	77	48	15	5	29	0.92	7	
DB 154	96	73	13	3	2	0.71	10	
DB 164b	113	60	18	3	5	0.36	20	
DB 208	174	65	22	3	–	1.20	17	
DB 210	177	73	10	4	3	2.02	16	
DB 219a	192	73	12	1	6	0.89	14	
Average		63	16	3.5	8	1.65	12	
DB 134	80	88	–	2	6	0.20	3	'Beef'
DB 164a	112	74	–	5	12	0.48	4	
DB 164c	116	81	–	5	7	0.20	4	
DB 166	120	76	–	3	13	0.68	4	
DB 185	149	85	–	1	9	0.49	3	
DB 209	175	88	–	2	6	0.48	4	
DB 211	180	83	–	2	10	0.63	5	
DB 219b	192	87	–	3	6	0.28	4	
Average		83	–	3	8.5	0.43	4	

n.d. not determined

length. Occasionally, the whole aragonitic bivalve fragment extinguishes uniformly between crossed-nicols. No pseudo-pleochroic shell mosaics or moulds infilled with granular calcite were found which suggests a very limited calcitisation. Calcite grains welding the aragonitic bivalve fragments are volumetrically insignificant which indicates limited cementation. Veins of ferroan calcite traverse the rock in all directions. These veins form a network which gives the 'rock' some degree of support.

High porosity is another important feature of these bands of the perished bivalves (Table 24). Porosity values are up to 40% and usually varies sympathetically with the aragonite content. The small calcite content which rarely exceeds 12% indicates limited cementation which in turn explains the high porosity values. It seems that although the 'rock' had suffered severe compaction, the change in the original porosity values is limited.

High organic carbon content is the third important characteristic feature of the perished bivalves . In fact the highest organic carbon content to be reported in all the Purbeck samples studied, was encountered in one of these bands (6.99% organic carbon in bed DB180). Clay and quartz contents vary considerably (Table 24). Pyrite, gypsum, sphalerite and occasionally barite occur in small quantities in most of the samples of the perished bivalves .

The high percentage of aragonite in the bands of perished bivalves raises questions regarding the preservation of skeletal aragonite in ancient sediments. Although skeletal aragonite has been reported from ancient sediments of late Devonian age (Grandjean *et al.*, 1964), and early Carboniferous (Hallam and O'Hara, 1962), it is well known that the abundance of aragonite in limestones decreases with the age of the host rock (Bathurst, 1975). The preservation of aragonite in ancient sediments can be related to the contents

of clay and organic matter. Bøggild (1930) reported that the limestones from Mesozoic strata in which aragonite still preserved has a large content of clay. He suggested that only 10-20% of clay is enough for the preservation of aragonite as long as possible. The bands of perished bivalves contain 12% of clay on average. Nevertheless, the clay content of the perished bivalve layers is not a critical factor in aragonite preservation since these layers are entirely enclosed in shale.

The role of organic matter in preserving aragonite in ancient sediments has been emphasised by Fuchtbaur and Goldschmidt (1964). They have shown that within the German Wealden (equivalent in part to Durlston Formation), molluscs enclosed in bituminous shale or oil escape solution whereas those in water-saturated coquina are replaced by calcite. The high content of organic matter in the Purbeck sediments has been emphasised below.

Because the preservation of aragonite and organic matter is closely connected, one assumes an early reduction in permeability of the host argillaceous sediment. This would prevent the oxidation and destruction of organic matter. Under such conditions the system is more or less closed and movement of the diagenetic solutions is very restricted. There is, however, a possibility that in the presence of organic acids small amounts of aragonite may dissolve although Kennedy and Hall (1967) suggested a mechanism by which an amino-acid, absorbed on the aragonite surface, could prevent its dissolution. Nevertheless, aragonite dissolution stops once the small amount of trapped pore-solutions is saturated with $CaCO_3$.

(e) Friable bivalve limestone

These are another group of limestones which may represent a diagenetic stage intermediate between the stages attained by the layers of perished bivalves and the bivalve biosparrudites. In outcrops, the layers of perished bivalves usually grade into

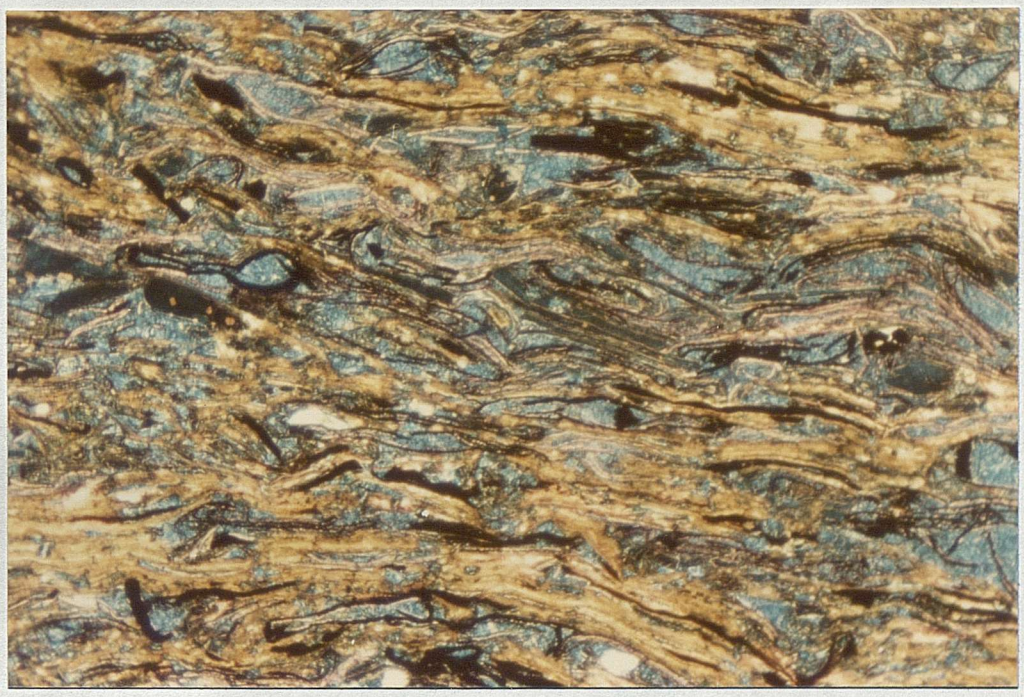

Fig. 84 Friable bivalve limestone rich in ostracods infilled with ferroan calcite. Most of the bivalves are still aragonitic (yellow). Thin-section stained with alizarin red-S and potassium ferricyanide. Plane polarised light Width of field 3.2 mm.
Chief Beef Beds: bed DB208, Durlston Bay

friable bivalve limestone which in turn passes laterally into bivalve biosparrudites.

Petrographically, these limestones consist predominately, of course, of bivalve fragments, although ostracods are locally abundant (Fig. 84). Most of the bivalves fragments are preserved as pseudo-pleochroic shell mosaics which are usually rich in Fe^{2+}. Pyrite is common especially in the calcitized bivalve fragments. Compactional features are numerous and usually predate the cementation phases. In these respects, the 'friable' bivalve limestones have some similarities with many of the bivalve biosparrudites described earlier in different parts of this work. However, the high aragonite content (10-26%) and the high porosity values (7-20%) are features in which the 'friable' bivalve limestones resemble the layers of perished bivalves .

Of particular interest are the porosity variations in relation to the contents of calcite, aragonite, clay and organic carbon of the bivalve biosparrudites, friable bivalve limestones and the bands of perished bivalves (Table 25). Porosity shows a sympathetic variation with the aragonite content (Fig. 85a). With the increase in the calcite contents due to cementation and calcitization of the aragonitic molluscs, porosity is appreciably reduced (Fig. 85b). The contents of clay and organic carbon have indirect effects on porosity (Fig. 85 c & d). Possibly their role is the preservation

Table 25. Average composition and porosity of the layers of perished bivalves , friable bivalve limestone and bivalve biosparrudites in the middle Purbeck Group of Durlston Bay.

	Calcite %	Aragonite %	Clay %	Organic Carbon %	Porosity (%)	Number of samples
Layers of perished bivalves	9	62	12	2.62	34	5
Friable bivalve limestone	63	16	8	1.65	12	8
Bivalve biospar-rudite	88	3	2	0.30	3	38

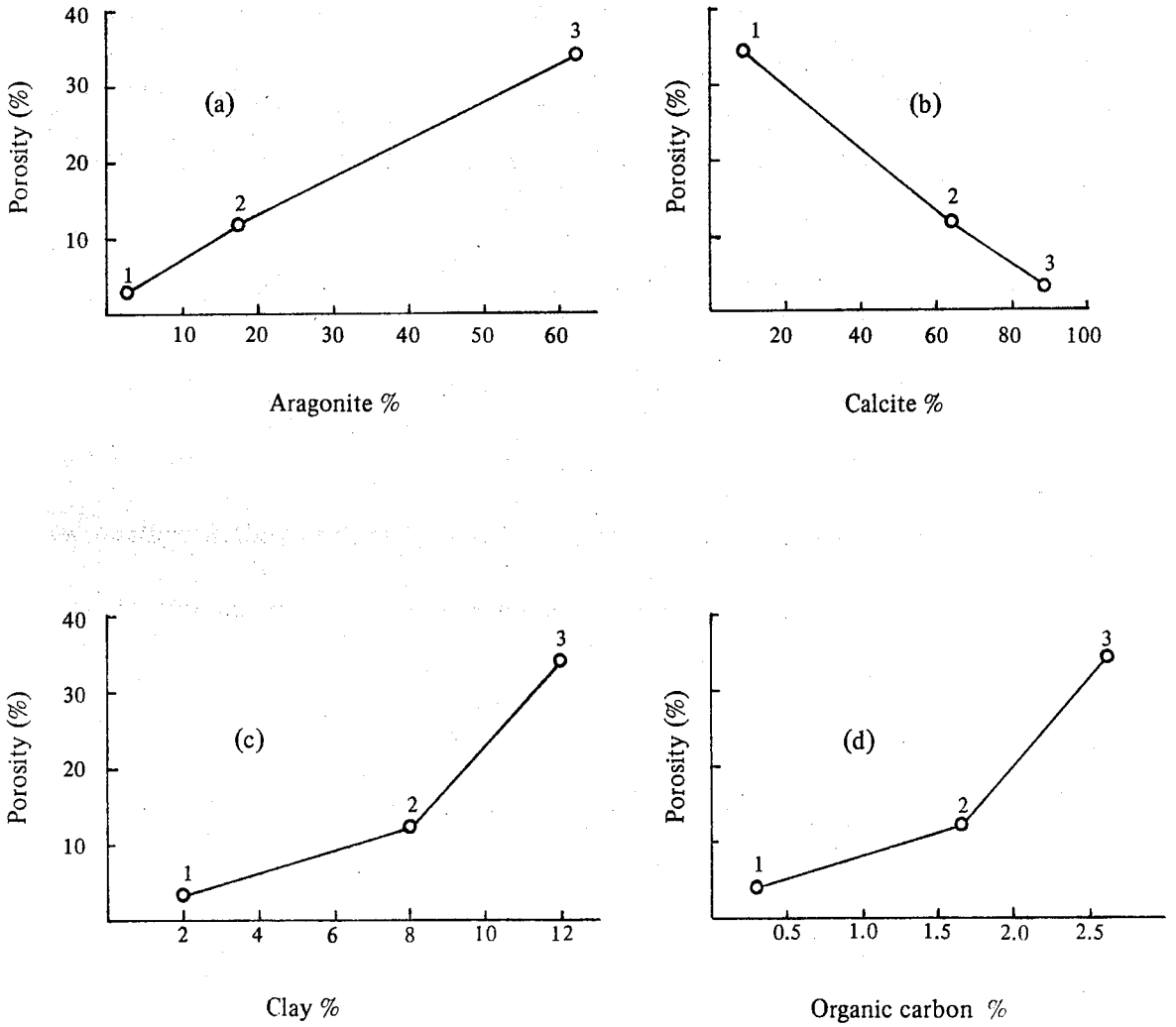

Fig. 85. Porosity variations in relation to the contents of aragonite, calcite, clay and organic carbon of the bivalve biosparrudites (1), friable bivalve limestone (2) and the layers of perished bivalves (3).

of aragonite and inhibiting calcite precipitation.

(f) Origin of the Purbeck 'beef'

Fibrous calcite, known as 'beef' is most common in the paper-shale, particularly those of the Chief Beef Beds, but it also occurs in various shales above and below the Cinder Beds. When the strata are disturbed by folding and faulting, the 'beef' layers are usually involved in the movement (Fig. 11). This suggests that the formation of 'beef' layers either predates folding and faulting or it is contemporaneous with the movement.

The 'beef' layers are usually 0.5-2 cm. in thickness. The maximum thickness to be recorded in the middle shales is 20 cm. This was observed in the Chief Beef Beds of Lulworth area. The 'beef' layers are usually medium dark grey (N6) in colour, but on weathering they turn into greyish red (5 R 4/2). Occasionally, they acquire a red stain of iron oxides which contains abundant selenite crystals. Commonly, the 'beef' layers have a flat surface. In other instances, when the surface is curved, the convex side is always directed upwards. In Worbarrow Tout, the 'beef' layers occur locally as series of broad domes in which thickness decreases away from the centre of each dome. The 'beef' layers usually consist of two bands separated by a thin film rich in clay and pyrite. The fibrous calcite crystals in the 'beef' layers are always normal to the bedding. Near the surface of the 'beef' layers, the calcite fibres are slightly curved.

The most important petrographic feature of 'beef' is that most of the calcite crystals are rich in Fe^{2+} (Fig. 86). Thin-sections normal and parallel to the 'beef' layers reveal clearly the nature of the cone-in-cone structure. The cones consist of bundles of fibrous calcite crystals orientated obliquely one to the others (Fig. 87). Each bundle is usually coated with a thin clay film (Figs. 86; 88).

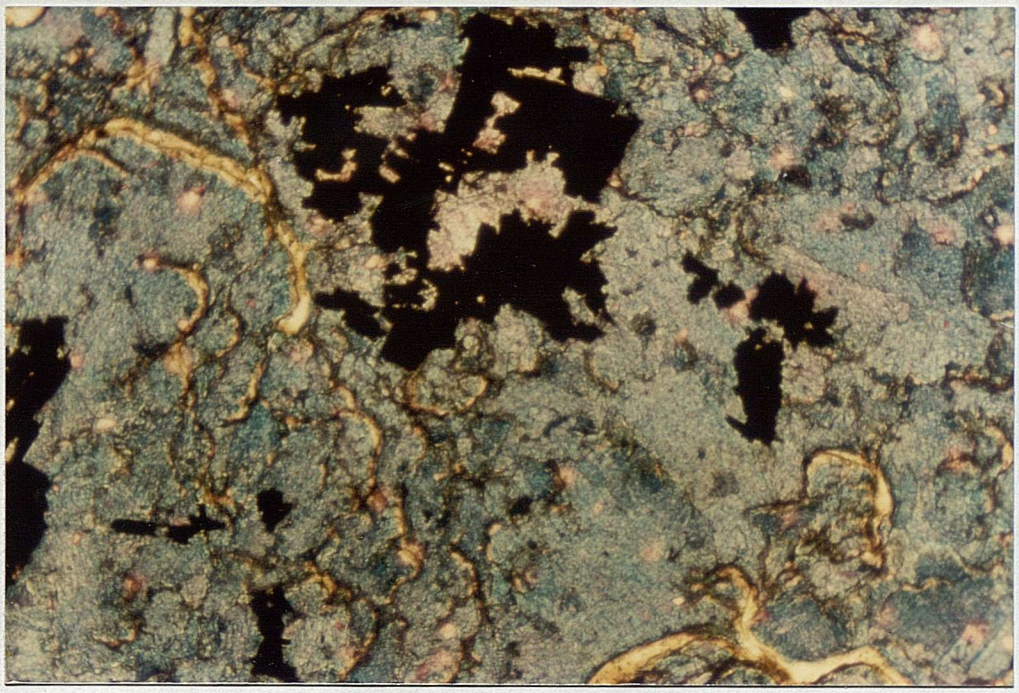

Fig. 86 Cross-section of 'beef' with staining revealing the high Fe^{2+} content. Clay (yellow) is common. Large pyrite crystals with well-developed faces are abundant. Thin-section stained with alizarin red-S and potassium ferricyanide.

Plane polarised light Width of field 3.2 mm.

Beef, *Corbula* Beds: bed DB164, Durlston Bay

Fig. 87 Vertical section in 'beef' showing the cone-in-cone structure. Thin-section stained with alizarin red-S and potassium ferricyanide.

Plane polarised light Width of field 3.2 mm.

'Beef', Chief Beef Beds, Durlston Bay

The majority of the calcite fibres are elongated in the direction of the optic-axis. In thin-sections cut parallel to the 'beef' layers, more than 70% of the calcite crystals have centred optic-axis figures. A few calcite crystals show pseudo-biaxial figures especially the large calcite crystals and those with twinning. Pyrite is more common along the surface of the 'beef' layers. It occurs as large crystals up to 2 mm. in diameter and characterised by well-developed crystal faces (Fig.86). Fractures are not common in the 'beef' layers, but when they occur, they are usually infilled with ferroan calcite.

Incipient development of beef was observed in many limestones, described above. However, this fabric is more frequent in the calcareous shales. Thin clay seams are usually associated with the incipient 'beef' in a way similar to the stylolitic insoluble residue (Fig. 89).

The composition of the beef layers is given in Table 24. Calcite content ranges from 74-88%. Most of the 'beef' has small contents of clay (6–13%) and detrital quartz (1–5%). Organic carbon content varies from 0.20–0.68%.

The occurrence of 'beef' in the Purbeck shales raises two related problems, i.e. the source of carbonate and the mechanism of formation. The layers of perished bivalves are the source of carbonate for the 'beef'. This is based on the following field observations and chemical criteria. 'Beef' is always associated with these layers. This was first discovered by Fisher (1856) who observed that the crystals of 'beef' are always shooting upwards from a layer of perished bivalves. The Sr contents of the 'beef' indicates redistribution of carbonates by aragonite dissolution and calcite reprecipitation (see Chapter 15).

It was mentioned before that preservation of aragonite indicates an early reduction

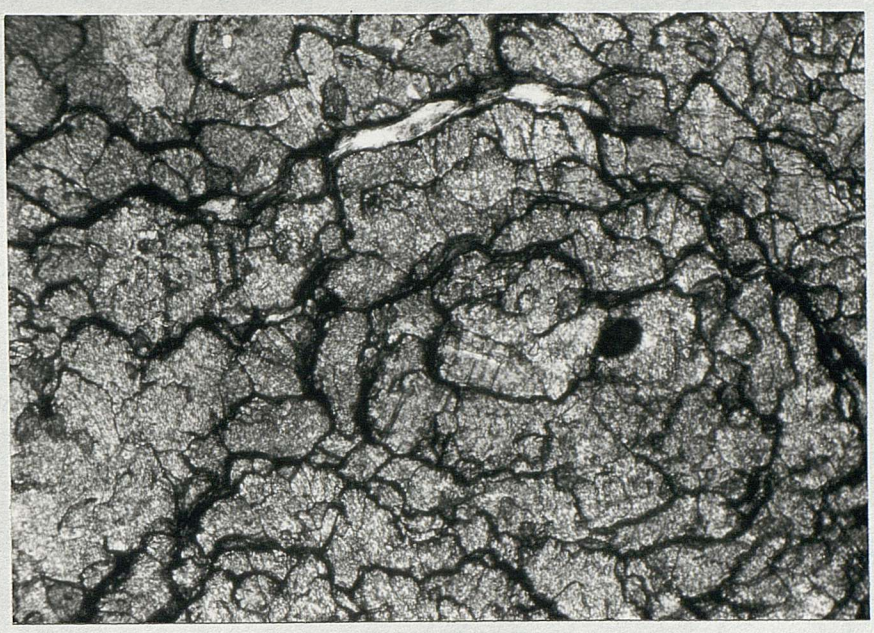

Fig. 88 Cross-section in beef showing circular bundles of calcite coated with clay (black).
Plane polarised light Width of field 2.9 mm.
'Beef', *Corbula* Beds: bed DB164, Durlston Bay

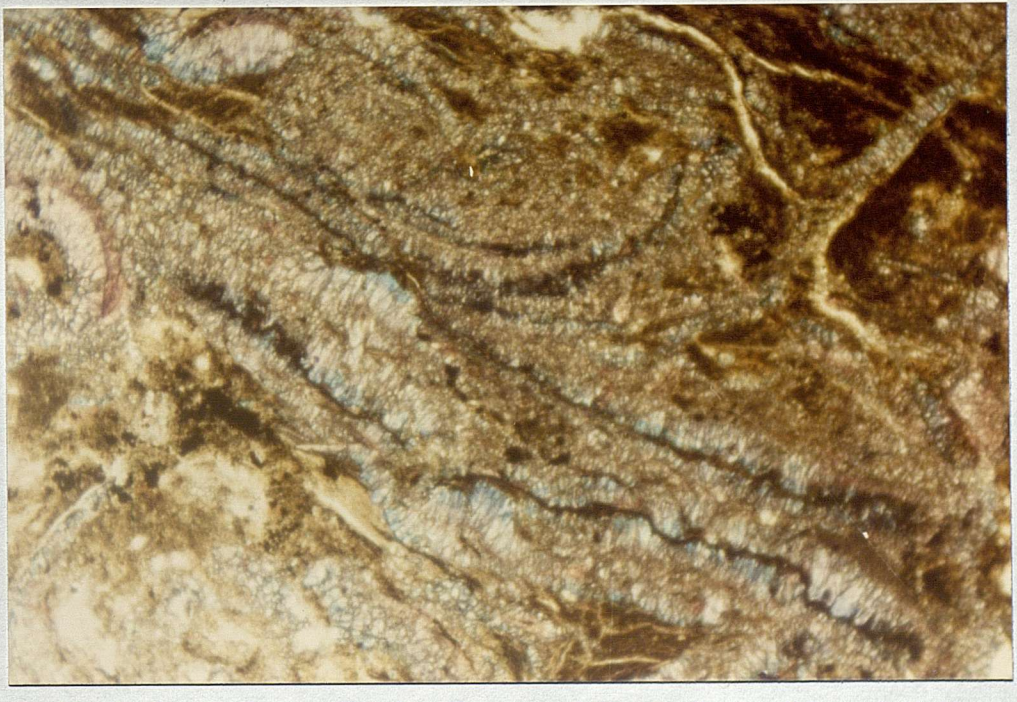

Fig. 89 Incipient development of 'beef' in calcareous shale. Note the clay seam between the beef layers.
Thin-section stained with alizarin red-S and potassium ferricyanide.
Plane polarised light Width of field 3.2 mm.
Calcareous shale, Marley Freshwater Beds: bed DB83, Durlston Bay

in permeability of the host shale. If permeability was reduced appreciably, the pore-solutions would have moved with such extreme slowness that equilibrium was almost completely reached between the surface of aragonite grains and the solutions. Under such conditions neither aragonite dissolution nor calcite precipitation would have taken place. However, before the system reached this state of equilibrium, the pore-solutions would have become saturated with $CaCO_3$ due to the early dissolution of some of the aragonite in the presence of organic acids. Precipitation of calcite from the pore-solutions is unlikely to have occurred unless the CO_2 pressure dropped. This implies departure from the equilibrium state which could not have been achieved without volume increase. Most probably the volume increase was obtained when the bedding surfaces were forced apart by growing fibrous calcite. Such mechanism is consistent with the occurrence of bent and curved fibres in the 'beef'.

However, a mechanism whereby the bedding planes could have been jacked open by water injection have been suggested by Shearman *et al.*, (1972). This mechanism implies active movement of vast quantities of water. If these solutions were saturated by $CaCO_3$, calcite precipitation would have occurred in the porous layers of perished bivalves rather than as 'beef'. On the other hand, if these solutions were under-saturated in $CaCO_3$ complete leaching of the aragonitic layers would have resulted. The high porosity (up to 40%) and high aragonite content (up to 75%) of the layers of perished bivalves indicates that water movement was in fact, very restricted.

10. HEAVY MINERALS OF THE MIDDLE PURBECK GROUP

The present research is restricted to the limestones although they are extremely poor in their heavy mineral content. Sandstones are not common and no specimen suitable for heavy mineral separation has been obtained from the shales. This may explain the lack of any published data concerning the heavy minerals in the Purbeck rocks of Dorset. The main objective of this account is to compare and contrast the heavy mineral assemblages of Lulworth and Durlston Formations. A search for possible source rocks has been attempted.

Heavy mineral separation was carried out for samples which were originally collected for petrographic and geochemical studies. Most of these samples were obtained from the middle Purbeck Group, particularly in the type-section of Durlston Bay. Additional samples were collected from the middle Purbeck rocks of Wiltshire and Sussex.

1. Mineralogy

Heavy minerals identified consist dominantly of opaque minerals, zircon, tourmaline, rutile, garnet, stauralite and kyanite (Table 26). Other minerals which occur in a frequency less than 1% of the non-opaque include anatase, brookite, epidote, barite, celestite, sphalerite and muscovite. Details of the most common non-opaque heavy minerals are given below.

(a) Zircon

This mineral occurs in all samples ranging from 28–75% of the non-opaques. Most of the zircon grains are colourless. Coloured varieties are not common, they often show zoning especially in the smaller grains. Distinct zoning in the colourless varieties is very rare. Rounding usually increases with progressive increase in grain size although

Table 26. Frequency distribution of heavy minerals in the middle Purbeck Group

Non-opaques are calculated as 100%
ρ = present, but less than 1%

Bed Number	Opaques	Zircon	Tourmaline	Rutile	Garnet	Staurolite	Kyanite	Others	Remarks
				DURLSTON BAY					
DB 214	59	71	13	7	4	2	–	3	Chief Beef Beds
DB 210	56	74	13	5	4	3	–	1	
DB 208	85	65	17	6	3	5	ρ	3	
DB 194	71	38	27	8	8	16	–	3	
DB 174	38	66	18	5	6	ρ	ρ	4	*Corbula* Beds
DB 161	67	43	19	8	7	12	11	–	
DB 159	60	28	24	7	6	18	16	1	
DB 157	45	40	9	14	5	27	4	1	
DB 151	55	68	8	5	9	5	2	3	Scallop Beds
DB 149	38	51	12	13	15	5	3	1	
DB 144	51	52	10	16	12	8	ρ	1	Intermarine Beds
DB 133	71	41	22	7	11	12	5	2	
DB 129	57	48	11	15	22	ρ	ρ	3	
DB 120	63	75	16	3	3	2	–	1	
DB 112	80	66	15	9	5	1	–	4	
DB 111	48	52	6	13	23	1	1	4	Cinder Beds
DB 110	45	71	11	8	8	–	–	2	Cherty Freshwater Beds
DB 102	52	55	10	12	20	1	–	2	
DB 101	51	70	6	10	7	1	–	6	
DB 99	38	54	23	9	7	ρ	–	6	
				OTHER DORSET LOCALITIES					
	57	52	19	6	5	7	10	1	*Corbula* Beds, Worbarrow Tout
	52	51	14	16	9	7	3	–	Scallop Beds, Herston (SZ/009787)
	57	29	26	10	20	3	12	–	Scallop Beds, Stair Hole
	59	49	19	18	5	5	1	3	Intermarine Beds, Dancing Ledge (SY/996776)
	53	38	26	6	16	6	6	2	Intermarine Beds, Worbarrow Tout
				WILTSHIRE					
	52	46	15	12	8	8	9	2	Above Cinder Beds, Vale of Wadour, Lady Down
				SUSSEX					
	58	65	10	21	3	–	–	1	Above Cinder Beds, Great Wood, Brightling (TQ/685219)

fine-grained zircons with higher degrees of rounding can be present. Some of the grains although still predominantly euhedral show some rounding of their terminations. Broken euhedral zircon grains are locally important. No thorough study of crystal elongation was made but, in general, zircons with length: breadth ratio of 2 : 1 or less predominate. This is in agreement with Poldervaart's (1955) study of sedimentary zircons.

(b) Tourmaline

Tourmaline ranges from 6–27% of the non-opaque heavy minerals. The brown varieties are the most abundant while the blue ones are less common. Parti-coloured (brown and blue) tourmaline grains are rare. The degree of rounding ranges from sub-angular to well-rounded (particularly egg-shaped). Euhedral tourmaline grains were sometimes encountered although they are not common. High concentration of black inclusions are frequently present in most of the euhedral grains.

(c) Rutile

Rutile occurs in all samples ranging from 3–21% of the non-opaque heavy minerals. The foxy-red variety is more abundant than the yellow rutile. Most of the grains vary from rounded to angular, euhedral grains are not common. Twinned rutile was encountered in few samples.

(d) Garnet

Garnet was identified in all samples varying from 3–22% of the non-opaque heavy minerals. The most abundant is the colourless variety. A few grains show a faint pink colour. Most of the garnet grains range from angular to subangular. Corroded grains are not common.

(e) Staurolite

The mineral is essentially confined to the Durlston Formation of Dorset. It was

found in beds belonging to the same formation in the Vale of Wadour, Wiltshire. Staurolite is present in small percentages but it occasionally reaches 27% of the non-opaque heavy minerals. The mineral is most common in the coarser fraction. Few grains have well-developed crystal faces and this suggests that there was some attrition. Corroded staurolite grains with ragged outlines are common. They have features similar to those described by Allen (1949a) as 'spires'.

(f) Kyanite

Kyanite is almost always accompanied with staurolite, both being characteristic minerals of the Durlston Formation of Dorset. Kyanite was also identified above the Cinder Beds in Wiltshire.

Kyanite ranges from 0 – 16% of the non-opaque heavy minerals. It occurs as elongated colourless grains. The most distinctive feature of kyanite in the Purbeck rocks is its ragged outlines; a feature similar to that described by Smithson (1942) in the middle Jurassic rocks of Yorkshire.

2. Evaluation of the heavy minerals: the limitations

Andel (1959) emphasised the importance of four processes which may modify the heavy mineral assemblages and consequently limit their interpretation in terms of source areas. These processes are: 1. weathering both in source area and depositional basin; 2. mechanical destruction during transportation; 3. selective sorting of minerals according to size, shape and density; and 4. chemical destruction after deposition capable of removing the less stable minerals. Evaluating heavy mineral assemblages implies the ability to eliminate or take into account all modifications the assemblages undergo between source rock and completed analyses.

(a) **Alteration of the assemblages by weathering**

Heavy minerals are greatly affected by chemical alteration in the source rocks and during deposition, particularly in broad regions of low relief. The role of weathering becomes less important as the rate of uplift and erosion increased (Stanley, 1965). The scarcity of feldspars and the dominance of stable minerals such as zircon, rutile and tourmaline suggests compositional maturity in both light and heavy mineral assemblages of the Purbeck rocks. Such maturity reflects the importance of weathering (or recycling), especially during the deposition of the Lulworth Formation.

(b) **Alteration of the assemblages by mechanical destruction**

This process was probably of minor importance during the Purbeck sedimentation. It has been found that there is negligible destruction of heavy minerals by mechanical wear in sediments transported by modern rivers for distances greater than 1000 kms. (Andel, 1959).

(c) **Alteration of the assemblages by selective sorting**

The composition of the heavy mineral assemblages of a sediment can be modified by sorting mainly according to size and shape. The effect of density variations is apparently much less than the effect of size. Densities of heavy minerals range from 2.85 (the cut off point in bromoform) to over 5.0 while sizes cover a wider range i.e. from approximately minimum of 0.03 mm. to larger than 0.5 mm. Zircon and rutile in the Purbeck sediments have a tendency to be enriched in the finer particle-sizes while kyanite and staurolite are more abundant in the coarser sizes. Garnet and tourmaline occupy

the intermediate range. Although sorting could be an important factor in concentrating certain heavy minerals in the Purbeck sediments, it is unlikely to be responsible for the removal of others.

(d) Alteration of the assemblages by post-depositional changes

After sedimentation heavy minerals can be modified by selective chemical destruction during diagenesis; a process which Pettijohn (1941) has called intrastratal solution. Although the world-wide importance of this process is still debated (Bramlette, 1941; Smithson, 1941; Krynine, 1942; Pettijohn, 1957; Andel, 1959; Gazzi, 1965; Stanley, 1965; Blatt and Sutherland, 1969; Grimm, 1973; Nickel, 1973), all agree that it does occur at least locally. In the Purbeck sediment, kyanite and stauralite are corroded by intrastratal solution, but it seems unlikely that diagenesis was so intense to remove important amounts of the heavy minerals. The occurrence of meta-stable carbonates such as aragonite in different horizons of the Purbeck Group, suggests that leaching of heavy minerals during diagenesis was of limited scale.

3. Possible source rock

A feature of the transition between the Jurassic and Cretaceous periods was the world-wide fall in sea-level (Hallam, 1969), and the development of brackish to freshwater conditions in many parts of the world (Anderson, 1974). Western Europe provides a good example of this fall, especially in early Cretaceous times (Allen, 1967a). By the end of the Portland marine sedimentation phase, much of southern England was exposed to land conditions (Wills, 1951). Exposed Paleozoic and Mesozoic rocks surrounding the Purbeck basin in southern England are possible sources of clastics including heavy minerals. The following is an attempt to locate sources from which the Purbeck detritus was derived.

Accessory minerals characteristic of the granite massifs in S.W. England and N. France were reported by Brammall (1928) and Groves (1931). The heavy mineral assemblages in the Purbeck of Dorset do not seem to indicate that there was a direct derivation from the granite massifs of Cornwall, Devon, Brittany or Normandy. On the other hand, the metamorphic rocks and sediments of Brittany would provide kyanite and staurolite. Neaverson (1925) and Latter (1926) suggest the Armorican massif of Brittany as the main source of kyanite and staurolite in the late Kimmeridge Clay and Portland Sand Formation respectively. The same source area has been also suggested for staurolite and kyanite in the Wealden sediments of the Weald (Allen, 1949a; 1959; 1967a & b; 1969). Due to the corroded nature of kyanite and staurolite in the Purbeck sediments, it is difficult to decide whether both minerals were directly derived from Brittany or recycled through late Jurassic sediments.

Wealden detrital tourmaline from Durdle Door suggests derivation from Armorica (Allen, 1972). Some of the Purbeck tourmaline could have derived from the same source.

The London-North Sea uplands could be possible source for some of the heavy minerals in the Purbeck sediments. During the Wealden times, these uplands consisted of an interior highland north of the Thames made principally of Upper Paleozoic rocks and a marginal lowland of Jurassic sediments to the south (Allen, 1954). In Sussex, Kent and Surrey the London uplands were important sources for the lower Wealden detritus including black iron ore, zircon, tourmaline, rutile and garnet (Allen, 1949a; 1960; 1961; 1967b; 1976). Undoubtedly, the Purbeck of Dorset should have received some sediments from the London uplands since their weathering began in late Jurassic times (Allen, 1967b) and they were fairly close.

4. Palaeogeographic implications

Recycling is a major difficulty in relating the heavy minerals in the Purbeck sediments to particular source rocks. It cannot be proved in all instances just whence the constituents of heavy minerals were derived. Also, it is not possible to prove conclusively the number of cycles of erosion and transportation to which the heavy minerals have been subjected.

In the Purbeck of Dorset, brackish and freshwater fauna shows a marked upward increase in the succession. There is an increase in the quantity and grain size of the clastics (including the heavy minerals) from the Lulworth Formation to the Durlston Formation. This indicates some important hydrological changes. The arrival of staurolite and kyanite (and kaolinite; see Chapter 11) in the Durlston Formation suggests that the drainage courses were able to affect source rocks which were difficult to drain at the time of Lulworth formation. There was probably increasing rainfall and/or decreasing evaporation from the Lulworth to the Durlston times. This is demonstrated by lithology; evaporites occur in the basal Purbeck while fluviatile sands and clays cap the Purbeck sequence. Additionally, the arrival of coarse clastics during the time of the Durlston Formation may also be the result of high relief developed on the surrounding land during the mid-Purbeck tectonics (Allen, 1967a; 1975).

11. GEOCHEMISTRY OF THE MIDDLE PURBECK SHALES

1. General

The data are presented separately in tabular and diagrammatic form and in the appendices. For brevity no sections repeating these data are given in the text. For each element, however, there follows a discussion and interpretation. Different approaches were applied in interpreting the present geochemical data; they include the following:

(a) Statistics

Initially, the chemical data of 200 samples representing the middle Purbeck limestones and shales were treated using the normal distribution statistics. It was found that the distribution of most of the elements was far from normality as indicated by their high skewness values. The whole population includes all gradations from almost pure limestones with 99% carbonates to shales containing up to 90% clay minerals. A decision had to be made to split the whole population into limestones and shales, as they were identified during the field work. Most of the rocks recognised in the field as shales or mudstones were found to contain more than 50% clays. Similarly, the limestone samples contain more than 50% carbonates. Only few samples occur near the shale-carbonate boundary and they were grouped with the limestones or the shales as appropriate. This procedure improved the skewness values of most elements when each new population was measured but some major and trace elements remained highly skewed.

Often when the distribution is unidentified or not positively known, nonparametric statistics may be applied (Flanagan, 1957). Their major disadvantage lies in the fact that large samples must be used in order to achieve power efficiency equal to that

of the normal distribution (Fenner and Hagner, 1967). Nonparametric and normal distribution statistics were applied and a fair agreement between both approaches was obtained. However, the normal distribution statistics were preferred for the reasons mentioned above. To avoid any bias, only the values of correlation coefficients at the 0.001 level of significance were considered. Throughout the present work, however, the value of the statistical data was not overestimated and it was treated with caution.

(b) Comparison with published data

The arithmetic means of the geochemical data obtained in the present work were compared with the corresponding averages for shales and limestones cited in literature. Many averages exist, but mainly the most widely quoted ones were preferred for comparison. Usually such averages are based on large numbers of geochemical data which represent samples from many geological periods. Averages of particular types of rocks such as those of freshwater and marine shales, were used for the problem of palaeosalinity.

2. Mineralogy

The distribution of the different minerals in the middle Purbeck shales is shown in Figs. 90 & 91. Average mineral composition of the entire shale suite is 68%.clay minerals, 15.4% carbonates and 11.6% quartz (Table 27). The middle Purbeck clays contain on average 7% kaolinite, 38% illite and 23% montmorillonite (this including the mixed-layer illite/montmorillonite).

The average mineralogic composition of shales reported by Leith and Mead (1915), Clarke (1924) and Shaw and Weaver (1965) is given in Table 27. By comparison, the middle Purbeck shales are characterised by low quartz content and high carbonate content.

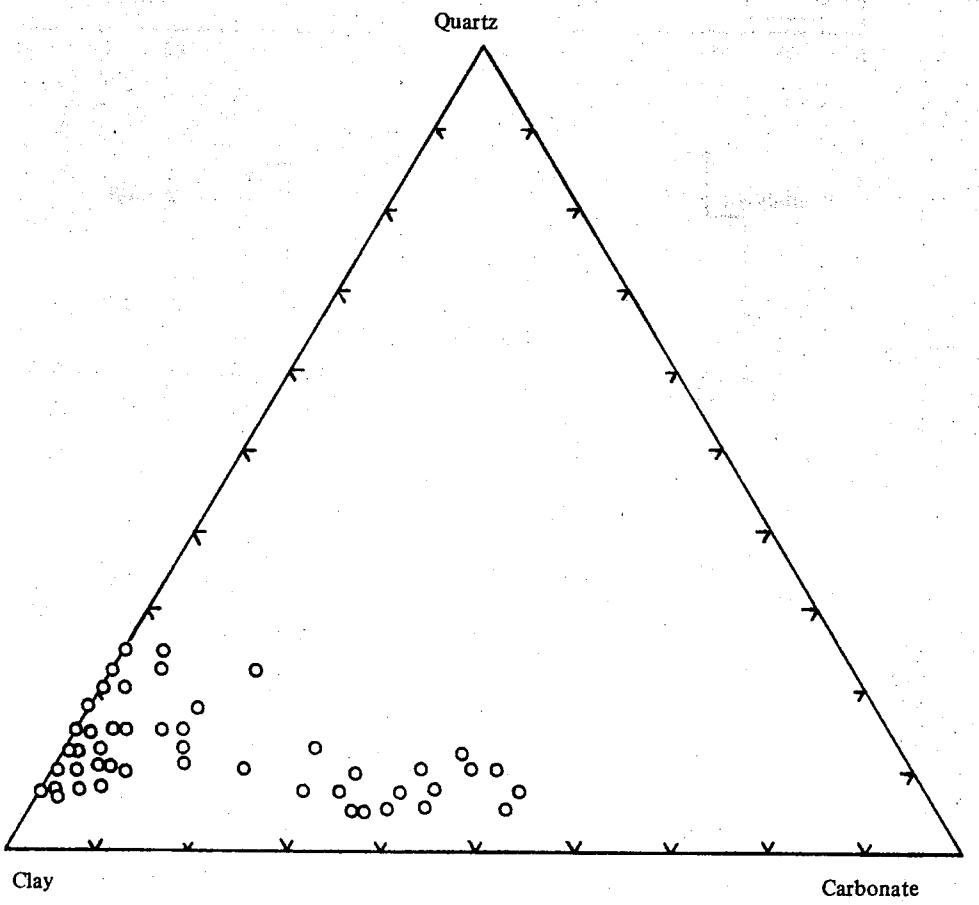

Fig. 90. Mineral composition at the middle Purbeck shales

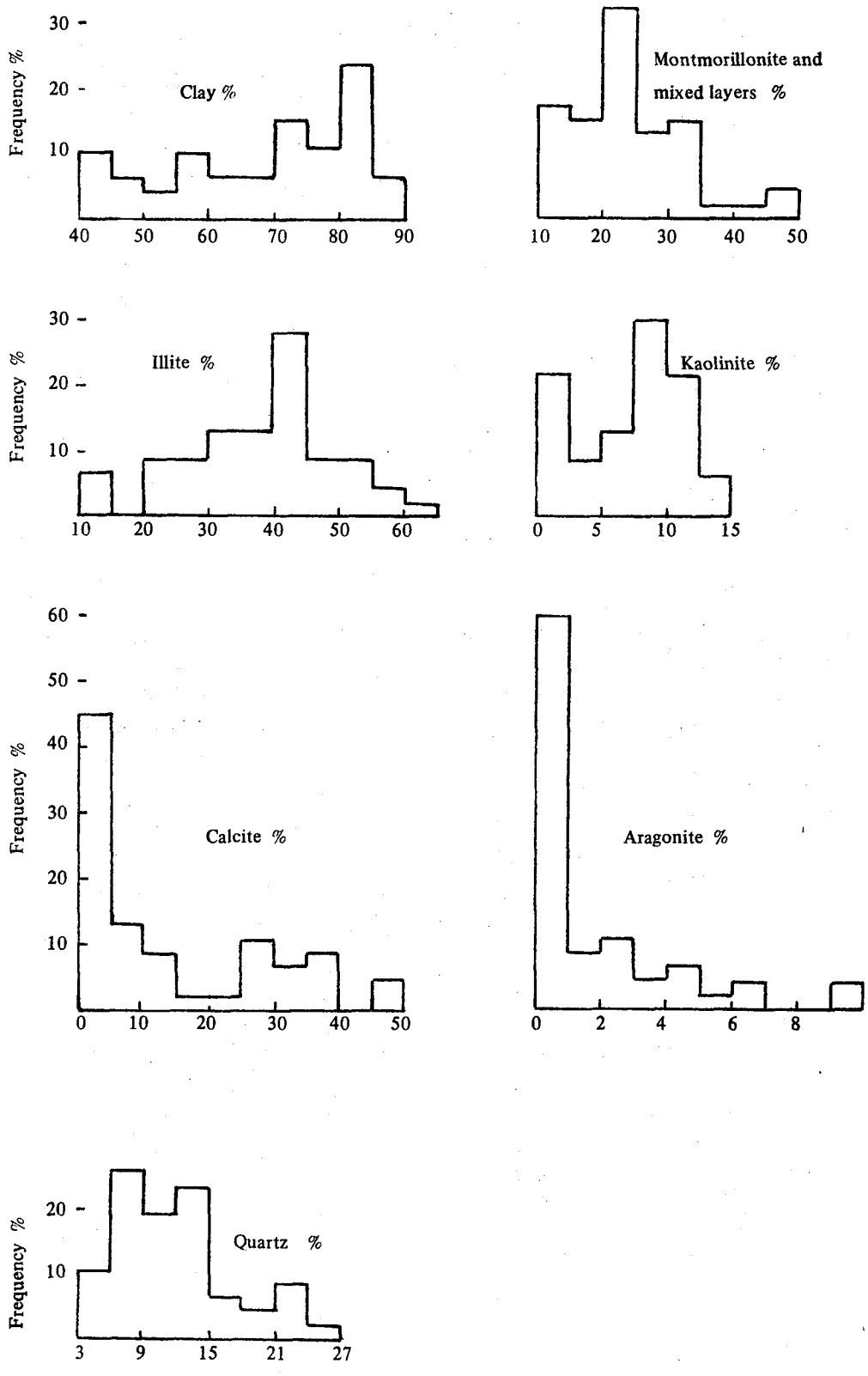

Fig. 91. Mineral distributions in the middle Purbeck shales

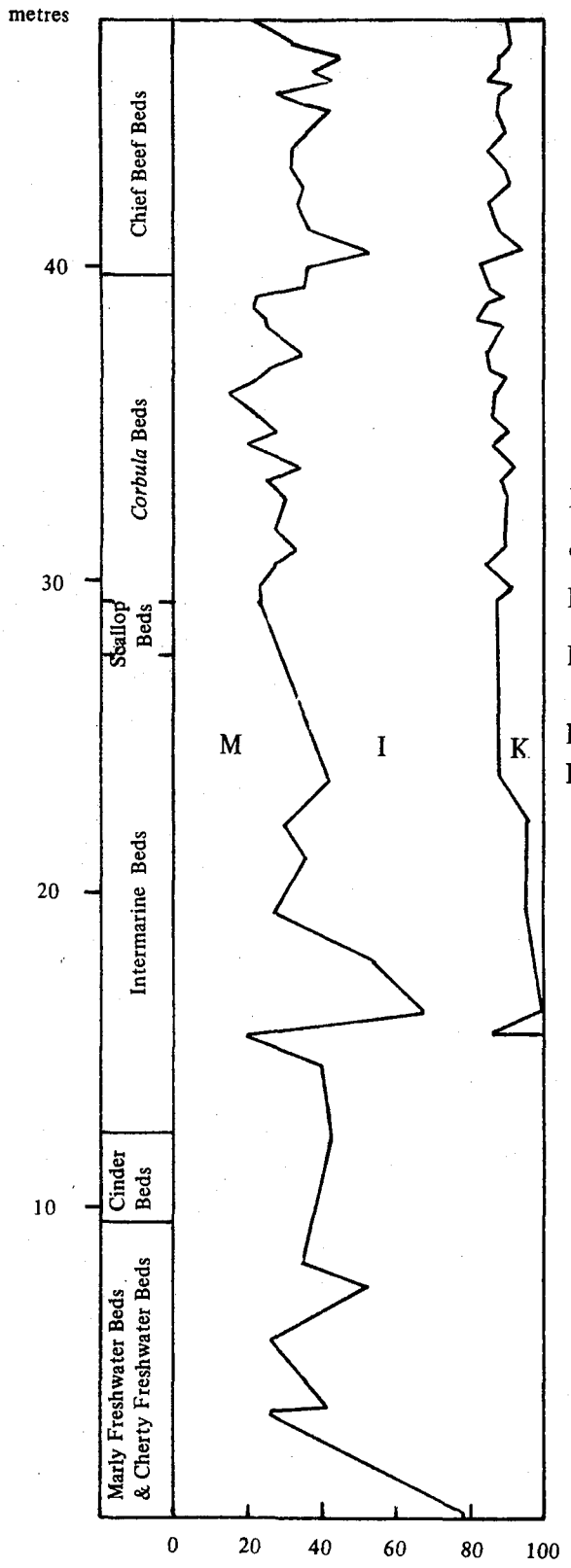

Fig. 92. Stratigraphic distribution of the clay minerals in the Middle Purbeck shales of Durlston Bay.

M : Montmorillonite (and the mixed-layer illite/montmorillonite)

I : Illite

K : Kaolinite

Table 27. Average shale composition (in percent)

	Leith & Mead (1915)[1]	Clarke (1924)[1]	Shaw & Weaver (1965)	Present work
Quartz	32	22.3	30.8	11.6
Feldspars	18	30.0	4.8	–
Clay minerals	34	25.0	60.9	68 [2]
Iron Oxides	5	5.6	<0.5	5.9
Carbonates	8	5.7	3.6	15.4
Organic matter	1	–	1	1.99
Other minerals	1	11.4	<2	<3 [3]

[1] Cited in Shaw and Weaver (1965)
[2] Including iron oxides
[3] Mainly gypsum

The stratigraphic distribution of clay minerals through the middle Purbeck shales is shown in Fig. 92. Illite and montmorillonite (and the mixed-layer illite/montmorillonite) are present in all samples. Kaolinite first appears in the Intermarine Beds and is then consistently present in beds of younger age.

3. Chemistry of the major elements

(a) Silicon

The silica content of the middle Purbeck shales varies from 25.4 – 57.5% (see Table 28 and Fig. 93). Average silica content is 46.7% corresponding to 55.2% calculated on carbonate-free basis. This latter value is very close to the average silica in shales reported by different authors (Table 29).

In the samples studied, silicon occurs in two phases: combined silica and quartz. Combined silica (total silica-quartz) is associated essentially with the clays as indicated from a strong positive correlation with the clay content ($r = 0.90$). The amount of quartz varies from nearly 4% to about 25%. It occurs as angular grains and is assumed

Table 28. Chemical composition of the middle Purbeck shales [1]

In percent	Min	Max	Average	S.D.	S.E.	SK
SiO_2	25.8	57.5.	46.7	8.74	1.27	−0.92
TiO_2	0.26	1.12	0.63	0.24	0.04	0.23
Al_2O_3	6.47	24.1	17.8	5.12	0.75	−0.88
Fe_2O_3	3.05	8.15	5.89	1.47	0.21	−0.44
MgO	1.23	9.10	2.14	1.48	0.22	3.90
CaO	0.69	25.2	8.08	7.77	1.34	0.82
Na_2O	0.28	1.23	0.50	0.17	0.03	2.42
K_2O	1.46	3.98	2.87	0.70	0.10	−0.41
CO_2	0.00	22.7	6.79	7.19	1.05	0.74
H_2O^+	3.02	9.42	6.02	1.68	0.25	0.05
Organic carbon	0.48	7.46	1.99	1.30	0.19	1.79
S	0.04	1.37	0.63	0.30	0.04	0.25
In ppm						
P	70	1405	347	238	35	2.68
Cl	117	9869	922	1678	245	4.44
V	70	233	145	49	7.2	0.05
Mn	50	1806	459	350	51	1.49
Ni	31	112	61	20	2.9	0.40
Cu [2]	27	49	35	4.5	0.8	1.27
Zn	39	178	93	33	4.8	0.52
Ga	8	26	18	5.2	0.8	−0.71
As	5	30	12	5.2	0.8	1.93
Rb	86	261	167	49	7.1	−0.37
Sr	127	1610	461	382	56	1.63
Zr	57	262	142	52	7.5	0.39
Ba	137	865	400	147	21	0.84
Ce	0.0	148	84	33	4.8	−0.18
Pb	11	36	24	7.1	1.0	0.07
Th	0.0	17	10	3.5	0.5	−0.58

[1] Based on 47 samples
[2] Based on 29 samples
SD = Standard deviation
SE = Standard error of the mean
SK = Skewness

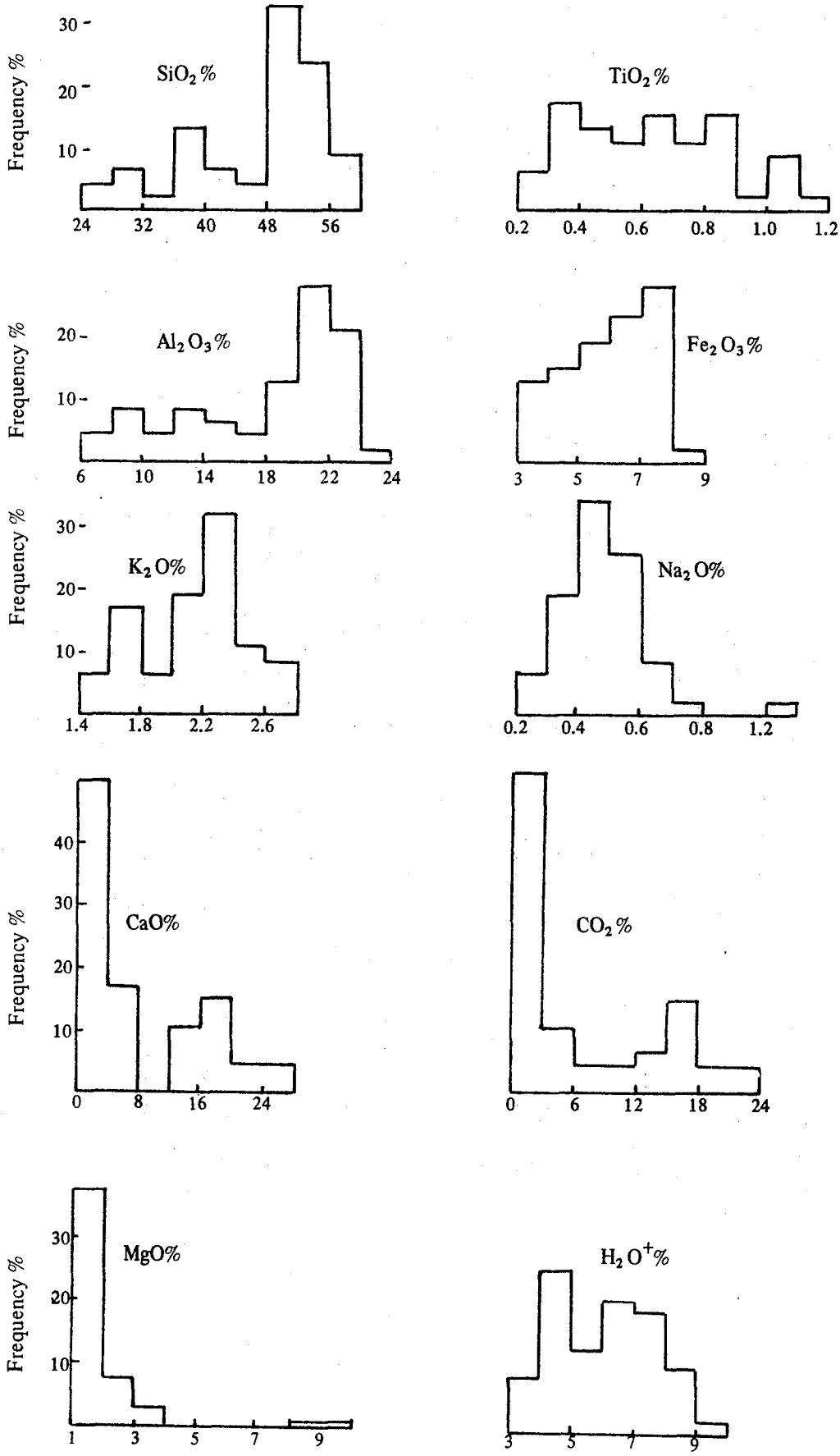

Fig. 93. Distribution of the major elements in the Middle Purbeck shales

Table 29. **Abundance of silica in shales**

	SiO_2 %
Clarke (1924)[1]	58.1
Rankama and Sahama (1950)	58.4
Green (1959)	51.8
Horn and Adams (1966)	55.7
Ronov and Migdisov (1971)	
a. Russian platform	52.2
b. N. American platform	56.4
Present work	47.6
	55.2 [2]

[1] Cited in Weaver (1958b)
[2] Calculated on carbonate-free basis

to be detrital in origin although small contributions from chemically precipitated silica may be included.

Detrital quartz is usually used as an indicator of grain size and hence of rate of sedimentation (Spears, 1964; Bloxam and Thomas, 1969). Spears (1964) used the ratio of free silica/combined silica (approximately quartz to clay ratio) as a measure of sorting during the time of sedimentation. Bloxam and Thomas (1969) used the ratio quartz/organic carbon as an index of sedimentation rate. The stratigraphic distribution of the ratios quartz/combined silica and quartz/organic carbon is shown in Fig. 94. The two ratios have the same trend as that of quartz. Such agreement encouraged the further investigation of additional indicators for sedimentation rates. They include the ratios TiO_2 /combined silica and Zr/combined silica. Both ratios agree well with the sedimentation rates based on quartz contents (Fig. 95).

The stratigraphic distribution of quartz contents, quartz/combined silica etc. suggests a marked upward increase in the sedimentation rates. This is in agreement with

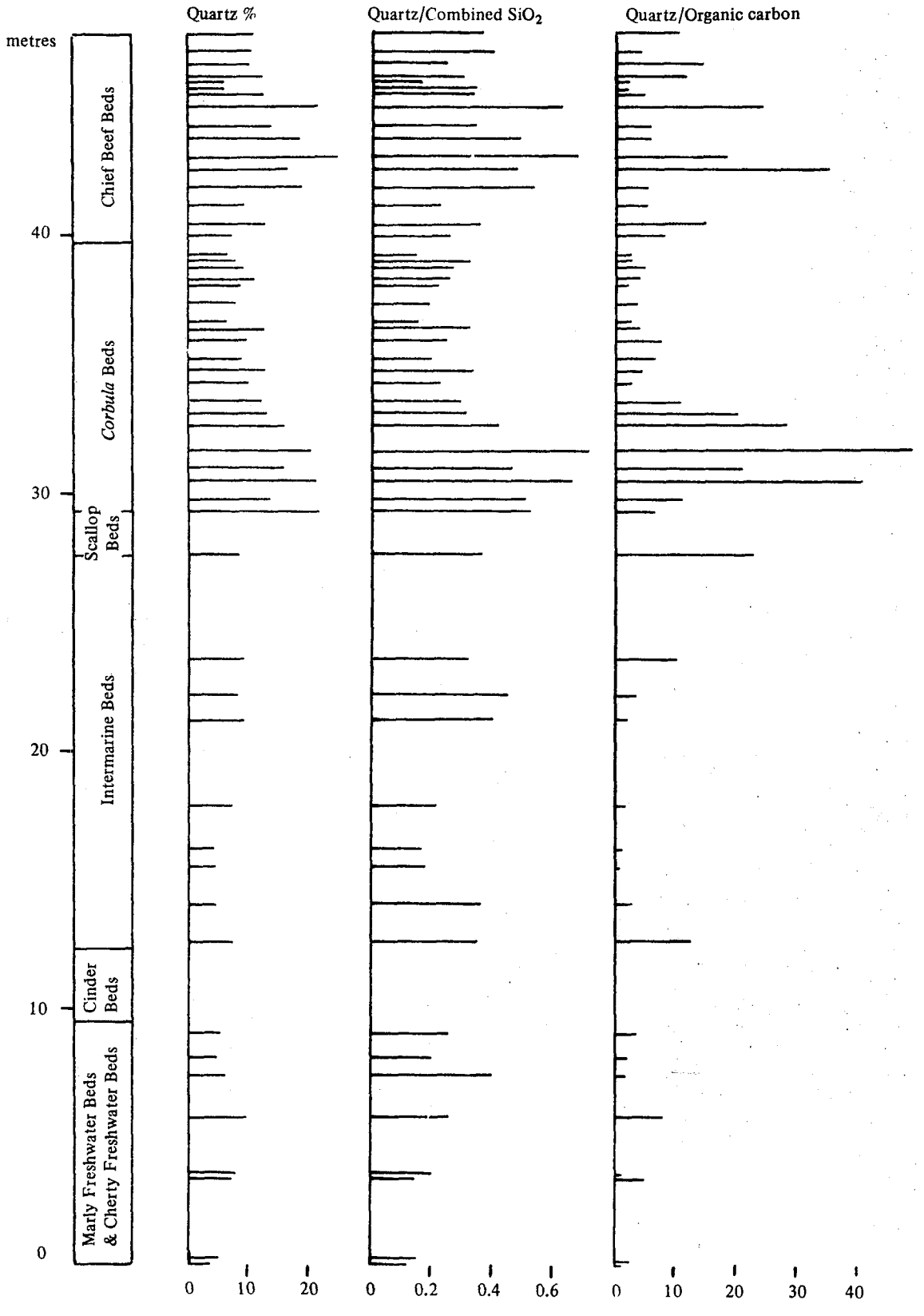

Fig. 94 Vertical variation of quartz, quartz/combined SiO_2 ratio and quartz/organic carbon ratio (for middle Purbeck shales)

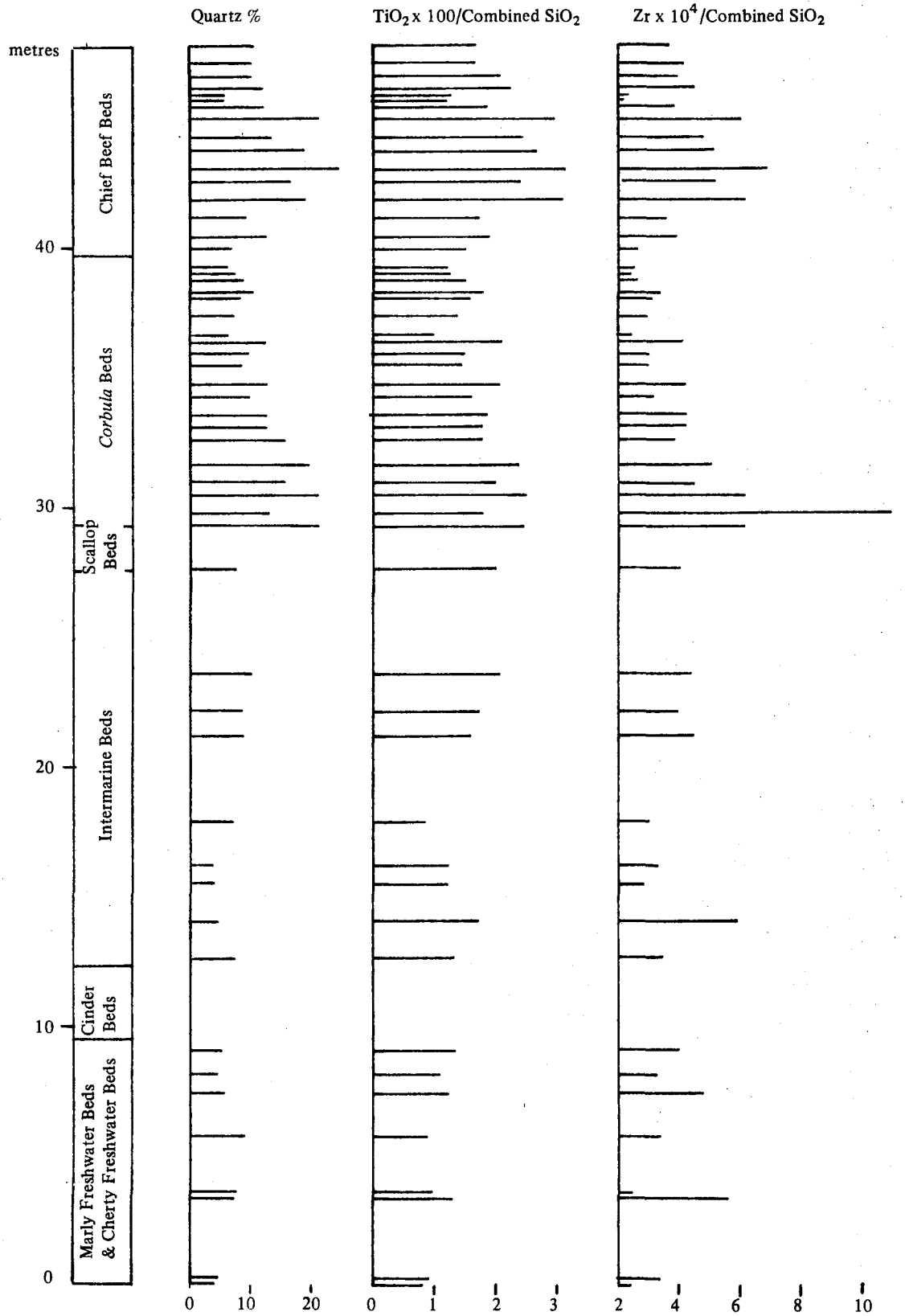

Fig. 95. Vertical variation of quartz, TiO_2 /combined SiO_2 ratio and Zr/ combined SiO_2 ratio (for middle Purbeck shales)

the influx of coarse detritals above the Cinder Beds. The causes for the higher sedimentation rate above the Cinder Beds was probably as mentioned above, increase in rainfall and perhaps development of higher reliefs in surrounding land.

(b) Titanium

In the middle Purbeck shales, titanium values range from 0.26 – 1.12% TiO_2 (see Table 28 and Fig. 93). The average TiO_2 content is 0.63% corresponding to 0.74% calculated on carbonate-free basis. This latter value is very close to the average TiO_2 content in shales (Table 30). The average TiO_2/Al_2O_3 ratio of the middle Purbeck shales is low in comparison with that of shales. This is attributed to the high alumina content of the present rocks (Table 30).

Table 30. Abundance of titanium and aluminium in shales

	TiO_2 %	Al_2O_3 %	TiO_2/Al_2O_3 [1]
Clarke (1924) [2]	0.65	15.4	0.042
Rankama and Sahama (1950)	0.77	15.1	0.051
Green (1950)	0.78	15.1	0.052
Turekian and Wedepohl (1961)	0.77	15.1	0.051
Horn and Adams (1966)	0.74	15.1	0.049
Ronov and Migdisov (1971)			
a. Russian platform	0.77	14.7	0.052
b. N. American platform	0.77	15.4	0.050
Present work	0.62	17.4	0.036
	0.74 [3]	21.0 [3]	

[1] Calculated by the present author
[2] Cited in Weaver (1958b)
[3] Calculated on carbonate-free basis

In the middle Purbeck shales, rutile, anatase and brookite have been identified in the HF acid insoluble residue (following the method of Raman and Jackson, 1965). Small amounts of titanium are to be expected in the clay structure since titanium sub-

stitutes for Fe^{3+} and Al^{3+} in the octahedral position and for Si^{4+} in the tetrahedral position (Tillmanns, 1970).

The TiO_2/Al_2O_3 ratios of the middle Purbeck shales are shown plotted against the quartz contents on Fig. 96. The objective is to calculate the amounts of Ti present in the clay structure. The correlation between the TiO_2/Al_2O_3 ratio and quartz content is highly significant ($r = 0.76$). This positive relation is due to the increased importance of TiO_2 minerals relative to the clays as the quartz content increases. The TiO_2/Al_2O_3 ratio for quartz-free shales (middle Purbeck) ranges from 0.009 to 0.020 corresponding to the minimum and maximum TiO_2/Al_2O_3 ratio associated with the silicate structure. Spears and Kanaris – Sotiriou (1975) found that the ratio of TiO_2 substituting in the clay minerals to the Al_2O_3 content is not greater than 0.025 which is close to the ratio of 0.020 calculated for the Purbeck shales. To calculate the minimum and maximum TiO_2 % present in the lattice of 'average' middle Purbeck clays, the following relations could be applied:

TiO_2/Al_2O_3	= 0.009	for minimum substitution
TiO_2/Al_2O_3	= 0.020	for maximum substitution

Assuming a Purbeck clay with 20% Al_2O_3, the TiO_2 present in the lattice exceeds 0.18% but not greater than 0.40%.

The TiO_2/Al_2O_3 ratio is related to grain size since the ratio increases from mudstone to siltstone to sandstone (Spears and Kanaris – Sotiriou, 1975; table 1). The low TiO_2/Al_2O_3 ratio in the middle Purbeck shales suggests that the sediments are weighted towards the clay-sized material. This is also reflected in the high alumina and low quartz content in the middle Purbeck shales in comparison with the 'average' shales (see Table 27 & 29).

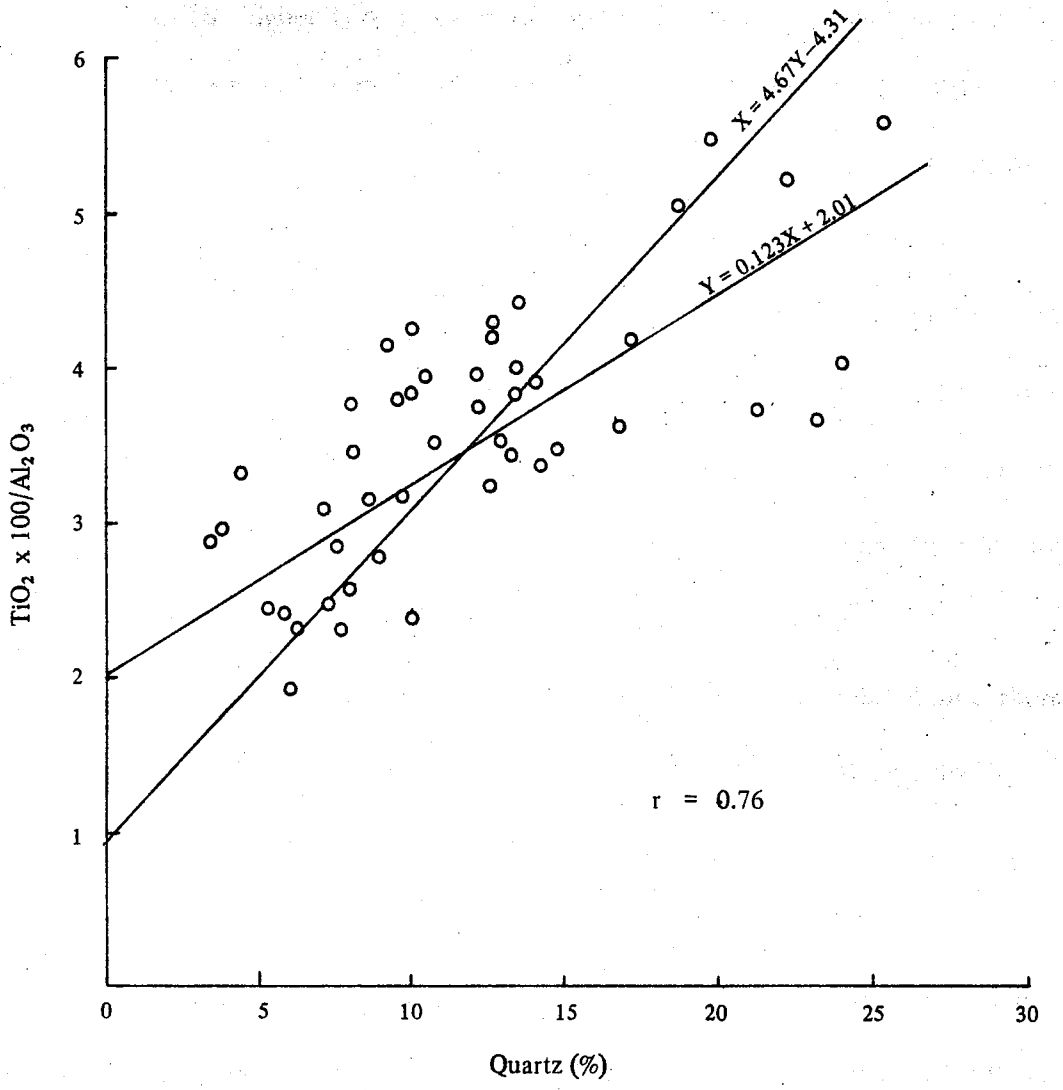

Fig. 96. Variation in the TiO_2/Al_2O_3 ratio with quartz content (for middle Purbeck shales)

Migdisov (1960) showed that the TiO_2/Al_2O_3 ratio of argillaceous sediments is approximately constant irrespective of climate and facies. On the other hand, as pointed out by Migdisov, the clays of humid epochs in general have higher average Al and Ti contents. The higher Ti contents in the shales of Durlston Formation in comparison with those of Lulworth Formation suggests change in the climatic conditions. The increased rainfall during the period of Durlston Formation has been emphasised before in Chapter 10.

Titanium has been suggested as a reliable indicator for distinguishing between marine and freshwater clays (Lebedev, 1967). Based on 937 clay samples from the lower Cretaceous and Jurassic clays (excluding the highly calcareous clay), Lebedev concluded that the average TiO_2 content from freshwater clays was 0.83% and from the marine and brackish clays was 0.63%. It is interesting to note that the 0.73% TiO_2 present in the middle Purbeck shales (calculated on carbonate-free basis) is equal to the average of the 0.83% TiO_2 and 0.63% TiO_2 reported by Lebedev for freshwater and marine-brackish clays.

(c) **Aluminium**

Individual samples in the middle Purbeck shales gave values between 6.47 – 24.1% Al_2O_3 (see Table 28 and Fig. 93). The average Al_2O_3 content is 17.8% corresponding 21% calculated on carbonate-free basis. Both values are higher than the average Al_2O_3 content shales reported by different authors (Table 30).

The stratigraphic distribution of Al_2O_3, calculated on carbonate-free basis, is more or less uniform. Only few horizons below the Cinder Beds are exceptionally low in Al_2O_3 content especially the Mammal Bed (bed Db83). The deficiency in alumina is accompanied by an increase in the MgO content as indicated from the following table.

	Al_2O_3/MgO	Combined SiO_2	Combined SiO_2/Al_2O_3
Middle Purbeck shales	8.32	35.1	1.97
Mammal Bed (average of two shale samples)	0.98	35.2	5.31

Dolomite was not found in the Mammal Bed suggesting that magnesium is essentially present in the clays. As a further check a sample from the Mammal Bed was treated with dilute acetic acid and later analysed for the major elements. Table 31 indicates that Mg is associated with the clays substituting for Al. The clays of the Mammal Bed are dominated by montmorillonite which constitutes about 80% of the clay minerals. This points to the montmorillonite as the essential host of Mg.

Table 31. Chemistry of a shale sample from the Mammal Bed before and after acetic acid treatment.

	before	after
SiO_2	40.2	54.0
TiO_2	0.31	0.52
Al_2O_3	6.47	10.50
Fe_2O_3	3.05	5.33
MgO	8.16	10.70
CaO	17.0	1.89
Na_2O	0.73	0.31
K_2O	1.94	2.80
CO_2	14.1	–
H_2O^+	3.02	5.10

(d) Iron

The iron content in the middle Purbeck shales varies from 3.05 – 8.15 % Fe_2O_3. The average value is 5.89% Fe_2O_3 which corresponds to 6.96% Fe_2O_3 calculated on carbonate-free basis. Both values are very close to the average Fe_2O_3 content in shales reported by different authors (Table 32).

Table 32 **Abundance of iron in shales**

	Fe_2O_3 % [1]
Clarke (1924) [2]	6.47
Rankama and Sahama (1950)	6.73
Green (1959)	6.48
Turekian and Wedepohl (1961)	6.72
Horn and Adams (1966)	5.55
Ronov and Migdisov (1971)	
a. Russian platform	6.24
b. N. American platform	4.63
Present work	5.89
	6.96 [3]

[1] Total iron contents given by the different authors are expressed here as ferric oxide
[2] Cited in Weaver (1958b)
[3] Calculated on carbonate-free basis

In the middle Purbeck shales, iron shows a strong positive correlation with Al besides the other clay-related elements. Also the stratigraphic distribution of Fe/Al ratio is more or less uniform suggesting the association of iron with the clays (Hirst, 1962; Spears, 1964).The strong negative correlation between Fe and the carbonates emphasises the detrital nature of Fe in the middle Purbeck shales.

The weathered shales especially in the Chief Beef Beds are occasionally heavily stained with iron oxides and commonly contain small amounts of gypsum. The amount of iron associated with pyrite before weathering is about 0.80% Fe_2O_3 (calculated from the average sulphur content of the middle Purbeck shales). The remaining Fe_2O_3 is about 5% and is mainly accommodated in the clays. Carroll (1958) suggested that the iron in shales occur in the following ways:

1. essential constituent of the clay minerals
2. minor constituent of the clay minerals
3. present as iron oxide film on the surface of the clays

Chlorite has not been recorded in the present study, thus suggesting that possibilities 2 and 3 as an explanation for the occurrance of iron in the middle Purbeck shales.

(e) Calcium, magnesium and carbon dioxide

In the middle Purbeck shales, the CaO content ranges from 0.69% – 25.2% while the CO_2 content varies from 0.0 – 22.7% (see Table 28 and Fig. 93). The averages of CaO and CO_2 are 8.08% and 6.79% respectively. These averages are generally higher than the values given for shales by different authors (Table 33).

Table 33. Abundance of CaO, MgO and CO_2 in shales.

	CaO %	MgO %	CO_2 %
Clarke (1924) [1]	3.11	2.44	2.63
Rankama and Sahama (1950)	3.12	2.32	
Green (1950)	7.20	3.32	6.08
Turekian and Wedepohl (1961)	3.09	2.49	
Horn and Adams (1966)	3.15	2.72	
Ronov and Migdisov (1971)			
a. Russian platform	5.17	3.04	4.84
b. N. American platform	4.72	3.35	5.13
Present work	8.08	2.14	6.79
	7.73 [2]	1.85 [2]	6.44 [2]

[1] Cited in Weaver (1958b)
[2] Average after excluding two shale samples from the Mammal Bed

Calcium in the middle Purbeck shales occurs essentially in the carbonate phase as indicated from the strong positive correlation between CaO and CO_2 (r = 0.99). Calcium which may be present as gypsum, of weathering origin, is about 1% CaO on average if the 0.63% S, which represents the average value in the middle Purbeck shale, is allocated for gypsum. The amount of Ca present in the clay is about 1% CaO, minimum Ca content in the middle Purbeck shales is 0.69% CaO. The remaining 6% CaO is present in the carbonate phase. Average CO_2 in the middle Purbeck shales is 6.79% which is higher than the

equivalent CO_2 associated with 6% CaO. This may be due to the fact that CO_2 determination is liable to errors when present in small quantities.

Magnesium content ranges from 1.23 – 9.1% MgO. The average value is 2.14% MgO. If two samples from the Mammal Bed are excluded, the average becomes 1.85% MgO. This value is lower than the average MgO in shales reported by different authors (Table 33).

The amount of Mg which may be present in the carbonate fraction of the middle Purbeck shales is about 0.2% MgO[1]. The remaining 1.65% MgO is essentially present in the clays. The exceptionally high Mg content of the Mammal Bed has been already discussed in some detail (see Al).

(f) Potassium and sodium

Potassium content in the middle Purbeck shales varies from 1.46 – 3.98% K_2O. The average value is 2.87 K_2O corresponding to 3.39% K_2O calculated on carbonate-free basis. This latter value is very close to the average K_2O in shales reported by different authors (Table 34). Feldspars have not been detected in the present shales suggesting that potassium is essentially present in the clay minerals particularly illite and to some extent in the mixed-layer illite/montmorillonite.

Sodium ranges from 0.28 – 1.25% Na_2O. The average value is 0.50% Na_2O which is lower than the average Na_2O content in shales (Table 34). About 16% of the average sodium content in the middle Purbeck shales is present as NaCl. The remaining 0.42% Na_2O (chloride-free sodium) is mainly present in the calcite structure since Na correlates positively with CaO, CO_2, and calcite. Sodium shows a strong negative correlation with Al_2O_3, K_2O, SiO_2 and most of the other clay-related elements.

---

[1] This value was calculated from the average Ca/Mg ratio of the middle Purbeck limestones.

Table 34. Abundance of K_2O and Na_2O in shales

	K_2O %	Na_2O %
Clarke (1924) [1]	3.24	1.30
Rankama and Sahama (1950)	3.25	1.31
Green (1959)	3.49	0.81
Turekian and Wedepohl (1961)	3.20	1.29
Horn and Adams (1966)	3.00	0.65
Ronov and Migdisov (1971)		
a. Russian platform	3.25	0.85
b. N. American platform	3.40	0.66
Present work	2.83	0.55
	3.39 [2]	

[1] Cited in Weaver (1958b)
[2] Calculated on carbonate-free basis

From the foregoing, it is clear that K and Na have two different hosts; clays and carbonates respectively. The Na/K ratio is, therefore, a good measure of the carbonate to clay ratio in the Purbeck shales.

4. Chemistry of the trace elements

(a) Vanadium

In the middle Purbeck shales, vanadium content varies between 70 and 233 ppmV (see Table 28 and Fig. 97). Average V content is 145 ppm which is close to the average value for shales reported by different authors (Table 35). Vanadium content calculated on carbonate-free basis is slightly higher than most of the averages in shales.

Vanadium is one of the elements enriched in the hydrolysate sediments (Goldschmidt, 1954). In the middle Purbeck shales, vanadium shows very strong positive correlation with Al ($r = 0.78$) indicating its association with the clays. In the clays, vanadium can be adsorbed and incorporate in the clay mineral structure or in iron oxide castings (Landergren, 1974). In the normal hydrolysate sediments most of the vanadium

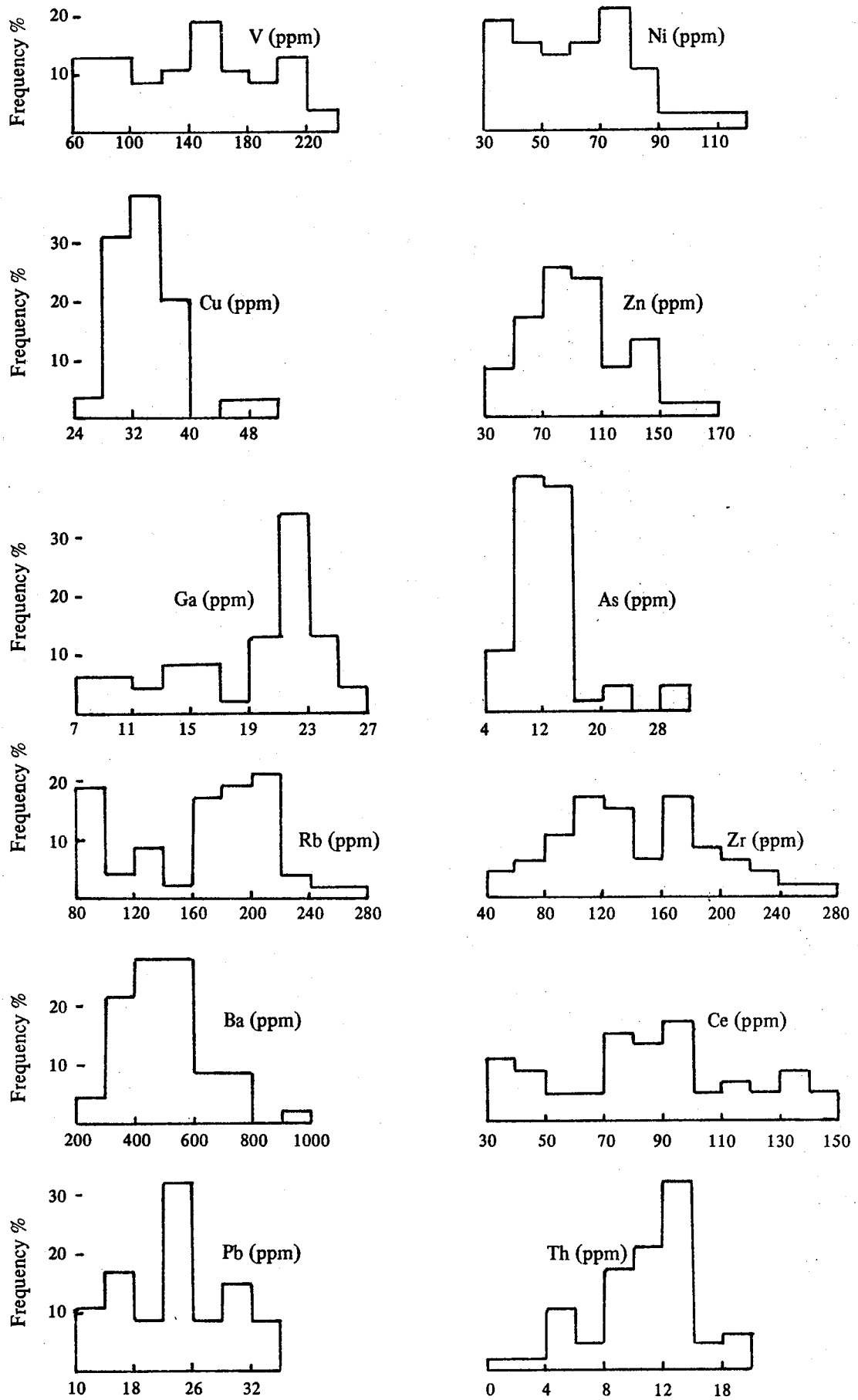

Fig. 97. Distribution of trace elements in the middle Purbeck shales

Table 35. Abundance of vanadium in shales

	V(ppm)
Rankama and Sahama (1950)	120
Green (1959)	130
Turekiam and Wedepohl (1961)	130
Horn and Adams (1966)	101
Landergren (1974)	159 [1]
Present work	145
	171 [2]

[1] Calculated by the present author from 167 marine and freshwater shales
[2] Calculated on carbonate-free basis.

is present as $(V04)^{3-}$ ion fixed as ferric vanadate in the limonite fraction. In the average marine hydrolysate sediments, the bulk of vanadium is present in the clay structure in the trivalent form in the same way as aluminium (Goldschmidt, 1954). In the middle Purbeck shales, the relation between vanadium and iron oxides is concealed by their strong correlation with aluminium. Nevertheless, the correlation between vanadium and aluminium is much stronger than that between vanadium and iron oxides (r = 0.78 and 0.56 respectively). This suggests that vanadium behaviour in the middle Purbeck shales has some similarities with that of marine hydrolysates. This may indicate an inherited marine nature since the depositorial environment of the middle Purbeck shales was dominated by brackish to freshwater conditions.

Vanadium shows strong sympathetic variation with Ti, Zr and quartz (r = 0.91, 0.62 and 0.59 respectively). With the carbonates, vanadium shows very strong negative correlation (r = −0.81). This indicates clearly the detrital nature of vanadium in the middle Purbeck shales.

Vanadium is usually high in bituminous sediments; a fact which is of a geochemical interest and economic importance. Its concentration is controlled not only

by the primary vanadium content of the organic matter but also by the reducing character of the environment (Landergren, 1974). In the middle Purbeck shales, vanadium shows a negative correlation with organic carbon. This is difficult to explain since reducing conditions existed during the time of sedimentation or at least below the water-sediment interface. Also the high organic carbon contents in the Purbeck shales suggest periods of reducing conditions. Lack of correlation between vanadium and reducing conditions suggests that most of the vanadium was incorporated in the clays before entering the Purbeck basin.

(b) Nickel

Individual samples in the middle Purbeck shales gave values between 31 ppm Ni and 112 ppm Ni (see Table 28 and Fig. 97). The average Ni content is 61 ppm which is close to the average Ni in shales reported by Turekian and Wedepohl (1961). On the other hand, the Purbeck average is much higher than the Ni values given Rankama and Sahama (1950), Green (1959) and Horn and Adams (1966) as shown from the following table.

Table 36. Abundance of nickel in shales

	Ni (ppm)
Rankama and Sahama (1950)	24
Green (1959)	21
Turekian and Wedepohl (1961)	68
Horn and Adams (1966)	29
Present Work	61

Nickel shows a strong positive correlation with the clays and a strong negative correlation with the carbonates indicating the detrital nature of nickel in the Purbeck clays. Nickel is one of the elements enriched in dark clays containing sulphides as well as the bituminous shales (Goldschmidt, 1954). This was not observed in the Purbeck

shales since nickel shows no correlation with sulphur and correlates negatively with organic carbon. Lack of correlation between nickel and sulphur is probably due to the weathered nature of the Purbeck shales at Durlston Bay. The negative correlation with organic carbon indicates that most of the nickel content in the Purbeck clays is detrital in nature. The relation between nickel and iron is difficult to evaluate since both have sympathetic relationship with the clays.

The Ni/Al ratio ranges between 3.48×10^{-4} and 13.53×10^{-4} and averages $\overline{6.90} \times \overline{10^{-4}}$. Samples with high Ni/Al ratio (compared with the average ratio) are mainly calcareous shales. This may suggest a possible leaching of nickel from the clays and relative enrichment in the calcareous shales. The Ni/Al ratio of the middle Purbeck shales shows a moderate positive correlation with the carbonate fraction ($r = 0.39$) which supports the observations concerning nickel mobility. Further more, the high nickel content in the bands of 'perished' bivalves (entirely enclosed in the shales) points to processes of enrichment. One of these bands (bed DB194) contains 105 ppm Ni which is about twice the average Ni in the middle Purbeck shales.

(c) **Copper**

In the middle Purbeck shales[1] Cu ranges from 27–49 ppm. The average Cu content is 35 ppm. which is close to the Cu content in shales reported by Green (1959), Horn and Adams (1966) and Wedepohl (1974); i.e. 40 ppm, 44 ppm, and 35 ppm respectively.

Wedepohl (1974) stated that the major transport of copper at the earth's surface and its accumulation in the sedimentary environment are connected with the detrital

---

[1] The Cu data for the calcareous shales (containing more than 15% carbonates calculated on quartz-free basis) are excluded. This is because Cu determination was found unreliable in the Purbeck limestones.

matter. This was not obvious in the present study since Cu has no correlation either with quartz or clay. Nevertheless, Cu shows a weak positive correlation with Ni, Zn and Pb which have a detrital nature.

Copper is often enriched in the bituminous shales. The Cu enrichment is attributed due to adsorption and reaction with the degraded organic matter, besides precipitation of copper sulphides (Wedepohl, 1974). In other words, bituminous shales during diagenesis act as a sink for different heavy elements especially Cu. This was not observed in the Purbeck shales although they are relatively rich in organic matter. Copper shows no correlation with organic carbon and correlates negatively with sulphur. This is probably due to the weathered nature of the Purbeck shales. Some of the original copper associated with the original reducing conditions is expected to oxidize and dissolve to the highly soluble copper sulphate.

(d) Zinc

Individual samples in the middle Purbeck shales gave values between 39 and 178 ppm. Zn. The distribution is moderately skewed (SK = 0.50) with about 50% of the population ranging between 70 and 110 ppm Zn. (Fig. 97). The average zinc content in the middle Purbeck shales is 93 ppm Zn. This value is more or less close to the average Zn content in shales reported by Green (1959) and Turekian and Wedepohl (1961) i.e. 80 ppm. and 95 ppm respectively. Horn and Adams (1966) gave a higher average for Zn in shales (130 ppm).

Zinc shows a moderate positive correlation with Fe and Al (r = 0.42 and 0.41 respectively), besides a large number of major and trace elements associated with the clay. Such behaviour points to the detrital nature of Zn in the middle Purbeck shales and suggests its occurrence in more than one phase mainly the clays and iron oxides. Wedepohl

(1972) suggested that the major transport and accumulation of Zn in sedimentary environmental occur mainly on the colloidal iron oxides and iron oxide coatings. The importance of adsorption of Zn on the clays has been experimentally proved by Krauskopf (1956).

In the middle Purbeck shales the ratio of Zn/Al (approximately Zn to clay ratio) throws some light on Zn mobility. The ratio correlates positively with CO_2 ($r = 0.43$) suggesting a possible mobilization of Zn and subsequent fixation in the carbonate fraction. Another independent evidence comes from the high Zn contents in the layers of 'perished' bivalves which are enclosed in the shales. In fact, the highest Zn contents recorded in the middle Purbeck rocks occur in these carbonate layers (DB164: 149 ppm Zn; DB192: 174 ppm Zn; DB194: 128 ppm Zn; DB198: 211 ppm Zn). These values suggest the layers of 'perished' bivalves are highly enriched in Zn (up to 10 times) compared with the Purbeck limestones.

It is difficult to relate the period of Zn mobilisation to the diagenetic history. Apart from the layers of 'perished' bivalves, the other middle Purbeck carbonates have normal Zn values. This may indicate that Zn mobilisation began after the main period of lithification. On the other hand, the low Zn contents of the 'beef' layers (associated with shales and predating faulting and folding) suggest that Zn mobilisation was completed before uplift.

(e) Gallium

Gallium in the middle Purbeck shales ranges from 8–26 ppm Ga (see Table 28 and Fig. 97). The average value is 18 ppm Ga corresponding to 26 ppm Ga calculated on carbonate-free basis. Both values are very close to the average Ga content in shales reported by Horn and Adams (1966) and Turekian and Wedepohl (1961) i.e. 23 and 19

ppm Ga respectively.

The association of Ga and Al in the sedimentary cycle is very close. Both elements are enriched in the hydrolysate sediments where Al is the essential host of Ga. As expected the Ga/Al ratio is more or less constant and the correlation between both elements in the middle Purbeck shales is highly significant (r = 0.95).

(f) **Arsenic**

Individual samples in the middle Purbeck shales gave values between 5 and 30 ppm As (see Table 28 and Fig. 97). The Purbeck average is 12 ppm As which is very close the average As in shales i.e. 13 ppm. As reported by Turekian and Wedepohl (1961) and Onishi (1967). Green (1959) and Horn and Adams (1966) gave lower values for As in shales i.e. 7–9 ppm and 9 ppm respectively.

In the sedimentary cycles, As has the tendency to become precipitated in the hydrolysate sediments. Onishi (1970) reported 1.5 ppm As in average igneous rocks against 13 ppm. As in shales. Arsenic is also enriched in the oxidate sediments mainly by adsorption on ferric hydroxides (Rankama and Sahama, 1950). Red beds are highly enriched in As up to 12 times compared with the average sedimentary rocks (see Table III in Cosgrove, 1972b). In the present rocks, As shows no correlation either with the clay content or with iron oxides.

Organic carbon is the main factor controlling As distribution in the middle Purbeck shales since both elements correlate positively (r = 0.48). The highest As content (30 ppm As) occurs in a sample which contains 7.46% organic carbon. Because As shows a sympathetic variation with organic carbon, a positive correlation is to be expected between As and S. This was not observed due to the weathered nature of the Purbeck shales at Durlston Bay.

Arsenic correlates positively with the carbonate fraction of the middle Purbeck shales suggesting that the calcareous shales are relatively enriched in As. Purbeck shales with less than 15% carbonates (calculated on quartz-free basis) contain 11.6 ppm As while the calcareous shales (with more than 15% carbonates) contain 13 ppm As. This was unexpected since carbonate rocks contain only 1 ppm As (Onishi, 1967); and the Purbeck limestones contain less than 2 ppm As on average. However, possible As mobilisation in the Purbeck clay and subsequent enrichment in the carbonate fraction may explain such anomaly.

(g) Rubidium

In the middle Purbeck shales, rubidium contents vary between 86 and 261 ppm (see Table 28 and Fig. 97). The average value is 167 ppm Rb which is very close to the averages of Rb in shales given by Turekian and Wedepohl (1961), Heir and Bellings (1970) and Reimer (1972) i.e. 140 ppm, 167 ppm and 155 ppm respectively.

The geochemistry of rubidium is very closely related to that of potassium. The main bulk of rubidium in the sedimentary cycle is enriched in the clays replacing potassium. In the middle Purbeck shales correlation between potassium, the 'host' element and rubidium, its 'companion' element, is highly significant ($r = 0.96$).

Rubidium is one of the elements which has been suggested as a palaeosalinity indicator. Degens *et al.*, (1957) reported high Rb content in the marine shales compared with freshwater shales. Campbell and Williams (1965) while working on some Canadian Cretaceous shales found that the K/Rb ratio of 250–300 is characteristic of the non-marine and brackish water shales while in the marine shales the K/Rb ratio ranges from 150–200. The K/Rb ratio of the middle Purbeck shales ranges from 122–189 and averages 172 which groups the middle Purbeck sediments with the ' marine' shales. This probably

reflects an inherited 'marine' nature of the Purbeck clays although their depositional environments were dominated by low salinities.

Another ratio of a particular interest is the Rb/Sr ratio. In shales older than about the Upper Carboniferous, the Rb/Sr ratio is generally above 1.0 while in younger shales, the ratio always below this value (Reimer, 1972). The average Rb/Sr ratio for the middle Purbeck shales is 0.36; in agreement with Reimer's conclusion about the increase of Sr in shales and the decrease of Rb and other alkalis since the Upper Carboniferous.

(h) Zirconium

Zirconium content of the middle Purbeck shales varies between 57 and 262 ppm (See Table 28 and Fig. 97). Average Zr content is 142 ppm which corresponds to 168 ppm calculated on carbonate-free basis. Both values are close to the average Zr contents in shales reported by Rankama and Sahama (1950), Green (1959), Turekian and Wedepohl (1961) and Horn and Adams (1966) i.e. 120 ppm, 200 ppm, 160 ppm and 142 ppm respectively.

Zircon has been identified in the heavy minerals as well as in the HF acid insoluble residue. Apart from zircon, zirconium may be present in the lattice of the clays. Degenhardt (1957) found variable quantities of Zr in the clay minerals. According to Nicholis and Loring (1962), some Zr can proxy for Al in the clay minerals.

Zirconium in the middle Purbeck shales correlates positively with clays and with quartz ($r = 0.46$ and 0.70 respectively). The higher correlation with quartz suggests the importance of Zr with the increase of grain size i.e. with the increase in sedimentation rate. The stratigraphic distribution of Zr/combined SiO_2 (approximately Zr to clay ratio) follows the same trend of sedimentation rates based on quartz contents (Fig. 95).

High Zr content in shales indicate intense weathering whereby the resistent

minerals could survive (Awasthi, 1970). It is already mentioned that the average Zr content in the middle Purbeck shales agrees well with the average Zr for shales. This suggests that the Purbeck clastics have not undergone many cycles of erosion and deposition before reaching the Purbeck basin.

(i) Barium

Individual samples gave values between 137–856 ppm Ba (see Table 28 and Fig. 97). The arithmetic mean of barium content of the middle Purbeck shales is 400 ppm which is not far from most of the Ba averages for shales reported by Rankama and Sahama (1950), Green (1959), Turekian and Wedepohl (1961) and Horn and Adams (1966) i.e. 460 ppm, 800 ppm, 580 ppm and 250 ppm respectively. More recently, Puchelt (1972) estimated the average Ba content in shales as 546 ppm.

In the middle Purbeck shales, Ba correlates strongly with K ($r = 0.67$) which suggests that important amounts of Ba being captured by K-minerals presumably the illite. This is explained by the similarity between ionic radii of Ba and K (Goldschmidt, 1954). Barium shows a strong positive correlation with Al ($r = 0.71$) which is higher than the Ba-K correlation. This may suggest additional Ba being adsorbed on the clays. Although barite was not detected in the middle Purbeck shales, the weak positive correlation between Ba and S ($r = 0.18$) may indicate minor contribution from barite.

Most probably the bulk of Ba transported to the Purbeck basin was associated with the clays, especially the illite. The strong positive Ba-Al correlation ($r = 0.71$), besides Ba weak correlation with quartz ($r = 0.20$) indicates Ba importance with the decrease in grain size. The stratigraphic distribution of Ba and quartz contents through the middle Purbeck (Fig. 98) suggests that Ba was relatively enriched in the clays accumulated during periods of slow sedimentation.

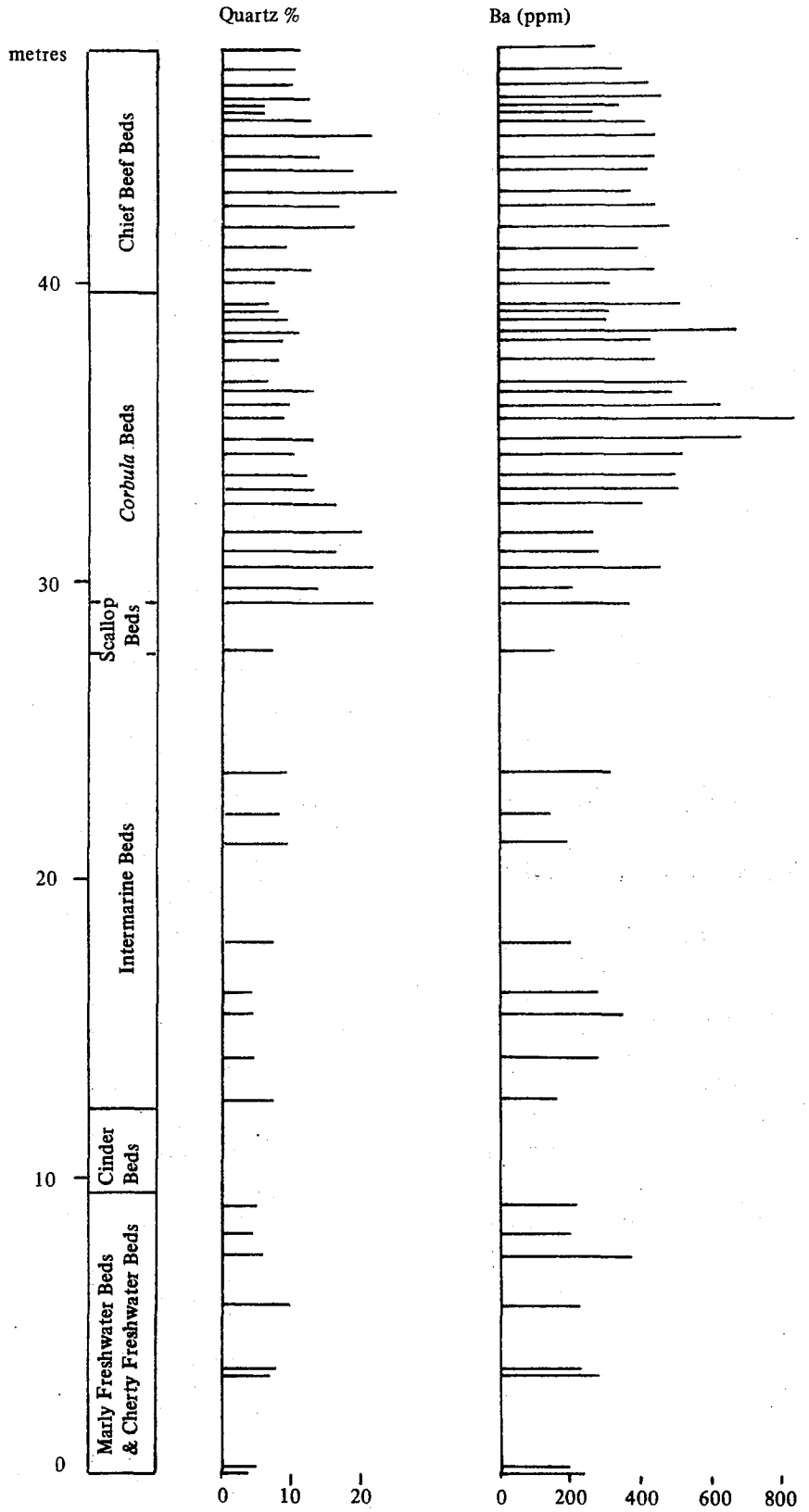

Fig. 98. Vertical variation of quartz and Ba (for middle Purbeck shales)

(j) Cerium

The cerium content of the middle Purbeck shales varies between values below the detection limit (20 ppm Ce) and 148 ppm. The average Ce content is 84 ppm. This value is higher than the average Ce content in shales given by Green (1959), Turekian and Wedepohl (1961) and Horn and Adams (1966) i.e. 30 ppm, 59 ppm, and 45 ppm respectively. The average Ce content of 8616 shale samples from the Russian platform is 67 ppm Ce (Ronov *et al.*, 1967). Although the Purbeck average is generally high, it is close to the Ce content of the Russian platform.

Cerium behaviour is better understood if the abundance of the other rare-earth (RE) is known[1]. Nevertheless, Ce shows very strong correlations with Al and most of the clay-related elements suggesting a detrital nature for Ce in the middle Purbeck shales.

(k) Lead

In the middle Purbeck shales, Pb ranges from 11–36 ppm (see Table 28 and Fig. 97). The distribution is more or less normal (SK = 0.07). The average Pb content is 23 ppm. This value is very close to the average Pb content in shales given by Rankama and Sahama (1950), Green (1959) and Wedepohl (1974b), ie. 20 ppm, 20 ppm and 24 ppm respectively. On the other hand, the Purbeck average is much lower than the value of 80 ppm Pb reported for shales by Horn and Adams (1966).

The geochemistry of Pb is dominated by its chalcophile and lithophile characters. The former is explained by its close association with S, Se and Te. The lithophile nature of Pb comes from its ionic size which makes it possible for Pb to replace K, Ba, Sr and

---

[1] The RE group consists of 14 elements occupying the 4f transitional period in the periodic system. The elements are subdivided into two sub-groups; the Ce (or light) rare-earths and the Y (or heavy) rare-earths (Haskin *et al.*, 1966).

even Ca (Goldschmidt, 1954).

In the middle Purbeck shales, Pb behaviour is dominated by its strong detrital nature. Lead correlates strongly with Ti, Zr and quartz contents (r = 0.91, 0.72 and 0.66 respectively). The strong negative correlation with the carbonates is a further evidence for the detrital nature of Pb. Gad *et al.*, (1969), while studying the chemistry of the Whitbian (Upper Lias) sediments of the Yorkshire coast, found that more than 70% of Pb is located in the clays, thus the bulk of Pb is detrital. Because the ionic radius of Pb^{2+} (1.32 Å) is very clost to that of potassium (1.33 Å), it is possible that important amounts of Pb could be present in the illite structure. Of particular interest is the Pb-Al correlation (r = 0.72) which is stronger than that between Pb and K (r = 0.58). This may suggest that some Pb being adsorbed on the clays. The Pb-Fe correlation (r = 0.55) is difficult to evaluate since both elements are heavily loaded on the clays.

The chalcophile nature of Pb is not obvious in the middle Purbeck shales since Pb shows no correlation with S. Lack of Pb-S correlation is attributed mainly due to the small amounts of S present in the middle Purbeck shales, besides the weathered nature of the succession at Durlston Bay. The amount of pyrite which might have occurred in the original sediments was less than 2% (calculated from the present average sulphur content). Considering the average of 80 ppm Pb in pyrite (Wedepohl, 1974b), the contribution from the 2% pyrite in the middle Purbeck sediments did not exceed 2 ppm Pb.

(l) Thorium

Most of the publications dealing with thorium include analytical data for uranium. The fractionation and distribution of thorium and uranium in sedimentary rocks is determined by the oxidation and leaching of uranium during weathering, with the

immobile thorium left behind in resistates or adsorbed on clays (Adams and Weaver, 1958). Therefore the Th/U ratio has been suggested as a sensitive indicator of sedimentary processes and environment (Pliler and Adams 1962; Kovalev, 1965; Bloxam and Thomas, 1969). Unfortunately, due to analytical difficulties, the uranium data for the middle Purbeck shales are not included in the present work.

Thorium content in the middle Purbeck shales varies from the detection limit (2 ppm) and 17 ppm Th. The average Th content of the present rocks is 10 ppm. This value is very close to the average Th content in shales reported by different authors (Table 37).

Table 37. Abundance of thorium in shales

	Th (ppm)
Rankama and Sahama (1950)	10
Green (1959)	12
Turekian and Wedepohl (1961)	12
Horn and Adams (1966)	13
Rogers and Adams (1969)	10–13
Ronov and Migdisov (1971)	
a. Russian platform	10.6
b. N. American platform	14.3
Present work	10.2
	12.1 [1]

[1] Calculated on carbonate-free basis

In the middle Purbeck shales, Th shows significant positive correlation with 14 elements which can be classified into four groups. The values of correlation coefficients are given to the right-hand side of each element.

Group 1 : Al(0.58), Ga(0.53), Si(0.53), Rb(0.44), K(0.40) and Fe(0.33)
Group 2 : Ti(0.67) and Zr(0.52)
Group 3 : Ce(0.55)
Group 4 : Pb(0.74), V(0.72), Ni(0.44), Ba(0.32) and Zn(0.25)

The first and second groups point to the residence sites of Th i.e. in the hydrolysate sediments and in the heavy resistate minerals. The second and third groups reflect the geochemical behaviour of Th since it occupies, geochemically, an intermediate position between the rare-earth metals, zirconium and uranium (Rankama and Sahama, 1950). Thorium correlation with the elements of the fourth group is difficult to explain especially in the case of Pb and V which have the highest correlation values with Th. However, Th correlation with the elements of the fourth group could be an apparent one since both are heavily loaded on the clays.

Thorium correlates negatively with CaO and CO_2, besides other elements which have sympathetic variation with the carbonates such as organic carbon, Mn, Sr and Na. It seems reasonable to conclude that Th in the middle Purbeck shales is mainly of detrital nature. This is indicated by Th positive correlation with the detrital components (clays, quartz, etc.) and its negative correlation with the non-detrital fraction particularly the carbonates.

5. Modification of elements during diagenesis

Potter *et al.*, (1963) claimed that the content of trace elements in ancient shales is not seriously modified by post-depositional diagenetic processes. In the middle Purbeck shales, as previously suggested, the possibility of Zn and Ni mobilisation during diagenesis cannot be ruled out. Also, the petrographic study of the Purbeck limestones suggests limited Fe mobilisation since the shales were the main source for Fe^{2+} in the ferroan calcite either in the late cements or in the 'beef' layers. Although the criteria for such mobilisation are tentative, it was felt that the subject should be treated again. It is hoped that this may emphasise the importance of diagenesis on the modification of certain elements in the shales.

Originally, the abnormally high Zn and Ni contents of the layers of perished bivalves (thin carbonate bands enclosed in the shales) drew the attention to the source of such enrichment. The other middle Purbeck limestones have 'normal' contents of Zn and Ni comparable with their averages in carbonate rocks (see chapter 12). Therefore, the shales are possible source of the high Zn and Ni in the layers of 'perished' bivalves.

If the movement of Zn and Ni during mobilisation was from the shales towards the carbonate layers (enclosed in the shale), one expects that the calcareous shale to be relatively enriched in Zn and Ni in comparison with the 'pure' shales. As a test for this possibility, the following procedure was applied. The shale suite of the middle Purbeck was split into two groups: 'pure' shale and calcareous shales[1]. To eliminate the effect of carbonate dilution, the element concentrations were calculated on carbonate-free basis. Table 38 indicates that Zn, Ni and Fe are relatively enriched in the calcareous shales in comparison with the 'pure' shales. Examination of the ratios Zn/Al, Ni/Al and Fe/Al

Table 38 Behaviour of Zn, Ni and Fe in the middle Purbeck shales[1]

	'Pure' shales	Calcareous shales
Clay %	77.8 (80.9)	52.7 (80.2)
Carbonate %	3.8	43.3
Quartz %	13.4 (13.9)	8.8 (13.4)
Fe_2O_3 %	6.75 (7.02)	4.52 (7.24)
Zn ppm	100 (104)	81 (130)
Ni ppm	68 (71)	50 (80)
Fe_2O_3/Al_2O_3	0.32	0.38
Zn/Al_2O_3	4.73×10^{-4}	6.88×10^{-4}
Ni/Al_2O_3	3.23×10^{-4}	4.17×10^{-4}

[1] Values in parentheses are calculated on carbonate-free basis

[1] The 'pure' shales are difined arbitrarily as those with more than 85% clays calculated on quartz-free basis; the other shale samples were considered as calcareous shales.

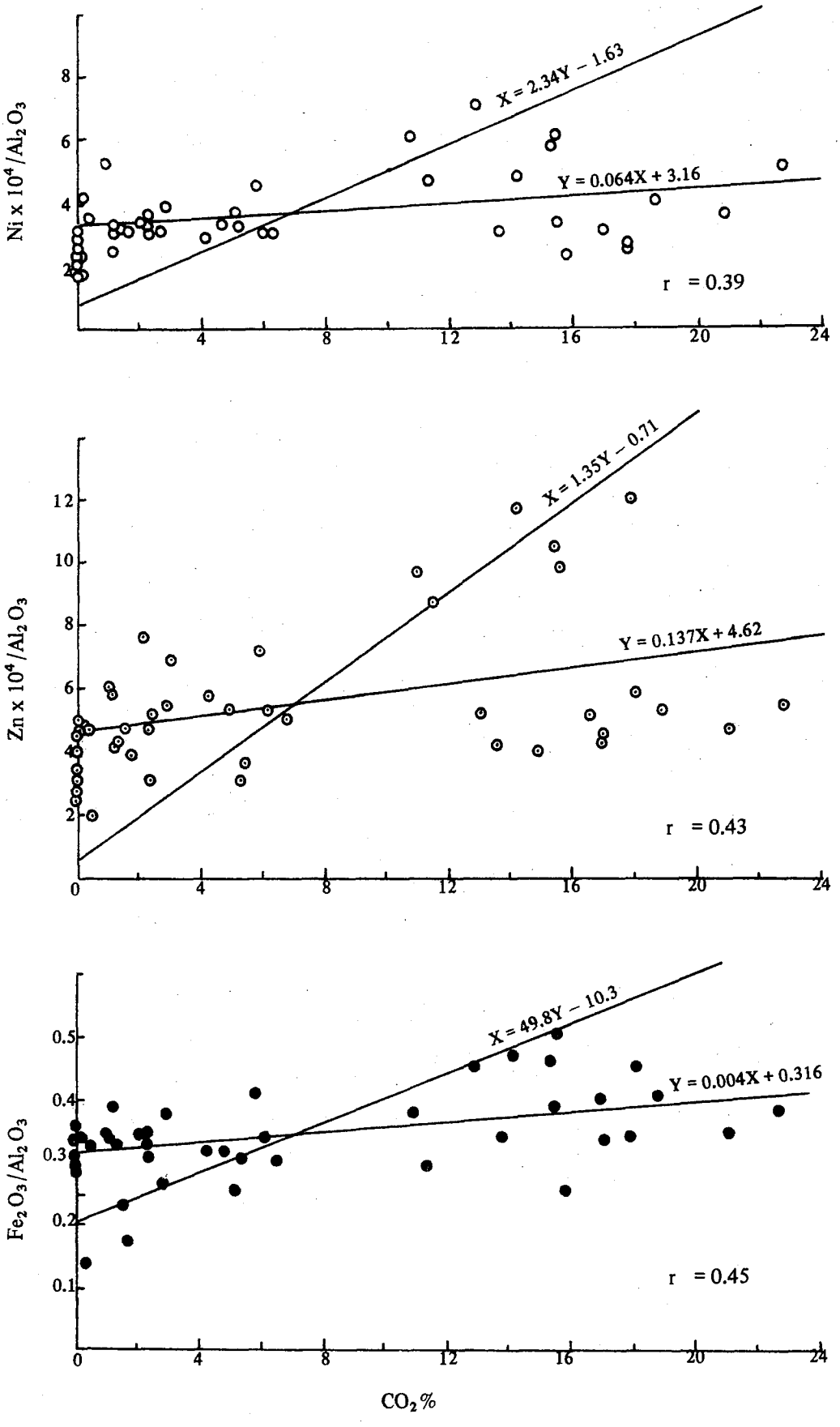

Fig. 99. A plot of Ni/Al, Zn/Al and Fe/Al against CO_2 (for middle Purbeck shales)

in the whole shale suite indicates that they have sympathetic variations with the contents of CO_2 (Fig. 99). Again this indicates that the calcareous shales are relatively enriched in Zn, Ni and Fe.

6. Trace elements and palaeosalinity of the middle Purbeck shales

To consider an element as an ideal palaeosalinity indicator, it must be affected only by water salinity. Other environmental parameters should have the minimum effect compared with water salinity. In addition, the element should not be seriously modified by post-depositional environment. Even if these limitations are satisfied, another difficulty arises from the fact that most of the shales are products of recycling. Boron anomalies were observed by Harder (1964) in Pleistocene sediments from northern Europe. These sediments were deposited in boron deficient freshwater lakes, but the clays contained much boron because they were derived from boron-rich Triassic sediments. Many boron anomalies are known in shales (Eagar, 1962; Eagar and Spears, 1964; Curtis, 1964; Spears, 1965; Cody, 1970), and probably resulted from recycling.

Several trace elements, including B, Ga, V, Li, Cr, Cu and Ni, have been proposed as palaeosalinity indicators for shales (Keith and Degens, 1959; Katchenkov, 1961 quoted in Landergren, 1974; Walker, 1962, 1963, 1964; Potter *et al.*, 1963; Tourtelot, 1964; Ordrof, 1969). More recently, Cody (1971) has ruled out any possible relationship between an element concentration in shale and palaeosalinity.

The average contents of V, Ni, Cu and Ga in the middle Purbeck shales, besides those of freshwater and marine shales are given in Table 39. These data indicate that: 1) Cu and Ga contents in shales cannot be related to palaeosalinity, and 2) V and Ni could be more abundant in marine shales compared with freshwater shales. The high V and Ni contents of the middle Purbeck shales indicate a possible marine origin. On the

Table 39. Distribution of V, Ni, Cu and Ga (ppm) in freshwater and marine shales.

	Freshwater	Marine	Middle Purbeck Shale (present work)
Vanadium			
Goldschmidt (1954)	120	200	145
Potter *et al.*, (1963)	53	134	
Tourtelot (1964)	93–101	158–243	
Katchenkov (1961 in Landergren, 1974)	120	180	
Nickel			
Potter *et al.*, (1963)	23	42	61
Tourtelot (1964)	19–23	32–53	
Copper			
Potter *et al.*, (1963)	16	28	35
Tourtelot (1964)	22–29	27–48	
Lebedev (1967)	46	44	
Wedepohl (1974)		23–65	
Gallium			
Degens *et al.*, (1958)	17	8	18
Potter *et al.*, (1963)	16	25	
Tourtelot (1964)	19–20	16–20	

other hand, the palaeontological evidences suggest that the environment of the middle Purbeck shales was dominated by brackish and freshwater conditions.

It seems that the middle Purbeck shales represent another case similar to the example of boron anomalies observed by Harder (1964). In this respect, it is interesting to note that the boron content of illite from the freshwater limestones from the middle and upper Purbeck was similar to that for illite from the marine Cinder Beds (Walker, 1964).

Generally, the great majority of clay minerals in argillaceous sediments are detrital

in origin and strongly reflect the characters of source material rather than those of the depositional environment (Weaver 1958 a & b; Mackenzie, 1965; Cosgrove and Salter, 1966 and many others). The detrital nature of the middle Purbeck clays has been emphasised in many parts of this study (see Fe, V, Ni, Zn, Zr, Ba, Pb and Th).

Therefore, the inherited marine nature of the Purbeck clays suggests derivation from older marine sediments. Throughout most of southern England, the Purbeck-Wealden sediments contain derived material (including illite-rich clays, glauconite, limestone and chert) from marine Upper Jurassic sources (Allen, 1960; Allen *et al.*, 1964; Allen and Keith 1965; West and Hooper, 1969).

12 GEOCHEMISTRY OF THE MIDDLE PURBECK LIMESTONES

1. Mineralogy

The average mineral composition of the present limestones is about 75% calcite, 5% aragonite, 10% clay minerals and 4% quartz. The distribution of these minerals is shown in Fig. 100. The composition of the main carbonate facies is summarised in Table 40. The bivalve biosparrudites contain the highest amount of calcite while the layers of perished bivalves consist of dominant aragonite. Generally, the clays are more abundant in the micritic limestones in comparison with the other facies.

2. Chemistry of the major elements

(a) Calcium, magnesium and carbon dioxide

In the middle Purbeck limestones, calcium ranges from 24.9 – 54.3% CaO whereas CO_2 varies between 20.8 and 43.5% (see Table 41 and Fig. 101). The distributions of both CaO and CO_2 are very similar as indicated from their histograms and skewness values (SK = –0.66 and –0.65 respectively). The average contents of CaO and CO_2 in the present limestones are 43.4% and 35.2% respectively. These values agree well with the contents of CaO and CO_2 reported for carbonate rocks by different authors (Table 42).

Table 42. Abundance of CaO, MgO and CO_2 in carbonate rocks

	CaO %	MgO %	CO_2 %	Ca/Mg[1]
Rankama and Sahama (1950)	42.6	7.91	41.6	6.38
Green (1959)	38.1	7.29	37.0	6.19
Turekian and Wedepohl (1961)	42.3	7.79	35.7	6.43
Horn and Adams (1966)	38.1	7.51		6.00
Ronov and Migdisov (1971)				
a. Russian platform	39.7	7.44	35.7	6.32
b. N. American platform	43.2	6.28	39.7	8.15
Present work	43.4	1.40	35.2	45.00

[1] Calculated by the present author

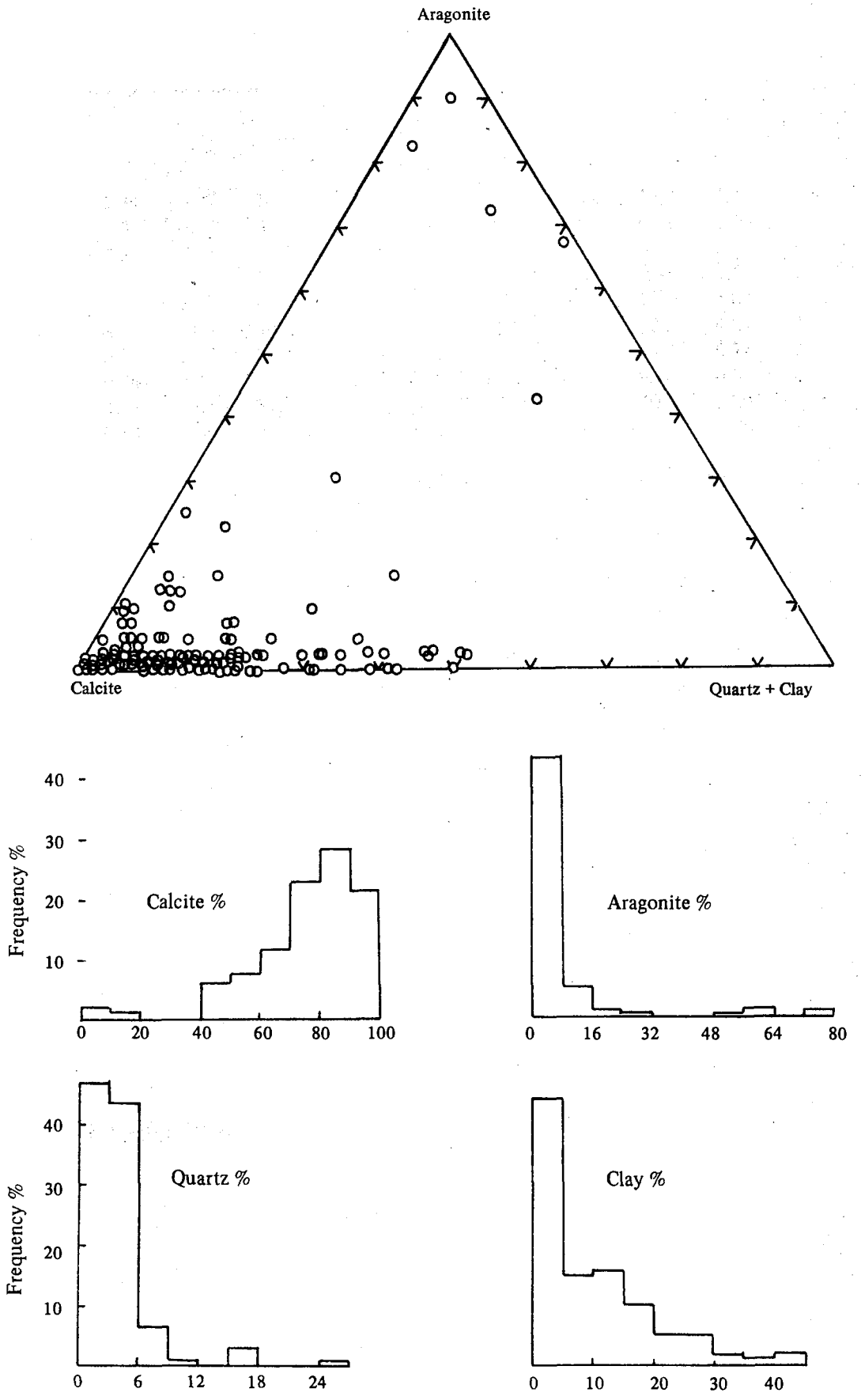

Fig. 100. Mineral composition of the middle Purbeck limestones

Table 40. Chemistry and mineralogy of the main carbonate facies in the Middle Purbeck Group of Durlston Bay

	1	2	3	4	5	6	7	8	9	10	11
In percent											
SiO_2	5.24	8.97	14.2	10.4	8.65	4.70	3.14	2.42	6.36	9.40	5.22
TiO_2	0.06	0.13	0.14	0.20	0.13	0.06	0.04	0.03	0.09	0.13	0.10
Al_2O_3	1.31	2.92	3.36	4.77	3.67	1.03	1.00	0.45	2.14	3.05	2.36
Fe_2O_3	0.82	1.52	1.67	1.74	1.66	0.63	3.91	0.88	3.53	3.64	1.63
MgO	1.77	1.85	4.52	1.19	1.14	1.12	0.91	1.11	1.07	0.70	0.80
CaO	46.4	41.2	34.9	38.1	42.4	48.2	45.3	50.5	42.7	39.0	46.2
Na_2O	0.90	0.83	0.86	0.74	0.71	0.89	0.71	0.84	0.75	0.76	0.72
K_2O	0.36	0.65	1.00	0.90	0.69	0.33	0.20	0.14	0.36	0.58	0.44
CO_2	40.4	33.3	31.9	31.6	35.0	38.9	36.3	40.4	34.9	30.6	36.5
H_2O^+	0.63	1.64	2.03	1.82	1.19	0.51	0.41	–	0.80	1.82	1.39
Organic carbon	0.62	1.88	0.62	0.72	0.56	0.24	1.77	0.30	1.65	2.62	0.43
S	0.19	0.29	0.29	0.28	0.32	0.15	1.25	0.22	0.92	0.78	0.24
Cl	0.19	0.12	0.15	0.09	0.06	0.09	0.06	0.11	0.11	0.15	0.02
In ppm											
P	498	349	425	306	343	243	240	323	263	443	176
V	17	28	39	56	29	16	12	9	21	31	22
Mn	947	869	633	1476	358	242	758	310	657	433	214
Ni	10	14	19	17	13	8	15	6	25	52	13
Rb	16	31	39	41	29	14	10	5	17	30	23
Sr	1309	1120	1003	262	568	478	637	769	1310	2201	657
Zr	33	46	48	37	27	21	19	20	35	64	22
Ba	239	238	143	98	354	148	133	226	643	154	98
In percent											
Calcite	85	74	71	72	76	88	82	89	63	9	83
Aragonite	1	2.5	2	–	2.5	0.5	1	3	16	62	–
Quartz	2.5	3.5	5	4	4	3	3	2	3.5	5	3
Clay	6	14	17	16	12	4.5	4.5	2	8	12	8.5
Ca/Mg ratio	31.1	26.4	9.1	37.9	44.1	51.0	59.0	53.9	47.3	66.0	68.4
Srx1000/Ca (atomic ratio)	1.81	1.74	1.84	0.44	0.86	0.63	0.90	0.97	1.96	3.61	0.91

1 Charophyte biomicrite
2 Ostracod biomicrite
3 Ostracod-gastropod biomicrite
4 Micrite and pelmicrite
5 Bivalve biomicrudite (Cinder Beds excluded)
6 Bivalve biomicrudite (Cinder Beds)
7 Ostracod biosparite
8 Bivalve biosparrudite
9 Friable bivalve limestone
10 Layers of perished bivalves
11 'Beef'

Table 41. Chemical composition of the middle Purbeck Limestones

In percent	Min	Max	Average	S.D.	S.E.	SK
SiO_2	0.11	31.1	7.73	7.52	0.64	1.40
TiO_2	0.01	0.38	0.09	0.08	0.007	1.07
Al_2O_3	–	9.56	2.41	2.48	0.21	1.04
Fe_2O_3	0.08	11.05	1.70	1.61	0.14	3.14
MgO	0.44	5.84	1.40	0.82	0.07	3.04
CaO	24.9	54.3	43.4	7.87	0.67	–0.66
Na_2O	0.43	1.20	0.80	0.14	0.01	0.11
K_2O	0.02	2.24	0.53	0.47	0.04	1.05
CO_2	20.8	43.5	35.2	5.77	0.49	–0.65
H_2O^+	–	4.61	1.04	1.15	0.10	0.81
Organic carbon	0.04	6.99	0.92	1.13	0.10	2.90
S	0.05	4.06	0.38	0.53	0.04	5.27
In ppm						
P	160	2613	372	263	22	5.12
Cl	162	8327	1005	1218	104	3.58
V	–	89	24	21	1.76	1.27
Mn	22	2291	555	394	34	1.71
Ni	–	105	15	14	1.16	3.00
Rb	–	109	24	24	2	1.14
Sr	227	4167	897	586	50	2.23
Zr	2	108	34	22	1.89	0.94
Ba	–	5436	267	624	53	6.52
Ce	–	129	26	28	2.41	1.07
Zn [2]	–	211	35			
Ga	–	9	2			
As	–	25	1.8			
Pb	–	26	3.4			
Th	–	9	2.5			

[1] Based on 137 samples collected from Durlston Bay; samples from the 'beef' layers are not included.

[2] The data of Zn, Ga, As, Pb and Th are based on 30 limestone samples

S.D. = standard deviation

S.E. = standard error of the mean

SK = skewness.

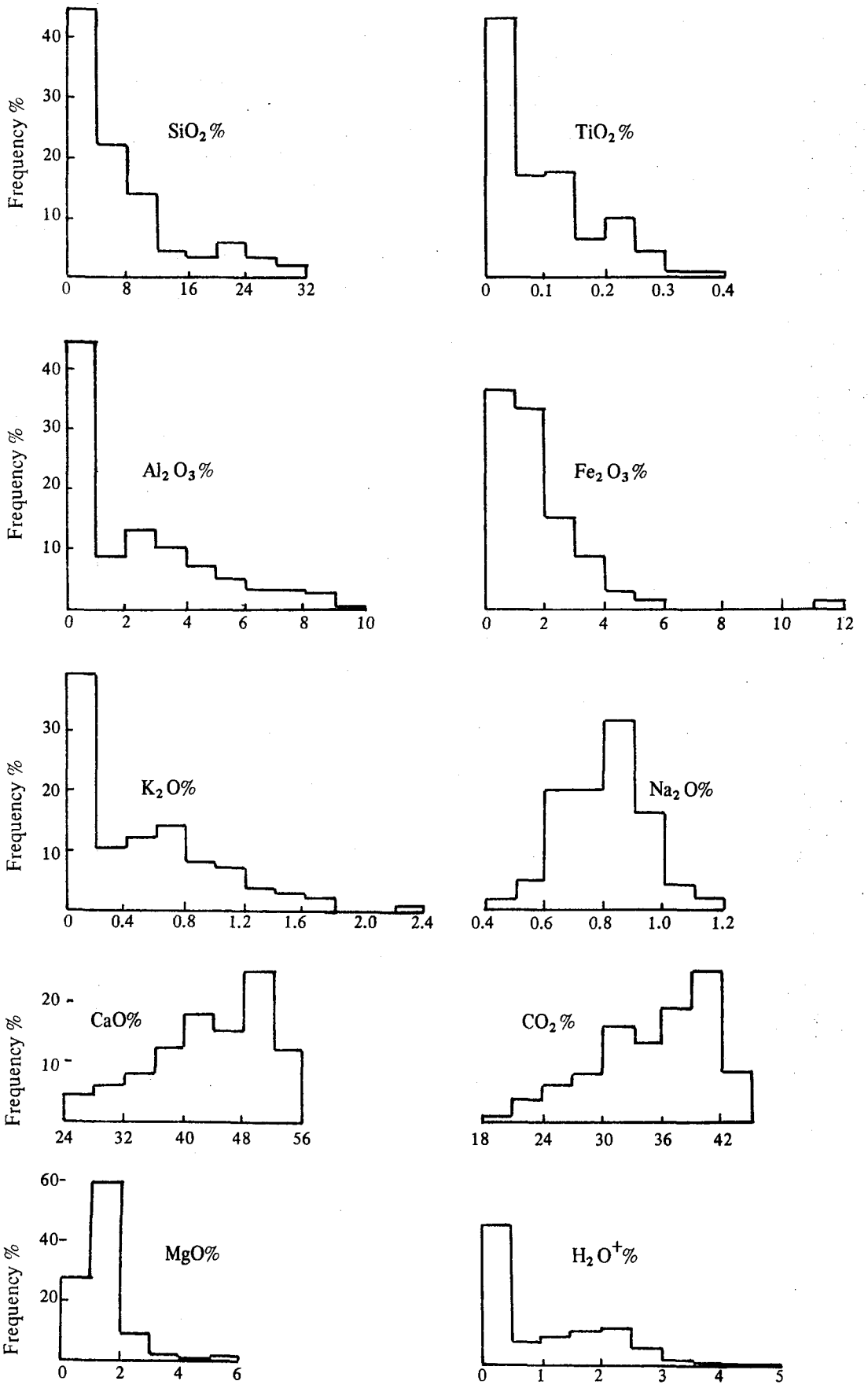

Fig. 101. Distribution of the major elements in the Middle Purbeck limestones

Calcium is entirely present in the carbonate phase as indicated from its strong positive correlation with CO_2 (r = 0.98). Clay and quartz represent the bulk of the non-carbonate fraction. Both correlate negatively with calcium (r = −0.91 and −0.60 respectively).

Magnesium in the present limestones ranges from 0.44 – 5.84% MgO (see Table 41 and Fig. 101). The average magnesium value is 1.4% MgO which is lower than that of carbonate rocks (Table 42). However, this is attributed to the scarcity of dolomite in the middle Purbeck rocks at Durlston Bay[1]. The amount of magnesium in the clay fraction is about 0.4% MgO (Table 43). The remaining is about 1% MgO and is present in the calcite structure (low-Mg calcite).

Although Ca/Mg ratio of the middle Purbeck limestones shows a wide range from 6–119, the distribution is not far from normality (SK = 0.39). The average Ca/Mg ratio in the present rocks is very high compared with that of carbonate rocks (Table 42). Obviously this is due to the low Mg content in the middle Purbeck limestones. The different limestone facies recognised in the present study vary considerably in respect to their Ca/Mg ratio (table 40). The ostracod-gastropod biomicrites (contain about 17% clay) have the lowest Ca/Mg ratio. These rocks were encountered in the Marly Freshwater Beds where the clays are relatively rich in Mg. The layers of perished bivalves (contain up to 75% aragonite) have the highest Ca/Mg ratio. In general, skeletal aragonite rarely contains more than 1 mole percent $MgCO_3$ (Chave, 1954).

In the present carbonates, the Ca/Mg ratio shows a marked increase from the biomicrites and biomicrudites towards the biosparites and biosparrudites (Table 42). This suggests that the sparry calcite cements contain less Mg in comparison with the

[1] Traces of dolomite were found only in one sample (bed DB133).

Table 43. Chemistry of the middle Purbeck limestones compared with the contribution from the clay-fraction [1 & 2]

	Average for all the limestones	Calculated contribution from the clay-fraction[3] for all the limestones
In percent		
SiO_2 (combined)[4]	4	5
TiO_2	0.09	0.09
Al_2O_3	2.41	2.54
Fe_2O_3	1.70	0.84
MgO	1.40	0.36
K_2O	0.52	0.41
In ppm		
V	24	21
Ni	15	9
Zn	35	9
Ga	2	1.8
As	1.8	1
Rb	24	24
Zr	34	20
Ba	267	60
Ce	26	12
Pb	3.4	2.4
Th	2.5	1

[1] Average clay content of the present limestones is about 10%

[2] Zn, Ga, As, Pb and Th were determined in 30 limestone samples which contain about 7% clay on average

[3] Based on the average composition of the middle Purbeck shales after correction for the non-clay fraction

[4] Combined SiO_2 = total silica – quartz.

carbonate mud. This seems to indicate a decrease in the Mg content as the crystal size of calcite increases. The 'beef' layers which consist mainly of coarse calcite crystals (up to few millimetres), have the lowest Mg content.

(b) Silicon, titanium, aluminium and potassium

The contents of the four elements in the present limestones are almost exclusively in the non-carbonate fraction particularly the clays. Calculated contribution from the average of 10% clay, present in the middle Purbeck limestones, are extremely close to the averages of the four elements in the whole limestone (Table 43). Again this can be inferred from strong positive correlations between the clay and the four elements (r = 0.91, 0.93, 0.96 and 0.96 respectively). Since the clays have strong sympathetic variations with the heavy resistate elements such as Ti and Zr, a detrital origin for the clay fraction of the present limestones is assumed.

The distribution of SiO_2, TiO_2, Al_2O_3, and K_2O in the middle Purbeck limestones are very similar (fig. 101). This is also reflected in their skewness values (SK = 1.40, 1.07, 1.04, and 1.05 respectively). The slight difference in the distribution of SiO_2 is due to the presence of variable amounts of quartz.

The ranges and averages of SiO_2, TiO_2, Al_2O_3 and K_2O are given in Table 44. Comparison with published data indicates that the contents of the four elements in the present limestones are very close to those of carbonate rocks.

Table 44. Abundance of SiO_2, TiO_2, Al_2O_3 and K_2O in carbonate rocks

	SiO_2 %	TiO_2 %	Al_2O_3 %	K_2O%
Rankama and Sakama (1950)	5.18		0.82	0.33
Green (1959)	8.56	0.07	2.46	0.19
Turekian and Wedepohl (1961)	5.14	0.07	0.79	0.33
Horn and Adams (1966)	7.26	0.06	1.70	0.29
Ronov and Migdisov (1971)				
a. Russian platform	8.27	0.13	1.65	0.57
b. N. American platform	6.68		1.48	0.26
Present work	7.68	0.09	2.46	0.53

(c) Iron

The content of iron in the present limestones ranges from 0.08 – 11.05% Fe_2O_3 (see Table 41 and Fig. 101). The distribution is highly skewed (SK = 3.14). The average value for the middle Purbeck limestones (1.70% Fe_2O_3) seems to be in agreement with the averages reported for carbonates (Table 45).

Table 45 Abundance of iron (expressed as Fe_2O_3) in carbonates

	Fe_2O_3 %	Fe/Al[1]
Rankama and Sahama (1950)	0.57	0.92
Green (1959)	1.86	1.00
Turekian and Wedepohl (1961)	0.54	0.83
Horn and Adams (1966)	1.73	0.90
Ronov and Migdisov (1971)		
a. Russian platform	1.28	1.02
b. N. American platform	1.40	1.25
Present work	1.70	0.93

[1] Calculated by the present author

From the above table it appears that the ratio of iron to aluminium is reasonably constant. This indicates association of the iron with the clay fraction in carbonate rocks. Iron in the present limestones occurs in the pyrite and in the clay. The amount of iron present as pyrite is little less than 1% Fe_2O_3 (calculated from the average sulphur value). The remaining Fe_2O_3 is little more than 0.70% and occurs in the clay fraction. This value is close to the contribution of the 10% clay present in the middle Purbeck limestones i.e. 0.84% Fe_2O_3 (see Table 43).

Iron shows sympathetic variations with quartz, aluminium, organic carbon and sulphur (r = 0.23, 0.42, 0.49 and 0.89 respectively). The higher correlation with sulphur and organic carbon indicates that important quantities of iron were precipitated as

sulphides in reducing environments. However, before precipitation the major transport of iron occurred mainly on the detrital matter as indicated from the positive correlation with the quartz and the clay.

(d) Sodium

Sodium was reported in all the middle Purbeck limestones ranging from 0.43–1.20% as Na_2O (see Table 41 and Fig. 101). The distribution is more or less normal (SK = 0.11). Average Na_2O content of the present limestones is much higher than the values reported for carbonate rocks by different authors (Table 46).

Table 46. Abundance of sodium in carbonate rocks

	Na_2O %
Rankama and Sahama (1950)	0.04
Green (1959)	0.08
Turekian and Wedepohl (1961)	0.05
Horn and Adams (1966)	0.05
Ronov and Migdisov (1971)	
a. Russian platform	0.29
b. N. American platform	0.16
Present work	0.80
	0.71 [1]

[1] Chloride-free Na expressed as Na_2O

X-ray spectrometry is not the ideal technique for Na determination although the instrumental precision was found satisfactory. It is difficult, therefore, to explain the apparent high Na levels considering that feldspars were rarely identified in the present rocks. Important contributions from sea water could be ruled our since all samples were washed thoroughly in deionised water before chemical analyses. Also the amount of sodium which may be present as NaCl is less than 11% of the total Na.

The striking feature of Na behaviour in the middle Purbeck limestones is that it

exceeds Cl on molar basis for a factor ranging from 2 – 40. Land and Hoops (1973) found that Na in Recent marine carbonates is present in excess of equimolar Cl concentration by at least of factor 6. This suggests that Na is not balanced by Cl concentration in both ancient and modern carbonates.

In the present rocks only about 0.065% Na is probably present as NaCl. The remainder of Na (0.71% Na_2O) is mainly present in the carbonates since chloride-free sodium correlates positively with CO_2 and negatively with Al_2O_3 (r = 0.61 and –0.51 respectively). Calcite is the main host of Na as indicated from positive correlation with both total Na and chloride-free Na (r = 0.45 and 0.51 respectively). No relation was found between aragonite and sodium.

3. Chemistry of Trace Elements

(a) Vanadium and nickel

The abundance of the two elements in the present limestones is controlled by the amounts of clay and iron oxide, hence they are grouped together. Table 47 gives the averages for V and Ni in these rocks compared with the results of other workers.

Table 47. Abundance of V and Ni in carbonate rocks

	V (ppm)	Ni (ppm)
Green (1959)	2 – 20?	20
Graf (1960)	15	12
Turekian and Wedepohl (1961)	20	20
Horn and Adams (1966)	13	13
Present work	24	15
	21 [1]	9 [1]

[1] Contribution of the clay fraction

From the table, it appears that V average is more or less similar to that of Ni. This may be

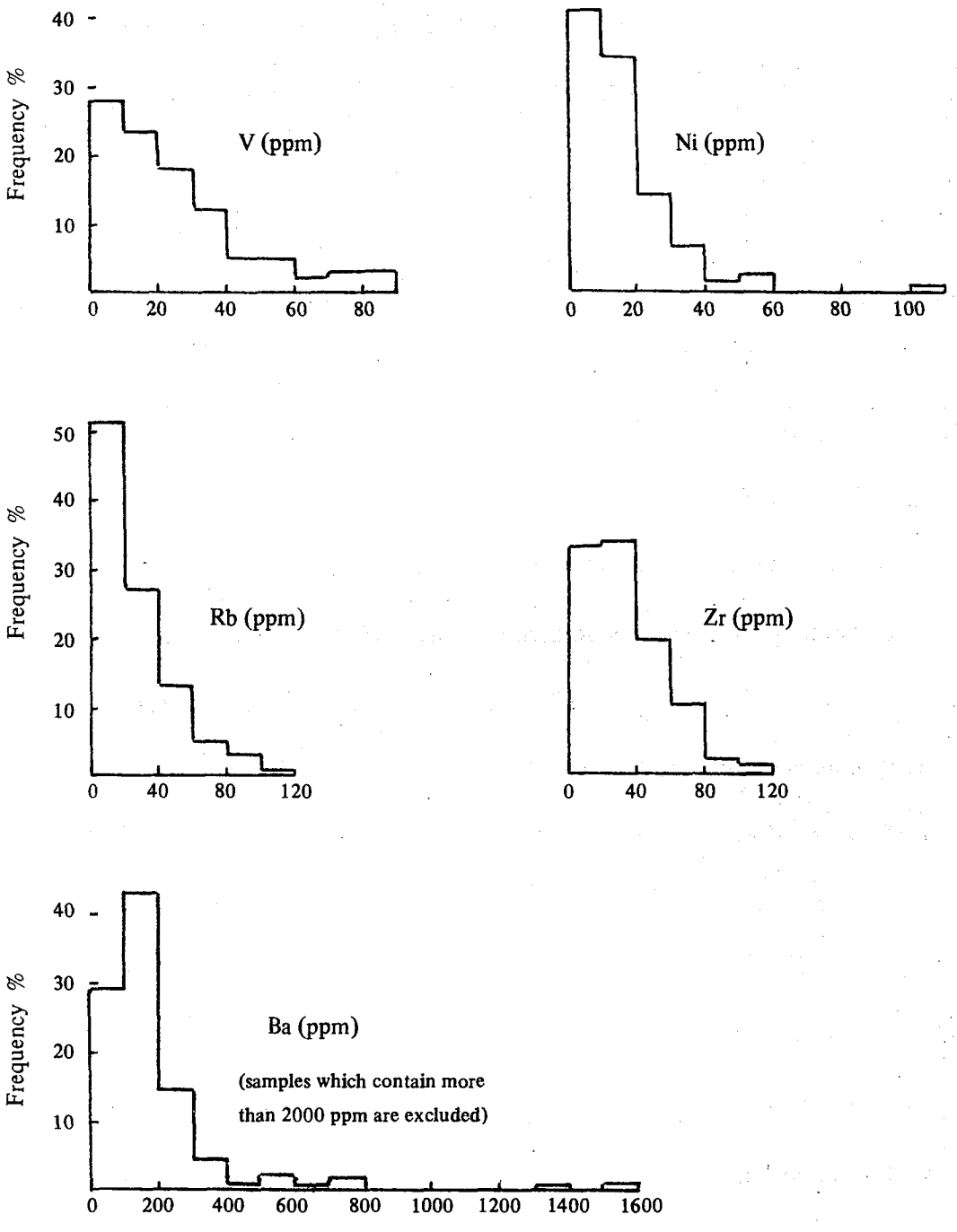

Fig. 102. Distribution of trace elements in the middle Purbeck limestones

the case in 'pure' carbonates, but with the increase of clay content V increases rapidly in comparison with Ni. This is due to the fact that V in argillaceous sediments is nearly 2–3 times the content of Ni (see Chapter 11).

Vanadium ranges from 0 – 89 ppm V. About 50% of the samples contain less than 20 ppm (Fig. 102). The vanadium distribution is approximately lognormal as indicated by the skewness values before and after log transformation (SK = 1.27 and –0.19 respectively). The average value for V in the middle Purbeck limestones is generally higher than the reported values for carbonates (see Table 47).

Nickel varies from 0 – 105 ppm Ni. More than 75% of the present limestones contain less 20 ppm (Fig. 102). The distribution of Ni is highly skewed (SK = 2.97). The skewness value drop to 0.12 after log transformation, thus suggesting lognormal distribution. The average nickel content in the middle Purbeck limestones is generally below the values quoted for carbonates (Table 47).

The behaviour of V and Ni in the middle Purbeck limestones is summarised in Table 48. Amongst the elements which control the distribution of V are: Al, Fe and organic carbon. The highest correlation with Al means that important amounts of V being incorporated in the clays. On the other hand, it seems that Fe and organic carbon are not important factors in the accumulation of V as indicated from lack of significant correlation between V and sulphur. It appears, therefore, that V relation with Fe and organic carbon is an apparent one since both elements are controlled by the distribution of the clay. Table 48 indicates that Ni has a strong affinity towards Fe, S and organic carbon. Since important amounts of Fe in the middle Purbeck limestones are present as pyrite, it is likely that Ni is mainly present in the sulphide phase replacing Fe.

Table 48. Correlation coefficients of V and Ni with Al, Fe, S and organic carbon in the middle Purbeck limestones

	V	Ni
Al	0.92	0.47
Fe	0.45	0.73
S	0.15	0.56
Organic carbon	0.33	0.44

Nickel is more enriched in the layers of perished bivalves (Table 40). These layers are enclosed in relatively thick shale units. The possibility of Ni mobilisation in the shales and subsequent fixation in the surrounding carbonates has been already discussed before (see Chapter 11).

(b) **Rubidium**

From the following table, it appears that there is no reliable average for Rb in carbonate rocks. Because the geochemistry of Rb is closely connected with that of K (see Chapter 11), it is assumed that K/Rb ratios should vary within a limited range. This can be observed in the shales, but in carbonate rocks the fluctuation in the K/Rb ratios is enormous (Table 49).

Table 49. Abundance of Rb(ppm) in carbonate rocks

	Carbonates		Shales
	Rb	K/Rb[1]	K/Rb[1]
Green (1959)	5	315	100–178
Turekian and Wedepohl (1961)	3	900	190
Horn and Adams	46	52	102
Present work	24	180	173

[1] Calculated by the present author

In the present limestones, Rb ranges from 0 – 109 ppm (see Table 41 and Fig. 102). The average value for Rb in the middle Purbeck limestones is 24 ppm. This value

is identical with the contribution from the clay fraction (Table 43). Rubidium correlation with K, Al and the clay fraction are highly significant (r = 0.98, 0.96 and 0.97 respectively). This indicates that Rb occurs entirely in the clays and particularly replacing K in clay minerals. The significant positive correlation between Rb and the heavy resistate elements such as Ti and Zr (r = 0.92 and 0.59 respectively) indicates a detrital origin for Rb in the present rocks.

(c) **Zirconium**

Individual samples range from 2 – 108 ppm Zr (see Table 41 and Fig. 102). The Zr average for the middle Purbeck limestones is 34 ppm. This value is higher than the reported averages for carbonate rocks (Table 50). The apparently high Zr average in the present rocks is the result of analytical difficulties (see below).

Table 50. Abundance of Zr in carbonate rocks

	Zr (ppm)
Green (1959)	20
Graf (1960)	17
Turekian and Wedepohl (1961)	19
Horn and Adams (1966)	18
Present work	34

Zircon correlates positively with the quartz and with most of the clay-related elements. This indicates that Zr is mainly associated with the detrital matter. Zircon is a major component of the heavy mineral suites (see Chapter 10), and it is probably the main source for Zr in the present limestones. Variable amounts of Zr may be present in the clay fraction (see chapter 11).

High Zr values are to be expected in carbonate rocks when X-ray spectrometry is used for Zr determination. The high Zr levels are attributed to the overlap between ZrK_{α}

and $SrK_{\beta 1}$. Although extra care was taken during the calibration processes, but with Sr values up to 4200 ppm and with Zr values down to zero, the overlap was unavoidable. This overlap was reflected in a positive correlation between Zr and Sr (r = 0.41). Similar Zr–Sr correlation was observed by Hirst and Dunham (1963) and was explained by spectral interference.

(d) Barium

In the present limestones, Ba ranges between values below the detection limit (13 ppm Ba) and 5436 ppm Ba (see Table 41 and Fig. 102). The wide range of Ba in the middle Purbeck limestones, is not unique. Ostrom (1957) and Graf (1960) gave the Ba range in carbonate rocks as 10 – 10000 ppm and <5–8000 ppm respectively. More recently Puchelt (1972) reported that Ba in carbonate rocks varies from 1 – 10000 ppm.

The average Ba content in the present limestones is 267 ppm. If three samples (containing more than 2000 ppm Ba each) are excluded, the average becomes 184 ppm. This value is not far from the reported averages for Ba in carbonates (Table 51). The average Ba for carbonates given by Turekian and Wedepohl (1961) is too low. They based their average value (10 ppm) on the barium content of modern molluscan shells; this seems to be too low a value for carbonate rocks.

In the middle Purbeck limestones, Ba shows a weak positive correlation (significant after log transformations) with the clay, S and Sr. The correlation between Ba and the clay is obvious since the middle Purbeck shales contain more Ba in comparison with the limestones. The association of Ba with the acid insoluble residue and presumably with the clay has been reported in carbonate rocks by several authors (Goldberg and Arrhenius, 1958; Migdisov, 1960; Weber, 1964; Veizer and Demovic, 1973; and others). Probably most of the Ba present in the clay fraction occurs in the silicate structure

Table 51. Abundance of Ba in carbonate rocks

	Ba (ppm)
Rankama and Sahama (1950)	120
Ostrom (1957)	260
Green (1959)	77–250
Graf (1960)	150
Turekian and Wedepohl (1961)	10
Present work	267
	184 [1]
	59 [2]

[1] The Purbeck average after excluding three samples with more than 2000 ppm
[2] Contribution of the clay fraction

replacing for K (see Chapter 11). The Ba–S correlation suggests that some Ba is present in the sulphate phase and this was confirmed by the presence of barite. The correlation between Ba and Sr could be due to the presence of few samples which are exceptionally high in both elements (e.g. bed DB94: 4196 ppm Sr and 2180 ppm Ba; bed DB164b: 1862 ppm Sr and 4260 ppm Ba).

The present limestones contain 10% clay on average. The contribution from this amount of clay is about 60 ppm Ba (see Table 43). The remaining Ba in the middle Purbeck limestones is about 200 ppm and occurs mainly as barite and probably in the carbonate phase.

(e) Cerium

X-ray spectrometry was not a satisfactory technique for Ce determination in the present limestones. Instrumental precision was poor and the detection limit (25 ppm Ce) is much higher than the amount of Ce present in carbonate rocks. Considering such limitations, it is difficult to evaluate Ce behaviour in the present limestones. Nevertheless, the following is a brief account concerning the 'observed' behaviour.

Individual samples range from 0 – 129 ppm Ce (see Table 41). The average value for Ce in the middle Purbeck limestones is 26 ppm. This average is too high compared with the reported averages for Ce in carbonate rocks (Table 52). The clay fraction of the present limestones contain about 12 ppm Ce. This value is not far from the average of Ce in carbonate rocks.

Table 52. Abundance of Ce in carbonate rocks

	Ce (ppm)
Turekian and Wedepohl (1961)	11.5
Horn and Adams (1966)	10.8
Ronov *et al.*, (1967)	6.5
Present work	26
	12 [1]

[1] Contribution of the clay fraction

Ce correlates positively with Al and negatively with CO_2 indicating its association with the clay fraction. One of the anomalies of the 'observed' Ce behaviour, in the middle Purbeck limestones, is its enrichment in some samples which contain abundant aragonite. This is not understood.

(f) Zinc, gallium, arsenic, lead and thorium

The five elements were only determined in 30 limestone samples. With so many values near to the detection limit, it was felt that any statistical treatment is not justified. The following table shows the averages of the five elements in the present limestones alongside values published by other workers. The table indicates that a fair agreement exists between the present averages and those for carbonate rocks.

The behaviour of Zn in the present carbonates has some interest. It is highly enriched (up to 211 ppm Zn) in the carbonates which are enclosed in relatively thick

Table 53. Abundance of Zn, Ga, As, Pb and Th (ppm) in carbonate rocks

	Zn	Ga	As	Pb	Th
Green (1959)	19	3	2.4	6–27	1.8
Graf (1960)	26	2.5	2.5	8	1.9
Turekian and Wedepohl (1961)	20	4	1	9	1.7
Horn and Adams (1966)	16	2.7	1.8	17	2
Onishi (1970)			1		
Ronov and Migdisov (1971)					
a. Russian platform					2.3
b. N. American platform					1.3
Wedepohl (1974b)				5	
Present work	35	2	1.8	3.4	2.5
	15 [1]		1 [2]		
Contribution of the clay fraction [3]	9.3	1.8	1	2.4	1

[1] Samples with more than 100 ppm Zn are excluded
[2] One sample with 25 ppm As is excluded
[3] Average clay content is 7%.

shale units. The characteristic features of these carbonates (layers of perished bivalves) are : 1) high porosity, and 2) high content of skeletal aragonite. Sphalerite is essential host for Zn in these layers. The high aragonite content in these carbonates (up to 75%) suggests that they remained porous since the time of deposition. Zinc enrichment, therefore, implies a connection with porosity (Fig. 103). This enrichment, as it was suggested before, is attributed to Zn mobilisation in the clays (see Chapter 11).

It is worth mentioning that the As content of 25 ppm was the highest value encountered in the present rocks (limestones and shales). This high As content was found in a limestone sample (bed DB135) rich in pyrite and organic carbon.

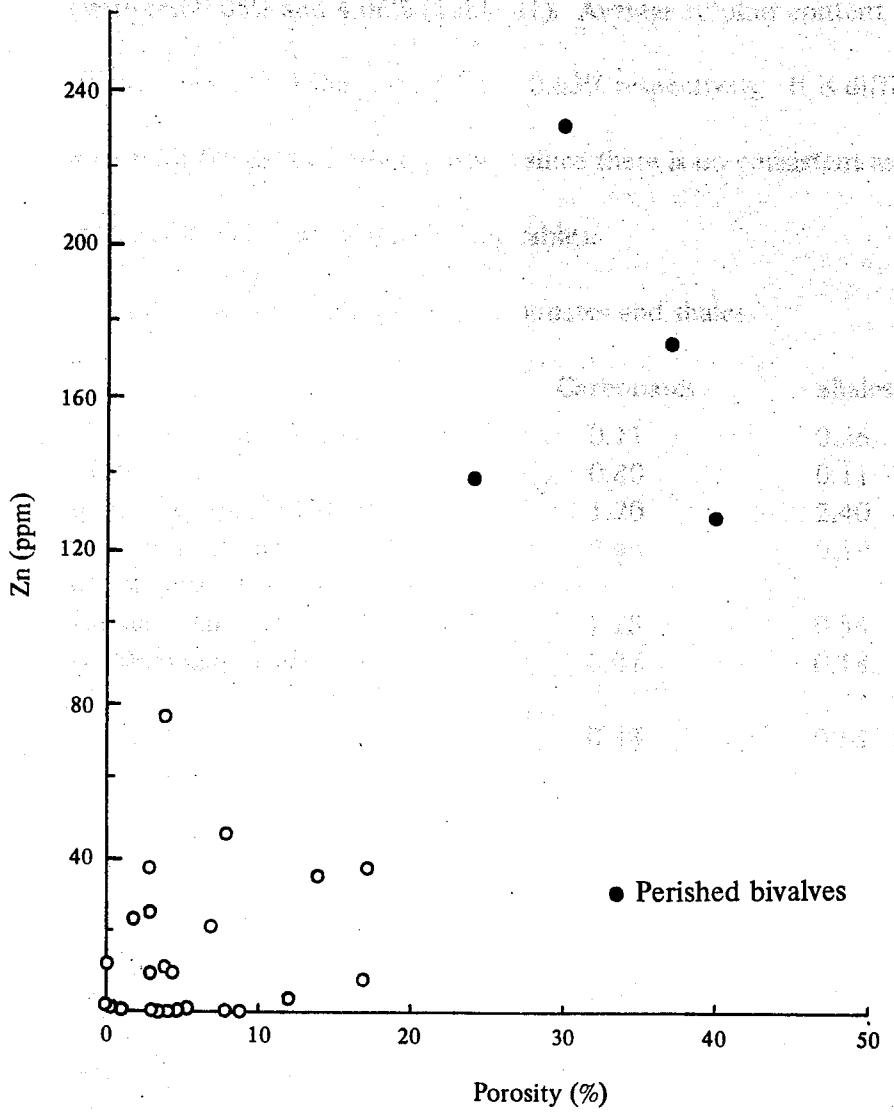

Fig. 103. A plot of Zn against porosity (for middle Purbeck limestones)

13. SULPHUR AND CHLORINE IN THE MIDDLE PURBECK ROCKS

1. Sulphur

In the present shales, sulphur ranges from 0.04 – 1.37% while in the limestones it varies between 0.05% and 4.06% (Table 41). Average sulphur content in the middle Purbeck limestones and shales is 0.38% and 0.63% respectively. It is difficult to compare these values with the data of other workers since there is no consistent averages for sulphur in carbonates and shales (see the following table).

Table 54. Abundance of sulphur (%) in carbonates and shales

	Carbonates	Shales
Rankama and Sahama (1950)	0.11	0.26
Green (1959)	0.80	0.11
Turekian and Wedepohl (1961)	1.20	2.40
Horn and Adams (1966)	0.46	0.19
Ronov and Migdisov (1971)		
a. Russian platform	1.28	0.54
b. N. American platform	0.07	0.18
Present work	0.38	0.63

The middle Purbeck shales differ from the limestones with respect to sulphur distribution and occurrences. The distribution in the limestones is lognormal while in the shales it is normal as indicated from the skewness values (SK = 5.27 and 0.26 respectively). After log transformation these values become 0.57 for the limestones and −1.79 for the shales. In the limestones sulphur occurs mainly in the iron sulphides as indicated from the strong positive correlation with Fe (r = 0.89). In the shales, sulphur is associated with the sulphate phase especially gypsum. Barite was rarely detected in the present shales but the weak correlation between S and Ba (r = 0.19) suggests that the mineral may be present. Sulphur and organic carbon are closely associated in the present limestones. This was not observed in the shales possibly due to the effect of

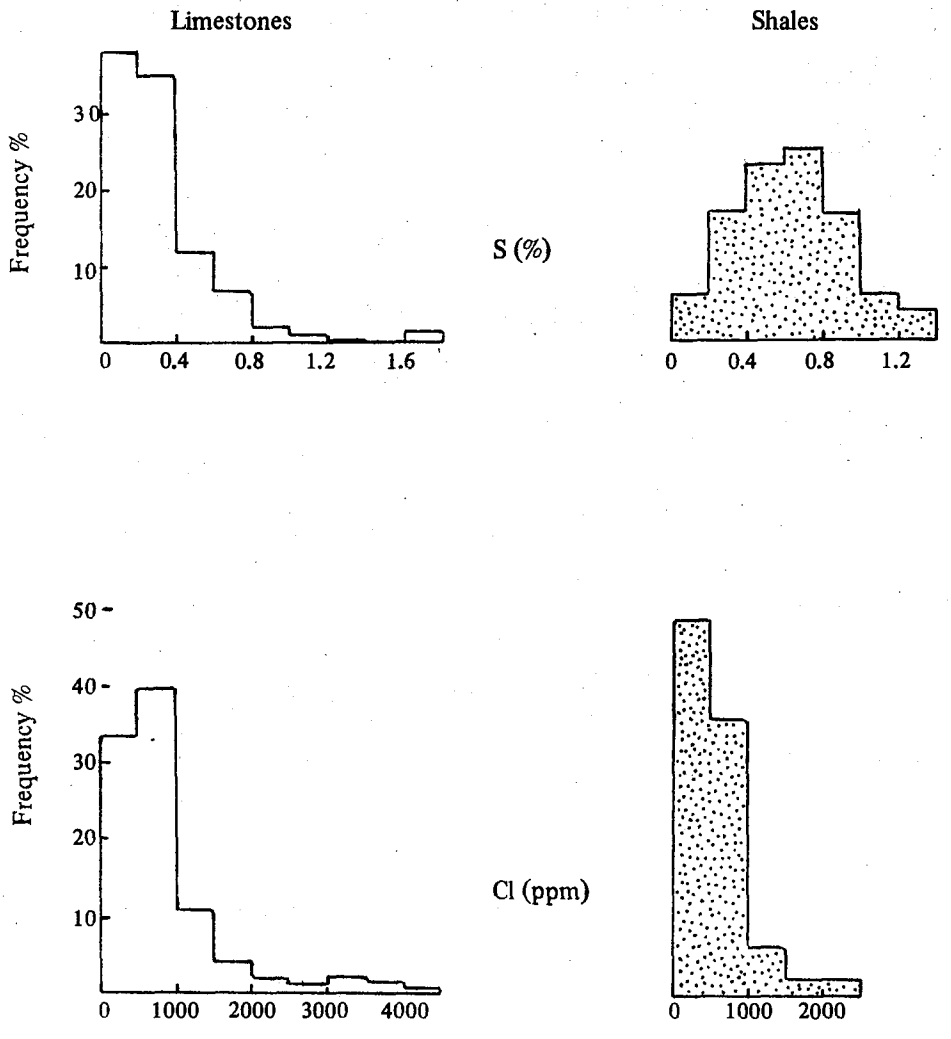

Fig. 104. Distribution of sulphur and chlorine in the middle Purbeck rocks. Samples which contain more than 2% S and 5000 ppm Cl are excluded from the histograms.

weathering.

The relation between sulphur and the trace elements of the middle Purbeck shales is obliterated by the weathering of the original sulphides. Weathering processes are also responsible for leaching of variable amounts of the original sulphur. Amongst the trace elements which are controlled by the distribution of sulphur in the present limestones are Zn, Ni, As and Pb.

The different petrographic types recognised in the middle Purbeck limestones vary considerably with respect to their sulphur contents (Table 40). The highest averages for sulphur were encountered in the ostracod biosparite, friable bivalve limestone and in the layers of perished bivalves 1.25%, 0.92% and 0.78% respectively. The high sulphur average for the ostracod biosparite is due to the high sulphur content (4.06%) in one sample obtained from bed DB214. If this sample is excluded, the sulphur content in the ostracod biosparite is not far from the average value in the middle Purbeck limestones. The high sulphur contents in the friable bivalve limestonesand in the layers of perished bivalves are attributed to secondary enrichment during diagenesis, besides the preservation of the original pyrite. The high contents of aragonite especially in the layers of perished bivalves (up to 75%) suggests that diagenetic events were 'frozen' at a very early stage. This explains the preservation of the original pyrite[1]. On the other hand, because these carbonates are highly porous (up to 40%), it seems probably that they acted as a 'sink' where different elements can accumulate. The high contents of Zn and Ni in the layers of perished bivalves were explained above in terms of secondary enrichment. It is probable, therefore, that some of the sulphur content in these carbonates is secondary in origin; and derived from the host shales.

---

[1] As shown above pyrite is rare in the early cemented *(type 3)* biosparrudites as a result of early oxidation.

2. Chlorine

The chlorine content in the present limestones ranges from 162–8327 ppm while in the shales it varies between 117 and 9869 ppm (Table 41). The chlorine distribution (Fig. 104) is highly skewed in both limestones and shales (SK = 3.58 and 4.44 respectively). The average value for chlorine in the present rocks are much higher than the values reported by different authors (Table 55). If the wild chlorine values (more than 2000 ppm) are excluded, the average becomes 680 ppm for limestones and 556 ppm for shales. These values are still high in comparison with the averages for chlorine in carbonates and shales. Contamination from sea water is not ruled out although the samples were washed thoroughly in deionised water. The high levels of chlorine in the present rocks are probably connected with the low accuracy of the method applied (X-ray spectrometry). Also, the high standard deviations (± 1218 ppm for limestones and ± 1678 ppm for shales) indicate low precision.

Table 55. Abundance of Cl (ppm) in carbonates and shales

	Carbonates	Shales
Rankama and Sahama (1950)	200	
Green (1959)	367	160
Graf (1960)	460	
Turekian and Wedepohl (1961)	150	180
Horn and Adams (1966)	305	170
Jones and Huang (1967)	131	103
Present work	1005	922
	680 [1]	556 [1]

[1] Samples with more than 2000 ppm Cl are excluded

In the present rocks, Cl shows strong positive correlation with Na suggesting that the bulk of Cl is present as NaCl. Walters and Winchester (1971) found that most of

the chlorine content of sediments occur in the water-soluble fraction. Apart from Na, chlorine has no relation with any of the major and trace elements either in the limestones or in the shales.

14. MANGANESE, PHOSPHORUS AND ORGANIC CARBON IN THE MIDDLE PURBECK ROCKS

The three elements are treated together since they show a common 'amphoteric' [1] behaviour. They correlate positively with the carbonate content of the shales whereas in the limestones they show sympathetic variation with the clay fraction. Such 'amphoteric' behaviour is attributed to the higher contents of Mn, P and organic carbon in the calcareous shales and argillaceous limestones in comparison with the 'pure' rocks [2] (see Table 56 and Fig. 105).

Table 56. Abundance of Mn, P and organic carbon in the middle Purbeck rocks[(a)]

	ppm Mn	ppm P	% Org.C	% Quartz	% Carbonate	% Clay
Pure limestones	478	342	0.66	2.7	87	4.1
	(491)	(351)	(0.68)		(89.5)	(4.2)
Argillaceous limestones	724	439	1.48	5.9	65	22.4
	(770)	(466)	(1.57)		(69)	(23.8)
Calcareous shales	691	458	2.61	8.8	34.3	52.7
	(758)	(502)	(2.86)		(37.6)	(57.8)
Pure shales	314	279	1.61	13.4	3.8	77.8
	(363)	(322)	(1.86)		(4.4)	(90)

[(a)] Values in parenthesis are calculated on quartz-free basis

1. Manganese

(a) In the shales

In the middle Purbeck shales, Mn content ranges from 50–1806 ppm. (Fig. 106). The average Mn value is 459 ppm which is lower than the reported averages for shales

[1] This term is borrowed from chemical terminology and not used in its strict sense.

[2] The 'pure' limestones are defined arbitrarily as those which contain less than 15% clay (calculated on quartz-free basis); the rest of the limestone population is classified as argillaceous limestone. The pure shales are those which contain less than 15% carbonate (calculated on quartz-free basis); the other shale samples are considered as calcareous shale.

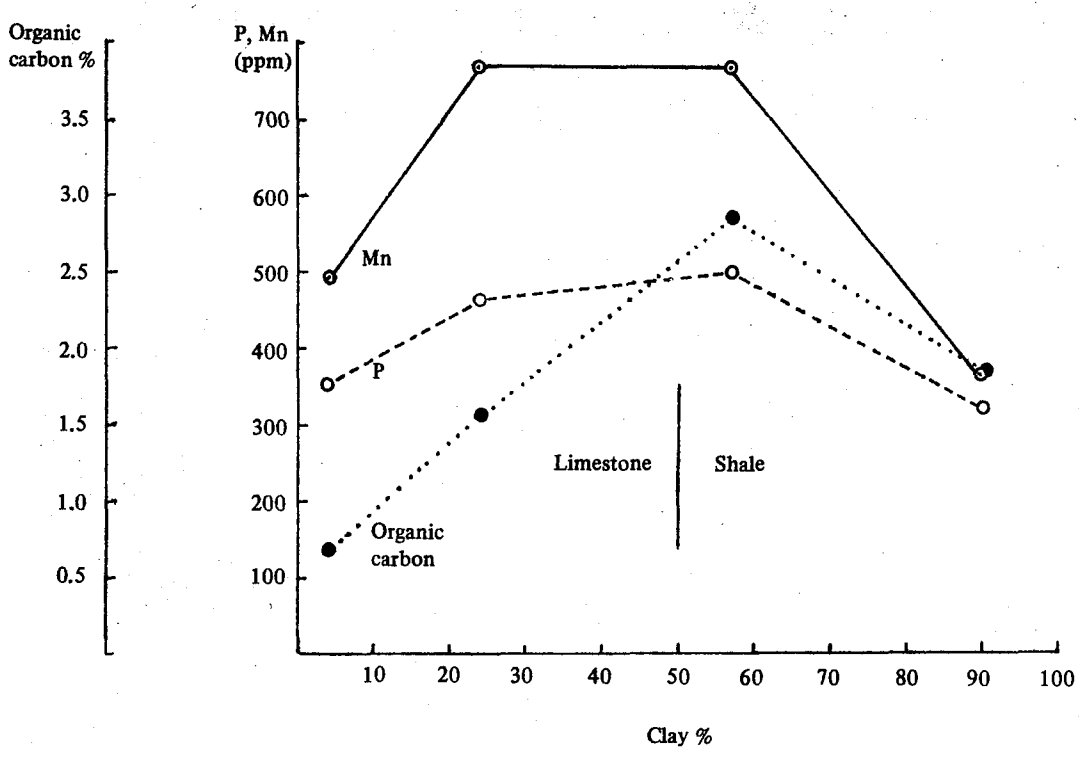

Fig. 105. Behaviour of organic carbon, P and Mn in the middle Purbeck rocks. Notice the inverse relation with the clay.

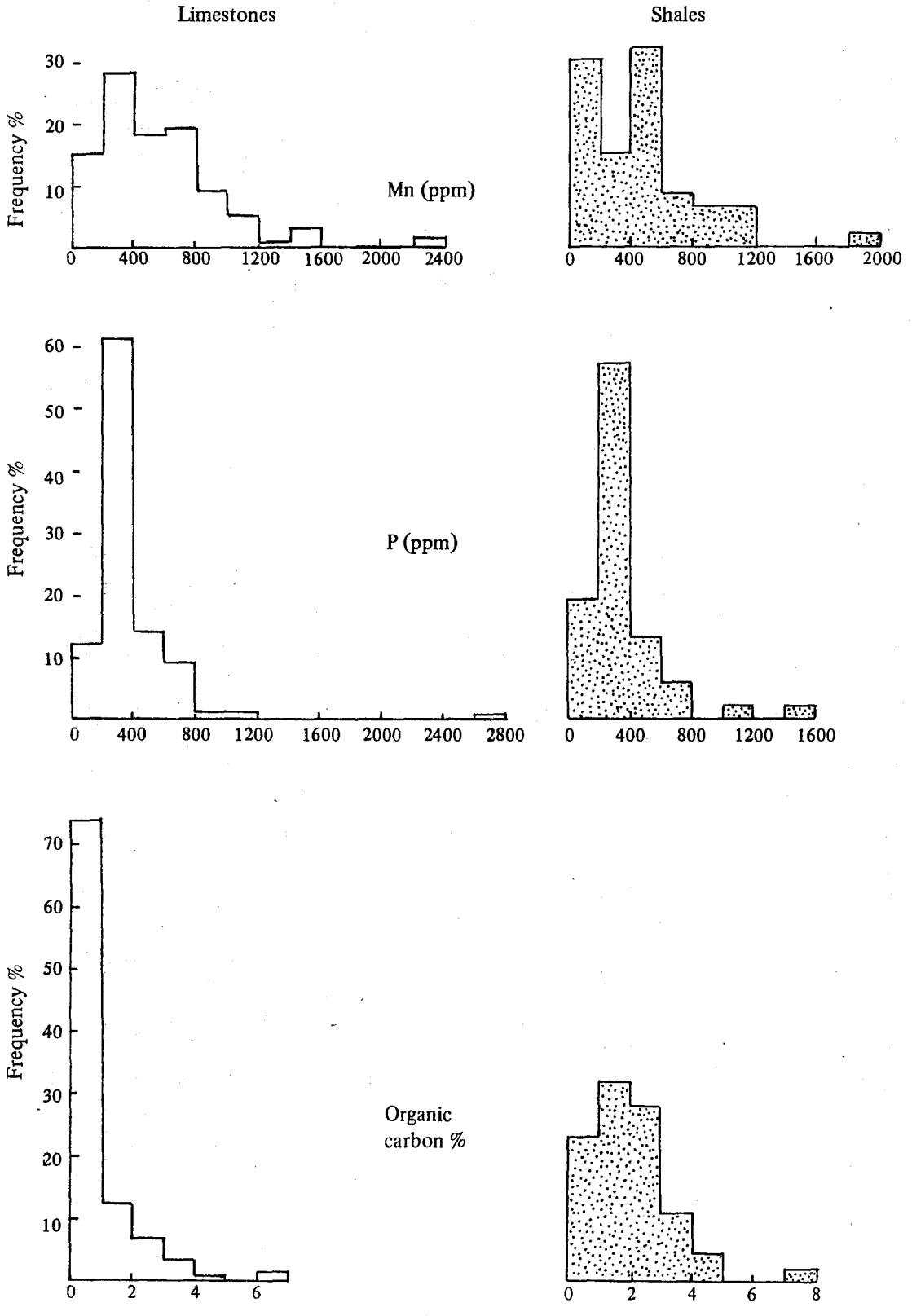

Fig. 106 Distribution of Mn, P and organic carbon

Table 57. Abundance of Mn (ppm) in shales and carbonates

	shales		carbonates	
	Mn	Mn/Fe[1]	Mn	Mn/Fe[1]
Rankama and Sahama (1950)	620	0.013	385	0.096
Turekian and Wedepohl (1961)	850	0.019	1100	0.289
Horn and Adams (1966)	575	0.015	842	0.103
Ronov and Migdisov (1971) (Russian platform)	527	0.012	310	0.035
Present work	459	0.011	555	0.098

[1] Calculated by the present author

(Table 57). When the calcareous shale samples are excluded, the average becomes 314 ppm Mn. This value is much lower than the average Mn content for shales.

Clay minerals very considerably in their Mn contents. Deer *et al.*, (1962a) gave the average Mn contents of clay minerals as follows: 2550 ppm for chlorite, 1700 ppm for vermiculite, 770 ppm for montmorillonite and illite. No Mn is present in kaolinite. The 'pure' shales in the middle Purbeck contain about 25% montmorillonite and mixed-layer clay minerals, 45% illite and 9% kaolinite while the carbonate content is less than 4%. According to the data of Deer *et al.*, (1962a), the 'pure' shales of the middle Purbeck may contain about 550 ppm Mn. This calculated Mn value is about 200 ppm Mn higher than the average value in the 'pure' shales (Table 56). Again, this suggests that the middle Purbeck clays are depleted in their Mn content.

The general rule is that Mn (and Fe) goes into solution at low redox potentials and precipitates at higher ones. The lowest stages of oxidation gives the most mobile ions while the highest stages are connected with fixation of Mn. Another important factor in the oxidation and reduction of Mn compounds is the acidity of the aqueous solutions

involved. Combination of low redox potentials and acid solutions usually results in leaching of appreciable amounts of Mn mainly as $Mn(HCO_3)_2$ (Rankama and Sahama, 1950). Reducing conditions are likely to have been operative during the deposition of the Purbeck clays particularly below the sediment-water interface, in the presence of organic matter. In such conditions leaching of Mn would have occurred at the time of deposition. This would account for the depletion of Mn in the Purbeck clays. It is difficult to locate the sites at which Mn was fixed. The calcareous shales, which contain much higher Mn in comparison with the 'pure' shales (Table 56), may be fixation sites. Additional Mn may have been leached when Zn, Ni and Fe were mobilised at a late stage of diagenesis (see Chapter 11). Mn was probably also mobilised.

Mn/Fe ratios of the shales are much lower than those of the limestones (Table 58). This indicates geochemical separation of Mn relative to iron in the carbonate in comparison with the clays. In the shales, Mn/Fe ratios show negative correlations with both quartz contents and quartz/organic carbon ratios (Fig. 107). This suggests an inverse relationship with the sedimentation rates.

Table 58. **Mn/Fe ratios of the middle Purbeck rocks**

	Mn/Fe
'Pure' limestones	0.120
Argillaceous limestones	0.051
Calcareous shales	0.024
'Pure' shales	0.007

Mn shows sympathetic variations with organic carbon, P, Sr, As and CO_2. On the other hand, the negative correlation between Mn and the clay contents results in a negative

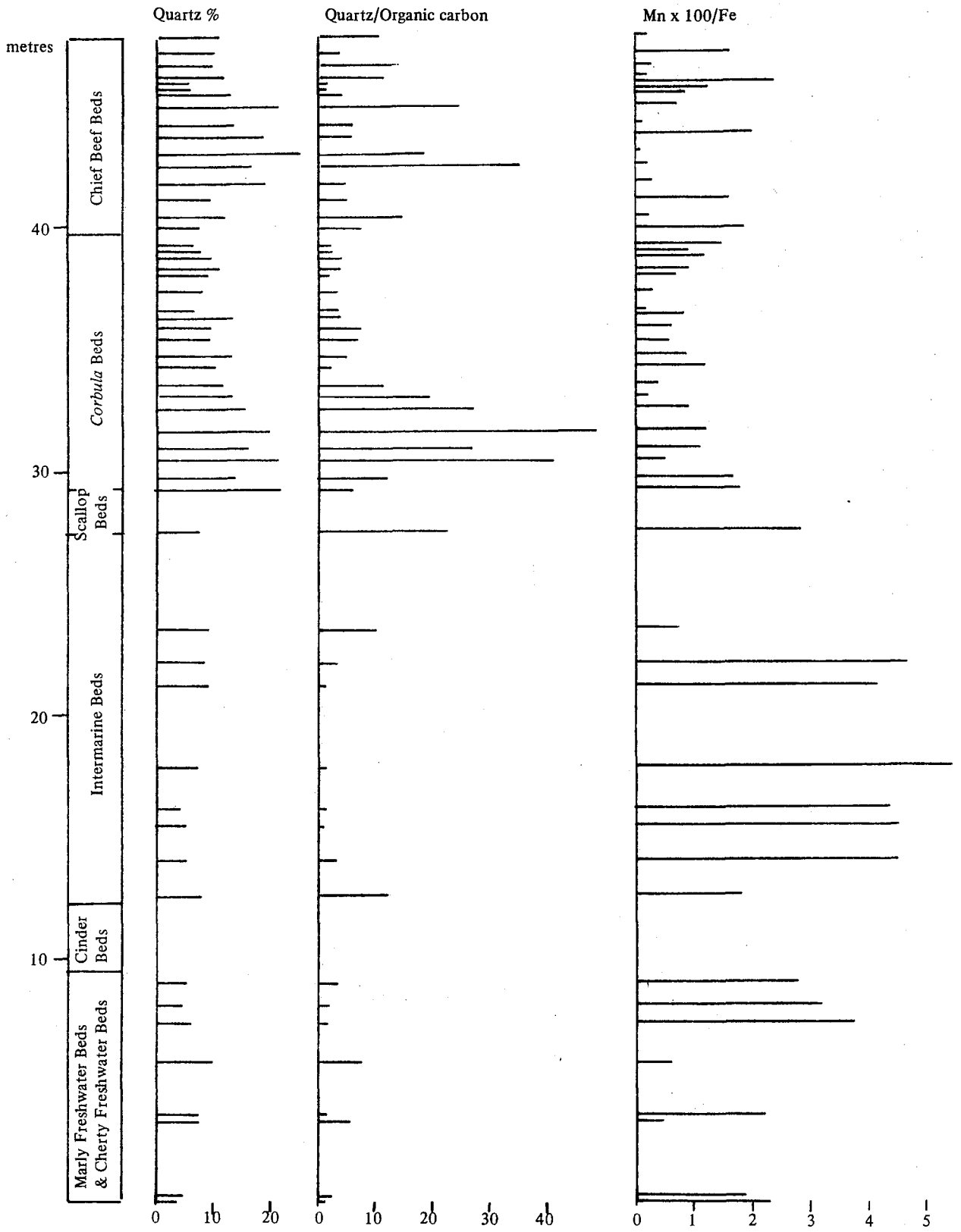

Fig. 107 Vertical variation of quartz, quartz/organic carbon ratio and Mn/Fe ratio (for middle Purbeck shales)

correlation between Mn and most of the elements associated with the clays. Such behaviour indicates that important amounts of Mn in the middle Purbeck shales are associated with the non-detrital fraction particularly the carbonates.

(b) In the limestones

The manganese content of the middle Purbeck limestones ranges from 22–2291 ppm (Fig. 106). The average Mn value is 555 ppm which falls in the range of Mn averages in carbonate rocks (Table 57). The relatively high Mn content of the argillaceous limestones (Table 56) in comparison with the 'pure' limestones suggests a sympathetic variation with the clay fraction. The association of Mn with the insoluble residue and presumably with the clays has been reported in carbonate rocks by many authors (Goldberg and Arrhenius, 1958; Migdisov, 1960; Weber, 1964; Veizer and Demovic, 1973 and others). Mn behaviour in the middle Purbeck limestones suggests some complications and not only a simple correlation with the clays.

Mn behaviour in the present limestones is better understood if one considers the stratigraphic distribution of Mn through the middle Purbeck sequence (Fig. 108). Low Mn contents are mainly confined to the limestones with abundant bivalve fragments. On the other hand, high Mn values are commonly found in the micritic limestones (the limestones of the Cinder Beds are exceptional). Such abrupt change in Mn contents with sharp change in lithology can be explained in terms of original mineralogy i.e. aragonite versus calcite. The volumetric importance of aragonite in the middle Purbeck bivalves has been emphasised before in the petrographic study. On the other hand, most of the micrites in the middle Purbeck have accumulated originally as calcite[1].

[1] There is no direct evidence available on the mineralogic composition of the original carbonate mud of the present rocks. Mineralogically, the primary carbonate mud would be high Mg-calcite and/or aragonite in the marine environment and low Mg-calcite in the non-marine environment (Friedman, 1968; Folk, 1974). According to palaeontology, the salinity in the middle Purbeck environments varied between brackish and freshwater with occasional 'marine' phases. It is reasonable, therefore, to assume that appreciable quantities of the carbonate mud in the present rocks were precipitated originally as low Mg-calcite.

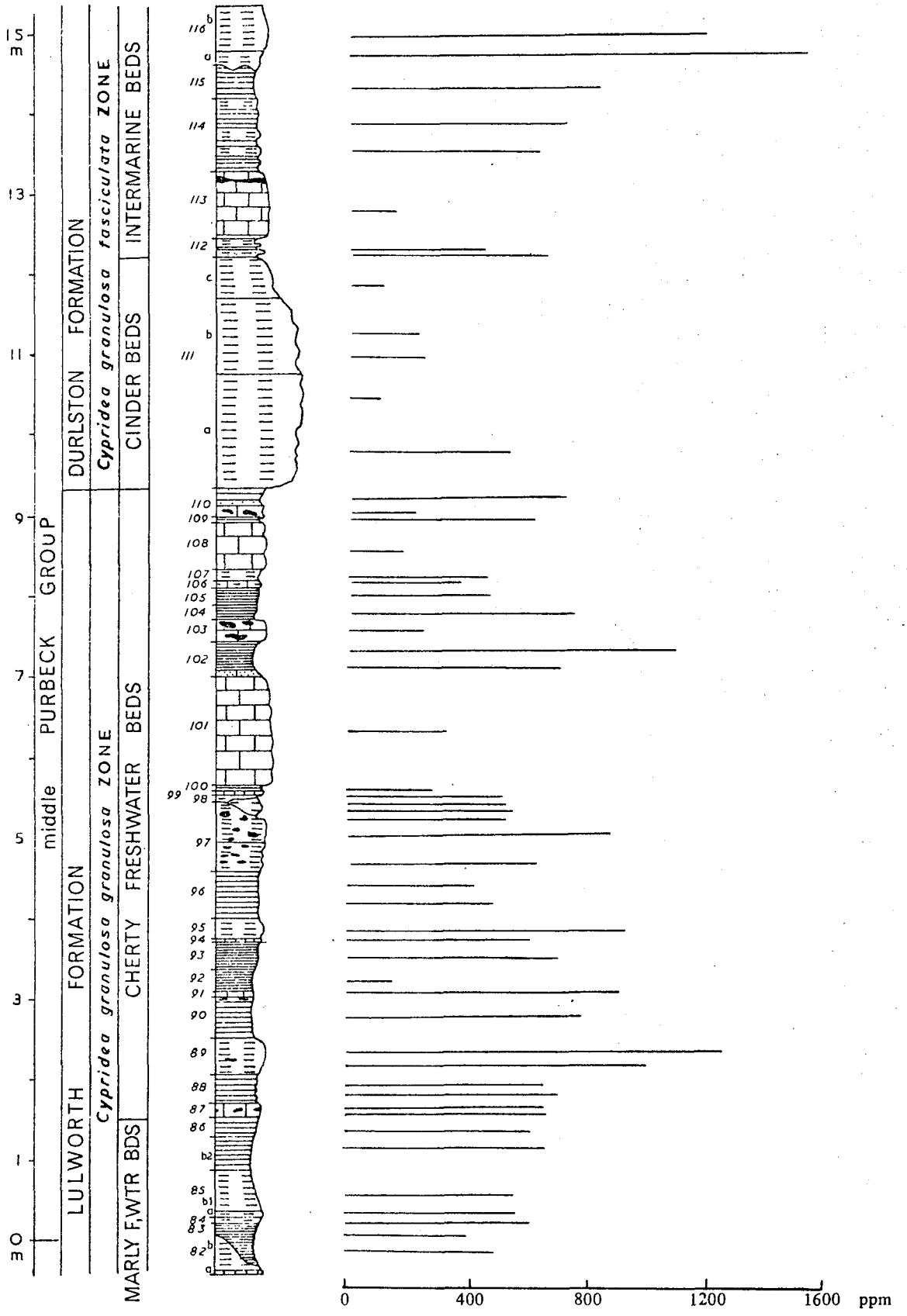

Fig. 108 Stratigraphic distribution of manganese content in the middle Purbeck Group of Durlston Bay (Key on Fig. 15).

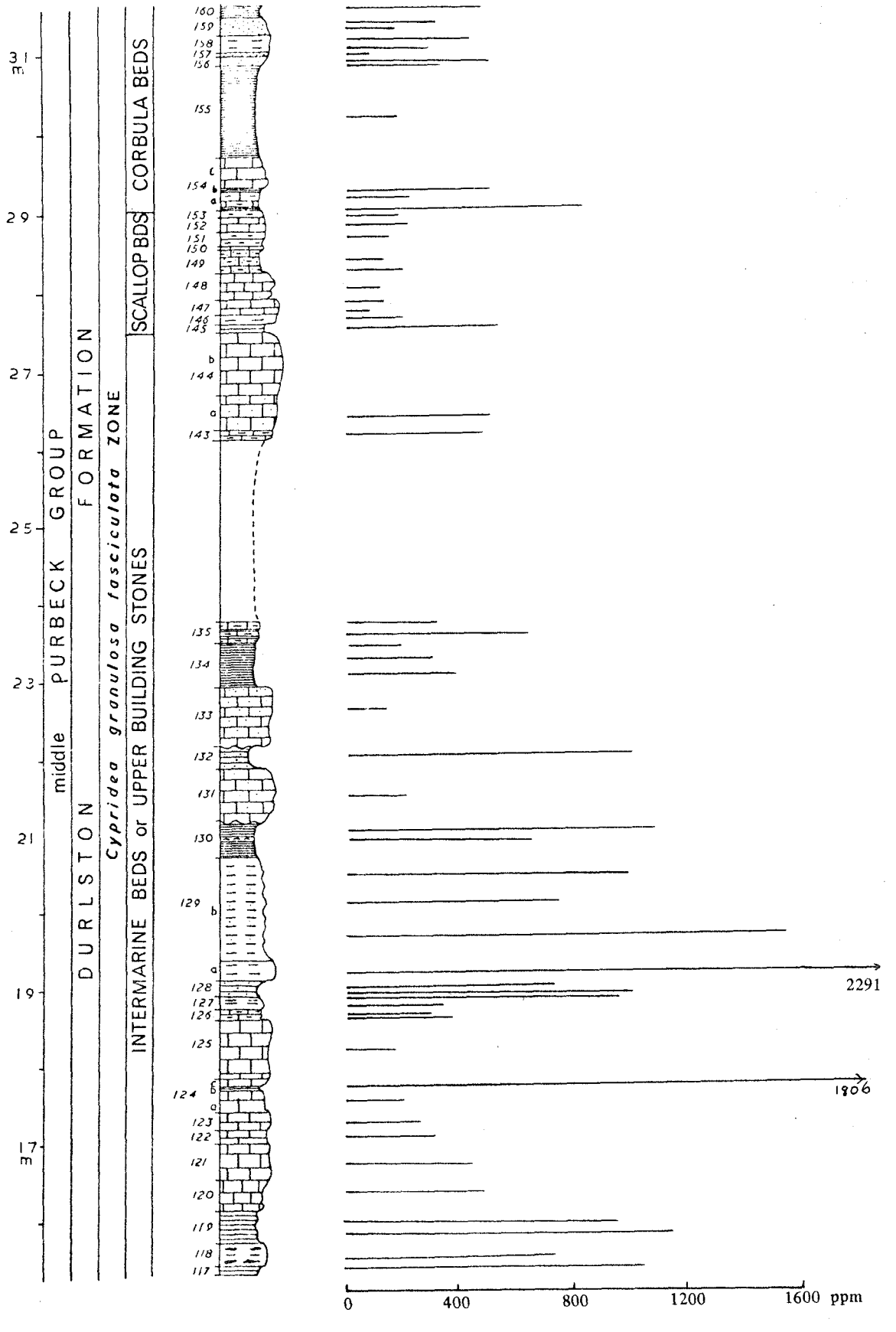

Fig. 108 (continued)

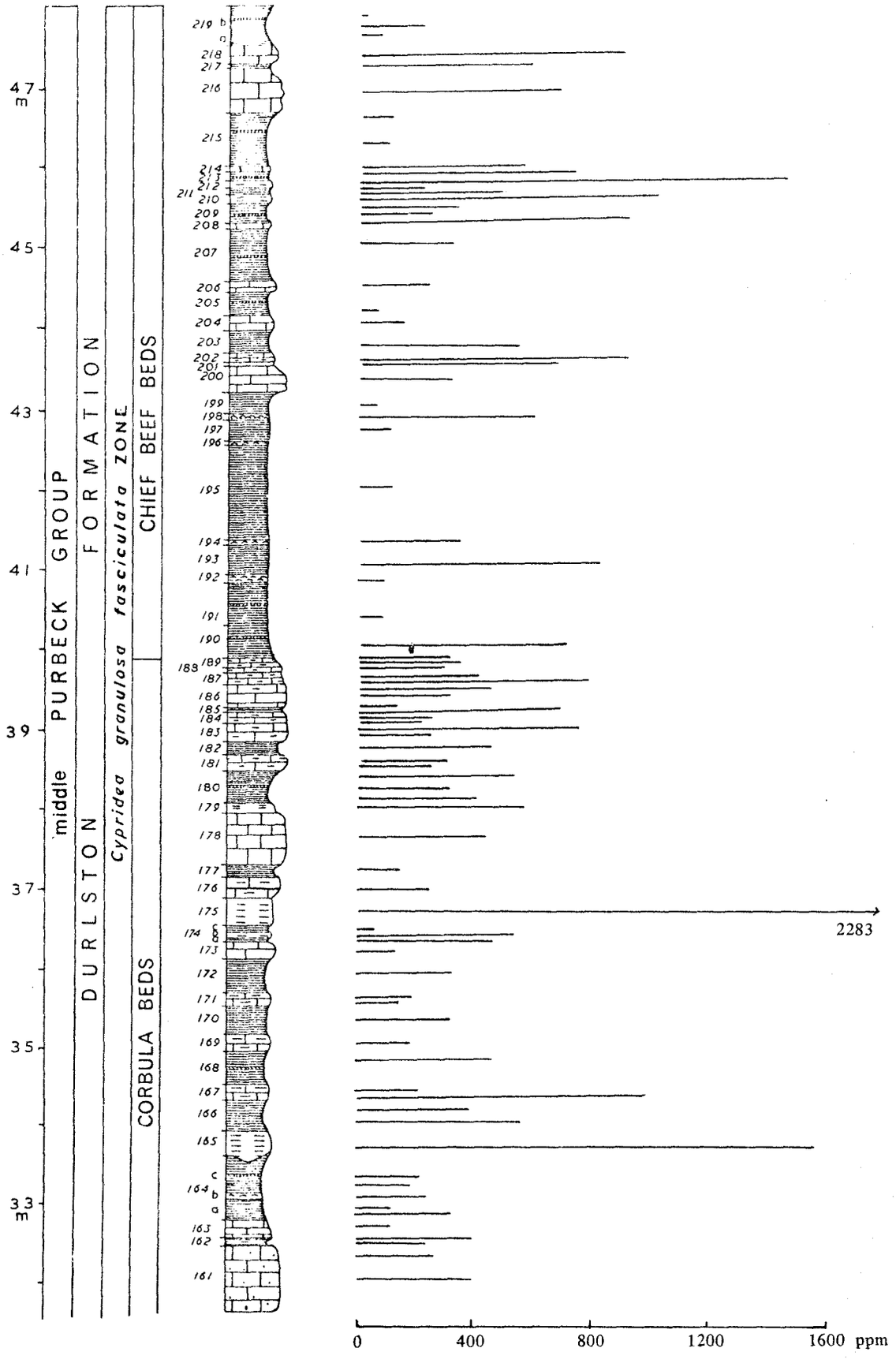

Fig. 108 continued.

In the calcite structure, Mn can substitute appreciably for Ca (natural Mn-rich calcite contains up to several percent $MnCO_3$ according to the data of Deer *et al.*, 1962b). On the other hand, much less Mn can substitute for Ca in the aragonite structure (Deer *et al.*, 1962b).

From the foregoing, it seems that the present Mn levels in the middle Purbeck limestones are good measures of the original carbonate mineralogy. If this is the case, then diagenesis had little effect on modifying the original Mn behaviour. Bencini and Turi (1974) while studying some Mesozoic carbonate rocks from Northern Apennines found that the original Mn content does not appear to have undergone serious changes during diagenesis especially during aragonite-calcite inversion.

It has been emphasised before that the 'micritic' limestones are generally higher in their Mn contents in comparison with the bivalve limestones. Although this was explained in terms of the original carbonate mineralogy (aragonite versus calcite), such differences in Mn contents may be related to different rates of Mn supply during the time of deposition. The 'micritic' limestones usually contain higher clay contents than the 'clean' bivalve limestones (see petrography). If the influx of clays was climatically controlled (humid versus arid conditions), this may explain Mn fluctuations. Under humid[1] conditions, the transporting medium is rich in organic acids and permits Mn to stay in solutions until it reaches the depositional environment (Wolf *et al.*, 1967).

Although the micritic limestones in the middle Purbeck contain up to 2300 ppm Mn, the Cinder Beds only contain 242 ppm Mn on average. If one sample with

---

[1] Humidity and aridity are used here in relative sense and do not imply geographic belts.

549 ppm Mn is excluded, the average becomes 170 ppm Mn. The Cinder Beds mostly consist of oyster fragments (*Liostrea distorta*) and a matrix of fine grained carbonate mud. Generally the oyster contents in the Cinder Beds are less than 40% of the rock volume. This may contain about 20–40 ppm Mn according to the data of Mn contents in the modern oyster *Crassostrea virginica* (Friedman, 1969). The remainder of Mn content in the Cinder Beds ranges from 130–150 ppm and is mainly present in the micrite fraction which usually exceeds 50% of the rock volume. Such low Mn content suggests that the micrites of the Cinder Beds are depleted in their Mn contents. If these micrites accumulated originally as aragonite then Mn deficiency is easily explained considering that much less Mn can substitute for Ca in the aragonite structure (Deer *et al.*, 1962b). However, there is no direct evidence available to confirm this possibility. On the other hand, the possibility of a limited Mn supply at the time of deposition cannot be ruled out.

2. **Phosphorus**

In the middle Purbeck, phosphorus content ranges from 160–2613 ppm in the limestones while in the shales it varies between 70 ppm and 1405 ppm (Fig. 106). Average phosphorus content in the middle Purbeck limestones and shales is 372 ppm and 335 ppm respectively. Table 59 suggests that there is no consistent average for phosphorus in sedimentary rocks particularly in the carbonates. This makes it difficult to compare phosphorus values in the middle Purbeck rocks with the published data. In this respect comparison could be biased or misleading. Nevertheless, the average phosphorus content of the middle Purbeck shales is lower than the quoted values for shales (Table 59). The middle Purbeck limestones are also depleted in their phosphorus content considering the local occurrences of vertebrate bones. However the presence of small phosphate nodules near the horizons rich in bone fragments suggests processes of leaching and precipitation.

Probably the middle Purbeck rocks lost some of their original phosphorus content due to diagenetic modifications.

Table 59. Abundance of phosphorus (ppm) in carbonates and shales

	Carbonates	Shales
Rankama and Sahama (1950)	175	740
Green (1959)	1100	770
Turekian and Wedepohl (1961)	400	700
Horn and Adams (1966)	281	733
Ronov and Migdisov		
a. Russian platform	240	471
b. N. American platform	659	419
Present work	372	335

Geologic systems characterised by enrichment in organic carbon are also enriched in their phosphorus contents (Wolf *et al.*, 1967). Ronov and Korizina (1960) in their study of phosphorus distribution in the Russian platform sediments found a strong positive correlation between phosphorus and organic carbon. In the middle Purbeck rocks, phosphorus has insignificant positive correlation with organic carbon. Lack of a strong correlation suggests that the original phosphorus contents were modified probably by processes of leaching.

It has been mentioned before that the hybrid rocks (argillaceous limestones and calcareous shales) have higher phosphorus content in comparison with the 'pure' rocks (Table 56). This also explains why phosphorus correlates positively with the clay content of the limestones and negatively with the clay content of the shales (Fig. 105). Such 'amphoteric' behaviour of phosphorus in the middle Purbeck rocks is difficult to explain. If this behaviour was inherited from the original sediments, then why do the hybrid rocks contain more phosphorus than with the 'pure' rocks? The high contents of organic matter in the calcareous shales and argillaceous limestones may explain

why the hybrid rocks contain more phosphorus since organic carbon and phosphorus are geochemically related (Orr, 1974). Although the occurrence of phosphate nodules suggests processes of local leaching and precipitation, it is difficult to envisage a mechanism by which diagenetic solutions can lead to selective enrichment.

3. Organic carbon[1]

Organic matter in the middle Purbeck limestones ranges from 0.04–6.99% while in the shales it varies between 0.48% and 7.46%. The distribution of organic matter in the middle Purbeck sediments is a lognormal one as indicated from the skewness values i.e. SK = 1.72 and 2.90 for limestones and shales respectively. After log-transformation, these values decrease to −0.03 for limestones and −0.18 for shales. In the middle Purbeck, more than 75% of the shale samples contain more than 1% organic matter whereas about 75% of the limestones are below this value (Fig. 106). This agrees well with the distribution of organic matter in sedimentary rocks (Hunt, 1961). Average contents of organic matter in the middle Purbeck limestones and shales are 0.92% and 1.99% respectively. These values are generally higher than the average contents of organic matter in limestones and shales reported by various authors (Table 60).

Organic matter and pyrite can be closely related if reducing conditions are maintained. In the Purbeck limestones, organic matter correlates positively

---

[1] Organic carbon refers to carbon present in chemical structures that may be traced back to biological activity. Carbon dioxide and graphite are not usually included because the inherited undertainty in assigning them to organic or inorganic origin although they may represent end members of organic carbon cycle (Welte, 1970).

The amount of organic carbon, in percent, is usually multiplied by a conversion factor to approximate the amount of total organic matter in the rock. The organic factor takes into account the type of organic material and the contents of its O, N, S and H. Conversion factors range from 1.07 to 1.40. The factor of 1.22 is widely quoted. It was determined by Forsman and Hunt (1958) from elemental analyses of twenty one organic residues. In the present study, the analytical organic carbon was considered equal to the amount of organic matter and no conversion factor was used. This decision had to be taken to compensate for any reduced phases which may increase the content of the analytical organic carbon (see Chapter 6).

Table 60. Abundance of organic matter (%) in carbonates and shales

	Carbonates	Shales
Green (1959)	0.20	0.62
Hunt (1961)	0.29	2.10
Geham (1962)	0.24	1.14
Ronov and Migdisov (1971)		
a. Russian platform	0.30	0.74
b. N. American platform	0.43	
Present work	0.92	1.99

with S and Fe (r = 0.49 for both) which indicates a sympathetic variation between organic matter and pyrite. Such close relation was not observed in the middle Purbeck shales possibly due to the effect of weathering.

Organic matter in the middle Purbeck limestones correlates positively with the clay contents. The opposite behaviour was observed in the Purbeck shales where organic matter shows a negative correlation with the clay contents. Such 'amphoteric' behaviour is due to the high contents of organic matter in the argillaceous limestones and calcareous shales (Table 56 and Fig. 105). Because organic carbon content in ancient limestones is commonly lower than that of ancient shales (Hunt, 1961), argillaceous limestones have higher contents of organic matter in comparison with the 'pure' limestones.

The organic matter in the middle Purbeck shales increases with the increase of the carbonate content. Such behaviour is puzzling considering that shales contain more organic matter than limestones. The probable explanation is that the production of organic matter was greater in the calcareous shales than in the 'pure' shales. Alternatively, one can argue that the content of organic matter is a function of grain

size. The low quartz content of the calcareous shales in comparison with the 'pure' shales (Table 56) suggests some differences in grain size. Furthermore, the stratigraphic distribution of organic matter in the middle Purbeck shales indicates that periods characterised by influx of detrital quartz are usually depleted in their organic content (Fig. 109).

Generally, the amount of organic carbon depends upon the climate and oxidising conditions in the environment of deposition. Systems such as the Carboniferous and Jurassic are known to be rich in organic matter whereas the Permo-Triassic is relatively poor (Hoefs, 1969). The Purbeck, however, represents a very short span in comparison with the main geologic periods such as Carboniferous and Jurassic etc., and this makes the comparison between the organic content in the Purbeck and that of the large units of limited significance. Nevertheless, the contents of organic matter in the middle Purbeck shales and limestones (0.92% and 1.99% respectively) are higher than the contents of organic matter in most of the geologic periods characterised by large organic productivity (see table 6 K-2 in Hoefs, 1969).

Originally, the Purbeck carbonates contained much higher organic matter for the following reasons. Recent carbonates usually contain higher organic matter than ancient carbonates whereas ancient shales are slightly higher in organic matter than the recent clays (Hunt, 1961). Geham (1962) suggested that carbonates lose more organic matter than do shales due to repeated exposures to meteoric waters. This was observed in the present work. The Purbeck carbonates which show the minimum diagenetic modifications, such as the layers of perished bivalves, contain much higher organic matter than the other Purbeck carbonates which were lithified under subaerial conditions.

The high organic matter in the Purbeck sediments has been observed before by

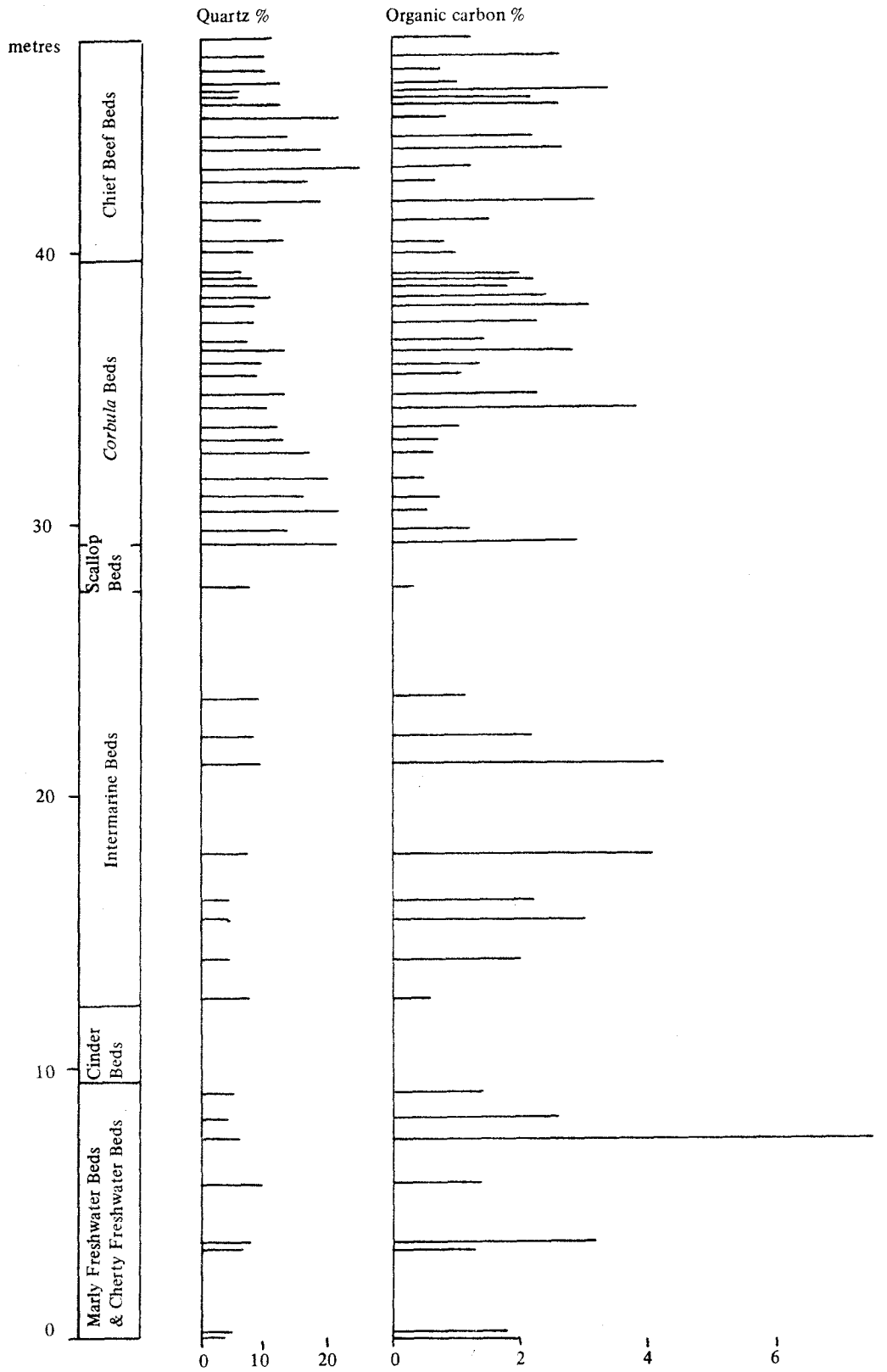

Fig. 109. Vertical variation of quartz and organic carbon contents (for middle Purbeck shales)

Strahan (1898). 'Impressive oil indications' in the Dorset coast were reported by Lees and Cox (1937). They suggested that some of the oil and bitumen are indigenous to the Purbeck sediments. On the other hand, they did not rule out the possibility of oil seepage by upward migration from the underlying Kimmeridge Clay although the sulphur content of the Purbeck residue is much lower than the Kimmeridge oil. The occurrence of bituminous limestones in the upper Purbeck Group at Peveril Point (intensively faulted and folded) could indicate local migration. However, most of the organic matter-rich horizons in the middle Purbeck Group are not affected by important fractures or faults. The low organic matter in the Portland Group (Lees and Cox, 1937) is a further evidence against important oil seepage from the underlying Kimmeridge Clay. To summarise, it seems that the bulk of the Purbeck 'oil' was generated from organic matter which was originally associated with the Purbeck sediments.

15. STRONTIUM IN THE MIDDLE PURBECK ROCKS

1. In the shales

In the present shales, Sr ranges from 127–1610 ppm (see Table 41 and Fig. 110). The average value is 462 ppm Sr which is generally above the Sr averages for shales reported by different authors (Table 61). This is mainly attributed to the high carbonate content in the middle Purbeck shales (see Table 27). When the calcareous shale samples are excluded, the average becomes 312 ppm Sr. This value agrees well with most of the Sr averages for shales. The Sr to Ca atomic ratio (expressed as Sr x 1000/Ca which is most familiar to geologists and geochemists, abbreviated: Sr/Ca ratio) indicates that shales are generally characterised by high ratios in comparison with the carbonates. This is mainly attributed to the low Ca content in shales.

Table 61. Abundance of Sr (ppm) in shales and carbonates

	Shales		Carbonates	
	Sr	Sr/Ca[1]	Sr	Sr/Ca[1]
Rankama and Sahama (1950)	170	3.49	425–765	0.64–1.15
Green (1959)	299	2.63	480	0.81
Turekian and Wedepohl (1961)	300	6.21	610	0.92
Horn and Adams	290	5.90	617	1.04
Present work	462	6.34	897	1.37

[1] Calculated by the present author

Strontium shows a significant negative correlation with Al ($r = -0.74$). The strong positive correlation with CO_2 ($r = 0.59$) suggests that Sr is incorporated with Ca in the carbonate phase. The plot of Sr against CO_2 suggests that about 250 ppm Sr is not accommodated in the carbonate. The location of this Sr quantity is difficult to explain. Small amounts of celestite may be present although the mineral was not

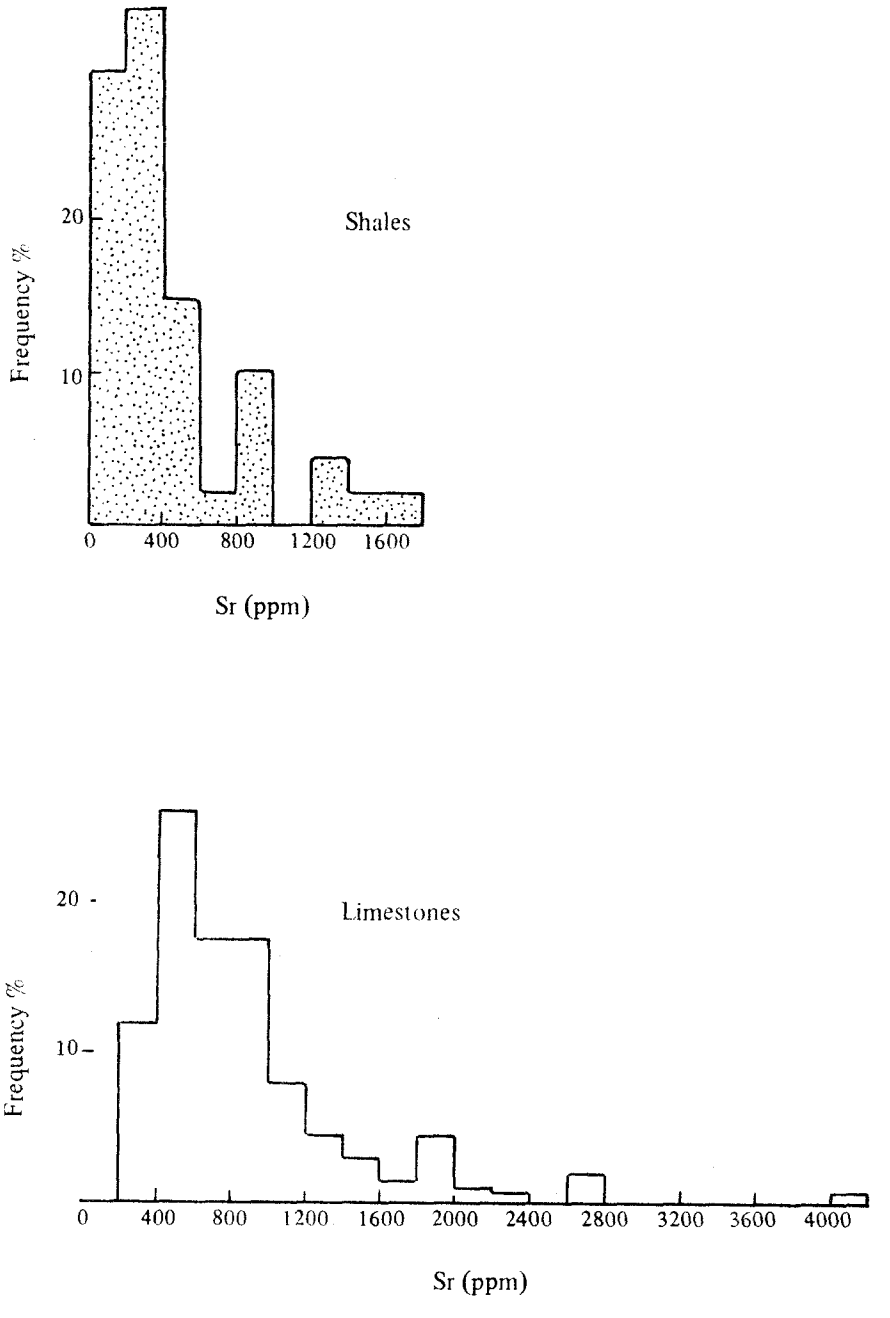

Fig. 110. Distribution of strontium in the middle Purbeck rocks

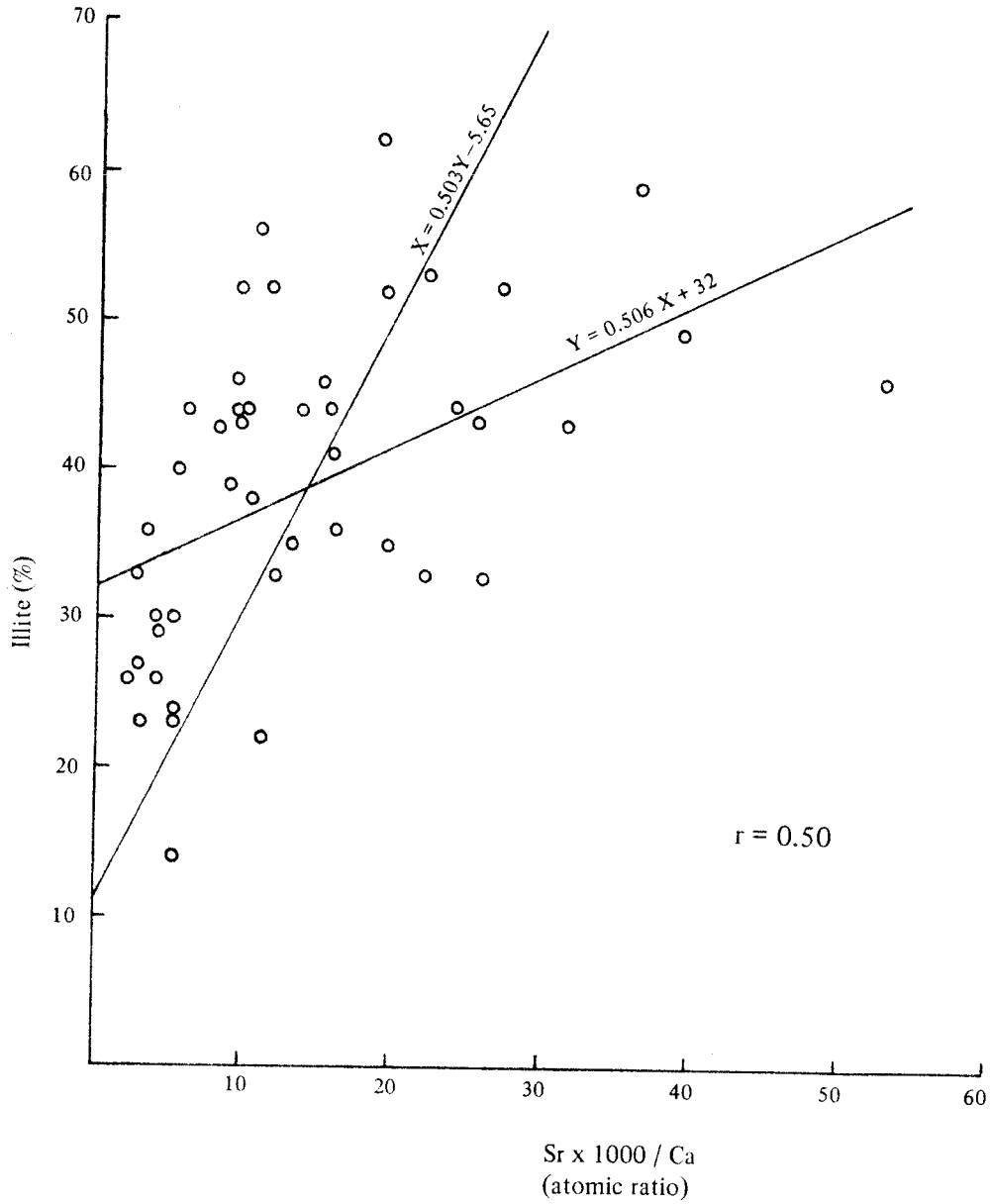

Fig. 111. Variation in the Sr/Ca ratio with illite content (for middle Purbeck shales)

detected. Strontium is known to substitute for K, Ca and Ba (Goldschmidt, 1954). The possibility of some Sr substituting for Ba is excluded since both elements correlate negatively. The relation between Sr and K is not visible since Sr is heavily loaded on the carbonate. When the calcareous samples were excluded, Sr relation with K became visible. So it appears that some Sr is replacing K in the interlayer of illite and illite/montmorillonite mixed layers.

The Sr/Ca ratio correlates positively with the clay ($r = 0.59$) and negatively with the carbonate ($r = -0.6$). The ratio is, therefore, a reflection of lithology i.e. carbonate versus clay. Since illite constitutes the greatest proportion of all clay minerals present in the middle Purbeck shales, the Sr/Ca ratio shows a positive correlation with illite content (Fig. 111).

2. In the limestones[1]

(a) General

It should be emphasised that the majority of ancient limestones contain less than

---

[1] Most investigations dealing with trace elements in carbonates are concerned with Sr; consequently a considerable amount of information is available concerning this element especially in Quaternary carbonate sediments and skeletons. A review of the extensive data available would be above the scope of this work. Nevertheless, it is relevant to consider some of the basic factors affecting Sr distribution in carbonates.

Recent carbonates are composed mainly of aragonite and/or calcite. The aragonite structure permits the incorporation of considerable amounts of Sr. As is known, strontianite also crystallises with the aragonite structure. On the other hand, Sr does not appear to substitute appreciably for Ca in the calcite structure.

The biochemistry of Sr in skeletal carbonates have been reviewed by Wolf *et al.*, (1967). They stated that Sr/Ca ratio in organisms primarily depend upon

1) the Sr/Ca ratio in the water medium;
2) salinity;
3) phylogenic factors;
4) temperature; and
5) crystal structure (polymorphism).

Strontium contents of inorganically formed carbonates can be interpreted in terms of Sr/Ca ratio of the precipitating solutions and temperature of precipitation (Kinsman, 1969; Kinsman and Holland, 1969). The relation between Sr/Ca ratio of the precipitating carbonate and Sr/Ca of the medium can be explained according to the following equation:

$$(Sr/Ca)_{solid} = K \times (Sr/Ca)_{liquid}$$

where K is the Sr partition coefficient. For calcite precipitating at 25°C, $K = 0.14 \pm 0.02$; for aragonite at 25°C, $K = 1.0 \pm 0.04$ (Kinsman and Holland, 1969).

Maximum loss of Sr occurs during early diagenesis before major cementation where aragonite changes into calcite (Kohle, 1965). The released Sr is usually present in the form of bicarbonate or chloride. The bulk of the released Sr to solution migrates into the sea; small amounts might precipitate as $SrSO_4$ (Rankama and Sahama, 1950).

500 ppm Sr (Kulp *et al.*, 1952; Bauch, 1968; Bathurst, 1975 and many others.). The Sr average for the middle Purbeck limestones is about 900 ppm. This value is also higher than the reported averages for carbonates (Table 61). As seen from Fig. 110, about 50% of the present limestones contain more than 800 ppm Sr. Thus it seems necessary to discuss the reasons for the high Sr content in the middle Purbeck limestones.

It might seem probable that the high Sr content in the present limestones is due to the presence of traces of celestite. To check this possibility, 36 limestone samples (representing the whole population) were treated with dilute HCl; the acid-soluble Sr was determined by atomic adsorption. The plot of HCl-soluble Sr against whole-rock Sr indicates that a celestite contribution is very improbable in most cases (Fig. 112). The contribution from Sr-carbonate minerals can be ruled out. Calciostrontianite was only identified in two exceptional samples which do contain celestite.

Bauch (1965; 1968) claimed that Sr content of limestones can be related the clay content. Bauch explained the retention of Sr in the clays by adsorption processes after Sr was set free during aragonite-calcite transition and been trapped in the pore solutions. This was not observed in the present study since Sr correlates negatively with the clay content in both limestones and shales (Fig. 113).

From the foregoing, the high Sr content of the present limestones cannot be fully explained in terms of secondary enrichment or Sr retention on the clay fraction. Therefore, it seems reasonable to assume that the high Sr content of the middle Purbeck limestones was inherited from the original sediments.

The Sr rich carbonates can be subdivided broadly into two groups: carbonates rich in skeletal aragonite and the biomicrites. In the first group (friable bivalve limestone and layers of perished bivalves, see Table 40), the high Sr content is attributed to the

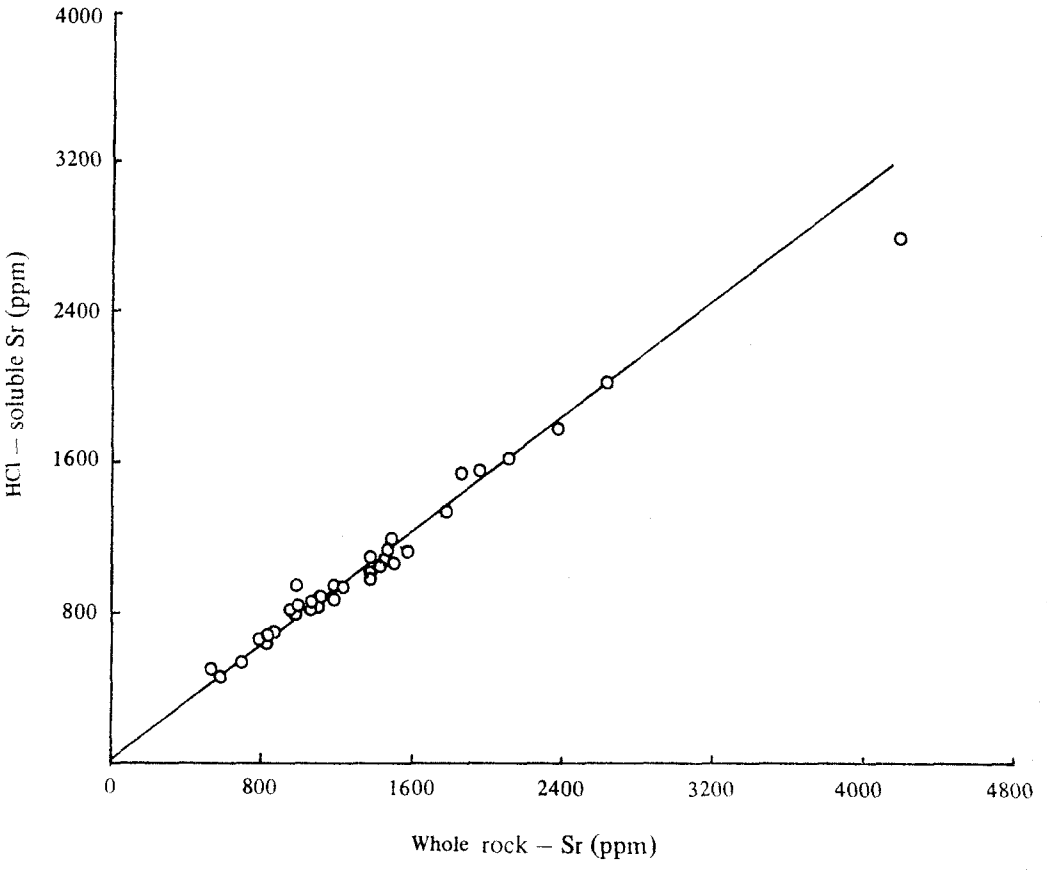

Fig. 112. A plot of whole rock – Sr against HCl – soluble Sr
(For middle Purbeck limestones)

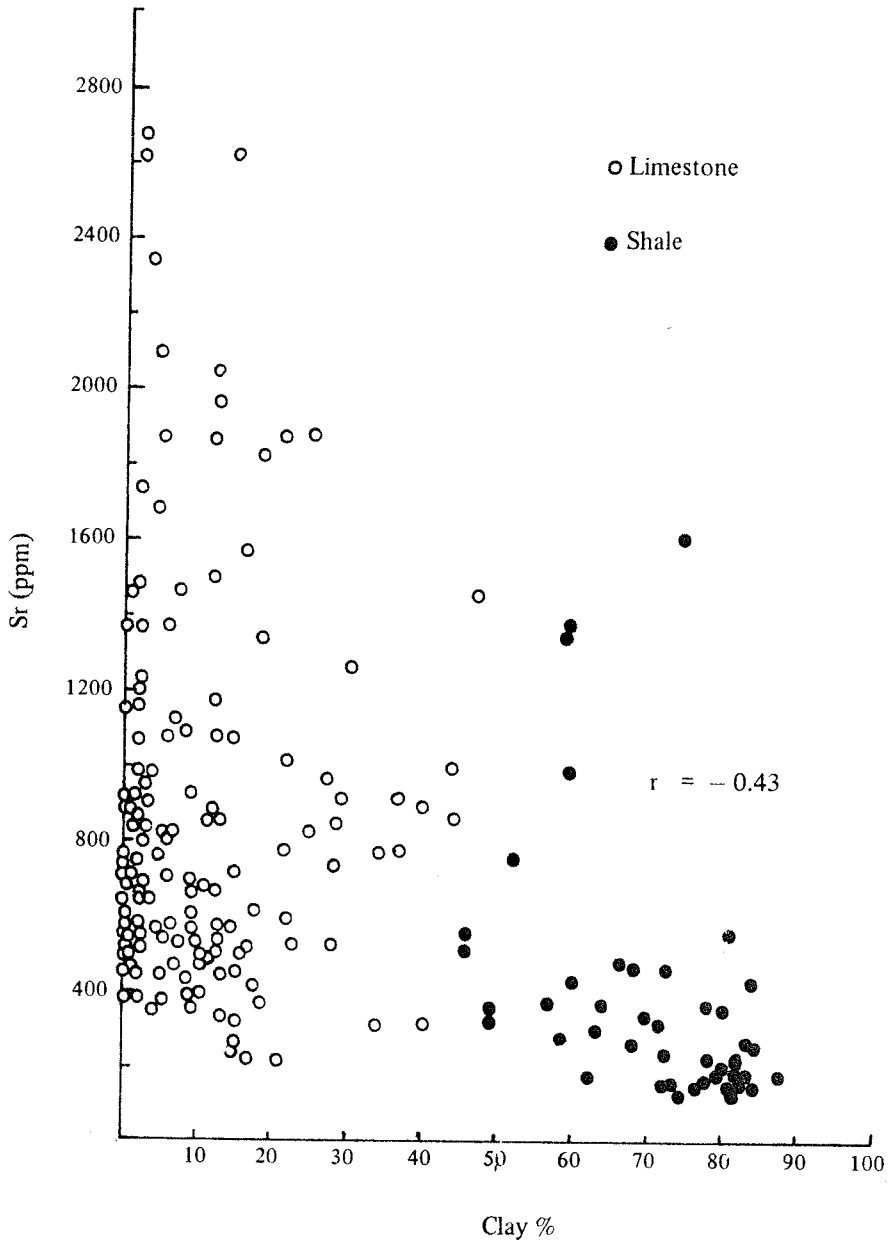

Fig. 113. The relation between Sr and clay content

conservation of aragonite. For example, in the layers of perished bivalves, Sr ranges from 1800–2670 ppm and averages 2200 ppm. These layers contain up to 75% skeletal aragonite. In contrast, the bivalve biosparrudites which represent a more advanced diagenetic stage, contain only 770 ppm Sr.

The carbonates of the second group (facies 1, 2 and 3 in Table 40), are dominated by micritic sediments which usually represent more than 50% of the rock volume. The average Sr values for the three facies is 1310, 1120 and 1000 ppm respectively, while aragonite is less than 3%. This suggests that Sr is mainly accommodated in the micrite fraction of these facies. But other limestones which consist essentially of micrite (facies 4 in Table 40), contain only 260 ppm Sr. Therefore, the high Sr content of facies 1, 2 & 3 indicates additional factors being involved in the retention of Sr in the calcite. Because such retention is confined to certain facies, Sr behaviour can be explained in terms of facies control.

(b) Facies control

The biomicrites always have high Sr content regardless of their stratigraphic position (below and above the Cinder Beds). On the other hand, most of the other facies which grade into or intercalate with the biomicrites have much lower Sr values. This suggests that modification during diagenesis cannot fully explain the high Sr content in these biomicrites. It is difficult to see how diagenesis could follow consistently, and in such detail, the facies boundaries. It appears, therefore, that Sr behaviour in some of the present limestones is facially controlled and most probably was inherited from the original sediments since the possibilities of secondary enrichment and Sr retention on the clay were improbable (see above).

Assuming that the above argument is correct, then the following suggestions

can be drawn.

1. Calcite was the main primary carbonate mud in the biomicrites (charophyte biomicrite, ostracod biomicrite and ostracod-gastropod biomicrite). If inorganic precipitation of aragonite had occurred in appreciable quantities, then maximum loss of Sr is to be expected during early diagenesis and before major cementation where aragonite changes into calcite (Kahle, 1965). In the present study, the value of 2500 ppm represents the quantity of Sr released due to skeletal aragonite-calcite transition. Therefore, it is difficult to explain the high Sr content in the biomicrites unless diagenesis was completed in a more or less closed system. But this is very improbable considering the high porosity of the biomicrites (up to 20%).

2. Provided that calcite was the main carbonate mud, then the high Sr concentrations in the biomicrites suggests high Sr/Ca ratios in the original medium of deposition[1]. Based on the present averages for Sr in these biomicrites, the Sr/Ca ratio in the depositional environment varied between 10 and 15 (using the Sr partition coefficient for calcite at 25°C given by Kinsman and Holland, 1969). The question of origin of these high Sr/Ca ratios which exceed those of river and marine waters (3.2 and 8.6 respectively; quoted in Kinsman, 1969), deserves a further thought[2].

(c) Sr-loss during diagenesis

The uncertainty in our knowledge of Sr behaviour during diagenesis is considerable especially in ancient carbonates. The following is an attempt to estimate the original

---

[1] According to palaeontology, most of these biomicrites have accumulated in lacustrine environments where salinity varied between brackish and freshwater. Desiccation cracks are the most common sedimentary feature observed in the biomicrites.

[2] Exceptionally high Sr/Ca ratios can occur in freshwater environments (c.f. Muller, 1968).

Sr content which might have occurred in the present limestones. Without starting with certain assumptions, it is very difficult to obtain an approximate value for Sr in the original sediments. These assumptions are given below:

1. The majority of the original sediments (which consisted of bioclastic debris and/or carbonate mud) had similar porosities.

2. Appreciable quantities of the original carbonate mud precipitated as calcite. Most of this calcite contained about 1000 ppm Sr (see facies control).

The average composition of the middle Purbeck carbonates was originally about 70% molluscan debris (other bioclastic fragments can be ignored) and about 30% carbonate mud. This estimate is based on bed thicknesses, carbonate content and abundance of micrite and molluscan debris. If we consider the Sr value of 2400 ppm in most molluscs (Bathurst, 1975), and the assumed Sr value of 1000 ppm for inorganic calcite, then the Sr content in the middle Purbeck carbonates was originally about 2000 ppm. Comparison with the present average of 900 ppm Sr then the net loss is about 1100 ppm Sr. This loss represents 55% of the original Sr value. If the average Sr content for the middle Purbeck limestones approached the average value for Jurassic rocks (260–330 ppm; quoted in Kahle, 1965), the net loss will be about 85%.

(d) Sr-porosity relation

The plot of porosity values against the Sr content of the middle Purbeck limestones is shown in Fig. 114. Two conclusions can be drawn:

1. There is no obvious relation between porosity and Sr values in most of the limestone samples which contain less than 5% skeletal aragonite. This is, however, the normal trend for most ancient limestones. In these rocks, both porosity and Sr are reduced to

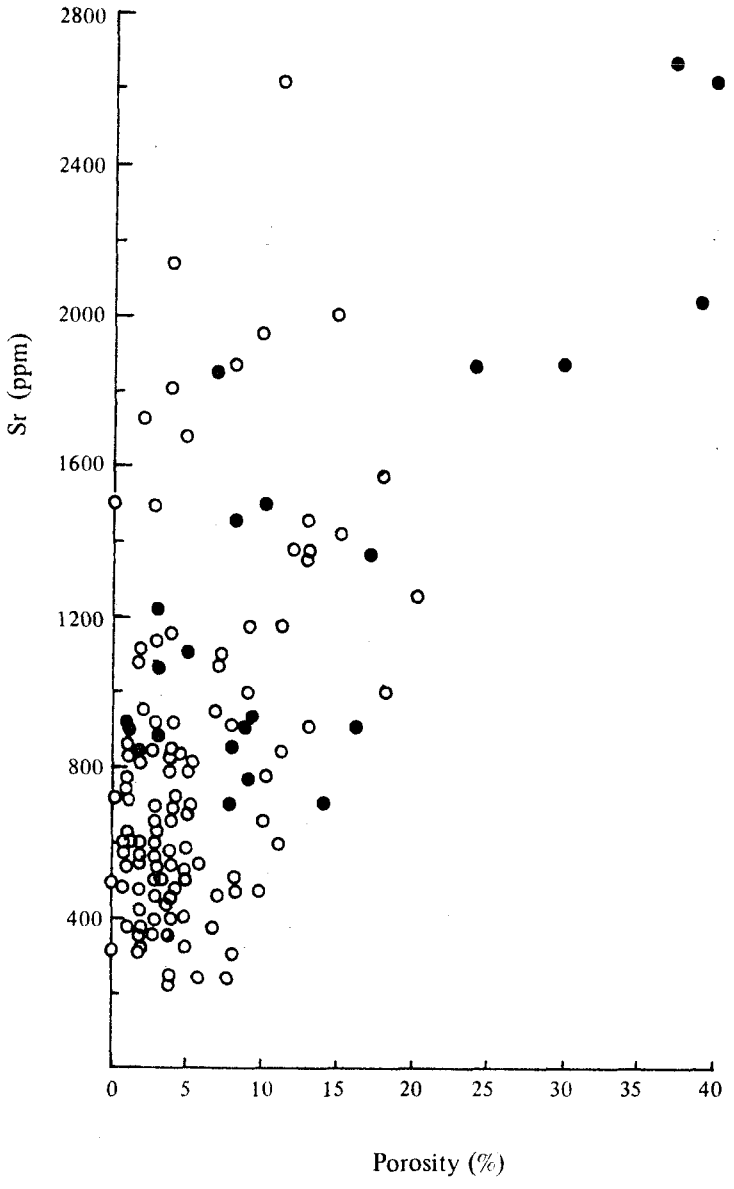

Fig. 114. A plot of Sr against porosity. The black dots represent samples which contain more than 5% aragonite (for middle Purbeck limestones)

base-levels[1].

2. Porosity shows a sympathetic variation with Sr in the carbonates which contain between 5 and 75% aragonite. The high porosity and Sr values for these carbonates are attributed to the conservation of aragonite. Such behaviour can be expected in Recent and Pleistocene carbonates since the reduction in porosity is accompanied by loss in Sr content. This suggests that some of the middle Purbeck carbonates have not yet reached the mature stage in carbonate diagenesis. The occurrence of carbonate bands with up to 40% porosity and up to 75% aragonite indicate that some of the Purbeck carbonates are still in the cementation stage.

(e) Sr in the 'beef'

The chemistry of fibrous calcite, known as beef, has some interest since it may reveal the nature of diagenetic fluids. As mentioned earlier, the majority of 'beef' layers occur at the top of carbonate layers which are rich in skeletal aragonite (layers of perished bivalves). This implies a connection between the growing calcite crystal in the 'beef' and aragonite dissolution.

In the present study, the Sr value of 2670 ppm was obtained in a layer of perished bivalves which contain about 75% aragonite. Therefore, Sr values up to 3560 ppm can be expected in pure skeletal aragonite. For simplicity assuming aragonite dissolution and calcite precipitation have occurred in a closed system, then the 'beef' crystal would contain between 420 and 560 ppm Sr during the early stages of growth. *(c.f.* Kinsman and Holland, 1969). Due to the low Sr uptake in the calcite, the Sr/Ca ratio in the

---

[1] Porosity of Recent carbonate mud and sand are normally 40–70%, but those of ancient carbonates are less than 5% (Bathurst, 1975). Also the Sr values of ancient limestones are generally less than 500 ppm while Recent carbonates contain up to 10000 ppm Sr (unpublished data on carbonate sands of the Egyptian Mediterranean coast).

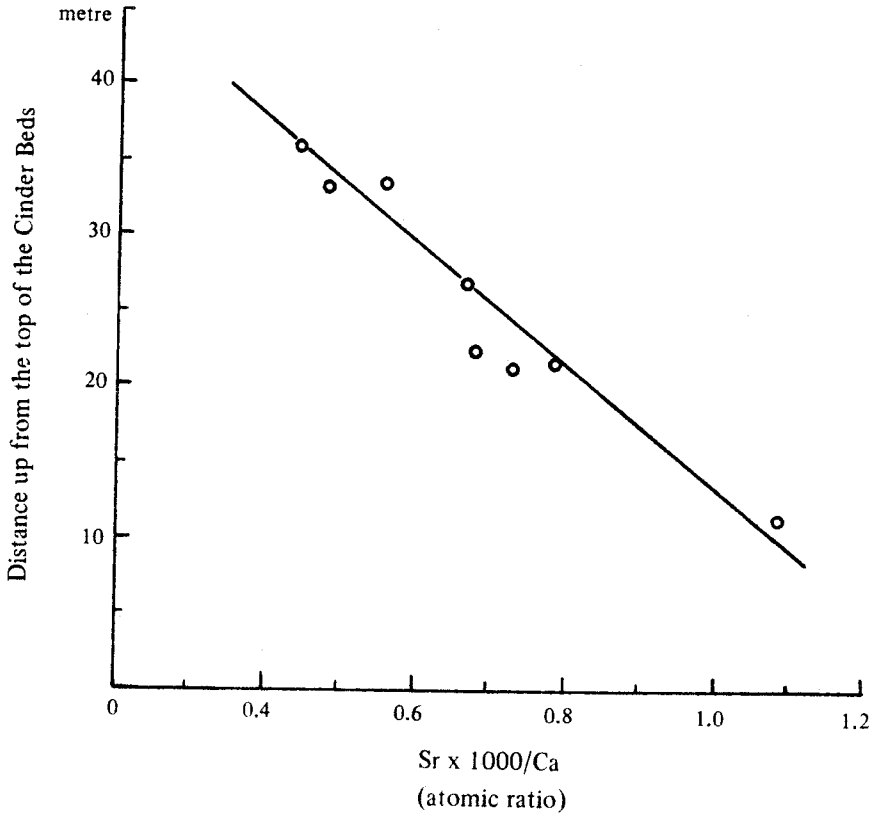

Fig. 115. Variation of Sr/Ca ratio of the 'beef' with depth.

residual solution increases gradually. Therefore the second generation of 'beef' should contain higher Sr content (between 700 and 1000 ppm Sr if 50% of the carbonates have precipitated in the early 'beef').

Since chemical analyses were performed on bulk samples, it was impossible to prove directly the nature of Sr zonation in the 'beef' crystal. However, the Sr values which were obtained for the 'beef' are consistent with the hypothetical model mentioned above. The high Sr value of 1060 ppm suggests that some of the 'beef' layers have precipitated from solution which contains high Sr concentration. This indicates that the 'beef' crystal can grow in a closed system although aragonite dissolution might have occurred in an open one. The low Sr content of 370 ppm, found in some of the 'beef' layers suggests flushing of Sr (in the residual solutions), probably by compaction, after precipitation of the early calcite crystals.

The stratigraphic distribution of Sr/Ca ratio of the 'beef' layers is shown in Fig. 115. It appears that this ratio decreases in an upward direction. If the 'beef' layers were formed from ascending solutions and not from the dissolution of local carbonates (aragonite in the present case), then the Sr/Ca ratio of the diagenetic fluids might have decreased upwards. But the Sr distribution in the middle Purbeck limestones indicates that Sr has no systematic vertical variation (Fig. 116). However, the nature of the middle Purbeck rocks as a limestone-shale sequence makes the movement of the pore fluids more complicated. The problem is further complicated in the presence of limestones which were originally lithified at different stages of diagenesis. Thus, the apparent decrease in the Sr/Ca ratio in the 'beef' layers with depth is not understood.

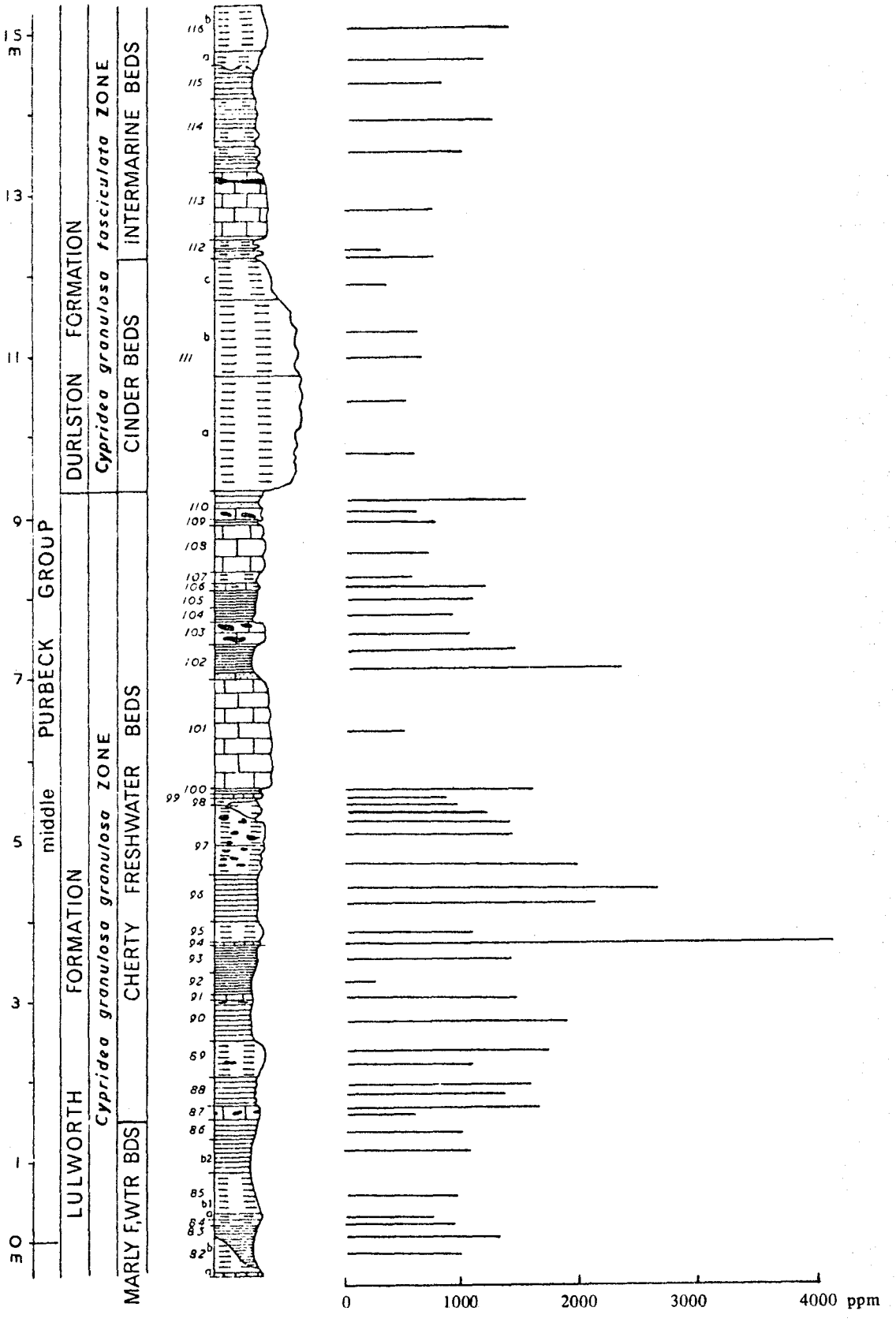

Fig. 116. Stratigraphic distribution of strontium in the middle Purbeck Group of Durlston Bay (Key on Fig. 15)

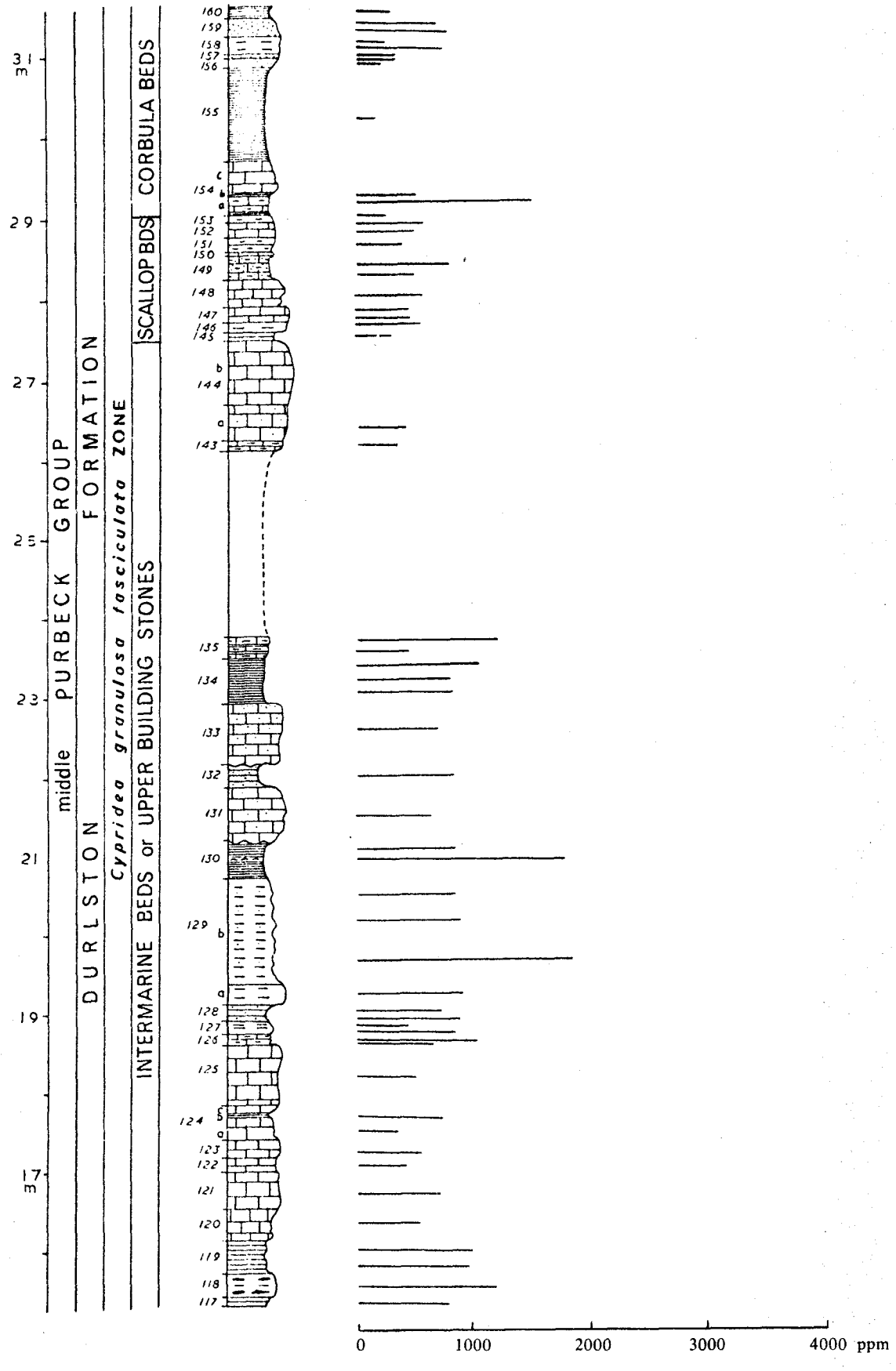

Fig. 116 continued.

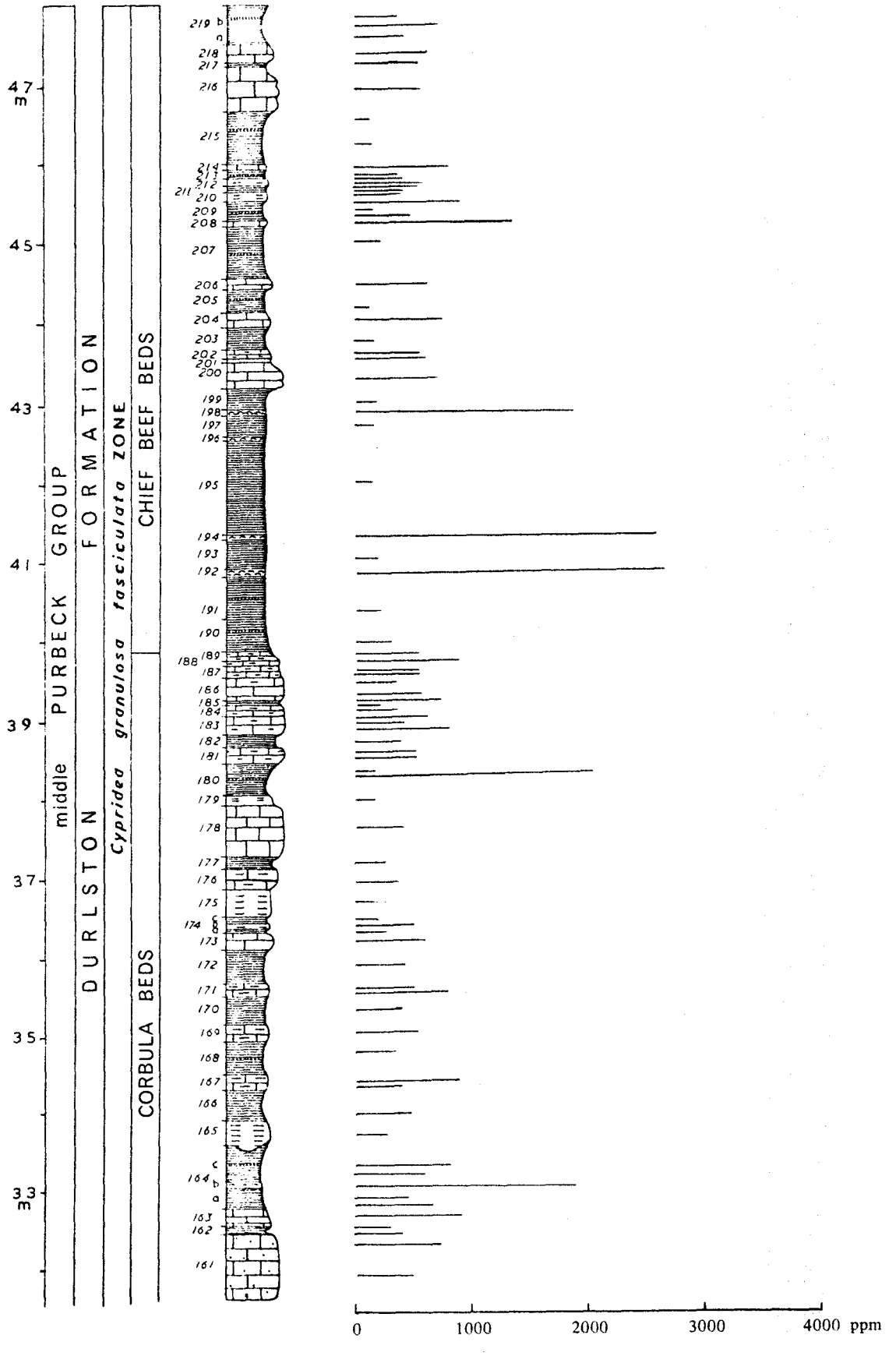

Fig. 116 continued

16. THE MIDDLE PURBECK SEDIMENTARY ENVIRONMENTS: INTERPRETATION AND SYNTHESIS

The following is an account on the sedimentary history of the middle Purbeck Group of Dorset. The palaeoenvironment cannot be interpreted entirely from sedimentological evidences. The results of sedimentological studies are considered in conjunction with previous palaeontological work particularly that of Anderson *et al.*, (1967) and Clements (1969).

After the shallow marine sedimentation of the Portland Group differential uplift produced in southern and south-eastern England a very shallow large lagoon or shallow gulf with restricted circulation of water. This resulted in high salinities and deposition of evaporites in the lower Purbeck strata (Brown, 1963; West, 1975). Later during deposition of the middle Purbecks salinities were lower probably because of increased rainfall (Anderson and Bazley, 1971). It was not, however, until during deposition of the Wealden that really humid conditions have prevailed as indicated by coarse clastics and much vegetation (Allen, 1975). Progressive climatic changes have to be considered when discussing the origin of the middle Purbeck strata. Other factors such as bathymetry and geometry of the basin must be taken into account. Because deposition occurred in a very shallow environment a long phase of subsidence was necessary to accommodate the whole thickness of the Purbeck strata. Although dessication cracks occur at several horizons, they may represent brief periods of emergence. Erosional surfaces that indicate long intervals of subaerial exposures are not common. The frequent occurrence of soils in the basal Purbeck (West, 1975), and their apparent absence in younger strata suggests progressive increase in the average subsidence rate.

There is palaeontological evidence of cyclic variation in salinity during deposition

of the Purbeck strata. Two series of salinity – controlled ostracod fauna have been recognised (Anderson *et al.*, 1967; Anderson and Bazley, 1971). C-phase fauna, in which species of the genus *Cypridea* predominate, result from conditions ranging from fresh-water to brackish (infrahaline-mesohaline, see Fig. 117). A contrasting S-phase with different species indicate more saline conditions. A complete faunicycle consists of an S-phase below and C-phase above. Anderson (in Anderson and Bazley, 1971) reported 39 faunicycles in the Purbeck Group of southern England but the stratigraphic positions of these in Durlston Bay have not been published.

The apparent positions of ostracod faunicycles in the middle Purbeck of Durlston Bay based on the ostracod data of Clements (1969) are shown in Fig. 3. The diagram indicates that some faunicycles can be correlated with lithology, especially above the Cinder Beds. Most of the limestones are relatively rich in ostracods of the S-phase species. In contrast, the shales are generally dominated by species of the genus *Cypridea* (C-phase species). Thus the sedimentary cycle consists of limestone below and shale above. The general agreement between faunicycles and lithocycles indicates that oscillations in salinity is the main reason for cyclicity during deposition of the middle Purbeck strata. The cyclic variations in salinity could have resulted from either climatic fluctuation (wet and dry periods) as suggested by Anderson (in Anderson and Bazley, 1971), or oscillations in the relative sea-level, a commonly proposed explanation for salinity oscillations in shallow-water sequences. Positive identification of the cause requires further investigation.

The environments in which the subdivisions (members) of the middle Purbeck Group are now considered in some detail.

Table 62. Summary of lithology and palaeontology of the middle Purbeck Group of Durlston Bay.

Subdivisions	Facies	Fossils
Chief Beef Beds	Bivalve biosparrudite Ostracod biosparite Ostracod biomicrite Shale	Bivalves: *Neomiodon, Unio* Gastropods: *Viviparus, Planorbis, Hydrobia* Ostracods: *Cypridea, Darwinula, Theriosynoecum, Macrodentina, Rhinocypris*
Corbula Beds	Bivalve biosparrudite Bivalve biomicrudite Algal pelmicrite with gypsum pseudomorphs Shale Calcareous sandstone	Bivalves: *Corbula, Pecten, Liostrea, Protocardia, Neomiodon* Gastropods: *Hydrobia, Procerithium, Theodoxus, Promathilda* Ostracods: *Macrodentina, Orthonotacythere, Cypridea, Dicrorygma, Rhinocypris, Darwinula* Foraminifers: ?
Scallop Beds	Bivalve biosparrudite Bivalve biomicrudite Calcareous shale Calcareous sandstone	Bivalves: *Pecten, Corbula, Liostrea* Gastropods: *Hydrobia, Viviparus, Theodoxus, Procerithium* Ostracods: *Dicrorygma, Macrodentina, Othonotacythere, Theriosynoecum, Scabriculocypris, Cypridea* Foraminifers: ?
Intermarine Beds	Bivalve biosparrudite Bivalve biomicrudite Ostracod biomicrite Charophyte biomicrite Calcareous shale Calcareous sandstone	Bivalves: *Neomiodon, "Cyclas", Liostrea* Gastropods: *Hydrobia, Viviparus, Ptychostylus, Planorbis, Theodoxus, Physa, Valvata.* Ostracods: *Cypridea, Darwinula, Theriosynoecum, Macrodentina* Vertebrates: Fish, Turtles, Dinosaurs Plants: Charophytes, *Ortonella*
Cinder Beds	Bivalve biomicrudite	Bivalves: *Liostrea, Protocardia, "Trigonia"* Annelids: *Serpula* Echinoids: *Hemicidaris* Vertebrates: Fish
Cherty Freshwater Beds & Marly Freshwater Beds	Charophyte biomicrite Ostracod biomicrite Ostracod-gastropod biomicrite Bivalve biosparrudite Calcareous shale	Bivalves: *Neomiodon, "Cyclas", Unio* Gastropods: *Valvata, Hydrobia, Viviparus, Planorbis, Physa* Ostracods: *Cypridea, Theriocynoecum, Darwinula, Fabanella* Sponges: *Spongilla* Vertebrates: Mammals, Turtles, Crocodiles, Fish Plants: Charophytes

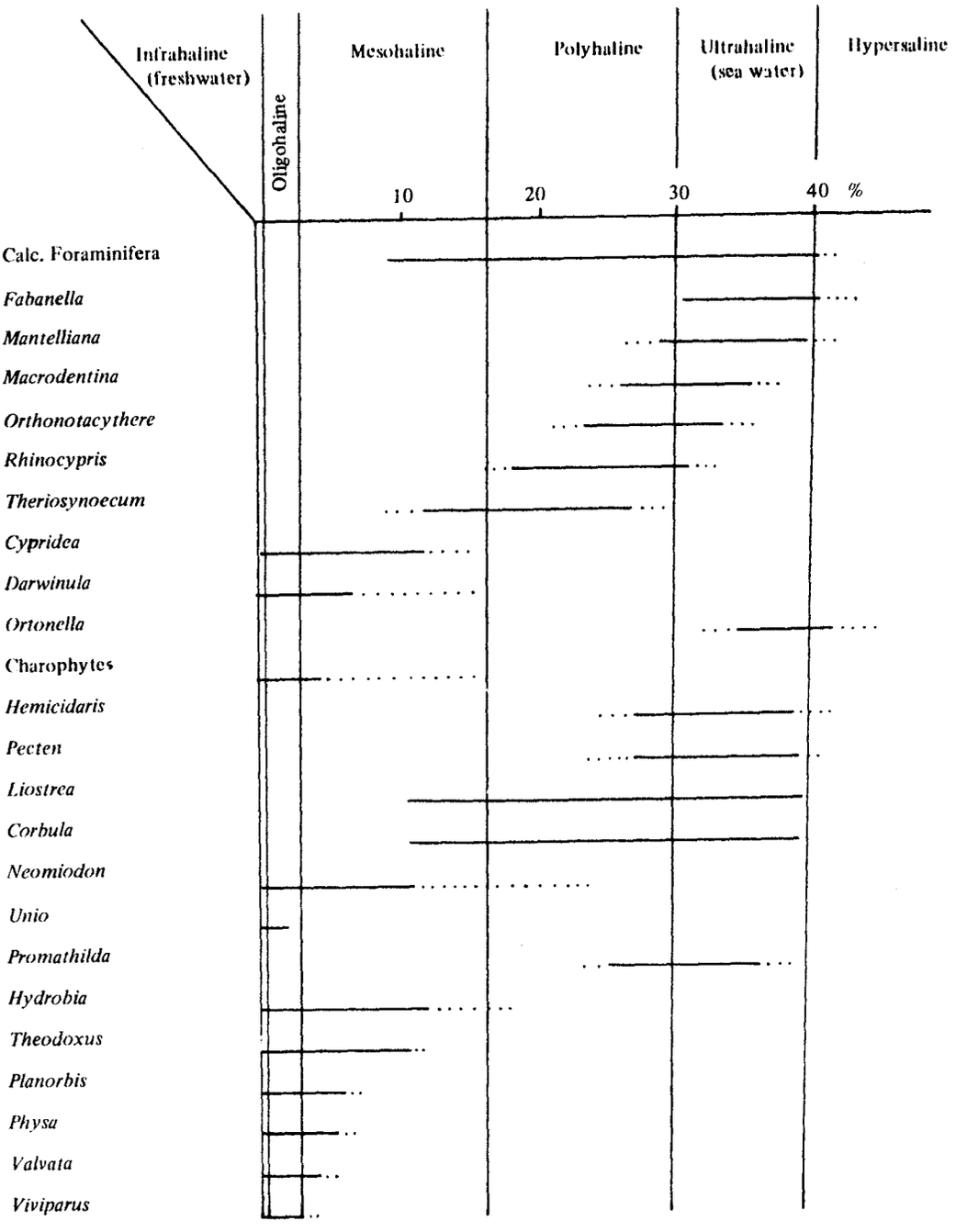

Fig. 117. Postulated salinity tolerance of certain elements of the middle Purbeck. Salinity classification is that used by Ager (1963).
Sources: Caspers (1957), Parker (1959), Johnson (1961), Brown (1963), Hudson (1963 a & b), Huckreide (1967), McGregor (1969), Anderson and Bazley (1971), Daley (1972) and Hudson and Palmer (1976).

1. Marly Freshwater Beds and Cherty Freshwater Beds.

Dilution of the former evaporite depositing lagoon in Dorset was brought about by inflowing freshwater. The land, presumably with rivers, existed to the west and to the north. The faunal assemblages (Table 62 and Fig. 117) imply the existence of a lake with salinities of less than 10‰. Rainfall was not, however, sufficient to introduce large quantities of coarse clastics. Thus a barrier between the lake and the open sea seems necessary to maintain such low salinities.

The lake had maximum extent, covering most of Dorset, at the time of deposition of the 'Flint Bed' (Harris, 1939). The bathymetric distribution of the gastropods *Physa*, *Valvata* and *Planorbis* in modern lakes (*c.f.* Kukal, 1971) suggests water depth in the range of 1 to 8 m. Living charophytes suggest similar range of water depth (Caspers, 1957). In Worbarrow area the lake may have been deeper where abundance of large stems of charophytes indicate that the plant were accumulated below the wave-base.

Water-levels in the lake undoubtedly fluctuated greatly in response to climatic changes. When evaporation exceeded rainfall, the lake dried completely and halite crystals and dessication cracks were formed.

The lake sediment was mainly carbonate mud and argillaceous material in addition to variable quantities of bioclastic debris of charophytes, ostracods, molluscs, sponges, fish and turtles. Most of the carbonate mud in the lake probably accumulated by physico-chemical precipitation of calcite caused by loss of CO_2 to the atmosphere and by photosynthetic action of algae (*c.f.* Terlecky, 1974). Some of the carbonate mud, however, may have been derived by shell comminution. Fragmentation of the fossils is probably due both to wave action and biological activity.

The bivalve biosparrudites occur extensively in the upper parts of the Cherty

Freshwater Beds. The granular calcite cement, lack of micrite matrix and fragmentation of most of the bivalves points to depositional environment in which wave action was continually effective. In the field the bivalve biosparrudites are not closely associated with biomicrites and biomicrudites. The biosparrudites were, therefore, not the result of winnowing of micrite from original biomicritic sediment, but instead were probably the result of a high rate of skeletal production.

2. Cinder Beds

The environments described above were destroyed by a marine invasion which marks the reestablishment of connection with the open sea. This marine transgression was initiated by a widespread earth-movement in north-west Europe (Allen, 1967b).

The Cinder Beds consist mainly of poorly-sorted oyster debris in a carbonate matrix (micrite and microspar). The fragmented nature of the oysters suggests high energy environments and the micrite mud probably have resulted from shell comminution. The microspar is a product of diagenetic size-enlargement of micrite. The small content of quartz and clay indicates limited supply of clastics from the surrounding land.

Oysters have a wide range of salinity tolerence, from 12% to 35% (Parker, 1959). The limited diversity of associated fauna in the Cinder Beds points to lower salinities. It is only in the middle part that the echinoid *Hemicidaris purbeckensis* occurs, thus suggesting salinities near 35%.

3. Intermarine Beds

Shortly after the regression of the Cinder Beds, a lake was developed once again over southern England. The lake sediments produced the limestones of the lower parts of the Intermarine Beds. They were mostly of carbonate mud, argillaceous material and debris of charophytes, gastropods (*Viviparus* and *Physa*) and ostracods (*Cypridea* and

Darwinula). The abundance of relatively large debris of plants and vertebrate bones suggests well vegetated swampy areas around the lake.

The remainder of the Intermarine Beds of Durlston Bay is mostly limestones intercalated with calcareous shale and mudstone. Traced westward the limestones interfinger with shales and sand and die out in the Ridgeway area (Fig. 13). The coarse grained limestone are composed of relatively large fragments of bivalves (mainly *Neomiodon* and occasionally *Liostrea*) with either interstitial micrite or spar. The biosparrudites could be the result of winnowing of micrite from original biomicrudites by intermittent waves. In general the bivalve biosparrudites indicate fairly high-energy depositional environments as is evident from the presence of cross-laimination and ripple marks.

The fine-grained limestones are represented mainly by ostracod biomicrites. The ostracod assemblages indicate wide ranges of salinity, from oligohaline to hypersaline. The common occurrence of desiccation cracks points to relative shallowness of the basin. Thus sedimentation has occurred mainly above the wave-base which would account for the fragmented nature of most of the ostracod valves.

The Intermarine Beds suggest important hydrologic changes. Since sediments accumulated mainly under brackish water conditions, a connection with the open sea was probably necessary. On the other hand, maintenance of brackish water conditions imply continuous inflow of freshwater to counterbalance the influx from the open sea. The arrival of coarse clastics near the margins of the basin (at Ridgeway) and appearance of new mineral assemblage (kaolinite, staurolite and kyanite) suggest more active rivers draining new source rocks. This activity was initiated by increasing precipitation and possibly also by uplift (Allen, 1967b).

At intervals, the rate of evaporation still exceeded the rate of influx of fresh and

marine waters as it had often done during early Purbeck times. During these periods most of the basin in Dorset was exposed to subaerial conditions and dessication cracks were developed. Herds of herbivorous dinosaurs roaming across the carbonate sand flats at these times left their tracks (Delair and Lander, 1973).

4. Scallop Beds

The main difference between the Scallop Beds and the preceeding Intermarine Beds is the marine character of the latter (see Table 62 and Fig. 117). Of particular interest is the association of species of the gastropods *Viviparus* and *Theodoxus* and the ostracod *Cypridea*, freshwater or oligohaline genera, with species of the bivalves *Pecten*, *Corbula* and *Liostrea*, euryhaline marine organisms. This points to mixing of the skeletal debris of organisms which have lived under different salinity conditions.

The dominant marine character of the Scallop Beds suggests relative rise in sea-level rather than low rainfall. Erosion was now active in the hinterland as indicated by influx of coarse quartz sand.

In Durlston Bay, the Scallop Beds consist mostly of bivalve biosparrudites and biomicrudites and a complete gradation exists between both facies. The rounding of the shell fragments and abundance of coarse quartz sand in the biosparrudites seem to indicate depositional environment in which waves were continually effective. Most of the micrite was removed under these conditions. Some of the micrite, however, was trapped in the shell cavities. The development of oolitic coatings on some of the bivalve fragments points to continued agitation in water saturated with calcium carbonate.

The bivalve biomicrudites are ill-sorted shell fragments in a matrix of micrite. Complete gradation from complete valves to micron-sized shell fragments suggests that some of the micritic sediments were derived from shell comminution.

5. *Corbula* Beds

These beds suggest maximum competition between carbonate deposition within the basin and supply of clastics from the surrounding land. For most of the *Corbula* Beds, sediments are evenly represented by limestone and shale. Sandstones are most common in the lower parts of the succession. The limestone facies are similar to those described in the Scallop Beds.

The fauna suggest salinities similar or higher than those of the Scallop Beds and thus continuous inflow of sea water. Short periods of hypersalinity, indicated by the presence of minor evaporites, are the highest known in the British Purbeck succession. Nevertheless, periods of much lower salinity (oligohaline–mesohaline) are indicated by gastropod and ostracod fauna of certain beds (see Table 62). Most probably the rainfall was greater than previously which resulted in the arrival of quantities of coarse clastics (Fig. 14).

6. Chief Beef Beds

The fauna of these beds (*Neomiodon, Unio, Viviparus, Planorbis, Cypridea, Darwinula* etc.) suggests a significant decrease in salinity. Such change could have been produced by increased rainfall and possibly by the lowering of relative sea-level. The environment was dominated by clastics sedimentation. Indeed, shale occupies 75% of the sequence at Durlston Bay. The presence of large fragments of trees at several horizons suggest a well-vegetated land.

17. SUMMARY AND CONCLUSIONS

It is the purpose of this chapter to summarise those conclusions mentioned earlier, and to draw attention to some important points that have arisen from the present study. Evidence and argument for the conclusions has been provided in the previous chapters.

1. Sedimentary environment

The middle Purbeck Group of Dorset consist of limestones and shales formed in extremely shallow water of various salinities. There was a general progressive increase in subsidence, rates of sedimentation and rainfall.

During the deposition of the Marly Freshwater Beds and Cherty Freshwater Beds there was a low-salinity lake which sometimes evaporated completely and which was barred from the sea.

After the well-known Cinder Beds marine transgression a low salinity lake was again developed and the lower part of the Intermarine Beds were formed.

During the deposition of the remainder of the Intermarine Beds there was a major inflow of freshwater bringing coarse clastics from new sources. It mixed with inflowing sea water.

The dominant marine character of the Scallop Beds and *Corbula* Beds suggests a relative rise in sea-level. A pecularity here are minor evaporites, the highest known in the British Purbeck succession.

The clastics of the Chief Beef Beds were formed during lower salinities, probably due to increased rainfall.

2. Geochemistry of the middle Purbeck shales

1. The Purbeck clays were derived mainly from older marine sediments. The detrital

character is evident from strong associations of the clay and the detrital components such as quartz, Ti, Zr, Ce and Th. The strong negative correlation between these components and carbonate is further evidence.

2. The marine origin is indicated from the behaviour of V, Ni, and Rb. Based on boron contents in the Purbeck illites, Walker (1964) came to a similar conclusion. Such a marine character is, however, an inherited one since other evidence from the middle Purbeck shales suggests predominantly brackish to freshwater environments. The heavy minerals point to the Jurassic and possibly Upper Palaeozoic sediments of the surrounding uplands as sources for most of the clay.

3. The clays have not undergone many cycles of erosion and deposition before reaching the Purbeck basin. The normal contents of the major and trace elements especially the resistates such as Ti and Zr support this conclusion.

4. There is a progressive increase in the sedimentation rate from the Lulworth Formation to the Durlston Formation. This is evident from the stratigraphic distribution of the following indicators of sedimentation rates:

- Quartz content
- Ti content
- Quartz/organic carbon ratio
- Quartz/combined silica ratio
- Zr/combined silica ratio
- Ti/combined silica ratio

Increasing rainfall and/or decreasing evaporation are main reasons for the higher sedimentation rates in the Durlston Formation. Such climatic change is also evident from the palaeontological data. Clay and heavy minerals suggest a similar climatic trend. The appearance of kaolinite, staurolite and kyanite in the sediments of Durlston Formation suggest more active rivers draining new source rocks. There is also increase in the

quantity and grain size of quartz and heavy minerals from the Lulworth Formation to the Durlston Formation. The climatic changes are well documented in the lithology; evaporites in the basal Purbeck but in contrast fluviatile sands and clay cap the Purbeck sequence. There is a possibility that the development of higher relief, which resulted from mid-Purbeck tectonism, enhanced sedimentation rates during the deposition of the Durlston Formation.

5. Post-depositional changes affected the distribution of P, Mn, Fe, Ni, and Zn. This led to relative enrichment of these elements in the calcareous shale in comparison with pure shale.

6. The following conclusions were reached with regard to residence sites:

a. Titanium is mainly present in rutile, brookite and anatase. Variable quantities (20–40% of the total Ti) occur in the silicate structures.

b. Iron is present as iron oxide film on the surface of the clays and as a minor constituent of the clay minerals. Pyrite is rarely recorded. Most of the Fe associated with the original pyrite has been lost during weathering.

c. Montmorillonite is the main host for Mg especially in the clay of the Marly Freshwater Beds. In these sediments Mg substitutes for Al.

d. Amongst the elements which substitute for K are Rb, Ba, Sr and Pb.

e. Vanadium, Ni, Zn and Cu are associated with the clay and iron oxides. Their exact sites are not known but it is possible that these elements are both adsorbed and incorporated in clays and iron oxides.

f. The elements which are associated with the carbonates include Na, Sr and Mn. The following parameters were found to be good measures of the carbonate/clay ratio:

- Na/K ratio
- Sr/Ca ratio
- Mn/Fe ratio

3. Geochemistry of the middle Purbeck limestones

1. There are no chemical criteria which, by themselves, are sufficient to indicate significant differences between the limestone facies recognised on sedimentological and palaeontological grounds. The present study illustrates very forcibly that the chemistry of limestones in the middle Purbeck is controlled chiefly by the clay content and by diagenetic modifications. Broadly the average composition of the middle Purbeck carbonates was 70% molluscan debris particularly bivalves (other bioclastic fragments are volumetrically less significant) and 30% carbonate mud. Most of the bivalves were built mainly of aragonite while appreciable quantities of carbonate mud had accumulated as calcite. Therefore the micritic sediments and the carbonates that consisted mainly of bivalves had originally different carbonate mineralogy. Clays are more abundant in the micritic sediments as compared with the bivalve limestones. Within the latter group there are limestones that were lithified before and after compaction. The unlithified counterpart of the bivalve biosparrudites contain up to 75% aragonite.

2. The contents of Al, K and Ti are almost exclusively associated with the clay fraction. Silicon occurs in two phases: quartz and combined silica in the clay minerals. The clay and iron oxides are the main hosts for Fe. The clay fraction shows strong sympathetic variations with the contents of Ga, Rb, V, Th, Zr and Ce. Amongst the trace elements which might have been enriched due to the presence of pyrite are: Zn, As, Ni and Pb.

3. Magnesium decreases from the biomicrites and biomicrudites towards the biosparrudites. This suggests that sparry calcite cements contain less Mg in comparison with the carbonate mud indicating a decrease in the Mg content as the crystal size of calcite increases. The 'beef' layers which consist of very coarse calcite crystals have the lowest content of Mg.

4. Sodium is not balanced by the content of chlorine. Only 11% of the sodium is present as NaCl. The remaining sodium is present in the calcite.

5. The middle Purbeck limestones (and shales) are generally rich in organic carbon due to high organic productivity during the time of deposition and due to favourable conditions of preservation. Originally the Purbeck carbonates contained much more organic matter in comparison with the present values. The loss is attributed mainly to repeated exposure to meteoric water during lithification. The carbonates which escaped important diagenetic modifications contain much more organic carbon than the carbonates that were early lithified under subaerial conditions or in the vadose zone. The limestones that were lithified after compaction have intermediate contents of organic carbon (Table 63).

6. Phosphorus is depleted in the limestones considering the local occurrence of vertebrate bones. Some of the original P might have been leached as indicated by the presence of phosphate nodules near the horizons that are rich in bone fragments.

7. Strontium values for the middle Purbeck limestones are much higher than most ancient carbonates. Significant contributions from dispersed traces of celestite and Sr-carbonate minerals can be ruled out. Also the possibility of Sr being adsorbed on the clay is excluded. Two groups of carbonates were found particularly rich with respect to Sr. In the first group, the high Sr content can be related to the conservation of skeletal aragonite and to the time of calcitization. The limestones in which calcitization of aragonite occurred after compaction contain much more Sr in comparison with the limestones that were lithified before compaction. High Sr concentration in the second group (charophyte biomicrite, ostracod biomicrite and ostracod-gastropod biomicrite) is due to the high Sr/Ca ratio in the original medium of deposition.

8. The Sr behaviour in the fibrous calcite, known as 'beef', indicates redistribution of carbonates by dissolution of aragonite and reprecipitation of calcite. The Sr range (370–1060 ppm) of the 'beef' layers suggests that the 'beef' crystals grew, in a closed system, from solutions which have increased gradually with respect to Sr/Ca ratio.

9. Manganese is much higher in the rocks that were originally dominated by inorganic precipitation of calcite such as the micritic limestones. In contrast, the bivalve biosparrudite that originally consisted of skeletal aragonite contains the lowest Mn content. The variation in Mn contents of the micritic limestones might have been controlled by Mn supply at the time of deposition. There are no significant differences in the Mn contents of the bivalve limestones that were lithified before, lithified after compaction or unlithified (Table 63). Thus the original Mn content does not appear to have undergone serious changes during aragonite-calcite inversion.

4. Diagenesis

Middle Purbeck shell beds fall in one of the three major categories. The salient features of which are summarised here (Fig. 118).

Pre-compaction lithification (type 3)

It is well-known that both calcitization of skeletal aragonite and precipitation of calcite cements occur in the early stages of the carbonate sediment diagenetic history particularly before compaction. The present study, however, indicates that less than 30% of the middle Purbeck shell beds were lithified before compaction.

Most of the early lithified limestones are thick units without shale intercalations. Lithification occurred in the vadose zone and occasionally under subaerial conditions. The products of pre-compaction lithification are characterized by the following:

1. No compaction.

Fig. 118. Purbeck shell limestones – simplified diagenetic scheme.

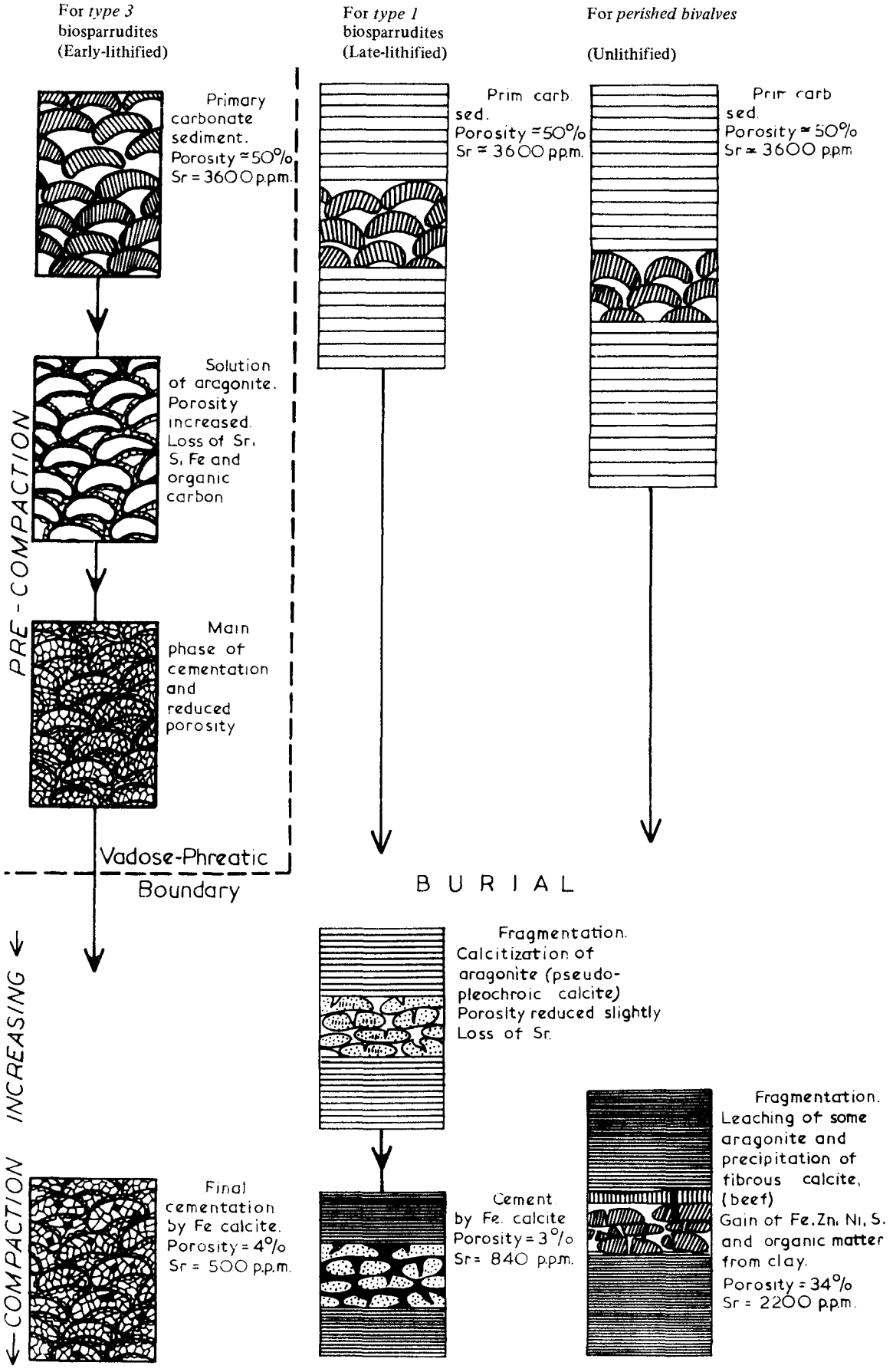

2. Appearance of the early calcite cements around the skeletal fragments near points of contacts (meniscus cement of Dunham, 1971).

3. Solution of skeletal aragonite and formation of cavities within the original micrite envelopes.

4. Reduction of porosity (primary and mouldic) by development of non-ferroan calcite cements.

Some of the early lithified limestones indicate final reduction of porosity in the phreatic zone.

Post-compaction lithification (type 1)

About 70% of the middle Purbeck shell beds were lithified after compaction and their diagenesis was to some extent retarded. The products of post-compaction diagenesis are characterised by the following:

1. Deformation of the allochems.

2. Scarcity of fabrics which indicate early dissolution of aragonite.

3. Large-scale development of pseudo-pleochroic calcite fabrics as mosaics replacing the former aragonite.

4. Coarse-crystalline ferroan calcite cements which postdate calcitization of aragonite.

The post-compaction diagenesis suggests rapid burial presumably due to rapid subsidence and sedimentation since water depth during deposition was in the order of few metres. Restricted movement of the diagenetic fluids was maintained under these conditions and the carbonate sediment, therefore, escaped early diagenetic modifications. Clay supply during deposition was the critical factor in reducing the effects of early diagenesis. Most of the limestones that were lithified after compaction are intercalated with relatively thick shale units.

Unlithified (perished bivalves)

The very thin carbonates (layers of perished bivalves) that are enclosed in relatively thick shale sequence, are unlithified. High aragonite content indicates that diagenesis was frozen at a very early stage due to early reduction in permeability by clays. This resulted from early compaction due to very rapid subsidence and sedimentation. The high porosity of these carbonates is due to limited cementation, perhaps partly because of the former presence of hydrocarbons in these layers. These aragonite layers were partly dissolved causing reprecipitation of fibrous calcite (beef).

Table 63. Mineralogy and chemistry of the bivalve carbonates in the middle Purbeck

	Pre-compaction lithification *(type 3)*	**Post-compaction lithification** *(type 1)*	**Unlithified** *(perished bivalves)*
In percent			
Aragonite	–	5	62
Calcite	93	87	9
Clay	1	2	12
Organic carbon	0.20	0.40	2.62
Fe_2O_3	0.40	1	3.64
S	0.16	0.25	0.78
In ppm			
P	240	280	440
Mn	360	300	430
Sr	500	840	2200
Ni	5	8	30
Zn	< 2	3	160
Porosity (%)	4	3	34

Comparative chemical composition of the bivalve limestones that were lithified before, after compaction or poorly lithified is given in Table 63. The early lithified strata

have low contents of Sr, P, S, Fe and organic carbon in comparison with the unlithified shell beds. The limestones that were lithified after compaction occupy intermediate positions. Migration of Ni, Zn, Fe and S and organic carbon from the clays into the unlithified carbonates has occurred. The significant diagenetic modifications in the bivalve carbonates of the middle Purbeck are summarised in Fig. 118 which also shows salient gains and losses of elements.

Thus the present limestones mainly result from two periods of calcitization of skeletal aragonite and precipitation of calcite cements. The time interval between the two periods was relatively long, since during this interval the sediments suffered compaction great enough to cause fragmentation and shell penetration. Examination of the individual beds indicates that the products of early and late lithification occur in broad cyclic sequences. The late lithified biosparrudites, however, are more abundant in the higher part of the succession (Fig. 3). Rate of supply of clay versus carbonate production is the major factor which influenced both the type of sediment deposited and the type of diagenesis.

Limestones with dominately late lithification are not common in the geologic column but are not, of course, confined to the Purbeck. They can be found in similar facies which are not only rich in organic matter but also with rapidly alternating limestones and shales.

REFERENCES

ADAMS, J.A.S. and WEAVER, C.E. 1958. Thorium to uranium ratios as indicators of sedimentary processes: an example of geochemical facies. *Bull. Am. Ass. Petrol. Geol.*, V. 42, p. 387–430.

ADLER, I. 1966. X-ray emission spectrography in geology. Elsvier, Amsterdam, 258pp.

AGER, D.V. Principles of Paleoecology. McGraw-Hill, New York, 371 pp.

AINARD, R. 1975. Microfaciès et paléoécologie du Purbeckien des régions de Nantua et Saint-Rambet (Jura méridional). Mise en evidence d'un horizon à *Anchispirocyclina lusitanica* EGGER. In Colloque sur la Limite Jurassique-Cretace. Lyon, France, 1973. (ed. Anon., 1975), p. 232–241.

ALBERSTADT, P.L. 1973. Depositional environments and origin of the fine-grained limestones of the Bigby-Cannon Formation (middle Ordvisian), Central Basin, Tennessee. *J. Sedim. Petrol.*, v. 43, p. 621–633.

ALLEN, P. 1949a. Wealden petrology: The Top Ashdown Pebble Bed and the Top Ashdown Sandstone. *Q. Jl. Geol. Soc. Lond.*, v. 104, p. 257–321.

ALLEN, P. 1949b. Notes on Wealden bone-beds. *Proc. geol. Ass.*, v. 60, p. 275–283.

ALLEN, P. 1954. Geology and geography of the London-North Sea Uplands in Wealden times. *Geol. Mag.*, v. 91, p. 498–508.

ALLEN, P. 1959. The Wealden environment: Anglo-Paris basin. *Phil. Trans. R. Soc.*, B, v. 242, p. 283–346.

ALLEN, P. 1960. Strand-line pebbles in the mid-Hastings Beds and geology of the London uplands. General features. Jurassic pebbles. *Proc. geol. Ass.*, v. 71, p. 156–168.

ALLEN, P. 1961. Strand-line pebbles in the mid-Hastings Beds and geology of the London uplands: Carboniferous pebbles. *Proc. geol. Ass.*, v. 72, p. 271–283.

ALLEN, P. 1967a. Origin of the Hastings facies in north-western Europe. *Proc. geol. Ass.*, v. 78, p. 27–105.

ALLEN, P. 1967b. Strand-line pebbles in the mid-Hastings Beds and the geology of the London uplands. Old Red Sandstone, New Red Sandstone and other pebbles. Conclusion. *Proc. geol. Ass.*, v. 78, p. 241–276.

ALLEN, P. 1969. Lower Cretaceous sourcelands and the North Atlantic. *Nature Lond.*, v. 222, p. 657–658.

ALLEN, P. 1972. Wealden detrital tourmaline: implications for northwestern Europe. *Q. Jl. geol. Soc. Lond.*, v. 128, p. 273–288.

ALLEN, P. 1975. Wealden of the Weald: a new model. *Proc. geol. Ass.*, v. 86, p. 389–437.

ALLEN, P. DODSON, M.H. and REX, D.C. 1964. Potassium-argon dates and the origin of the Wealden glauconite. *Nature Lond.*, v. 202, p. 585–586.

ALLEN, P. and KEITH, M.L. 1965. Carbon isotope ratios and palaeosalinities of Purbeck-Wealden carbonates. *Nature Lond.*, v. 208, p. 1278–1280.

ANDEL, T.H. VAN 1959. Reflections on the interpretation of heavy mineral analyses. *J. Sedim. Petrol.*, v. 29, p. 153–163.

ANDERMAN, G. and KEMP, J.W. 1958. Scattered X-ray as internal standards in X-ray emission spectroscopy. *Analyt. Chem.*, v. 30, p. 1306–1309.

ANDERSON, F.W. 1941. Ostracoda from the Portland and Purbeck Beds at Swindon. *Proc. geol. Ass.*, v. 51, p. 373–384.

ANDERSON, F.W. 1966. New genera of Purbeck and Wealden Ostracoda. *Bull. Br. Mus. nat. Hist. (Geology).*, v. 11, p. 435–446.

ANDERSON, F.W. 1971. The sequence of ostracod faunas in the Wealden and Purbeck of Warlingham Borehole. *Bull. geol. Surv. Gt. Br.*, v. 36, p. 122–138.

ANDERSON, F.W. 1974. The Jurassic–Cretaceous transition: the non-marine ostracod fauna. In: The Boreal Lower Cretaceous (ed. Casey, R. and Rowson, P.F.). Seel House Press, Liverpool, p. 101–110.

ANDERSON, F.W., BAZLEY, R.A.B. and SHEPHARD-THORN, E.R. 1967. The sedimentary and faunal sequence of the Wadhurst Clay (Wealden) in boreholes at Wadhurst Park, Sussex. *Bull. Geol. Surv. Gt. Br.*, v. 27, p. 171–235.

ANDERSON, F.W. and BAZLEY, R.A.B. 1971. The Purbeck Beds of the Weald (England). *Bull. geol. Surv. Gt. Br.*, v. 34, 174p.

ANONYMOUS. 1974. La Manche: Notice Explicative (explanation of the 1:1000,000 geological map of the English Channel) Bureau de Recherches Geologique et Minières, Orléans, France, 17p.

ANONYMOUS. 1975. Colloque sur la limite Jurassique-Crétacé Lyon, France, 1973 Mémoires du Bureau de Recherches Geologique et Minières, no. 86, 393 pp.

ARKELL, W.J. 1933. The Jurassic System in Great Britain. Clarendon Press, Oxford, 681pp.

ARKELL, W.J. 1938. Three tectonic problems of the Lulworth district: Studies on the middle limb of the Purbeck fold. *Q. Jl. geol. Soc. Lond.*, v. 94, p. 1–54.

ARKELL, W.J. 1941. The gastropods of the Purbeck Beds. *Q. Jl. geol. Soc. Lond.*, v. 97, p. 79–128.

ARKELL, W.J. 1945. The names of the strata in the Purbeck and Portland stone quarries. *Proc. Dorset. nat. Hist. Arch. Soc.*, v. 66, p. 158.

ARKELL, W.J. 1947. The geology of the country around Weymouth, Swanage, Corfe and Lulworth. *Mem. geol. Surv. U.K.* 386 p.

ARKELL, W.J. and TOMKEIEFF, S.I. 1953. English rocks terms, chiefly as used by miners and quarrymen. Oxford Univ. Press, London 139p.

AWASTHI, N. 1970. Some aspects of the Krol formation of Himalaya, India. *Contr. Min. Petr.*, v. 28, p. 192–220.

AUSTEN, J.H. 1852. A guide to the geology of the Isle of Purbeck, and the south-west coast of Hampshire. Blandford, 8V.

BATHURST, R.G.C. 1964. The replacement of aragonite by calcite in the molluscan shell wall. In: Approaches to paleoecology. (eds. Imbrie, J. and Newell, N.D.). Wiley, New York, p. 357–376.

BATHURST, R.G.C. 1966. Boring algae, micrite envelopes and lithification of molluscan biosparites. *Geol. J.*, v. 5., p. 15–32.

BATHURST, R.G.C. 1975. Carbonate sediments and their diagenesis. Elsevier, Amsterdam, 658pp.

BAUCH, W.M. 1965. Strontiumgehalte in süddeutschen Malmkalken. *Geol. Rundschau*, v. 55, p. 86–96.

BAUCH, W.M. 1968. Outlines of distribution of Sr in marine limestones. In: Recent developments in carbonate sedimentology in Central Europe (eds. Muller, G. and Friedman, G.M.), Springer, Berlin, p. 106–115.

BEAR, F.E. 1964. Chemistry of soil (ed. Bear, F.E.) Reinhold Publishing Corporation, New York, 515 pp.

BENCINI, A. and TURI, A. 1974. Mn distribution in the Mesozoic carbonate rocks from Lima Valley, Northern Apennines. *J. Sedim. Petrol.*, v. 44., p. 774–782.

BLATT, H. and SUTHERLAND, B. 1969. Intrastratal solution and non-opaque heavy minerals in shales. *J. Sedim. Petrol.*, v. 39, p. 591–600.

BLOXAM, T.W. and THOMAS, R.L. 1969. Palaeontological and geochemical facies in the *Gastrioceras subcrenatum* marine-band and associated rocks from the North Crop of the South Wales Coalfield. *Q. Jl. geol. Soc. Lond.*, v. 124, p. 239–281.

BØGGILD, O.B. 1930. The shell structure of the mollusks. *Kgl. Danske Videnskab. Selskab. Mat. Fys. Medd.*, 9. p. 231–325.

BRAMLETTE, M.N. 1941. The stability of minerals in sandstone. *J. Sedim. Petrol.*, v. 11, p. 32–36.

BRAMMALL, A. 1928. Dartmoor detritals: a study in provenance. *Proc. geol. Ass.*, v. 39, p. 27–48.

BRISTOW, H.W. and FISHER, O. 1857. Comparative vertical sections of the Purbeck strata of Dorsetshire. *Geol. Surv.*, Vertical Sections. Sheet no. 22.

BRISTOW, H.W. and WHITAKER, W. 1859. Horizontal Sections. *Geol. Surv.* Sheet no. 56.

BROWN, P.R. 1963, Algal limestones and associated sediments in the basal Purbeck of Dorset. *Geol. Mag.*, v. 1001. p. 565–573.

BROWN, P.R. 1964. Petrography and origin of some Upper Jurassic beds from Dorset, England. *J. Sedim. Petrol.*, v. 34, p. 254–269.

BROWN, P.R. 1966. Pyritization in some molluscan shells. *J. Sedim. Petrol.*, v. 36. p. 1149–1152.

CAMPBELL, F.A. and WILLIAMS, G.D. 1965. Chemical composition of shales of the Manville group (Lower Cretaceous) of Central Alberta, Canada. *Bull. Am. Ass. Petrol. Geol.*, v. 49, p. 81–87.

CAROZZI, A. 1948. Étude stratigraphique et micrographique du Purbeckien du Jura Suisse. Thèse no. 1123, Univ. de Genève.

CARROLL, D. 1958. The role of clay minerals in the transportation of iron. *Geochim. Cosmochim. Acta.*, v.14, p. 1–28.

CASEY, R. 1962. The ammonites of the Spilspy Sandstone and the Jurrassic-Cretaceous boundary. *Proc. geol. Soc. Lond.*, no. 1589, p. 95–100.

CASEY, R. 1963. The dawn of the Cretaceous period in Britain. *Bull. S.-East. Un. scient. Socs.*, v. 117, 1 – 15.

CASEY, R and GALLOIS, R.W. 1973. The Sandringham Sands of Norfolk. *Proc. Yorks. geol. Soc.*, v. 40, p. 1-22.

CASPERS, H. 1957. Black Sea and Sea of Azov. In: Treatise on marine ecology and paleoecology. (ed. HEDGPETH, J.W.) *Mem. geol. Soc. Am.*, 67, v. 21 p. 801-890.

CAYEUX, L. 1935. Les roches sédimentaires de France. Roches Carbonatées. Masson et Cie, Paris. 463 pp.

CHAPMAN, F. 1906. Note on an ostracodal limestone from Durlston Bay, Dorset. *Proc. geol. Ass.* v. 19, p. 283-285.

CHAVE, K.E. 1954. Aspects of the biochemistry of magnesium: 1. Calcareous marine organisms. *J. Geol.* v. 62, p. 266-283.

CLEMENTS, R.G. 1969. Contribution to Section on the Purbeck Beds. In Guide for Dorset and south Somerset. International Field Symposium on the British Jurassic (ed. Torrens, H.S.), Keele Univ., Figs. 35-37 .

CLEMENTS, R.G. 1973. A study of certain non-marine Gastropoda from the Purbeck Beds of England. Unpubl. Thesis, Hull Univ., 491 pp.

CODY, R.D. 1970. Anomalous boron content of two continental shales in eastern Colorado. *J. Sedim. Petrol.* v. 40, p. 750-754.

CODY, R.D. 1971. Adsorption and reliability of trace elements as environment indicators for shales. *J. Sedim. Petrol.*, v. 41, p. 461-471.

CODY, R.D. 1976. Growth and early diagenetic changes in artificial gypsum crystals grown within bentonite muds and gels. *Bull. geol. Soc. Am.* v. 87, p. 1163-1168.

COLLEY, H. and DAVIES, P.J. 1969. Ferroan and non-ferroan calcite cements in Pleistocene-Recent carbonates from the New Hebrides. *J. Sedim. Petrol.*, v. 39, p. 554-558.

COSGROVE, M.E. 1972a. The geochemistry of the red beds of south-east England, including the Permian volcanics. Unpubl. Thesis. Southampton Univ., 136pp.

COSGROVE, M.E. 1972b. The geochemistry and mineralogy of the Permian red beds of south-west England. *Chem. geol.*, v. 11, p. 31-47.

COSGROVE, M.E. and HEARN, E.W. 1966. Structures in the Upper Purbeck Beds at Peveril Point, Swanage, Dorset. *Geol. Mag.*, v. 103, p. 498-507.

COSGROVE, M.E. and SALTER, D.L. 1966. The stratigraphical distribution of kaolinite in the post-Armorican formations of south-west England. *Proc. Ussher Soc.*, v. 1, p. 249-252.

COSGROVE, M.E. and SULAIMAN, A.M.A. 1973. A rapid method for the determination of quartz in sedimentary rocks by X-ray diffraction incorporating mass absorption correction. *Clay Miner.* v. 10, p. 51-55.

CURTISS, C.D. 1964. Studies on the use of boron as a paleoenvironmental indicator. *Geochim. Cosmochim. Acta,* v. 28, p. 1125-1137.

DALEY, B. 1972. Macrovertebrate assemblages from the Bembridge Marls (Oligocene) of the Isle of Wight, England, and their environmental significance. *Palaeogr. Palaeoclimat. Palaeoecol.* v. 11, p. 11-32.

DAMON, R. 1884. Geology of Weymouth, Portland, and the coast of Dorsetshire. 2nd ed. Weymouth, 250pp.

DAVIES P.J. and TILL, R. 1968. Stained dry cellulose peels of ancient and recent impregnated carbonate sediments. *J. Sedim. Petrol.*, v. 38, p. 234-237.

DEER, W.A., HOWIE, R.A. and ZUSSMAN, J. 1962a. Rock-forming minerals. Longmans, London, v. 3, 270pp.

DEER, W.A., HOWIE, R.A. and ZUSSMAN, J. 1962b. Rock-forming minerals. Longmans, London, v. 5, 371pp.

DEGENHARDT, H. 1957. Untersuchungen zur geochemischen Verteilung des Zirkoniums in der Lithosphäre. *Geochim. Cosmochim. Acta.*, v. 11, p. 279-309.

DEGENS, E.T., WILLIAMS, E.G. and KEITH, M.L. 1957. Environmental studies of Carboniferous sediments. Part I: Geochemical criteria for differentiating marine from freshwater shales. *Bull. Am. Ass. Petrol. Geol.*, v. 41, p. 2427-2455.

DEGENS, E.T., WILLIAMS, E.G. and KEITH, M.L. 1958. Environmental studies of Carboniferous sediments. Part II: Application of geochemical criteria. *Bull. Am. Ass. Petrol. Geol.*, v. 42, p. 981-997.

DELAIR, J.B. and LANDER, A.B. 1973. A short history of the discovery of reptilian footprints in the Purbeck Beds of Dorset, with notes on their stratigraphical distribution. *Proc. Dorset nat. Hist. Arch. Soc.*, v. 94, p. 94-

DEMBOWSKA, J. and MAREK, S. 1975. Dévelopment du bassin de sédimentation sur la basse plaine de Pologne à la limite du Jurassique et du Crétacé. In Colloque sur la Limite Jurassique-Crétacé. Lyon, France, 1973 (ed. Anon., 1975), p. 110-116.

DICKSON, J.A.D., 1965. A modified staining technique for carbonates in thin-section. *Nature, Lond.* v. 205, p. 587.

DICKSON, J.A.D., 1966. Carbonate identification and genesis as revealed by staining. *J. Sedim. Petrol.*, v. 36, p. 491-505.

DIETRICH, R.V. 1960. Calciostrontianite from Pulaski and Rockingham counties, Virginia. *Am., Miner.*, v. 45, p. 1119-1124.

DONOVAN, R. and FOSTER, R.J. 1972. Subaqueous shrinkage cracks from the Caithness Flagstone series (Middle Devonian) of Northeast Scotland. *J. Sedim. Petrol.*, v. 42, p. 309-317.

DONZE, P. and LE HEGARAT, G. 1972. Le Berriasien, étage charnière entre le Jurassique et le Crétacé; ses équivalents continentaux en Europe du Nord. *24th Int. Geol. Congr. Canada.* Section 7, p. 515-523.

DRUMMOND, P.V.C., 1970. The Mid-Dorset Swell. Evidence of Albian-Cenomanian Movements in Wessex. *Proc. geol. Ass.*, v. 81, p. 679-714.

DUNHAM, R.J. 1971. Meniscus cement. In: Carbonate Cements (ed. Bricker, O.P.), Johns Hopkins Press, Baltimore, Md., p. 297-300.

EAGAR, R.M.C. 1962. Boron content in relation to organic carbon in certain sediments of the British Coal Measures. *Nature, Lond.*, v. 196, p. 428-431.

EAGAR, R.M.C. and SPEARS, D.A. 1966. Boron content in relation to organic carbon and to palaeosalinity in certain British Upper Carboniferous sediments: *Nature, Lond.*, v. 209, p. 177-181.

EL-SHAHAT, A. 1968. Geological and mineralogical studies of some sand deposits in the Nile Delta. Unpubl. Thesis. Ain Shams Univ., Cairo, 88pp.

EVAMY, B.D. 1969. The precipitational environment and correlation of some calcite cements deduced from artificial staining. *J. Sedim. Petrol.*, v. 39, p. 787-793.

EVAMY, B.D. and SHEARMAN, D.J. 1965. The development of overgrowths from echinoderm fragments. *Sedimentolog.*, v. 5, p. 211-233.

FENNER, P. and HANGER, A.F. 1967. Correlation of variations in trace elements and mineralogy of Esopus Formation, Kingston, New York. *Geochim. Cosmochim Acta*, v. 31, p. 237-261.

FISHER, O. 1856. On the Purbeck strata of Dorsetshire. *Trans. Camb. Phil. Soc.*, v. 9, p. 551-581.

FITTON, W.H. 1835. Notice on the junction of Portland and Purbeck strata on the coast of Dorsetshire. *Proc. geol. Soc.*, v. 2, p. 185-187.

FITTON, W.H. 1836. Observations on some of the strata between the chalk and the Oxford Oolite, in the south-east of England. *Trans. geol. Soc.*, v. 4, p. 103-388.

FLANAGAN, F.G. 1957. Semi-quantitative spectrographic analysis and rank correlations in geochemistry. *Geochim. Cosmochim. Acta.*, p. 315-322.

FOLK, R.L. 1959. Practical petrographic classification of limestones. *Bull. Am. Ass. Petrol. Geol.*, v. 43, p. 1-38.

FOLK, R.L. 1965. Some aspects of recrystallization in ancient limestones. In: Dolomitization and limestone diagenesis (eds. Pray, L.C. and Murray, R.C.), *Soc. Econ. Pal. Min. Spec. Publ.* 13, Tulsa, p. 14-48.

FOLK, R.L. 1974. The natural history of crystalline calcium carbonate: Effect of magnesium content and salinity. *J. Sedim. Petrol.*, v. 44, p. 40-53.

FORBES, E. 1851. On the succession of strata and distribution of organic remains in Dorsetshire Purbecks. *Rept. Br. Ass.* for 1850, p. 79-81.

FORSMAN, J.P. and HUNT, J.M. 1958. Insoluble organic matter (kerogen) in sedimentary rocks of marine origin. In: Habitat of Oil. (ed. Weeks, L.G.). *Am. Ass. Petrol. Geol.*, Tulsa, p. 747-778.

FRIEDMAN, G.M. 1964. Early diagenesis and lithification in carbonate sediments. *J. Sedim. Petrol*, v. 34, p. 777-813.

FRIEDMAN, G.M. 1968. The fabric of carbonate cement and matrix and its dependence on salinity of water. In: Recent development in carbonate sedimentology in Central Europe (ed. Muller, G. and Friedman, G.M.), Springer, Berlin, p. 11-20.

FRIEDMAN, G.M. 1969. Trace elements as possible environmental indicators in carbonate sediments. In: Depositional environments in carbonate rocks (ed. Friedman, G.M.), *Soc. Econ. Pal. Min., Spec. Publ.* 14, Tulsa, p. 193-198.

FUCHTBAUER, H. and GOLDSCHMIDT, H. 1964. Aragonitische Lumachellen im bituminosen Wealden des Emslandes. *Beitr. Miner. Petrog.*, v. 10, p. 184-197.

GAD, M.A., CATT, J.A. and LE RICHE, H.H. 1969. Geochemistry of the Whitbian (upper Lias) sediments of the Yorkshire Coast. *Proc. Yorks. geol. Soc.*, v. 37, p. 105-139.

GAZZI, P. 1965. On the heavy mineral zones in the geosyncline series. Recent studies in the Northern Apennines, Italy. *J. Sedim. Petrol.*, v.35, p. 109-115.

GEHAM, H.M. Jr. 1962. Organic matter in limestones. *Geochim. Cosmochim. Acta.*, v. 26. p. 885-897.

GIBBS, R.J. 1965. Error due to segregation in quantitative clay mineral X-ray diffraction mounting techniques. *Am. Miner.* , v. 50, p. 741-751.

GODDARD, E.N. *et al.*, 1970. Rock-colour chart. *Geol. Soc. Am.* Boulder, Colorado.

GOLDBERG, E.D. and ARRHENIUS, G.O.S. 1958. Geochemistry of Pacific pelagic sediments. *Geochim. Cosmochim. Acta.* v. 13, p. 153-212.

GOLDSCHMIDT, V.M. 1954. Geochemistry. Clarendon Press, Oxford. 730pp.

GRABAU, A.W., 1913. Principles of stratigraphy. Reproduced by Dover Publications Inc. New York. N.Y. 1960, v. 1, 1185pp.

GRAF, D.L. 1960. Geochemistry of carbonate sediments and sedimentary carbonate rocks. I – IV. Illinios. *St. geol. Surv., Circ.*, 297, 298, 301, 308: 250pp.

GRANDJEAN, J., GREGOIRE, C. and LUTTS, A. 1964. On the mineral components and the remnants of organic structures in shells of fossil molluscs. *Bull. Classe. Sci. Acad R. Belg.* v. 50, p. 562-595.

GREEN, J. 1959. Geochemical table of the elements for 1959. *Bull. Geol. Soc. Am.*, v. 70, p. 1127-1184.

GRIFFITHS, J.C. 1967. Scientific methods in the analysis of sediments. McGraw-Hill, New York, 502pp.

GRIMM, W.–D., 1973. Stepwise heavy mineral weathering in the Residual Quartz Gravel, Bavarian Molasse (Germany), *Contr. Sedimentology*. Stuttgart, v. 1, p. 103-125.

GROVES, A.W. 1931. The unroofing of the Dartmoor granite and the distribution of its detritus in the sediments of southern England. *Q. Jl. geol. Soc. Lond.*, v. 87 p. 62-96.

HALLAM, A. 1969. Tectonism and eustasy in the Jurassic. *Earth Sci. Rev.*, v. 5, p. 45-68.

HALLAM, A. and O'HARA, M.J. 1962. Aragonitic fossils in the Lower Carboniferous of Scotland, *Nature, Lond.* v. 195, p. 273-274.

HARDER, H. 1964. To what extent is boron a marine index element. *Geochem. Int.*, v.1, p. 105-112.

HARLAND, W.B. *et al.*, 1972. A concise guide to stratigraphic procedures. *Q. Jl. geol. Soc. Lond.*, v. 128, p. 295-305.

HARRIS, T.H. 1939. British Purbeck Charophyta. *Brit. Mus. nat. Hist. Lond.*, 83pp.

HASKIN, L.A., *et al.*, 1966. Meteoric, solar and terrestrial rare-earth distributions. In: Physics and Chemistry of the Earth. Pergamon Press, Oxford, v. 7, p. 167-322.

HECKEL, P.H. 1972. Recognition of ancient shallow marine environments. In: Recognition of ancient sedimentary environments. *Soc. Econ. Pal. Min.*, Spec. Publ. 16, Tulsa, p. 226-286.

HEIR, K.S. and BILLINGS, G.K. 1970. Rubidium. In: Handbook of Geochemistry (ed. Wedepohl H.K.), Springer, Berlin, v. 2, p. 37K1-37K3.

HINDE, G.J. 1912. A monograph of the British fossil sponges. V. I. Sponges of Palaeozoic and Jurassic strate. *Palaeontogr. Soc. (Monogr.).*, 264pp.

HIRST, D.M. 1962. The geochemistry of modern sediments in the Gulf of Paria I. *Geochim. Cosmochim. Acta., v. 26, p. 309-334.*

HIRST, D.M. and DUNHAM, K.C. 1963. Chemistry and petrography of the Marl Slate of S.E. Durham, England. *Econ. Geol.*, v. 58, p. 912-940.

HOEFS, J. 1969. Carbon In: Handbook of Geochemistry (ed. Wedepohl, K.H.), Springer, Berlin, v. 2., p. 6K1-6K6.

HORN, M.K. and ADAMS, J.A.S. 1966. Computer-derived geochemical balance and element abundances. *Geochim. Cosmochim. Acta.*, v. 30, p. 279-297.

HORWOOD, A.R. 1911. On the layers of the molluscan shell. *Geol. Mag.*, v. 48, p. 406-418.

HOWITT, F. 1964. Stratigraphy and structure of the Purbeck inliers of Sussex (England). *Q. Jl. Geol. Soc. Lond.*, v. 120, p. 77-113.

HOUSE, M.R. 1961. The structure of the Weymouth anticline. *Proc. geol. Ass.* v. 72, p. 221-238.

HUCKRIEDE, R. 1967. Molluskenfaunen mit limnischen und brachischen elementen aus Jura, Serpulit und Wealden NW.-Deutschlands und ihre palaogeographische Bedeutung. *Beih. geol. Jb.*, 67, 263p.

HUDSON, J.D. 1962. Pseudo-pleochroic calcite in recrystallized shell limestones. *Geol. Mag.*, v. 99, p. 492-500.

HUDSON, J.D. 1963a. The recognition of salinity-controlled mollusc assemblages in the Great Estuarine Series (middle Jurassic) of the Inner Hebrides. *Palaeontology*, v. 6, p. 318-326.

HUDSON, J.D. 1963b. The ecology and stratigraphical distribution of the invertebrate fauna of the Great Estuarine Series. *Palaeontology*, v. 6. 327-348.

HUDSON, J.D. 1970. Algal limestones with pseudomorphs after typsum from the middle Jurassic of Scotland. *Lethaia*, v. 3, p. 11-40.

HUDSON, J.D. and PALFRAMAN, D.F.B. 1969. The ecology and preservation of the Oxford Clay fauna at Woodham, Buckinghamshire. *Q. Jl. geol. Soc. Lond.*, v. 124, p. 387-418.

HUDSON, J.D. and PALMER, J.J. 1976. A euryhaline oyster from the middle Jurassic and origin of the true oysters. *Palaeontology*, v. 19, p. 79-93.

HUNT, J.M. 1961. Distribution of hydrocarbons in sedimentary rocks. *Geochim. Cosmochim. Acta.*, v. 22, p. 37-49.

INGAMELLS, C.O. and SUHR, N.H. 1967. Chemical and spectrochemical analysis of standard carbonate rocks. *Geochim. Cosmochim. Acta.*, v. 31, p. 1347-1350.

JOFFE, J. 1967. The 'dwarf' crocodiles of the Purbeck Formation, Dorset: A reappraisal. *Palaeontology*, v. 10, p. 629-639.

JOHNSON, J.H. 1961. Limestone-building algae and algal limestones. Colorado School of Mines, Boulder Colorado, 297pp.

JONES, D. 1958. Displacement of microfossils. *J. Sedim. Petrol.*, v. 28, p. 453-467.

JONES, T.R. 1885. On the ostracoda of the Purbeck formation, with notes on the Wealden species. *Q. Jl. geol. Soc. Lond.*, v. 41, p. 311-353.

JONES, W.D. and HUANG, W.H. 1967. Distribution of chlorine in terrestial rocks. *Geochim. Cosmochim. Acta.* v. 31, p. 35-49.

KAHLE, C.F. 1965. Strontium in oolitic limestones. *J. Sedim. Petrol.*, v. 35, p. 846-856.

KEITH, M.L. and DEGENS, E.T. 1959. Geochemical indicators of marine and freshwater sediments. IN: Researches in geochemistry. (ed. Albson, P.H.), John Wiley and Sons, N.Y., p. 38-61.

KENDAL, A.C. 1975. Post-compactional calcitization of molluscan aragonite in a Jurassic limestone from Saskatchewan, Canada. *J. Sedim. Petrol.*, v. 45, p. 399-404.

KENNEDY, W.J. and HALL, A. 1967. The influence of organic matter on the preservation of aragonite in fossils. *Proc. geol. Soc. Lond.*, no. 1643, p. 253-255.

KESLING, R.V. 1961. Reproduction of ostracoda. In: Treatise on Invertebrate Paleontology (ed. MOORE, R.C.), *Q. Arthropoda 3*, p. Q17-Q19.

KINSMAN, D.J.J. 1969. Interpretation of Sr^{2+} concentrations in carbonate minerals and rocks. *J. Sedim. Petrol.*, v. 39, p. 486-508.

KINSMAN, D.J.J. and HOLLAND, 1969. The co-precipitation of cations with $CaCO_3$ – IV. The coprecipitation of Sr^{2+} with aragonite between 16° and 96° C. *Geochim. Cosmochim. Acta.*, v. 33, p. 1-18.

KOVALEV, V.A. 1965. Geochemical aspects of investigation of the Th/U ratio in sedimentary rocks. *Geochem. Int.*, v. 2, p. 861-864.

KRAUSKOPF, K.B. 1956. Factors controlling the concentration of thirteen rare metals in the sea-water. *Geochim. Cosmochim. Acta.*, v. 9, p. 1-32.

KRYNINE, P.D. 1942. Provenance versus mineral stability as a controlling factor in composition of sediments (abst.). *Bull. geol. Soc. Am.*, v. 53, p. 1850-1851.

KULP, J.L., TUREKIAN, K. and BOYD, D.W. 1952. Strontium content of limestones and fossils. *Bull. geol. Soc. Am.*, v. 63, p. 701-716.

KUKAL, Z. 1971. Geology of Recent sediments. Central Geol. Surv., Prague, Academic Press, London, 490 pp.

LAND, L.S. and HOOPS, G.K. 1973. Sodium in carbonate sediments and rocks: a possible index to the salinity of diagenetic solutions. *J. Sedim. Petrol.*, v. 43, p. 614-617.

LAND, L.S., MACKENZIE, F.T. and GOULD, S.J. 1969. Pleistocene history of Bermuda. *Bull. geol. Soc. Am.*, v. 78, p. 993-1006.

LALICKER, C.G. 1949. Principles of petroleum geology. Appleton-Century-Crofts, Inc., New York, 377pp.

LANDERGREN, S. 1974. Vanadium. In Handbook of Geochemistry. (ed. Wedepohl, H.K.) Springer, Berlin, v. 2, p. 23K1-23K5.

LATTER, M.P. 1926. Petrology of Portland Sand of Dorset. *Proc. geol. Ass.*, v. 37, p. 73-91.

LEAKE, P.E. *et al.*, 1969/70. The chemical analyses of rock powders by automatic X-ray fluorescence. *Chem. Geol.*, v. 5, p. 7-86.

LEES, G.M. and COX, P.T. 1937. The geological basis of the present search for oil in Great Britain. *Q. Jl. geol. Soc. Lond.*, v. 93, p. 156-194.

LEBEDEV, B.A. 1967. Trace elements in marine and freshwater clays. *Geochem. Int.*, v. 4. p. 821-824.

LINDHOLM, R.C. and FINKLEMAN ,R. B. 1972. Calcite staining: semiquantitative determination of ferrous iron. *J. Sedim. Petrol.*, v. 42, p. 239-242.

LIVINGSTON , H.D. and THOMPSON, G. 1969. Cited in Thompson, G., *et al.*, 1970.

LLOYD, A.J. 1964. The Luxembourg Colloquium and the revision of the stages of the Jurassic System. *Geol. Mag.*, v. 101, p. 249-259.

LOVE, L.G. 1964. Early diagenetic pyrite in fine grained sediments and the genesis of sulphide ores. In Sedimentaolgy and Ore genesis. (ed. Amstutz, G.C.), Elsevier Amsterdam, p. 11-17.

LOVE, L.G. 1967. Early diagenetic iron sulphides in Recent sediments of the Wash (England). *Sedimentology*, v. 9, p. 327-352.

LYELL, C. 1855. Manual of Elementary Geology. London, 655pp.

MACKENZIE, R.C. 1965. The origin of clay minerals in soils. *Proc. Ussher Soc.* v. 1, p. 134-151.

MASSON, P.H. 1955. An occurrence of gypsum in southwest Texas. *J. Sedim. Petrol.*, v. 25, p. 72-77.

MATHEWS, R.K. 1967. Diagenetic fabrics in biosparites from the Pleistocene of Barbados, West Indies, *J. Sedim. Petrol.*, v. 37, p. 1147-1153.

McGREGOR, D.L. 1969. The productive potenial, life history and parasitism of the freshwater ostracod *Darwinula stevensoni* (Brady and Robertson), IN: The Taxonomy, Morphology and Ecology of Recent Ostracods (ed. Neale, J.W.). Oliver and Boyd Ltd., Edinburgh, p. 194-221.

MEYER, C.J. 1872. On the Wealden as a fluvio-lacustrine Formation, and on the relation of the so-called "Pundfield Formation" to the Wealden and Neocomian. *Q. Jl. geol. Soc. Lond.*, v. 28, p. 243-255.

MIGDISOV, A.A. 1960. On the titanium/aluminium ratio in sedimentary rocks. *Geochemistry (U.S.S.R.)* English transl., v. 2, p. 178-194.

MILLIMAN, J.D. 1974. Marine Carbonates. Springer, Berlin, 375 pp.

MILLMAN, J.D. and BORNHOLD. 1973. Peak height versus peak intensity analysis of X-ray diffraction data. *Sedimentology*, v. 20, p. 445-448.

MILNER, H.B. 1962. Sedimentary Petrography. Macmillan, New York, N.Y., 2 v. 1358pp.

MITCHELL, R.S. and PHARR, R.F. 1961. Celestite and calciostrontianite from Wise County, Virginia. *Am. Min.*, v. 46, p. 189-195.

MÜLLER, G. 1968. Exceptionally high strontium concentrations in freshwater onkolites and mollusk shells of Lake Constance. In: Recent developments in carbonate sedimentaolgy in Central Europe. (eds. Müller, G. and Friedman, G.M). Springer, Berlin, p. 116-127.

NEAVERSON, E. 1923. The petrography of the Upper Kimmeridge Clay and Portland Sand in Dorset, Wiltshire, Oxfordshire and Buckinghamshire. *Proc. geol. Ass.*, v. 36, p. 240-256.

NICKEL, E. 1973. Experimental dissolution of light and heavy minerals in comparison with weathering and intrastratal solution. *Contr. Sedimentology, Stuttgart*, v. 1, 1-68.

NICHOLIS, G.D. and LORING, D.H. 1962. The geochemistry of some British Carboniferous sediments. *Geochim. Cosmochim. Acta.*, v. 26, p. 181-223.

ONISHI, H. 1970. Arsenic. In: Handbook of Geochemistry (ed. Wedepohl, H.K.), Springer Berlin, v. 2, p. 33O1.

OSTROM, M.E. 1957. Trace elements in Illinois Pennsylvanian limestones. *Illinois St. geol. Surv.*, Circ. 243, p. 1-34.

ORR, W. 1974. Sulphur. In: Handbook on Geochemistry (ed. Wedepohl, K.H.), Springer, Berlin, v. 2, p. 16L1-16L19.

ORDORF, R. 1968. Ein Beitrag zur Geochemie des Lithiums in Sedimentgesteinen. *Geochim. Cosmochim. Acta.* v. 32, p. 191-208.

OLDERSHAW, A.E. and SCOFFIN, T.P. 1967. The source of ferroan and non-ferroan calcite cements in the Halkin and Wenlock limestones. *Geol. J.* , v. 5, p. 309-320.

OWEN, R. 1871. Monograph of the fossil Mammalia of the Mesozoic Formations. *Palaeontogr. Soc. (Monogr.)*, 115pp.

PARKER, R.H. 1959. Macro-invertebrate assemblages of central Texas coastal bays and Laguna Madre. *Bull. Am. Ass. Petrol.Geol.*, v. 43, p. 2100-2166.

PETTIJOHN, F.J. 1941. Persistence of heavy minerals and geologic age. *J. Geol.*, v. 49, p. 610-625.

PETTIJOHN, F.J. 1957. Sedimentary Rocks. Harper, New York, 526pp.

PHILLIPS, W.J. 1964. The structure in the Jurassic and Cretaceous rocks on the Dorset coast between White Nothe and Nupe Bay. *Proc. geol. Ass.*, v. 75, p. 373-405.

PLILER, R. and ADAMS, J.A.S. 1962. The distribution of thorium, uranium and potassium in the Mancos Shale. *Geochim. Cosmochim. Acta.*, v. 26, p. 1115-1135.

POLDERVAART, A. 1955. Zircon in rocks. I. Sedimentary rocks. *Am. J. Sci.*, v. 253, p. 433-461.

POTTER, P.E., SHIMP, N.F. and WITTERS, J. 1963. Trace elements in marine and freshwater argillaceous sediments. *Geochim. Cosmochim. Acta.*, v. 27, p. 669-694.

PUCHELT, H. 1972. Barium. IN: Handbook of Geochemistry (ed. Wedepohl, K.H.), Springer, Berlin, v. 2, p. 56K1-56K8.

PUGH, M.E. 1969. Algae from the lower Purbeck limestones of Dorset. *Proc. Geol. Ass.*, v. 79, p. 513-523.

RAMAN, K.V. and JACKSON, M.L. 1965. Rutile and anatase determination in soils and sediments. *Am. Min.*, v. 50, p. 1086-1094.

RANKAMA, K. and SAHAMA, Th.G. 1950. Geochemistry. The University of Chicago Press, 911pp.

REIMER, Th. 1972. The evolution of the rubidium and strontium content of shales. *N. Jb. Miner. Abh.*, v. 116, p. 167-195.

RIDD, M.F. 1973. The Sutton Poyntz, Poxwell and Chaldon Herring Anticlines: a reinterpretation. *Proc. geol. Ass.*, v. 84, p. 1-8.

ROGERS, J.J.W. and ADAMS, J.A.S. 1969. Thorium. In: Handbook of Geochemistry (ed. Wedepohl, K.H.), Springer, Berlin, V. II. p. 90K1-90K5.

RONOV, A.B. and KORZINA, G.A. 1960. Phosphorus in sedimentary rocks. *Geochemistry (U.S.S.R.)* English Transl., v. 8, p. 805-829.

RONOV, A.B., BALASHOV, Yu.A., and MIGDISOV, A.A. 1967. Geochemistry of the rare earths in the sedimentary cycle. *Geochem. Int.*, v. 4, p. 1-17.

RONOV, A.B. and MIGDISOV, A.A. 1971. Geochemical history of the sedimentary cover of the Russian and North American platforms. *Sedimentology*, v. 16, p. 137-185.

SALTER, D.L. and WEST, I.M. 1965. Calciostrontianite in the based Purbeck Beds of Durlston Head, Dorset. *Min. Mag.*, v. 35, p. 146-150.

SARJEANT, W.A. 1974. A history and bibliography of the study of fossil vertebrate footprints in the British Isles. *Palaeogeogr. Palaeoclimatol. Palaeoecol.*, v. 16, p. 265-378.

SCHULTZ, L.G. 1964. Quantitative interpretation of mineralogical composition from X-ray and chemical data for Piere shale. *U.S. geol. Surv. Proff. Papers* 391C.

SCHWARZACHER,W.1961.Petrology and structure of some Lower Carboniferous reefs in north-western Ireland. *Bull. Am. Ass. Petrol. Geol.*, v. 45, p. 1481-1503.

SHAPIRO, L. and BRANNOCK, W.W. 1962. Rapid analysis of silicate, carbonate and phosphate rocks. *U.S. geol. Surv. Bull.* 1144A, p. 1-56.

SHAW, D.B. and WEAVER, C.E. 1965. The Mineralogical composition of shales. *J. Sedim. Petrol.*, v. 35, p. 213-222.

SHEARMAN, D.J. 1966. Origin of marine evaporites by diagenesis. *Bull. Inst. Mining Met.*, v. 77, p. 208-215.

SHEARMAN, D.J. and SKIPWITH, P.A.De. 1965. Organic matter in Recent and ancient limestones and its role in their diagenesis. *Nature, Lond.*, v. 208, p. 1310-1311.

SHEARMAN, D.J., MOSSOP, G., DUNSMORE, H. and MARTIN, M. 1972. Origin of gypsum veins by hydraulic fracture. *Bull. Inst. Mining Met.*, v. 81, p. 149-155.

SHOVER, E.F. 1964. Clay-mineral environmental relationships in COSCO (U.PENN). clays and shales, North Central Texas. *Clay and Clay Minerals, Proc. 12th Conf.*, Pergamon Press, New York, p. 431-443.

SIMPSON, G.G. 1928. A catalogue of the Mesozoic Mammalia in the Geological Department of the British Museum. *Br. Mus. (Nat. Hist)*, 208p.

SPEARS, D.A. 1964. The major element geochemistry of the Mansfield marine band in the Westphalian of Yorkshire. *Geochim. Cosmochim. Acta.*, v. 28, p. 1679-1696.

SPEARS, D.A. 1965. Boron in some British Carboniferous sedimentary rocks. *Geochim. Cosmochim. Acta.*, v. 29, p. 315-328.

SPEARS, D.A. and KANARIS-SOTIRIOU, R. 1976. Titanium in some Carboniferous sediments from Great Britain. *Geochim. Cosmochim. Acta.*, v. 40, p. 345-351.

SMITHSON, F. 1941. The alteration of detrital minerals in the Mesozoic rocks of Yorkshire. *Geol. Mag.* v. 78, p. 97-112.

SMITHSON, F. 1942. The middle Jurassic rocks of Yorkshire: A petrological and palaeogeographical study. *Q. Jl. geol. Soc. Lond.*, v. 98, p. 27-59.

SORBY, H.C. 1879. Address to the Geological Society. *Q. Jl. geol. Soc. Lond.*, v. 35, p. 56-95.

STANLEY, D.J. 1965. Heavy minerals and provenance of sands in flysch of central and southern French Alps. *Bull. Am. Ass. Petrol. Geol.*, v. 49, p. 22-40.

STENZEL, H.B. 1971. Oysters. In: Treatise on Invertebrate Palaeontology (ed. Moore, R.C.), N. Bivalvia, 3, p. N953-N1224.

STEPHEN, L.K. and HUBERT, J.F. 1969. Dispersal patterns and diagenesis of oolitic calcarenite in the Ste. Genevieve Limestone (Mississippian), Missouri. *J. Sedim. Petrol.*, v. 39, p. 954-968.

STOKKE, P.R. and CARSON, B. 1973. Variation in clay mineral X-ray diffraction results with the quantity of sample mounted. *J. Sedim. Petrol.*, v. 43, p. 957-964.

STRAHAN, A. 1898. The Geology of the Isle of Purbeck and Weymouth. *Mem. Geol. Surv. U.K.*, 278 pp.

SULAIMAN, A.M.A. 1972. The geochemistry of the Namurian argillites of Ireland. Unpubl. Thesis. Southampton Univ., 267 pp.

SYLVESTER-BRADLEY, P.C. 1949. The ostracod genus *Cypridea* and the zones of the Middle and Upper Purbeck. *Proc. Geol. Ass.*, v. 60, p. 125-153.

TERLECKY, P.M. Jr. 1974. The origin of late Pleistocene and Holocene marl deposits. *J. Sedim. Petrol.*, v. 44, p. 456-465.

THOMPSON, G., BANKSTON, D.C. and PASLEY, S.M. 1970. Trace element data for reference carbonate rocks. *Chem. Geol.*, v. 6, p. 165-170.

TICKELL, F.G. 1965. The techniques of sedimentary mineralogy. Elsevier, Amsterdam, 220pp.

TILLMANNS, E. 1970. Titanium. In: Handbook on Geochemistry (ed. Wedepohl, H.K.) Springer, Berlin, v. 2, p. 22A1-22A5.

TOURTELOT, H.A. 1964. Minor element composition and organic carbon content of marine and nonmarine shale of Late Cretaceous age in the western interior of the United States. *Geochim. Cosmochim. Acta.*, v. 23, p. 1579-1604.

TOWNSON, W.G. 1975. Lithostratigraphy and deposition of the type Portlandian. *Q. Jl. geol. Soc. Lond.*, v. 131, p. 619-638.

TROSTAL, L.J. and WYNNE, D.J. 1940. Determination of quartz (free silica) in refractory clays. *J. Am. Ceram. Soc.*, v. 23, p. 18-22.

TUREKIAN, K.H. and WEDEPOHL, K.H. 1961. Distribution of elements in some major units of the earth's crust. *Bull. Geol. Soc. Am.*, v. 72, p. 175-192.

VEIZER, J. and DEMOVIČ, R. 1973. Environmental and climatic controlled fractionation of elements in the Mesozoic carbonate sequence of Western Carpathians. *J. Sedim. Petrol*, v. 43, p. 258-271.

WALKER, C.T. 1962. Separation techniques in sedimentary geochemistry illustrated by studies of boron. *Nature, Lond.*, v. 194, p. 1073-1074.

WALKER, C.T. 1963. Size fractionation applied to geochemical studies of boron in sedimentary rocks. *J. Sedim. Petrol.*, v. 33, p. 694-702.

WALKER, C.T. 1964. Depositional environment of Purbeck Formation. *Geol. Mag.* v. 101, p. 189-190.

WALTERS, L.J. and WINCHESTER, J.W. 1971. Neutron activation analysis of sediments for halogens using the Szilard-Chalmers reaction. *Analyt. Chem.*, v. 43, p. 1020-1025.

WEAVER, C.E. 1958a. A discussion on the origin of clay minerals. In: Clay and Clay Minerals. *Nat. Acad. Sci. Nat. Res. Council.* Publ. 566, p. 159-193.

WEAVER, C.E. 1958b. Geologic interpretation of argillaceous sediments. Part 1. Origin and significance of clay minerals in sedimentary rocks. *Bull. Am. Ass. Petrol.Geol.*, v. 42, p. 254-271.

WEBER, J.N. 1964. Trace elements composition of dolostones and dolomites and its bearing on the dolomite problem. *Geochim. Cosmochim. Acta.*, v. 28, p. 1817-1868.

WEBSTER, T. 1816. Letters from Dorset. In: A Description of the Principal Picturesque Beauties, Antiquities, and Geological Phenomena of the Isle of Wight (author: Englefield, H.).

WEBSTER, T. 1826. Observations on the Purbeck and Portland Beds. *Trans. geol. Soc.*, ser. 2, v. 2, p. 37-44.

WEDEPOHL, K.H. 1972. Zinc. In: Handbook on Geochemistry (ed. Wedepohl, K.H.) Springer, Berlin, v. 2, p. 30K1-30K13.

WEDEPOHL, K.H. 1974a. Copper. In: Handbook on Geochemistry (ed. Wedepohl, K.H.) Springer, Berlin, v. 2, p. 29K1-29K10.

WEDEPOHL, K.H. 1974b. Lead. In: Handbook on Geochemistry (ed. Wedepohl, K.H.) Springer, Berlin, v. 2, p. 82K1-82K9.

WELTE, D. 1969. Organic geochemistry of carbon. In: Handbook on Geochemistry (ed. Wedepohl, K.H.) Springer, Berlin, v. 2, p. 6L1-6L30.

WEST, I.M. 1960. On the occurrence of celestine in the Caps and Broken Beds at Durlston Head, Dorset. *Proc. geol. Ass.*, v. 71, p. 391-401.

WEST, I.M. 1964. Evaporite diagenesis in the Lower Purbeck Beds of Dorset. *Proc. Yorks. geol. Soc.*, v. 34, p. 315-330.

WEST, I.M. 1965. Macrocell structure and entrolithic veins in British Purbeck gypsum and anhydrite. *Proc. Yorks. geol. Soc.*, v. 35, p. 47-58.

WEST, I.M. 1975. Evaporites and associated sediments of the basal Purbeck Formation (Upper Jurassic) of Dorset. *Proc. geol. Ass.* v. 86, p. 205-225.

WEST, I.M. and HOOPER, M.J. 1969. Detrital Portland chert and limestone in the Upper Purbeck Beds at Friar Waddon, Dorset. *Geol. Mag.*, v. 106, p. 277-280.

WESTON, C.H. 1848. On the geology of Ridgeway, near Weymouth. *Q. Jl. geol. Soc. Lond.*, v. 4., p. 245-256.

WETHERED, E. 1890. On the occurrence of fossil forms of the genus *Chara* in the middle Purbeck strata of Lulworth, Dorset. Proc. Cotteswold, p. 101-103.

WILLS, L.J. 1951. A palaegeographical atlas of the British Isles and adjacent parts of Europe. Blackie and Son Ltd., London, 63 pp.

WOLF, K.H., CHILINGAR, G.V. and BEALS, F.W. 1967. Elemental composition of carbonate skeletons, minerals and sediments. In: Carbonate Rocks (eds. Chilingar, G.V., Bissel, H.J. and Fairbridge, R.W.) Elsevier, Amsterdam, p. 23-152.

WOODWARD, H.B. 1895. The Middle and Upper Oolitic Rocks of England (Yorkshire excepted). *Mem. geol. Surv. U.K.*, p. 499.

YOUNG, J.T. 1878. On the occurrence of a freshwater sponge in the Purbeck limestone. *Geol. Mag.*, v. 5. p. 220-221.

APPENDICES

These are in four parts. Parts A, B and C give the details of the chemistry of the middle Purbeck rocks at Durlston Bay. Mineralogy is also included in these parts on the basis of four components: calcite, aragonite, quartz and clay. Details of the mineral composition of the shales are given in Part D. All samples are listed according to bed numbers given in Fig. 3.

Abbreviations used are:

B:	'Beef'
CH:	Chert
LS:	Limestone
Pb:	Perished bivalves
SH:	Shale
SS:	Sandstone

PART A

Sample No.	1	199	3	4	5	6	7	8
Bed No.	DB83	DB83	DB84	DB85a	DB85b1	DB85b2	DB86	DB87
In percent								
SiO_2	40.2	39.3	21.9	3.20	3.17	11.1	20.5	1.54
TiO_2	0.31	0.32	0.18	0.04	0.08	0.13	0.18	0.02
Al_2O_3	6.47	6.80	4.30	0.66	1.88	2.92	4.35	0.05
Fe_2O_3	3.05	3.15	1.98	0.64	1.04	1.45	2.20	0.25
MgO	8.16	9.10	5.84	2.07	3.88	5.05	3.29	1.22
CaO	17.0	15.4	29.6	48.4	42.3	35.5	32.1	52.4
Na_2O	0.73	1.23	0.99	0.98	0.84	0.86	0.76	0.95
K_2O	1.94	1.96	1.28	0.23	0.57	0.92	1.22	0.06
CO_2	14.1	15.3	27.6	39.4	37.3	33.5	29.1	42.7
H_2O^+	3.02	4.60	2.09	–	1.24	1.93	2.77	–
Organic Carbon	1.92	1.66	0.48	0.11	0.20	0.59	1.21	0.12
S	0.24	0.09	0.32	0.20	0.23	0.32	0.29	0.15
Cl	0.04	0.69	0.24	0.10	0.10	0.10	0.17	0.04
In ppm								
P	1043	1405	373	291	347	609	372	358
V	72	82	44	10	27	35	49	9
Mn	494	420	632	588	574	688	638	682
Ni	32	40	24	8	10	17	23	5
Rb	88	86	47	7	22	39	49	–
Sr	987	1347	957	751	981	1068	1004	600
Zr	88	115	49	17	35	49	58	18
Ba	230	213	107	70	158	122	184	165
Ce	37	33	27	–	33	–	28	–
In percent								
Calcite	27	29	61	85	82	76	63	95
Aragonite	5	5	2	4	3	–	3	2
Quartz	4	5	6	2	3	3	8	2
Clay	59	59	27	4	4	15	22	–
Lithology	SH	SH	LS	LS	LS	LS	LS	LS

Sample No.	9	10	11	12	13	14	15	16
Bed No.	DB87	DB88	DB88	DB89	DB89	DB90	DB91	DB92
In percent								
SiO_2	8.47	13.5	13.4	5.94	3.98	10.8	5.81	53.1
TiO_2	0.04	0.15	0.14	0.09	0.05	0.15	0.03	0.58
Al_2O_3	0.65	3.38	3.11	2.00	0.85	3.19	0.72	18.9
Fe_2O_3	1.22	1.75	1.86	1.06	0.62	1.67	2.57	6.33
MgO	2.76	2.40	2.49	2.04	1.70	4.95	1.99	3.51
CaO	42.0	36.8	36.9	43.4	49.0	36.1	45.1	1.93
Na_2O	1.06	0.80	0.80	0.83	1.01	0.74	0.78	0.31
K_2O	0.18	0.88	0.80	0.63	0.33	1.03	0.20	3.98
CO_2	36.6	31.5	31.3	36.3	40.2	30.4	36.1	0.40
H_2O^+	–	2.36	2.36	1.50	–	2.30	–	6.25
Organic Carbon	0.62	1.86	2.40	0.19	0.25	0.81	0.41	1.24
S	0.10	0.18	0.18	0.16	0.17	0.20	0.62	0.47
Cl	0.74	0.12	0.11	0.07	0.07	0.08	0.06	0.04
In ppm								
P	668	249	263	413	892	680	252	132
V	18	29	33	22	15	35	10	131
Mn	677	729	672	1024	1284	805	935	160
Ni	27	17	17	10	11	24	8	68
Rb	8	37	32	26	11	44	8	261
Sr	1678	1336	1573	1118	1739	1870	1462	257
Zr	40	71	67	31	48	66	22	257
Ba	248	262	318	344	121	120	213	287
Ce	–	31	29	–	–	–	80	30
In percent								
Calcite	83	70	68	81	89	67	68	1
Aragonite	–	1	3	2	2	2	14	–
Quartz	7	5	6	3	2	1	3	7
Clay	4	18	16	7	2	21	7	84
Lithology	LS	LS	LS	LS	LS	LS	LS	SH

Sample No.	17	18	19	20	21	22	23	193
Bed No.	DB93	DB94	DB95	DB96	DB96	DB97	DB97	DB97
In percent								
SiO_2	41.5	2.98	6.89	3.30	9.88	7.07	3.74	1.76
TiO_2	0.36	0.04	0.10	0.04	0.08	0.07	0.03	0.02
Al_2O_3	10.6	0.38	2.13	0.71	2.08	1.63	0.44	0.11
Fe_2O_3	4.76	0.79	0.97	0.42	1.24	0.96	1.05	0.47
MgO	3.27	1.39	2.06	2.59	3.84	2.84	1.84	1.87
CaO	14.6	48.6	43.3	46.7	37.3	42.4	46.9	51.4
Na_2O	0.47	0.86	0.86	1.10	0.91	0.81	1.20	0.85
K_2O	2.64	0.15	0.67	0.23	0.66	0.45	0.16	0.12
CO_2	12.9	39.0	35.8	38.8	30.8	32.8	37.8	42.8
H_2O^+	4.15	–	1.51	1.22	2.23	1.88	–	–
Organic Carbon	3.36	0.37	0.40	0.87	3.67	1.90	0.40	0.36
S	0.40	0.37	0.17	0.18	0.28	0.30	0.10	0.09
Cl	0.03	0.06	0.12	0.37	0.28	0.19	0.83	0.23
In ppm								
P	246	350	424	447	452	286	766	303
V	78	–	25	6	26	15	10	11
Mn	717	612	1032	496	436	637	892	552
Ni	76	10	14	7	13	11	9	9
Rb	152	–	29	6	32	21	7	4
Sr	1380	4169	1078	2098	2618	1962	1373	1415
Zr	91	77	26	33	50	33	40	29
Ba	233	2180	220	191	237	290	568	144
Ce	58	29	–	–	–	–	–	–
In percent								
Calcite	29	84	81	86	68	74	86	97
Aragonite		4	1	3	2	–	–	–
Quartz	8	3	4	2	4	4	2	1
Clay	59	3	8	4	14	12	6	1
Lithology	SH	LS	LS	LS	LS	LS	LS	LS

Sample No.	194	195	24	75	26	27	28	29
Bed No.	DB97	DB97	DB98	DB98	DB99	DB100	DB101	DB102
In percent								
SiO_2	92.0	90.3	9.63	5.81	3.42	50.5	0.95	2.53
TiO_2	0.02	0.01	0.07	0.05	0.02	0.37	0.02	0.05
Al_2O_3	–	–	2.44	1.60	0.19	15.7	–	0.41
Fe_2O_3	0.42	0.24	1.50	1.21	0.47	6.57	0.25	0,47
MgO	0.32	0.29	2.00	1.75	1.25	3.66	1.18	1.60
CaO	2.88	5.78	40.2	46.1	49.0	6.22	53.3	49.9
Na_2O	0.21	0.23	1.02	0.81	0.91	0.52	1.01	0.80
K_2O	0.06	0.02	0.58	0.42	0.11	3.81	0.06	0.18
CO_2	2.97	5.62	32.4	37.3	38.3	5.80	41.7	39.6
H_2O^+	–	–	1.82	1.19	–	5.05	–	–
Organic Carbon	0.16	0.24	0.22	0.16	0.60	1.31	0.24	0.96
S	0.08	0.03	0.07	0.06	0.12	0.04	0.10	0.11
Cl	0.03	0.06	0.32	0.09	0.10	0.06	0.08	0.07
In ppm								
P	106	107	534	619	293	218	160	240
V	12	10	23	20	7	125	6	5
Mn	50	66	562	548	527	268	335	727
Ni	12	3	15	10	5	72	5	7
Rb	2	–	31	24	5	217	2	4
Sr	142	121	1186	919	842	1610	494	2354
Zr	–	–	50	34	7	135	5	83
Ba	33	70	375	134	186	234	135	385
Ce	–	–	–	–	–	57	–	35
In percent								
Calcite	6	13	74	85	84	7	93	90
Aragonite	–	–	–	–	3	7	1	–
Quartz	92	90	5	2	4	10	1	2
Clay	–	–	12	9	2	74	–	3
Lithology	Ch	Ch	LS	LS	LS	SH	LS	LS

Sample No.	30	31	32	33	34	35	36	37
Bed No.	DB102	DB103	DB104	DB105	DB106	DB107	DB108	DB109
In percent								
SiO_2	34.4	3.68	25.5	9.94	2.53	6.03	6.71	23.6
TiO_2	0.32	0.04	0.23	0.10	0.03	0.09	0.02	0.24
Al_2O_3	8.51	0.37	6.93	2.49	0.41	2.02	0.05	7.18
Fe_2O_3	4.34	0.30	3.48	1.21	0.62	1.02	0.22	2.99
MgO	2.73	1.24	2.37	2.16	1.21	1.68	1.24	1.89
CaO	18.1	49.6	24.5	39.8	50.9	44.2	53.3	29.3
Na_2O	0.60	0.87	0.63	0.91	0.84	0.83	1.14	0.74
K_2O	1.87	0.17	2.24	0.81	0.20	0.64	0.08	1.68
CO_2	15.5	37.1	22.0	32.5	41.8	35.7	42.7	24.2
H_2O^+	3.83	–	3.57	1.76	–	0.84	–	2.79
Organic Carbon	7.46	0.69	2.27	1.13	0.21	0.36	0.16	1.61
S	1.37	0.12	0.41	0.14	0.11	0.11	0.09	0.11
Cl	0.05	0.09	0.10	0.34	0.11	0.08	0.29	0.06
In ppm								
P	266	323	556	327	249	260	192	293
V	71	7	60	34	9	21	8	72
Mn	1127	257	768	477	390	427	178	630
Ni	53	4	48	14	8	10	6	36
Rb	88	4	109	36	7	30	–	78
Sr	1453	1112	908	1081	1189	578	698	770
Zr	118	51	69	39	29	32	16	75
Ba	381	188	198	105	71	73	97	216
Ce	48	–	46	–	31	–	–	36
In percent								
Calcite	31	80	48	74	88	81	96	55
Aragonite	4	5	2	–	7	–	1	1
Quartz	10	3	4	5	2	2	1	5
Clay	46	5	37	12	2	13	–	34
Lithology	SH	LS	LS	LS	LS	LS	LS	LS

Sample No.	38	39	42	197	41	196	40	43
Bed No.	DB110	DB110	DB111a	DB111a	DB111b	DB111b	DB111c	DB112
In percent								
SiO_2	59.7	6.09	5.92	6.34	3.35	3.28	4.61	2.14
TiO_2	–	0.11	0.08	0.08	0.03	0.03	0.06	0.04
Al_2O_3	–	2.40	1.75	1.65	0.29	0.31	1.17	0.50
Fe_2O_3	0.19	1.43	1.02	0.79	0.36	0.37	0.63	0.61
MgO	0.58	1.50	1.24	1.25	0.99	0.91	1.23	1.09
CaO	19.7	42.8	46.1	45.9	51.0	50.4	47.7	51.0
Na_2O	0.41	0.98	0.84	0.87	0.87	1.04	0.81	0.76
K_2O	0.03	0.51	0.43	0.53	0.14	0.14	0.40	0.13
CO_2	15.2	32.7	39.2	36.4	40.6	40.0	38.2	40.6
H_2O^+	–	1.06	1.10	0.92	–	–	0.52	–
Organic Carbon	0.20	3.40	0.17	0.28	0.11	0.36	0.30	0.06
S	0.07	0.34	0.31	0.08	0.14	0.15	0.07	0.17
Cl	0.16	0.15	0.08	0.17	0.06	0.07	0.09	0.06
In ppm								
P	118	203	292	343	160	170	249	394
V	3	26	16	26	10	11	16	9
Mn	223	753	549	109	224	225	105	677
Ni	2	13	10	9	7	6	7	7
Rb	–	21	21	22	5	5	17	5
Sr	554	1501	569	520	661	638	357	695
Zr	19	63	15	27	19	17	25	14
Ba	959	227	57	392	41	113	139	29
Ce	–	–	–	–	–	–	–	27
In percent								
Calcite	35	71	86	83	92	91	87	89
Aragonite	–	3	3	–	–	–	–	3
Quartz	61	3	3	3	3	3	3	2
Clay	–	12	5	8	2	2	5	2
Lithology	SS	LS	LS	LS	LS	LS	LS	LS

Sample No.	44	45	46	47	48	50	49	51
Bed No.	DB112	DB113	DB114	DB114	DB115	DB116a	DB116b	DB117
In percent								
SiO_2	30.8	0.66	6.24	18.1	17.6	0.91	2.75	25.4
TiO_2	0.33	0.01	0.10	0.22	0.20	0.02	0.04	0.25
Al_2O_3	8.31	–	2.52	5.98	5.68	0.21	0.68	8.80
Fe_2O_3	3.72	0.09	1.06	2.30	2.14	0.15	0.45	3.24
MgO	1.74	1.05	1.75	1.85	1.65	1.20	1.51	1.78
CaO	25.8	53.3	42.6	33.3	33.7	52.1	50.1	25.9
Na_2O	0.71	0.94	0.81	0.61	0.66	0.96	0.90	0.60
K_2O	1.49	0.04	0.57	1.29	1.14	0.08	0.20	1.41
CO_2	20.8	41.6	34.4	26.0	28.0	43.1	37.2	22.1
H_2O^+	3.44	–	1.79	2.83	2.25	–	–	2.80
Organic Carbon	0.62	0.23	0.50	1.92	0.47	0.22	1.16	3.16
S	0.61	0.07	0.38	0.22	0.54	0.08	0.19	0.76
Cl	0.04	0.08	0.06	0.02	0.03	0.06	0.09	0.04
In ppm								
P	633	254	328	428	563	274	691	507
V	70	6	26	37	50	8	11	73
Mn	475	163	632	732	841	1568	1195	1029
Ni	27	5	13	31	21	5	9	28
Rb	86	–	27	65	63	2	9	87
Sr	322	694	953	1246	819	1146	1367	777
Zr	77	50	35	77	50	22	34	60
Ba	144	53	174	280	218	83	200	348
Ce	46	–	–	37	27	–	–	33
In percent								
Calcite	46	91	77	56	64	98	91	48
Aragonite	2	3	1	3	–	–	–	3
Quartz	8	1	2	5	4	1	2	4
Clay	40	–	11	30	25	–	2	37
Lithology	LS	LS	LS	LS	LS	LS	LS	LS

Sample No.	52	53	54	55	56	57	58	59
Bed No.	DB118	DB119	DB119	DB120	DB121	DB122	DB123	DB124a
In percent								
SiO_2	0.97	1.72	25.8	0.83	0.33	3.77	0.73	2.57
TiO_2	0.02	0.03	0.26	0.01	0.01	0.04	0.01	0.03
Al_2O_3	0.13	0.54	8.94	0.08	–	0.97	–	0.62
Fe_2O_3	0.21	0.75	3.08	0.17	0.08	0.47	0.08	0.45
MgO	1.23	0.95	1.73	0.98	0.92	1.12	0.97	1.19
CaO	52.5	51.7	24.8	52.8	54.3	47.9	53.1	50.6
Na_2O	0.85	0.95	0.59	0.99	0.99	0.81	0.98	0.84
K_2O	0.08	0.12	1.46	0.05	0.03	0.24	0.05	0.17
CO_2	41.5	40.9	21.1	41.4	43.0	39.5	41.5	41.1
H_2O^+	–	–	4.61	–	–	–	–	–
Organic Carbon	0.93	0.59	2.16	0.14	0.08	0.43	0.12	0.18
S	0.22	0.34	0.70	0.05	0.05	0.16	0.07	0.17
Cl	0.06	0.06	0.02	0.35	0.40	0.06	0.14	0.03
In ppm								
P	414	221	371	221	187	273	193	191
V	8	–	74	6	5	13	5	11
Mn	736	1141	958	479	437	312	264	203
Ni	–	6	33	–	5	7	–	6
Rb	3	5	89	–	–	14	–	7
Sr	1177	978	998	549	692	434	587	371
Zr	29	24	67	7	11	16	8	6
Ba	51	1398	271	–	235	107	48	56
Ce	–	32	36	–	–	28	–	–
In percent								
Calcite	93	93	48	94	98	90	93	92
Aragonite	1	–	–	–	–	–	1	1
Quartz	1	1	4	1	–	2	1	1
Clay	2	2	44	–	–	4	–	3
Lithology	LS	LS	LS	LS	LS	LS	LS	LS

Sample No.	60	61	62	63	64	65	66	67
Bed No.	DB124b	DB125	DB126	DB126	DB127	DB127	DB128	DB128
In percent								
SiO_2	37.9	1.59	5.98	2.31	1.26	11.5	20.9	13.8
TiO_2	0.29	0.02	0.09	0.03	0.02	0.15	0.22	0.16
Al_2O_3	12.2	0.03	2.74	0.45	0.08	4.42	6.42	7.57
Fe_2O_3	4.63	0.11	1.60	0.60	0.32	1.56	2.65	1.70
MgO	1.77	1.00	1.18	1.04	1.00	1.31	2.20	1.70
CaO	18.4	52.8	44.1	51.3	53.2	38.2	29.8	36.8
Na_2O	0.51	0.94	0.65	0.96	0.82	0.72	0.50	0.70
K_2O	1.83	0.06	0.55	0.15	0.06	1.03	1.45	1.04
CO_2	15.5	40.6	36.3	40.9	41.9	33.0	24.2	30.3
H_2O^+	3.14	–	1.11	–	–	1.94	3.45	2.45
Organic Carbon	4.04	0.06	0.40	0.37	0.18	0.42	2.61	0.98
S	0.98	0.06	0.28	0.22	0.18	0.14	0.45	0.34
Cl	0.01	0.10	0.02	0.09	0.04	0.02	0.03	0.04
In ppm								
P	462	217	234	195	250	269	351	318
V	83	8	28	9	5	38	52	45
Mn	1806	174	372	290	338	968	988	719
Ni	41	–	15	10	5	20	30	20
Rb	113	3	31	4	–	50	70	47
Sr	749	526	661	1064	884	464	900	776
Zr	82	10	25	18	11	28	55	45
Ba	209	30	222	59	121	102	133	73
Ce	70	–	67	54	–	–	38	38
In percent								
Calcite	25	92	79	88	86	73	52	66
Aragonite	10	–	3	5	9	3	3	3
Quartz	7	4	3	2	2	3	7	5
Clay	52	–	9	2	–	16	29	22
Lithology	SH	LS	LS	LS	LS	LS	LS	LS

Sample No.	68	69	70	71	72	73	74	75
Bed No.	DB129a	DB129b	DB129b	DB129b	DB130	DB130	DB131	DB132
In percent								
SiO_2	3.35	8.83	4.65	6.38	22.8	31.9	2.48	25.8
TiO_2	0.05	0.12	0.04	0.10	0.21	0.37	0.03	0.30
Al_2O_3	0.56	3.54	0.40	2.89	5.52	8.90	0.46	8.15
Fe_2O_3	0.93	1.66	0.52	1.23	3.26	3.65	0.40	3.06
MgO	1.07	1.35	0.98	1.30	1.09	1.98	1.13	1.92
CaO	47.8	37.5	47.6	42.2	31.4	21.2	51.4	25.2
Na_2O	0.92	0.83	0.93	0.88	0.62	0.61	0.91	0.63
K_2O	0.91	0.66	0.19	0.51	0.98	1.55	0.17	1.77
CO_2	39.0	30.7	37.9	32.7	24.3	18.7	41.3	22.7
H_2O^+	–	2.23	–	2.27	2.46	4.61	–	4.16
Organic Carbon	1.90	6.65	0.42	3.35	2.07	4.14	0.18	2.19
S	0.43	0.93	0.19	0.48	0.26	0.47	0.18	0.71
Cl	0.18	0.39	0.19	0.13	0.03	0.02	0.10	0.02
In ppm								
P	274	277	287	256	418	361	288	512
V	15	29	12	24	49	95	11	86
Mn	2291	1538	754	983	655	1080	210	1000
Ni	10	22	6	14	22	37	4	42
Rb	9	32	7	29	53	92	5	90
Sr	925	1847	905	847	1805	882	640	848
Zr	35	82	46	57	102	101	11	73
Ba	142	154	115	138	19	185	92	137
Ce	–	40	–	35	60	91	40	42
In percent								
Calcite	86	44	78	68	16	36	91	46
Aragonite	3	26	9	6	40	7	3	2
Quartz	3	5	4	4	15	9	2	8
Clay	3	12	2	13	18	40	2	44
Lithology	LS	LS	LS	LS	PB	LS	LS	LS

Sample No.	76	77	78	80	81	82	83	84
Bed No.	DB133	DB134	DB134	DB134	DB135	DB135	DB143	DB144a
In percent								
SiO_2	0.73	21.8	53.1	3.68	5.20	1.26	3.95	2.76
TiO_2	0.01	0.27	0.82	0.08	0.05	0.02	0.02	0.02
Al_2O_3	–	7.90	22.0	1.45	2.35	0.21	0.16	–
Fe_2O_3	0.40	5.20	5.77	0.88	11.03	0.94	0.95	0.39
MgO	0.91	1.26	1.72	0.82	1.04	1.03	1.10	0.77
CaO	52.9	30.7	5.04	48.8	32.2	51.7	50.0	50.9
Na_2O	0.63	0.43	0.45	0.68	0.71	0.77	0.66	0.72
K_2O	0.04	0.98	2.84	0.28	0.33	0.08	0.14	0.04
CO_2	39.5	27.4	5.16	39.0	27.8	40.8	40.2	40.4
H_2O^+	–	2.22	6.08	0.37	1.05	–	–	–
Organic Carbon	0.16	0.92	1.16	0.20	3.19	0.83	0.08	0.04
S	0.18	1.26	0.72	0.14	4.00	0.41	0.27	0.16
Cl	0.06	0.02	0.07	0.02	0.03	0.06	0.04	0.06
In ppm								
P	250	339	167	152	242	256	256	196
V	4	83	225	14	56	12	12	6
Mn	146	393	301	211	646	329	485	509
Ni	4	37	84	9	57	10	9	7
Rb	–	51	172	12	18	3	5	3
Sr	712	842	812	1063	466	1205	375	457
Zr	13	55	172	41	8	31	6	14
Ba	69	152	323	43	92	203	75	82
Ce	–	120	101	89	90	33	61	–
In percent								
Calcite	88	48	12	88	60	80	91	92
Aragonite	2	15	–	–	3	13	–	–
Quartz	2	5	12	2	2	2	3	4
Clay	–	29	73	6	7	2	2	–
Lithology	LS	LS	SH	B	LS	LS	LS	LS

Sample No.	85	86	87	88	89	90	91	92
Bed No.	DB145	DB146	DB147	DB147	DB148	DB149	DB149	DB151
In percent								
SiO_2	26.4	3.65	2.33	3.46	1.42	21.3	9.58	6.30
TiO_2	0.38	0.06	0.02	0.04	0.03	0.21	0.10	0.12
Al_2O_3	9.56	1.10	0.06	0.12	0.37	5.29	1.46	2.70
Fe_2O_3	2.79	0.78	0.34	0.55	0.44	2.91	1.49	1.18
MgO	1.43	0.95	0.94	1.03	1.01	1.13	1.00	1.09
CaO	29.8	49.5	50.7	50.3	51.9	32.2	43.0	44.6
Na_2O	0.65	0.79	0.77	0.63	0.71	0.65	0.64	0.83
K_2O	1.66	0.28	0.05	0.10	0.12	0.95	0.35	0.56
CO_2	25.6	40.3	39.6	38.8	41.6	26.6	34.3	36.4
H_2O^+	2.40	0.31	–	–	–	1.82	0.41	0.85
Organic Carbon	0.30	0.23	0.04	0.04	0.08	0.49	0.18	0.34
S	0.14	0.23	0.10	0.12	0.21	0.73	0.35	0.35
Cl	0.03	0.06	0.06	0.07	0.10	0.05	0.07	0.07
In ppm								
P	232	279	227	228	176	277	325	191
V	89	14	9	14	8	59	22	31
Mn	547	202	94	153	126	198	147	151
Ni	26	7	6	8	6	24	10	12
Rb	62	11	2	3	4	44	14	27
Sr	316	541	457	464	551	489	826	402
Zr	79	16	26	52	10	80	48	24
Ba	148	50	156	77	97	128	108	130
Ce	46	–	35	30	–	38	45	–
In percent								
Calcite	57	90	89	88	93	60	74	81
Aragonite	1	1	1	–	1	–	4	2
Quartz	7	2	5	5	2	16	11	3
Clay	34	6	–	1	2	16	6	9
Lithology	LS	LS	LS	LS	LS	LS	LS	LS

Sample No.	93	94	95	96	97	98	99	100
Bed No.	DB152	DB153	DB154a	DB154b	DB154b	DB155	DB156	DB156
In percent								
SiO_2	3.68	5.11	5.40	2.29	36.4	56.0	15.1	51.6
TiO_2	0.02	0.09	0.82	0.04	0.42	0.83	0.22	0.73
Al_2O_3	0.05	2.39	21.9	0.63	13.2	22.9	6.20	20.6
Fe_2O_3	0.72	2.18	6.71	2.30	4.44	5.23	2.07	6.38
MgO	1.06	1.05	1.90	0.85	1.55	1.91	1.32	2.00
CaO	49.1	45.4	2.62	47.6	18.4	1.49	34.9	5.34
Na_2O	0.69	0.80	0.41	0.86	0.52	0.53	0.75	0.50
K_2O	0.06	0.43	3.16	0.14	2.04	3.26	1.08	2.89
CO_2	37.9	37.2	2.40	37.7	17.7	1.47	29.5	5.33
H_2O^+	–	0.86	5.95	–	4.18	6.32	2.06	5.74
Organic Carbon	0.14	0.61	2.88	0.57	1.77	0.55	0.18	0.79
S	0.34	0.66	0.71	0.69	0.77	0.28	0.22	0.62
Cl	0.03	0.04	0.01	0.04	0.02	0.08	0.03	0.09
In ppm								
P	461	223	210	265	335	187	636	251
V	7	26	140	10	75	155	42	169
Mn	224	191	839	231	517	191	360	511
Ni	5	12	67	11	38	78	18	70
Rb	2	19	178	4	91	198	58	161
Sr	490	595	260	1494	517	174	227	335
Zr	25	19	200	38	262	203	40	163
Ba	163	119	376	60	219	465	135	380
Ce	35	33	94	52	73	115	44	84
In percent								
Calcite	88	81	2	73	38	3	67	12
Aragonite	–	3	4	13	2	–	–	–
Quartz	4	2	21	3	13	23	5	16
Clay	–	9	69	2	44	63	21	70
Lithology	LS	LS	SH	LS	SH	SH	LS	SH

Sample No.	101	102	103	104	105	106	107	108
Bed No.	DB157	DB157	DB158	DB159	DB159	DB160	DB161	DB161
In percent								
SiO_2	41.8	40.0	9.81	21.0	31.1	55.4	6.90	4.47
TiO_2	0.03	0.12	0.17	0.07	0.23	0.77	0.09	0.03
Al_2O_3	0.19	4.40	4.56	1.50	7.77	18.4	2.73	0.41
Fe_2O_3	0.64	4.07	1.48	1.05	3.24	5.66	1.27	0.48
MgO	0.68	0.83	1.11	0.78	1.14	2.00	1.18	1.04
CaO	28.2	21.5	39.9	37.1	25.0	6.68	43.4	48.2
Na_2O	0.51	0.44	0.86	0.59	0.61	0.42	0.62	0.85
K_2O	0.11	0.74	0.84	0.33	1.36	3.01	0.62	0.14
CO_2	21.5	18.4	32.6	28.6	32.2	5.00	33.5	39.7
H_2O^+	–	1.82	1.99	0.89	2.91	4.84	1.11	–
Organic Carbon	0.30	2.17	0.58	0.56	1.39	0.48	0.36	0.35
S	0.23	0.11	0.22	0.19	0.55	0.51	0.21	0.17
Cl	0.05	0.04	0.04	0.06	0.08	0.02	0.06	0.06
In ppm								
P	291	401	400	358	462	317	360	327
V	–	35	31	20	58	118	26	–
Mn	84	298	443	187	319	487	391	267
Ni	7	56	16	8	31	58	13	8
Rb	6	35	43	13	61	160	30	5
Sr	498	722	257	794	724	298	493	739
Zr	22	53	28	27	56	164	18	13
Ba	2481	363	209	107	410	376	69	1571
Ce	–	47	35	35	51	113	36	–
In percent								
Calcite	48	32	74	56	49	11	74	89
Aragonite	–	10	–	9	4	–	2	1
Quartz	52	36	4	17	17	25	4	7
Clay	–	15	15	6	28	64	11	2
Lithology	SS	LS	LS	LS	LS	SH	LS	LS

Sample No.	109	110	111	112	117	113	115	116
Bed No.	DB162	DB162	DB163	DB164	DB164a	DB164b	DB164c	DB164c
In percent								
SiO_2	28.1	53.1	1.83	8.26	51.2	2.50	50.6	4.85
TiO_2	0.26	0.69	0.02	0.14	0.68	0.05	0.74	0.08
Al_2O_3	3.07	21.1	0.04	3.73	19.6	1.22	20.1	21.0
Fe_2O_3	2.67	6.45	1.09	2.74	7.60	4.67	7.34	1.63
MgO	0.89	2.14	0.93	0.86	1.67	0.70	1.57	0.70
CaO	29.0	4.53	50.6	40.9	2.71	42.8	1.52	46.0
Na_2O	0.48	0.46	0.80	0.64	0.53	0.75	0.43	0.67
K_2O	0.69	3.31	0.05	0.60	3.25	0.24	3.37	0.40
CO_2	24.6	4.83	39.9	32.5	1.22	34.5	–	35.5
H_2O^+	1.09	5.59	–	1.50	6.35	0.49	7.97	2.45
Organic Carbon	0.27	0.55	0.44	0.48	0.66	0.36	0.97	0.20
S	0.61	0.61	0.33	0.64	0.82	1.67	0.83	0.70
Cl	0.02	0.09	0.04	0.01	0.12	0.06	0.06	0.02
In ppm								
P	330	439	218	237	277	242	257	182
V	31	185	6	28	154	–	190	20
Mn	239	405	118	329	120	249	194	222
Ni	28	71	7	29	48	24	64	16
Rb	29	181	–	34	193	9	205	21
Sr	397	307	919	671	466	1862	580	826
Zr	108	139	16	30	163	30	165	21
Ba	777	408	111	120	510	4260	690	102
Ce	32	95	–	57	65	38	87	59
In percent								
Calcite	56	9	87	74	3	60	–	81
Aragonite	–	2	4	–	–	18	–	–
Quartz	25	16	2	5	13	3	12	5
Clay	11	72	–	12	69	5	81	7
Lithology	LS	SH	LS	B	SH	LS	SH	B

Sample No.	118	119	120	121	122	123	124	125
Bed No.	DB165	DB166	DB166	DB167	DB167	DB168	DB169	DB170
In percent								
SiO_2	9.25	47.1	6.47	10.5	1.43	53.1	6.20	49.5
TiO_2	0.16	0.61	0.20	0.19	0.03	0.85	0.09	0.57
Al_2O_3	4.40	19.9	3.37	4.85	0.52	22.2	3.26	22.5
Fe_2O_3	1.62	6.75	1.80	1.66	0.80	7.57	1.87	7.51
MgO	1.16	1.81	0.90	1.35	0.96	2.19	1.06	1.89
CaO	38.5	6.51	44.2	39.5	51.3	1.58	44.3	2.63
Na_2O	0.76	0.43	0.59	0.63	0.85	0.39	0.80	0.40
K_2O	0.90	3.18	0.64	0.97	0.13	3.94	0.63	3.63
CO_2	32.0	6.05	33.3	30.9	42.4	1.17	35.4	1.27
H_2O^+	2.22	6.24	1.08	1.91	–	7.65	0.97	6.45
Organic Carbon	0.96	3.86	0.68	0.72	0.32	2.35	0.52	1.03
S	0.26	0.78	0.34	0.31	0.21	0.48	0.41	0 76
Cl	0.04	0.07	0.02	0.04	0.14	0.08	0.07	0.07
In ppm								
P	323	322	200	315	686	615	491	401
V	34	137	27	47	12	177	24	157
Mn	1563	563	370	986	222	464	181	314
Ni	15	63	16	17	8	78	15	72
Rb	42	172	32	44	4	218	29	215
Sr	316	480	659	404	922	366	522	418
Zr	28	120	24	32	28	168	14	119
Ba	117	513	79	208	148	675	129	865
Ce	–	94	41	27	54	132	27	73
In percent								
Calcite	73	14	76	70	89	3	77	3
Aragonite	–	4	–	–	8	–	3	–
Quartz	3	10	3	4	1	13	2	8
Clay	15	66	13	18	1	80	13	84
Lithology	LS	SH	B	LS	LS	SH	LS	SH

Sample No.	126	127	128	129	130	131	132	133
Bed No.	DB171	DB171	DB172	DB173	DB174a	DB174b	DB174c	DB175
In percent								
SiO_2	1.95	7.68	48.2	1.26	53.5	6.48	49.5	9.25
TiO_2	0.03	0.14	0.56	0.03	0.84	0.10	0.44	0.20
Al_2O_3	0.87	4.02	20.4	0.72	22.4	5.74	23.2	4.56
Fe_2O_3	0.73	1.48	7.73	0.61	7.28	2.06	7.09	1.43
MgO	0.96	1.04	1.70	1.16	1.98	1.05	1.60	1.16
CaO	49.9	41.9	4.93	52.6	2.86	42.7	0.90	39.6
Na_2O	0.90	0.72	0.38	0.89	0.37	0.67	0.44	0.77
K_2O	0.19	0.76	3.21	0.14	3.80	0.74	3.81	0.71
CO_2	41.0	33.5	2.93	42.4	2.34	35.1	–	31.6
H_2O^+	–	1.53	8.66	–	7.32	0.86	8.59	1.64
Organic Carbon	0.28	0.68	1.27	0.30	2.83	1.13	1.57	0.71
S	0.15	0.26	1.76	0.19	0.58	0.47	0.72	0.26
Cl	0.02	0.06	0.04	0.10	0.04	0.13	0.14	
In ppm								
P	700	265	336	318	711	829	132	235
V	5	31	148	6	218	25	146	84
Mn	151	188	329	150	468	545	94	2283
Ni	7	12	81	7	77	18	45	15
Rb	9	37	183	4	201	33	244	32
Sr	830	490	381	584	237	486	175	258
Zr	15	22	111	4	170	21	102	38
Ba	732	105	657	527	470	120	531	95
Ce	–	–	86	37	145	33	43	–
In percent								
Calcite	90	74	7	96	5	78	–	72
Aragonite	3	2	–	–	–	2	–	–
Quartz	1	3	10	1	13	2	7	4
Clay	3	13	78	2	78	11	88	15
Lithology	LS	LS	SH	LS	SH	LS	SH	LS

Sample No.	134	135	136	137	138	139	140	141
Bed No.	DB176	DB177	DB178	DB179	DB180	DB180	DB180	DB181
In percent								
SiO_2	8.51	48.3	0.29	13.3	48.7	6.6	51.2	6.67
TiO_2	0.15	0.56	0.01	0.24	0.63	0.12	0.77	0.12
Al_2O_3	3.97	22.2	0.04	5.36	23.0	2.94	22.3	3.70
Fe_2O_3	1.66	7.58	0.97	2.16	8.15	2.80	7.73	1.37
MgO	1.02	1.55	0.90	1.24	2.06	0.60	1.78	1.06
CaO	41.6	2.14	51.5	36.2	2.14	39.0.	2.81	43.4
Na_2O	0.62	0.44	0.77	0.69	0.41	0.70	0.40	0.77
K_2O	0.71	3.36	0.04	1.10	3.73	0.64	3.33	0.73
CO_2	33.5	0.50	41.6	31.1	2.08	31.2	2.32	36.2
H_2O^+	1.37	8.59	–	1.59	7.76	3.69	4.43	0.96
Organic Carbon	0.84	2.23	0.32	0.48	3.14	6.99	2.47	0.57
S	0.34	0.83	0.40	0.31	0.82	0.89	0.99	0.21
Cl	0.11	0.04	0.04	0.09	0.06	0.09	0.07	0.06
In ppm								
P	355	416	362	360	229	1111	225	334
V	40	134	8	51	157	33	155	24
Mn	254	155	441	582	411	315	536	245
Ni	13	51	6	20	80	37	84	13
Rb	35	204	2	50	213	32	201	33
Sr	337	248	389	232	150	2042	185	529
Zr	23	120	2	41	123	57	145	18
Ba	58	437	112	81	452	151	683	133
Ce	33	89	70	30	87	102	91	30
In percent								
Calcite	76	1	94	71	5	8	5	79
Aragonite	–	–	–	–	–	63	–	3
Quartz	4	8	1	5	9	4	11	3
Clay	14	85	–	17	81	12	80	10
Lithology	LS	SH	LS	LS	SH	PB	SH	LS

Sample No.	142	143	144	145	146	147	148	149
Bed No.	DB181	DB182	DB183	DB183	DB184	DB184	DB185	DB185
In percent								
SiO_2	10.4	41.8	1.18	9.41	11.2	31.4	50.0	4.14
TiO_2	0.17	0.50	0.03	0.17	0.14	0.31	0.56	0.07
Al_2O_3	4.52	16.2	0.43	3.87	5.69	13.4	24.1	2.17
Fe_2O_3	1.95	5.54	1.01	1.40	2.95	4.36	6.55	1.57
MgO	1.16	1.56	0.91	1.15	1.02	1.28	1.78	0.79
CaO	40.4	15.4	50.1	40.8	36.8	19.9	3.35	47.4
Na_2O	0.80	0.66	0.77	0.69	0.59	0.55	0.47	0.73
K_2O	0.89	2.61	0.10	0.73	1.00	2.14	3.55	0.45
CO_2	32.3	13.7	39.9	34.5	30.9	17.0	2.83	37.4
H_2O^+	1.17	4.04	–	1.16	2.31	5.52	6.85	0.88
Organic Carbon	0.57	1.75	0.34	0.66	1.26	2.35	1.97	0.49
S	0.21	0.76	0.29	0.29	0.43	1.06	0.50	0.14
Cl	0.10	0.24	0.04	0.04	0.02	0.10	0.14	0.07
In ppm								
P	576	599	487	669	558	762	246	145
V	33	109	6	38	38	86	135	21
Mn	309	448	251	750	210	261	689	130
Ni	17	52	6	14	19	41	80	8
Rb	42	134	3	36	52	115	214	24
Sr	509	376	814	395	611	361	223	717
Zr	29	89	19	28	26	58	115	14
Ba	68	320	75	85	173	315	508	129
Ce	41	95	48	–	30	74	87	42
In percent								
Calcite	71	29	82	77	66	35	4	85
Aragonite	2	2	9	2	4	4	3	–
Quartz	4	9	–	5	5	8	7	1
Clay	17	57	2	10	18	49	83	9
Lithology	LS	SH	LS	LS	LS	SH	SH	B

Sample No.	150	151	152	153	154	155	156	157
Bed No.	DB186	DB186	DB187	DB187	DB188	DB189	DB189	DB190
In percent								
SiO_2	0.96	6.22	6.22	17.5	1.49	6.25	19.6	36.2
TiO_2	0.02	0.12	0.09	0.20	0.03	0.10	0.22	0.42
Al_2O_3	0.06	3.18	2.74	6.77	0.46	3.19	7.67	15.1
Fe_2O_3	2.08	1.59	2.50	3.20	1.37	2.32	4.06	5.77
MgO	0.91	1.06	0.98	1.07	0.96	1.08	1.04	1.23
CaO	50.7	43.4	44.0	33.2	51.3	43.5	30.6	14.7
Na_2O	0.81	0.65	0.82	0.67	0.85	0.76	0.62	0.54
K_2O	0.04	0.64	0.50	1.11	0.12	0.56	1.29	2.23
CO_2	41.4	35.8	36.8	28.7	42.3	35.4	26.1	10.9
H_2O^+	–	1.08	0.45	2.30	–	1.28	3.22	5.87
Organic Carbon	0.84	0.71	0.68	0.77	0.31	0.55	1.37	0.99
S	0.79	0.30	0.44	0.54	0.23	0.23	0.48	1.35
Cl	0.03	0.07	0.04	0.03	0.07	0.08	0.04	0.03
In ppm								
P	397	279	307	307	402	1147	2613	249
V	6	29	23	17	11	17	62	118
Mn	319	450	777	402	278	341	302	707
Ni	6	14	9	6	9	11	23	94
Rb	2	31	26	56	3	26	63	127
Sr	551	359	580	519	895	870	556	288
Zr	5	14	14	33	16	20	40	76
Ba	119	209	139	5436	63	577	612	329
Ce	–	–	56	61	–	42	64	77
In percent								
Calcite	94	81	81	63	87	72	56	25
Aragonite	–	–	3	2	9	8	4	–
Quartz	1	3	4	6	2	3	5	8
Clay	–	10	7	23	1	12	28	58
Lithology	LS	LS	LS	LS	LS	LS	LS	SH

Sample No.	158	159	160	161	162	163	164	165
Bed No.	DB191	DB192	DB193	DB194	DB195	DB197	DB198	DB199
In percent								
SiO_2	49.5	1.99	49.0	1.33	55.6	53.0	14.3	57.3
TiO_2	0.69	0.04	0.69	0.02	1.12	0.86	0.27	1.04
Al_2O_3	20.6	0.59	20.7	0.40	20.8	20.7	5.80	18.8
Fe_2O_3	7.51	3.41	7.19	5.11	6.03	7.15	3.64	5.69
MgO	1.43	0.51	1.62	0.44	1.53	1.52	0.87	1.52
CaO	2.30	47.3	3.47	44.3	0.69	1.51	33.1	1.24
Na_2O	0.42	0.90	0.32	0.72	0.29	0.46	0.88	1.05
K_2O	2.93	0.13	3.18	0.08	3.38	3.19	1.09	2.81
CO_2	–	35.3	1.00	34.0	–	0.04	28.3	–
H_2O^+	9.40	–	8.46	–	7.29	7.38	2.96	7.40
Organic Carbon	0.88	1.62	1.53	1.44	3.23	0.49	0.96	1.20
S	0.83	0.88	0.75	1.63	0.23	0.58	0.25	0.53
Cl	0.05	0.03	0.02	0.04	0.01	0.16	0.56	0.99
In ppm								
P	231	297	343	174	261	217	216	253
V	159	11	182	5	219	207	58	195
Mn	84	86	824	350	110	113	580	50
Ni	38	38	112	105	52	39	59	38
Rb	193	4	190	–	207	198	59	175
Sr	199	2671	192	2618	155	170	1867	173
Zr	147	48	137	43	224	182	72	226
Ba	436	166	391	199	476	442	237	385
Ce	75	84	148	129	130	97	98	125
In percent								
Calcite	–	14	2	6	–	–	1	–
Aragonite	–	68	–	75	–	–	62	–
Quartz	13	2	9	2	19	17	4	25
Clay	81	2	83	2	77	78	25	73
Lithology	SH	PB	SH	PB	SH	SH	PB	SH

Sample No.	166	167	168	169	170	171	172	173
Bed No.	DB200	DB201	DB202	DB203	DB204	DB205	DB206	DB207
In percent								
SiO_2	1.56	16.9	6.60	56.3	0.14	54.6	0.11	56.5
TiO_2	0.03	0.21	0.10	1.06	0.01	0.97	0.01	1.05
Al_2O_3	0.54	6.17	2.98	21.2	–	21.8	–	20.5
Fe_2O_3	1.33	3.28	1.52	3.86	0.89	6.79	1.79	6.18
MgO	0.92	1.16	0.97	1.63	0.99	1.71	0.98	1.38
CaO	50.7	34.5	43.2	2.05	53.9	1.18	52.8	0.72
Na_2O	0.86	0.60	0.76	0.34	1.01	0.35	0.91	0.28
K_2O	0.14	1.10	0.60	3.15	0.02	3.50	0.02	2.84
CO_2	41.5	29.1	35.6	1.71	42.8	–	43.0	–
H_2O^+	–	2.70	1.67	6.51	–	7.90	–	7.58
Organic Carbon	0.45	2.63	1.34	2.68	0.16	2.19	0.44	0.88
S	0.28	0.26	0.38	0.40	0.19	0.34	0.50	0.50
Cl	0.06	0.02	0.10	0.05	0.02	0.05	0.03	0.03
In ppm								
P	163	181	247	307	163	195	237	189
V	11	64	22	213	6	216	6	217
Mn	300	662	895	542	156	57	235	321
Ni	6	26	13	70	5	50	8	65
Rb	6	51	27	164	–	222	2	188
Sr	700	590	562	150	768	127	616	134
Zr	12	44	25	190	8	195	8	214
Ba	62	170	235	426	22	453	16	446
Ce	58	51	–	114	–	104	–	130
In percent								
Calcite	92	66	81	3	95	–	96	–
Aragonite	2	–	–	–	2	–	2	–
Quartz	2	8	4	19	–	14	–	22
Clay	2	22	9	74	–	82	–	75
Lithology	LS	LS	LS	SH	LS	SH	LS	SH

Sample No.	174	175	176	177	178	179	180	181
Bed No.	DB208	DB209	DB209	DB210	DB210	DB211	DB211	DB211
In percent								
SiO_2	0.75	3.51	51.7	3.21	9.94	30.9	5.01	6.58
TiO_2	0.02	0.08	0.74	0.05	0.17	0.31	0.08	0.11
Al_2O_3	0.09	1.49	19.2	1.03	4.47	13.1	2.58	3.87
Fe_2O_3	4.45	1.41	6.14	4.34	1.85	5.17	1.91	2.52
MgO	0.76	0.66	1.57	0.87	1.05	1.38	0.79	1.07
CaO	47.3	49.3	5.58	43.9	40.1	20.6	45.9	42.8
Na_2O	0.69	0.86	0.39	0.80	0.84	0.64	0.75	0.79
K_2O	0.05	0.31	2.92	0.24	0.76	1.89	0.49	0.69
CO_2	37.9	38.6	4.18	36.7	31.2	16.9	36.4	33.5
H_2O^+		0.84	6.21	0.52	2.30	3.54	1.27	1.91
Organic Carbon	1.02	0.48	2.85	2.02	2.52	2.14	0.63	1.13
S	1.15	0.04	0.47	1.04	0.26	1.03	0.08	0.21
Cl	0.05	0.01	0.05	0.23	0.09	0.07	0.01	0.02
In ppm								
P	223	169	237	255	236	350	172	653
V	7	20	168	15	39	70	22	30
Mn	910	252	333	779	1009	475	220	997
Ni	51	8	66	17	15	39	8	15
Rb	–	16	173	12	38	98	26	34
Sr	1367	438	236	905	379	346	510	588
Zr	14	13	148	21	37	57	17	35
Ba	136	104	394	118	137	276	105	153
Ce	84	66	91	53	28	59	33	74
In percent								
Calcite	65	88	8	73	70	37	83	72
Aragonite	22	–	2	10	1	2	–	4
Quartz	3	2	13	4	3	6	2	2
Clay	–	6	73	5	19	49	10	15
Lithology	LS	B	SH	LS	LS	SH	B	LS

Sample No.	182	183	184	185	186	187	188	189
Bed No.	DB212	DB213	DB214	DB215	DB215	DB216	DB217	DB218
In percent								
SiO_2	8.27	39.2	3.51	55.5	51.8	2.16	36.5	0.29
TiO_2	0.14	0.43	0.04	1.00	0.87	0.03	0.45	0.01
Al_2O_3	3.41	17.8	0.72	24.0	20.6	0.32	11.5	–
Fe_2O_3	2.40	4.42	11.1	5.72	7.92	1.72	5.11	1.30
MgO	0.97	1.53	0.78	1.68	1.46	0.96	2.39	0.92
CaO	39.7	16.7	33.5	0.83	1.26	49.1	19.0	53.5
Na_2O	0.61	0.50	0.60	0.29	0.37	0.73	0.53	0.76
K_2O	0.61	2.39	0.15	3.29	2.89	0.12	1.88	0.03
CO_2	31.9	15.8	28.0	0.32	–	37.9	18.0	43.5
H_2O^+	2.09	4.37	–	6.73	8.03	–	4.15	–
Organic Carbon	2.50	3.45	4.81	1.07	0.71	0.55	2.50	0.39
S	0.46	0.39	4.06	0.09	0.82	0.36	0.35	0.19
Cl	0.03	0.01	0.04	0.08	0.06	0.03	0.02	0.06
In ppm								
P	238	318	309	189	185	197	249	206
V	27	98	12	233	163	10	106	5
Mn	1446	736	579	91	139	675	586	884
Ni	16	42	38	104	72	4	31	4
Rb	33	135	8	223	194	5	94	–
Sr	416	368	796	152	176	570	534	620
Zr	43	81	23	199	168	16	106	10
Ba	140	344	166	465	407	58	347	74
Ce	63	61	46	131	124	–	49	–
In percent								
Calcite	70	33	62	–	–	88	40	99
Aragonite	2	3	4	1	–	–	1	–
Quartz	4	6	4	13	10	2	11	1
Clay	14	64	3	85	84	2	44	–
Lithology	LS	SH	LS	SH	SH	LS	SH	LS

Sample No.	190	191	192
Bed No.	DB219a	DB219b	DB129b
In percent			
SiO_2	47.2	4.09	5.67
TiO_2	0.63	0.03	0.10
Al_2O_3	14.8	1.46	1.98
Fe_2O_3	4.35	3.02	1.35
MgO	1.46	0.80	0.73
CaO	12.1	46.4	46.8
Na_2O	0.47	0.82	0.76
K_2O	2.24	0.32	0.40
CO_2	11.4	37.4	38.0
H_2O^+	4.08	0.72	0.97
Organic Carbon	1.25	0.89	0.28
S	0.20	0.45	0.07
Cl	0.03	0.03	0.02
In ppm			
P	70	252	173
V	171	16	22
Mn	56	218	22
Ni	69	26	10
Rb	131	16	20
Sr	434	699	368
Zr	130	17	15
Ba	280	54	100
Ce	72	44	73
In percent			
Calcite	15	73	87
Aragonite	10	12	—
Quartz	14	1	3
Clay	60	6	6
Lithology	SH	LS	B

PART B

Sample Number	6	7	18	23	28	31
Bed Number	DB8562	DB86	DB94	DB97	DB101	DB103
In ppm						
Zn	22	37	11	3	–	1
Ga	4	5	1	1	–	–
As	3	2	–	–	–	–
Pb	–	4	–	2	–	–
Th	–	4	4	4	6	7

Sample Number	32	42	41	40	51	52
Bed Number	DB104	DB111a	DB111b	DB111c	DB117	DB118
In ppm						
Zn	38	10	–	–	45	–
Ga	8	2	–	1	10	–
As	14	–	–	–	19	–
Pb	10	8	7	–	11	–
Th	5	–	6	5	–	4

Sample Number	56	76	80	81	91	94
Bed Number	DB121	DB133	DB134	DB135	DB149	DB154
In ppm						
Zn	–	–	1	37	24	25
Ga	–	–	2	3	2	3
As	–	–	–	25	–	–
Pb	5	–	7	26	7	–
Th	–	–	9	4	5	–

Sample Number	102	104	113	116	118	133
Bed Number	DB157	DB159	DB164b	DB164c	DB165	DB175
In ppm						
Zn	46	–	139	28	12	10
Ga	5	2	2	2	5	5
As	3	–	3	3	3	–
Pb	–	–	–	–	7	–
Th	–	–	2	4	–	4

Sample Number	154	159	161	164	174	175
Bed Number	DB188	DB192	DB194	DB198	DB208	DB209
In ppm						
Zn	–	174	128	211	8	18
Ga	1	–	–	6	–	2
As	–	–	6	–	–	–
Pb	6	9	9	4	–	–
Th	4	4	–	–	–	–

Sample Number	184	191
Bed Number	DB214	DB219b
In ppm		
Zn	77	85
Ga	1	2
As	3	3
Pb	–	–
Th	–	–

PART C

Sample Number	1	199	16	17	27	30
Bed Number	DB83	DB83	DB92	DB93	DB100	DB102
In ppm						
Cu	39	36	32	32	45	33
Zn	77	72	39	56	116	85
Ga	8	8	20	13	21	10
As	7	7	11	22	30	30
Pb	11	11	24	15	11	13
Th	3	8	10	5	22	--
Sample Number	54	60	73	75	78	95
Bed Number	DB119	DB124b	DB130	DB132	DB134	DB154a
In ppm						
Cu	29	36	33	37	36	35
Zn	43	63	49	46	70	117
Ga	8	13	10	9	20	23
As	9	13	15	12	15	8
Pb	15	14	16	13	33	25
Th	10	8	7	5	16	13
Sample Number	97	98	100	106	110	117
Bed Number	DB154b	DB155	DB156	DB160	DB162	DB164a
In ppm						
Cu	23	35	31	38	35	39
Zn	161	109	77	94	108	84
Ga	13	22	21	16	22	21
AS	14	8	15	9	10	11
Pb	19	27	25	22	23	26
Th	11	12	12	5	12	9
Sample Number	115	119	123	125	128	130
Bed Number	DB164b	DB166	DB168	DB170	DB172	DB174a
In ppm						
Cu	34	37	32	38	36	27
Zn	103	107	131	101	142	72
Ga	22	19	24	22	21	24
As	12	14	10	9	11	12
Pb	25	23	31	24	21	31
Th	12	10	12	11	10	12

Sample Number	132	135	138	140	143	147
Bed Number	DB174c	DB177	DB180	DB180	DB182	DB184
In ppm						
Cu	27	33	31	38	34	26
Zn	61	108	178	104	70	59
Ga	32	24	26	22	15	12
As	13	15	11	13	22	9
Pb	14	22	25	29	17	13
Th	5	9	9	13	7	14

Sample Number	148	157	158	160	162	163
Bed Number	DB185	DB190	DB191	DB193	DB195	DB197
In ppm						
Cu	31	31	35	38	32	31
Zn	134	148	84	129	95	58
Ga	20	15	22	21	21	22
As	17	7	9	13	9	9
Pb	19	18	27	31	36	30
Th	10	12	12	15	17	13

Sample Number	165	169	171	173	176	179
Bed Number	DB199	DB203	DB205	DB207	DB209	DB211
In ppm						
Cu	35	39	31	34	31	29
Zn	60	84	75	96	113	59
Ga	19	22	23	21	20	14
As	9	14	8	10	12	15
Pb	32	36	24	34	25	14
Th	13	17	12	13	9	5

Sample Number	183	185	186	188	190
Bed Number	DB213	DB215	DB215	DB 217	DB219
In ppm					
Cu	29	49	36	29	34
Zn	74	138	105	69	134
Ga	16	23	21	12	17
As	13	5	8	12	7
Pb	16	32	35	24	22
Th	9	13	10	9	11

PART D

Sample Number	1	199	16	17	27	30
Bed Number	DB83	DB83	DB92	DB93	DB100	DB102
In percent						
Montmorillonite & illite/mont.	46	46	5	24	21	24
Illite	13	13	84	35	59	22
Kaolinite	–	–	–	–	–	–
Quartz	4	5	7	8	10	10
Calcite	27	29	1	29	7	31
Aragonite	5	5	–	–	7	4

Sample Number	54	60	73	75	78	95
Bed Number	DB119	DB124b	DB130	DB132	DB134	DB154a
In percent						
Montmorillonite & illite/mont.	30	28	14	13	31	16
Illite	14	23	24	29	33	44
Kaolinite	–	1	2	2	9	9
Quartz	4	7	9	8	12	21
Calcite	48	25	36	46	12	2
Aragonite	–	10	7	2	–	4

Sample Number	97	98	100	106	110	117
Bed Number	DB154b	DB155	DB156	DB160	DB162	DB164a
In percent						
Montmorillonite & illite/mont.	10	17	23	17	22	17
Illite	30	36	39	40	43	44
Kaolinite	4	10	8	7	7	8
Quartz	13	23	16	25	16	13
Calcite	38	3	12	11	9	3
Aragonite	2	–	–	–	2	–

Sample Number	115	119	123	125	128	130
Bed Number	DB164b	DB166	DB168	DB170	DB172	DB174a
In percent						
Montmorillonite & illite/mont.	28	13	22	19	12	18
Illite	46	44	49	53	56	52
Kaolinite	7	9	9	12	10	8
Quartz	12	10	13	8	10	13
Calcite	–	14	3	3	7	5
Aragonite	–	4	–	–	–	–

Sample Number	132	135	138	140	143	147
Bed Number	DB174c	DB177	DB180	DB180	DB182	DB184
In percent						
Montmorillonite & illite/mont.	23	30	20	20	12	11
Illite	52	41	52	46	36	33
Kaolinite	13	14	9	14	9	5
Quartz	7	8	9	11	9	8
Calcite	–	1	5	5	29	35
Aragonite	–	–	–	–	2	4

Sample Number	148	157	158	160	162	163
Bed Number	DB185	DB190	DB191	DB193	DB195	DB197
In percent						
Montmorillonite & illite/mont.	27	21	44	30	26	27
Illite	44	27	33	43	43	44
Kaolinite	12	10	4	10	8	7
Quartz	7	8	13	9	19	17
Calcite	4	25	–	2	–	–
Aragonite	3	–	–	–	–	–

Sample Number	165	169	171	173	176	179
Bed Number	DB199	DB203	DB205	DB207	DB209	DB211
In percent						
Montmorillonite & illite/mont.	23	24	30	32	20	16
Illite	42	38	46	33	44	26
Kaolinite	8	12	8	10	9	4
Quartz	25	19	14	22	13	6
Calcite	–	3	–	–	8	37
Aragonite	–	–	–	–	2	2

Sample Number	183	185	186	188	190
Bed Number	DB213	DB215	DB215	DB217	DB219
In percent					
Montmorillonite & illite/mont.	23	32	39	14	25
Illite	23	43	35	26	30
Kaolinite	8	11	10	4	6
Quartz	6	13	10	11	14
Calcite	33	–	–	40	15
Aragonite	3	1	–	1	10